ARYLNITRENES: A SYNTHETIC APPROACH TOWARDS AMINO-IMINO-AZEPINES

By

CHARLES G. YOUNGER, B.Sc.

A Thesis

Submitted to the School of Graduate Studies

in Partial Fulfilment of the Requirements

for the Degree

Doctor of Philosophy

McMaster University

ARYLNITRENES: A SYNTHETIC APPROACH TOWARDS AMINO-IMINO-AZEPINES

DOCTOR OF PHILOSOPHY (1992) **McMASTER UNIVERSITY**

(Chemistry) **Hamilton, Ontario**

TITLE: Arylnitrenes: A Synthetic Approach Towards Amino-Imino-Azepines

AUTHOR: Charles G. Younger, B.Sc. (University of Western Ontario)

SUPERVISOR: Professor R.A. Bell

NUMBER OF PAGES: xiv, 246

ABSTRACT

The chemistry of substituted phenylnitrenes was investigated to discern the mechanism and factors involved in the preparation of 3H-dihydroazepines. Synthetic utility of this phenylnitrene reaction was explored through the photolysis of a series of non-symmetric phenylazides. Phenylnitrene production via the photolysis or thermolysis of phenylazides as well as through the deoxygenation of aryl-nitro compounds was compared. Results indicated the photolysis reaction was superior in yielding azepine products. The intermediates involved in the ring expansion reaction of the phenylnitrenes were computer modelled using a semi-empirical molecular orbital calculation that aided in the prediction of the observed product yields. In addition, the azirine intermediates derived from the photolysis of diamido-phenylazides were chemically trapped *in situ* confirming their presence in the complicated phenylnitrene mechanism. Kinetic data from the chemical trapping of the intermediates formed from the photolysis of 3-acetamido-4-trifluoroacetamido-phenylazide showed the azirine intermediate was formed directly from the singlet phenylnitrene. The didehydroazepine intermediate was formed from the azirine intermediate and not directly from the singlet phenylnitrene. The computational data were used to determine the substituents necessary to preferentially yield the desired azepine product. Finally, in an attempt to synthesize an amino-imino-azepine, 4,5-substituted 3H-dihydroazepines were synthesized selectively from 3,4-substituted phenylazides. However, attempts at oxidizing and/or deprotecting the 3H-dihydroazepines failed because of the harsh reaction conditions employed.

ACKNOWLEDGEMENTS

Throughout the course of this thesis I am grateful for the guidance and friendship given by my supervisor, Dr. R.A. Bell. From our many conversations, including both research and recreation, he has made the years at McMaster enjoyable.

The Chemistry faculty at McMaster, especially my committee members, Dr. N.H. Werstiuk and Dr. J. Warkentin. I would also like to thank Dr. B.E. McCarry and Dr. M.A. Brook for filling in when committee members were away.

I am also grateful for the technical assistance given by Dr. Donald (Don) W. Hughes and Brian G. Sayer for their NMR expertise and Dr. Richard Smith and F. Ramelan for their mass spectral mastery.

For the photochemistry advise, I appreciated the help of Dr. W.J. Leigh and cohorts, especially Mark and Greg. Their continued optimism and input inaugurated me into photochemistry and conference life.

Dr. R.F. Childs, John, George, Brad and Teresa for the use of the photolysis equipment.

I am deeply grateful to my labmates, Dr. Fred Capretta and Rob Maharajh. Their antics in the lab (and Fred's out of the lab) provided much needed entertainment at critical times.

I wish to thank my family for their support and encouragement especially throughout my studies.

Finally, I would like to thank my wife Jodi, for her support, encouragement and sympathetic ear for all the ups and downs endured throughout this thesis and for reminding me that there is more to life than chemistry (along with K. and K.). I hope someday I can do the same for you.

TABLE OF CONTENTS

LIST OF TABLES

LIST OF FIGURES

SYMBOLS AND ABBREVIATIONS

ε	molar extinction coefficient
CI MS	chemical ionization mass spectrometry
DDQ	2,3-dichloro-5,6-dicyano-1,4-benzoquinone
DMF	dimethylformamide
DMSO-d6	deuterated dimethylsulphoxide
EI MS	electron impact mass spectrometry
EtOAc	ethylacetate
FID	Free Induction Decay
HET-CORR	Heteronuclear Shift Correlated NMR
HRMS	high resolution mass spectrometry
IR	infrared
ISC	intersystem crossing
J	Nuclear Magnetic Resonance coupling constant
LR HET-CORR	Long Range Heteronuclear Shift Correlated NMR
MRI	Magnetic Resonance Imaging
NMR	Nuclear Magnetic Resonance
ppm	parts per million
Q_s	spin density
RF	radiofrequency
T_1	spin-lattice relaxation time
T_2	spin-spin relaxation time
THF	tetrahydrofuran
TLC	thin layer chromatography
UV	ultraviolet

Chapter 1

Magnetic Resonance Imaging and Amino-Imino-Azepines

1.1 Magnetic Resonance Imaging Contrast Agents

1.1.1 Introduction

Imaging techniques in medicine have progressed dramatically over the years to expand and enhance diagnostic medicine. There are many types of medical imaging techniques including: X-ray imaging and computer tomography (CT), ultrasound, positron emission tomography (PET), and nuclear magnetic resonance imaging (MRI). MRI is rapidly becoming the most valuable imaging technique available in medicine, as well as in chemical and engineering designs, due to its noninvasive nature. It uses nonionizing radiation (as opposed to X-rays), and modest magnetic fields. One of MRI's biggest deterrents is the initial capital for the apparatus. With the intense research in superconducting magnets, the cost of MRI machines is dropping as technology progresses. Other problems include relatively long data collection times and the occasional lack of diagnostic specificity[1a]. To overcome the problem of specificity, imaging enhancing agents are used.

The resolution of present day MRI instruments are routinely better than all other imaging techniques available[1]. Magnetic resonance capabilities include the ability to image cross sections, image flow, chemical shift determinations, perfusion and diffusion[1b]. Image enhancements can be made through the use of contrast agents but, unlike most imaging agents which are visualized directly, MRI agents themselves are not visualized. The agents change the local environment allowing image enhancement. To understand how

MRI contrast agents operate, the theory behind NMR and specifically MRI must be addressed.

1.1.2 Pulsed Nuclear Magnetic Resonance

Continuous wave (CW) NMR measures the emission or absorption of energy at a particular frequency during the variation of the magnetic field strength. Pulsed NMR is different from CW NMR in that the response of the system is measured after a radio frequency (RF) pulse has been applied. The pulse excites the entire frequency range and the response is collected over the same range under consideration. The sum of all the magnetizations can be expressed as a bulk magnetization, **M** (see Figure 1.1). During a pulse, $\mathbf{M}_o$ is perturbed by an oscillating RF field and the frequency response spectrum is collected and digitally processed mathematically by a Fourier transformation (FT). To understand how this system operates, the rotating frame vector model can be used[2a] as shown in Figure 1.1.

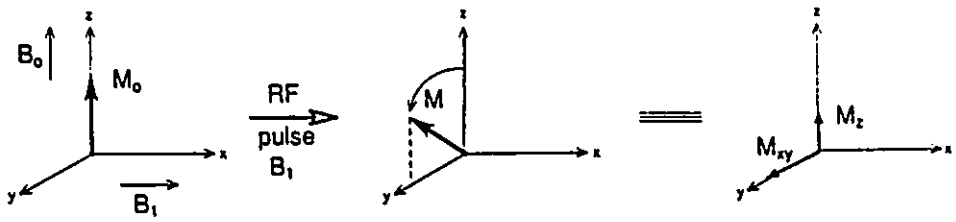

***Figure 1.1** Effect of a radiofrequency pulse on the bulk magnetization using the rotating frame of reference.*

Initially the system will have $\mathbf{M}_o$ in the direction of the static magnetic field, B_o. When an RF pulse, B_1, in the x-axis is applied, the magnetization is tipped towards the

y-axis. This bulk magnetization, **M**, can be viewed as containing two components, one in the z-axis, $\mathbf{M}_z$, and one in the xy-plane, $\mathbf{M}_{xy}$. The extent of rotation from the z-axis into the y-axis is dependent on the flip angle, θ. Hypothetically this magnetization should remain indefinitely about the z-axis although in reality it decays back to its equilibrium value $\mathbf{M}_o$ over time by processes referred to as *relaxation.*

1.1.3 Relaxation

After an RF pulse, $\mathbf{M}_z$ is smaller in magnitude than $\mathbf{M}_o$, and a new magnetization in the xy-plane, $\mathbf{M}_{xy}$, is created. The mechanism of relaxation can be classified as belonging to one of two types. The first type is relaxation of $\mathbf{M}_z$ back to $\mathbf{M}_o$ along the z-axis and the second is of $\mathbf{M}_{xy}$ back to its equilibrium value of zero.

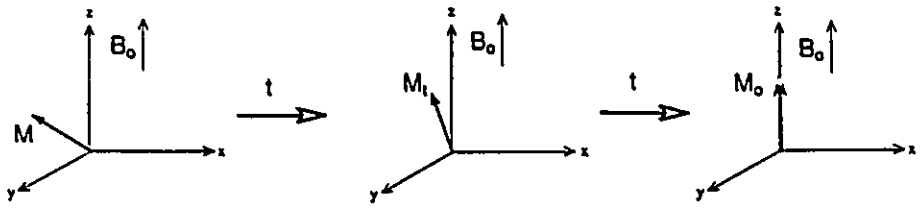

Figure 1.2 *Vector diagram of the relaxation of the bulk magnetization, M, back to it's equilibrium value of M_o after a RF pulse.*

Relaxation of $\mathbf{M}_z$ back to $\mathbf{M}_o$ requires an interaction between the spins of the nuclei and the surroundings. It is therefore described as spin-lattice or longitudinal relaxation. This rate, R_1, is first order and is typically measured by the relaxation time constant T_1.

$$R_1 = 1/T_1 \qquad (1.1)$$

The loss of magnetization in the xy-plane back to zero is achieved by two processes. Relaxation occurs both by spin-lattice relaxation back to the z-axis and by dephasing of the spins such that the net xy-magnetization, $\mathbf{M}_{xy}$, is zero. The dephasing of the components does not require any change in energy and therefore it can occur faster than spin-lattice relaxation. This type of relaxation is called spin-spin or transverse relaxation and is denoted by R_2 (the relaxation rate constant) and T_2 (the relaxation time constant).

$$R_2 = 1/T_2 \tag{1.2}$$

Because R_2 involves both spin-spin and spin-lattice processes, this relaxation is always equal to or faster than spin-lattice relaxation ($R_2 \geq R_1$). The effect of T_2 relaxation is important since short T_2 times (fast decay) result in line broadening of the acquired spectra.

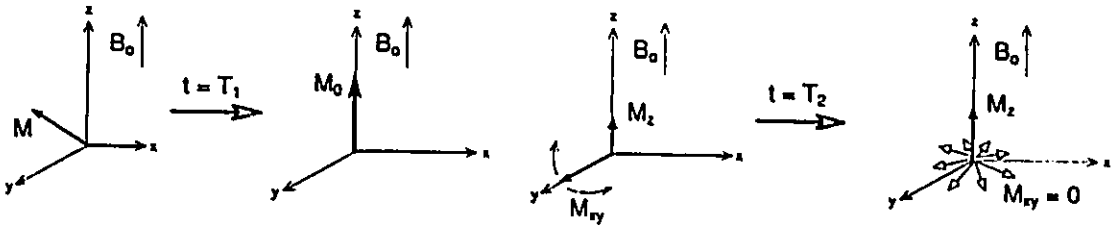

***Figure 1.3** Vector diagram of the longitudinal and transverse relaxation of the bulk magnetization.*

1.1.4 Magnetic Resonance Imaging (MRI)

The frequency of a resonance for a particular nucleus in a magnetic field is given by the Larmor equation[2a]:

$$\omega = \gamma B \tag{1.3}$$

Because the frequency ω is proportional to the field strength B, a field gradient perpendicular to the static magnetic field during imaging imparts spatial localization to a particular nucleus. One scan produces a one dimensional projection with the frequency of the signal describing the locale of the nucleus and the amplitude describing the abundance of nuclei at that locale (Figure 1.4). By acquiring multiple scans from multiple angles, a two dimensional slice can be formed and by stacking slices, a complete three dimensional image is created.

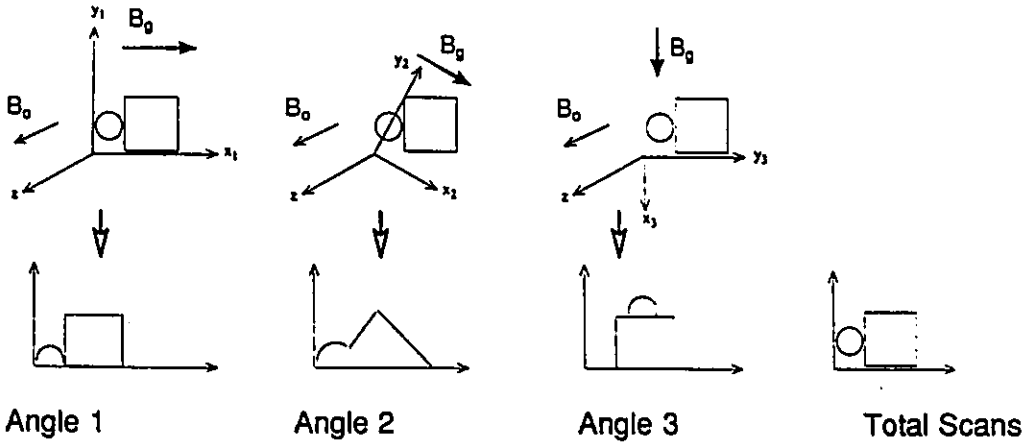

Multiple angles generate multiple silhouettes that construct a 2D image.

***Figure 1.4** Theory of images obtained through magnetic resonance imaging.*

Three MRI imaging techniques are used in practice in which the signal intensity acquired is weighted by T_1, T_2 and normal proton concentration[1a]. By using different pulse sequences, by varying the pulse angles and the delays between pulses, the intensity of the image can be optimized for each of these imaging techniques. For example, long delays between pulses may allow T_2 relaxation to occur completely while the system may still be relaxing via T_1.

1.1.5 Magnetic Resonance Contrast Media

There are two distinct classes of magnetic resonance contrast agents which affect the relaxation rate, or *relaxivity*, and are referred to as T_1 and the T_2 agents[3]. T_1 agents increase the relaxation rate of water molecules via a fluctuating local magnetic field generated by a proximal paramagnetic ion[3a,3c]. T_2 agents produce microscopic magnetic field gradients such that, when a water molecule diffuses by, the coherence of magnetic spin of the entire molecule is lost[3a,3c] causing the intensity of the acquired signal to be reduced. The dose of the agent required must be sufficient to provide a 10-20% enhancement of the image to be detectable by MRI[3c].

T_1 agents tend to be large macromolecules such as human serum albumin (HSA) bound to a paramagnetic ion[3e]. Because of the large size of the molecules, they exhibit slow tumbling *in vivo* allowing large relaxivity towards the surroundings. Enhancements of the relaxivity of two-to ten-fold have been found with HSA bound to paramagnetic species[3e].

T_2 agents are smaller paramagnetic molecules that create localized field gradients *in vivo* after injection. The magnitude of the field gradient is dependent on the magnetic moment, γ, of the ion with the standard agents tending to be gadolinium (III) complexes.

1.1.6 Theory of Relaxivity

Paramagnetic species increase both $1/T_1$ and $1/T_2$ of water molecules and the observed relaxation rate ($R_{1(obs.)}$ or $R_{2(obs.)}$) is a combination of both diamagnetic and paramagnetic relaxation rates.

$$R_{i(obs.)} = R_{i(diamagnetic)} + R_{i(paramagnetic)} \qquad i=1,2 \qquad (1.4)$$

The amount of relaxation enhancement depends on the distance between the water

molecules and the metal ion as well as on the duration of the interaction. The paramagnetic metal ion creates a fluctuating local magnetic field but is only operative within a distance of 5 Å from the affected aqueous hydrogen atoms[3b]. There are two mechanisms by which the ion can affect the relaxation rate of the water molecules; the first is labelled *inner-sphere* and the second is *outer-sphere relaxation.*

Inner-sphere relaxation occurs when a water molecule is coordinated to a paramagnetic ion or hydrogen bonded to the complex ion species. This type of interaction has been extensively studied and equations have been developed to describe the phenomenon in detail[3b] with the interaction being strongly dependent on the number of water molecules coordinated to the paramagnetic ion. Inner-sphere T_1 relaxation stems from the chemical exchange of the bulk water molecules with the primary coordination sphere of the water molecules to the paramagnetic ion[3c].

Outer-sphere relaxation occurs when a water molecule diffuses by a paramagnetic species without any binding[3a]. Therefore the residence time of the water in the vicinity of the ion is quite low and consequently the relaxation enhancement is small for outer-sphere relaxation.

Inner-sphere relaxation Outer sphere relaxation

Figure 1.5 *Types of relaxation mechanisms.*

1.1.7 MRI Contrast Agents

Ideally an MRI contrast agent should appreciably increase the relaxation rate of the water while remaining biocompatible. Paramagnetic ions, such as gadolinium (III), other paramagnetic lanthanides and transition metals, as free ions exhibit large relaxivities but they tend to be quite toxic and exhibit non-specific biodistribution[3b,3c]. To overcome this predicament, the metals are chelated to biocompatible ligands and therefore numerous chelants are being developed to meet the demands for an ideal MRI contrast agent[3]. Some of the more common MRI contrast agents are shown in Figure 1.6 with two of the most widely used agents being diethylenetriaminepentaacetic acid (DTPA) and tetraazacyclododecane-*N,N',N'',N'''*-tetraacetic acid (DOTA).

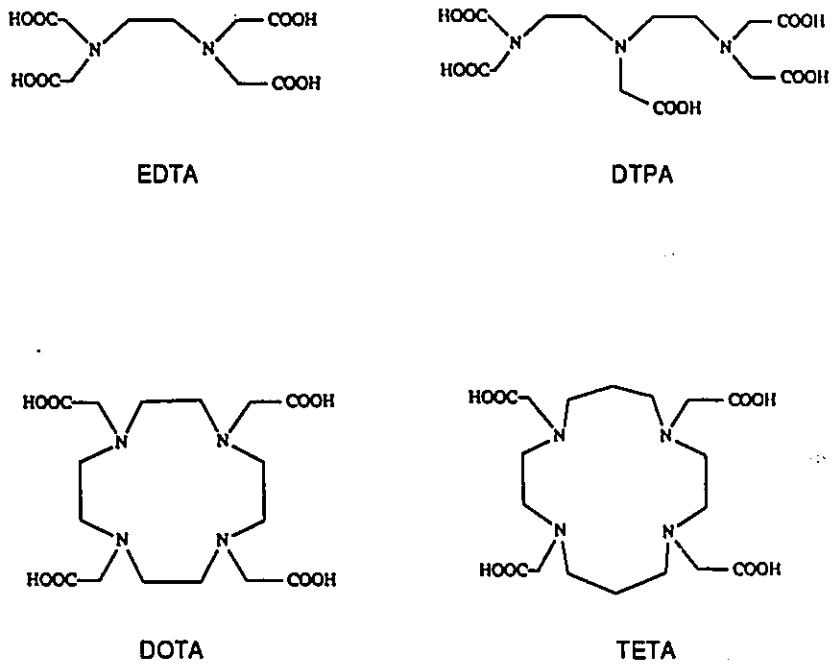

Figure 1.6 *A sample of MRI contrast agents.*

Table 1.1 shows the importance of water coordination in increasing the relaxivity. Although this increased coordination dramatically increased the relaxivity, it also increased the toxicity of the paramagnetic species. As a result, considerable research is being devoted to new chelants for MRI[3] and in 1990, Gd(DTPA) was the only contrast agent approved for clinical use in the United States[3c] with Gd(DOTA) only in clinical trials in Europe[1a].

Table 1.1 *Longitudinal relaxivities (R_1) as a function of coordinated water molecules and acute LD_{50} values for gadolinium (Gd) complexes.*

Species	Coordinated Water Molecules	Relaxivity R_1 ($mM^{-1}s^{-1}$)	Mouse LD_{50} (mmol kg^{-1})
Gd^{3+} (aqueous)	8,9	9.1	0.1 - 1.4
Gd(EDTA)	2,3	6.6	0.3
Gd(DTPA)	1	3.7	>10
Gd(DOTA)	1	3.4	>10
Gd(TETA)	0	2.1	N.A.
Gd(TTHA)	0	2.0	6

Analysis of Table 1.1 clearly shows the importance of water coordination to permit inner-sphere interactions. Both Gd(TETA) and Gd(TTHA) are said to be operating through the outer-sphere mechanism since no water molecules can enter into the primary coordination sphere.

1.1.8 Rational for the Synthesis of Amino-imino-azepines

The thermodynamic and kinetic stability of the metal complex is critical *in vivo* to

overcome toxicity problems and therefore the metal ion must be tightly coordinated to the chelant molecule. The tight chelation limits water coordination and thus lower relaxivity can occur. To overcome this problem, we proposed the development of an innovative chelant that can both bind the metal tightly and permit spin density from the metal to reach the water molecules through hydrogen bonding of water to the chelate. The proposed chelants are the amino-imino-azepines which have never been synthesized before.

1.1.9 Amino-imino-azepines

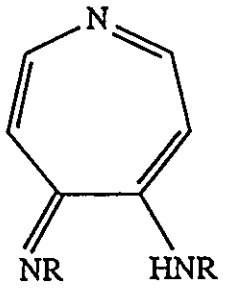

Amino-imino-azepines

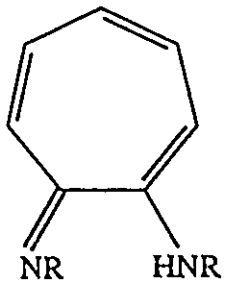

Amino-troponeimines

In the mid 1960's, Eaton *et al.*[4] synthesized a series of amino-troponeimines that transmitted large quantities of spin density from metal ions out into the π-system of the seven membered ring. We proposed the synthesis of an analogous seven membered nitrogen heterocycle, the amino-imino-azepines (shown above). The amino-imino-azepines were proposed as MRI chelants because they were anticipated to transmit spin density from the metal out into the ring π-system and subsequently to the nitrogen atom of the azepine ring. The nitrogen atom would presumably hydrogen bond to nearby water molecules allowing the inner-sphere mechanism of relaxation to occur while still allowing tight binding between the chelant and the metal ion.

Initially, theoretical calculations of spin density transmission on amino-imino-azepines chelated to a paramagnetic metal ion was investigated. Computer modelling of both amino-troponeimines and amino-imino-azepines was carried out to determine if spin density was transmitted out to the nitrogen atom of the azepine.

1.2 Molecular Modelling

1.2.1 Introduction

In the recent advances in computing, molecular modelling has been a very effective scientific method for the analysis and comprehension of chemical reactions[5]. *Ab initio* calculations, presently the most accurate molecular modelling method, are difficult for large molecules such as azepines because of the length of computation time (CPU) required. Simpler computer models such as MMX[6a] are more rapid but they incorporate too many approximations. The electronic stability from conjugation is not sufficiently reflected in the energy minima calculated. An alternative method is through the use of semi-empirical calculations such as those in the AMPAC or MOPAC programs[5b,5c]. These programs use shorter CPU time than *ab initio* methods and smaller file sizes while still incorporating both electronic and geometric considerations in the calculations. The AMPAC program uses either the MINDO/3, MNDO (modified neglect of diatomic overlap) or AM1 (Austin Model 1) Hamiltonians in the molecular orbital calculation. These Hamiltonians are less accurate quantum mechanical models than *ab initio* methods because they incorporate larger estimations to increase the speed of the calculations.

The AMPAC program uses initial atomic coordinates for a molecule obtained from

a simpler computer modelling program such as MMX or from crystallographic coordinates and then optimizes the geometry using one of the Hamiltonians selected. With the advent of faster and more powerful computers, general purpose quantum mechanical models have been made more feasible in many laboratories. These semi-empirical programs yield results that are comparable to *ab initio* methods but require at least 100 times less CPU time[5c]. This allows calculations on standard VAX computers and even on personal computers (PC's) to be completed in reasonable times.

During the course of study, molecular modelling was used in three major areas. The first area was the modelling of the amino-imino-azepines in order to determine if these systems project spin density from a paramagnetic metal centre out into the nitrogen heterocycle. This was desired as discussed earlier to determine if amino-imino-azepines complexed to paramagnetic metals would be useful as MRI contrast agents. The second experiment involved the modelling of a series of meta- and para-substituted phenylnitrenes and their ring expanded products to determine if semi-empirical methods (specifically the AMPAC program) can be used to predict product distributions. This area is discussed in more detail in Chapter 4. The final experiment was designed around a specific azide photolysis to aid in the understanding of the mechanism more thoroughly, at least for the particular system in question. The azide of particular interest was the 3-acetamido-4-trifluoroacetamido-phenylazide because of its unusual chemistry and this compound is discussed in detail in Chapter 5.

1.2.2 Amino-imino-azepines

In order to determine computationally if amino-imino-azepines would allow the transmission of spin density out into its π-system, the simple ring system was modelled

using the AMPAC program. The amino-troponeimines that Eaton *et al.*[4] synthesized were also modelled to determine if the model was representative and consistent with their observed data. The amino-imino-azepine metal complexes were modelled to determine specifically if spin density from the metal is transmitted onto the lone pair of the nitrogen atom of the azepine ring.

1.2.3 Theory of Spin Density Transmission

In tetrahedral nickel (II) complexes, π-bonding involves the interaction of half-filled Ni^{2+} d-orbitals and filled ligand p-orbitals of a π-bonded ligand[4g]. Because of the presence of unpaired electrons of the paramagnetic Ni^{2+} ion, the electrons from the ligand and the metal are delocalized throughout the conjugated π-system. Therefore spin density from the metal may be transmitted out into the ligand. This interaction can be measured from the isotropic hyperfine contact interaction shifts observed in the proton nuclear magnetic resonance spectrum (^{1}H NMR) of the ligand[4].

1.2.4 Theory of Spin Density

A single orbital containing a single electron, including its spin factor (or spin-orbital), can be defined in quantum mechanics as[7a]:

$$A\alpha \qquad (1.5)$$

where A is the orbital and α is the spin state (or β for the opposite spin state). Since an orbital is a function of position in space, it can be described by a position vector, r. Similarly the spin state can be defined by its spin, s. Because the spin component can only exist as +½ or -½, the spin component has zero probability of being different from +½

in state α. This means the certainty of finding spin +½ in state α (written as α(s)) vanishes unless s=+½ and similarly, β(s) vanishes unless s=-½.

The Schrödinger wave function for an electron in a single spin-orbital, Aα, can be described as[7a]:

$$\Psi_A(x) = A(r)\alpha(s) \tag{1.6}$$

where x represents both the spatial and spin components. Therefore the probability, P, of finding an electron in spin-orbital Aα is:

$$P = |\Psi_A(x)|^2 dx \tag{1.7}$$

$$\begin{aligned} P &= |A(r)\alpha(s)|^2 drds \\ &= A^*(r)\alpha^*(s)A(r)\alpha(s)drds \end{aligned} \tag{1.8}$$

Equation 1.8 is just the density function, ρ(x), for the probability, P, of finding an electron in element dr with spin between s and s+ds[7a]:

$$\begin{aligned} P(r) &= |\Psi_A(x)|^2 dx \\ &= \rho(x)dx \end{aligned} \tag{1.9}$$

In BRA-KET notation equation 1.9 can be written as:

$$\begin{aligned} P &= \rho(x)dx \\ &= \langle A\alpha | A\alpha \rangle \end{aligned} \tag{1.10}$$

If a three electron system is analyzed, such as the three π-electrons in the allyl radical, there are three spin-orbitals:

$$A\alpha,\ A\beta,\ B\alpha \tag{1.11}$$

Using a one determinant molecular orbital (MO) approximation with two α-electrons and

one β-electron, the Schrödinger wave function can be written for this system as:

$$\Psi = \frac{1}{\sqrt{3}} |A\alpha A\beta B\alpha| \tag{1.12}$$

The one-electron contribution to the energy can be expressed as the sum of the individual one electron matrix elements:

$$<\Psi|\Sigma h(i)|\Psi> = <A\alpha|h|A\alpha> + <A\beta|h|A\beta> + <B\alpha|h|B\alpha> \tag{1.13}$$

Equation **1.13** is essentially the density function in terms of components of α-spin and β-spin electrons. The Σh(i) is the one-electron Hamiltonian for the i'th electron and therefore a typical one-electron matrix element in longer form can be expressed as:

$$<A\alpha|h|A\alpha> = \int A^*(r_1)\alpha^*(s_1)h(1)A(r_1)\alpha(s_1)dr_1ds_1 \tag{1.14}$$

$$= \int_{\substack{s_1'=s_1 \\ r_1'=r_1}} h(1)A(r_1)\alpha(s_1)A^*(r_1')\alpha^*(s_1')dr_1ds_1$$

where r_1' and s_1' are the position vector and spin component, respectively, after operation of the Hamiltonian but before integration. However, the one electron contribution can also be expressed as a function of the density matrix, $\rho_1(x_1;x_1')$, where x_1 represents both the volume element r_1 and spin state s_1:

$$<\Psi|\Sigma h(1)|\Psi> = \int_{x_1'=x_1} h(1)\rho_1(x_1;x_1')dx \tag{1.15}$$

The density matrix can therefore be expressed as a function of α- and β-spin components:

$$\rho_1(x_1;x_1') = [A(r_1)A^*(r_1') + B(r_1)B^*(r_1')]\alpha(s_1)\alpha^*(s_1') + A(r_1)A(r_1')\beta(s_1)\beta(s_1') \tag{16}$$

Equation 1.16 shows that the density matrix is composed of separate α- and β-spin components and from this relation the probability of finding an electron can also be described as a function of separate α- and β-spin components:

$$P_1(r_1) = P_1^{\alpha}(r_1) + P_1^{\beta}(r_1) \qquad (1.17)$$

For the allyl radical, the electron density for the α-electrons is:

$$P^{\alpha} = |A|^2 + |B|^2 \qquad (1.18)$$

and for the β-electrons is:

$$P^{\beta} = |A|^2 \qquad (1.19)$$

The spin density, $Q_s(r_1)$, is defined as[7a]:

$$Q_s(r_1) = \frac{1}{2}(P_1^{\alpha}(r_1) - P_1^{\beta}(r_1)) \qquad (1.20)$$

Thus the spin density of an atom can be determined by subtracting all the β-electron densities from all the α-electron densities associated with that particular atom and dividing the total by two (as shown in Equation 1.20).

1.2.5 Modelling Studies

Initially the simple allyl radical was modelled to simplify the mathematics involved and to assess the computer model's reliability. In an allyl radical, spin density can be predicted to be either positive or negative on different atoms[4f]. The allyl radical is said to have positive π-spin density associated with the terminal carbons (C_1 and C_3) and negative π-spin density associated with the central carbon (C_2)[4f]. The allyl radical was therefore modelled using AMPAC to determine if AM1 could reliably calculate spin densities. The

allyl radical was initially drawn and minimized using the program PCMODEL. This geometry (Figure 1.7) was subsequently imported into the AMPAC program and minimized using the AM1 Hamiltonian in conjunction with an unrestricted Hartree-Fock (UHF) calculation. The UHF calculates the secular determinants of the α- and β-electrons independently in order to compute separate α- and β-eigenvectors so that the electron spin densities on each atom could be calculated. A restricted Hartree-Fock (RHF) calculation calculates the secular determinants such that the eigenfunction is an eigenvalue of the Schrödinger wavefunction while in a UHF calculation this is only an approximation.

The spin density on each atom, Q_s, was calculated by subtracting one half the total number of beta electron eigenvectors (high spin) from one half the total number of alpha electron eigenvectors (low spin) on a particular atom (see equation 1.20)[7a]. The AMPAC program calculated the electron energy levels for both the α- and β-electrons and then the electrons were divided into filled orbitals calculated by AMPAC so that only the filled α- and β-orbitals were used in the spin density calculation.

The spin density calculations on the allyl radical were performed initially to ascertain the reliability of the model. AMPAC calculates one s-orbital and three p-orbitals on each atom (larger than hydrogen) such that the p-orbitals are aligned along the x- y- and z-axes of the coordinate space in AMPAC as shown in Figure 1.8 (designated as AMPAC space here). The spin density on the hydrogen atoms are in an s-type orbital and therefore they were obtained directly from the eigenvectors calculated by the AMPAC program (Figure 1.7). The π-orbitals on the radical were aligned perpendicular to the xy-plane in AMPAC space during the calculation and thus the π-contribution to the spin density was obtained directly from the p_z-orbitals in AMPAC space.

For example in the allyl radical, there are 17 electrons; nine α-electrons and eight β-electrons. Therefore the total α-electron density on H_1 was found to be 0.42030 and the total β-electron density was found to be 0.46590 manifesting a spin density on H_1 as -0.0228. Similarly the spin densities on $H_{1'}$, H_2, H_3 and $H_{3'}$ along with the π-spin densities on C_1, C_2 and C_3 were calculated. The π-spin densities were compared to McConnell's calculations[7b] and the results (Table 1.2) were similar in sign but the magnitudes were different.

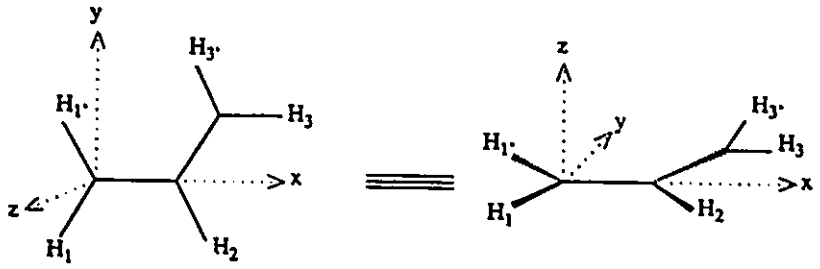

Figure 1.7 *Alignment of the allyl radical for the AMPAC calculation.*

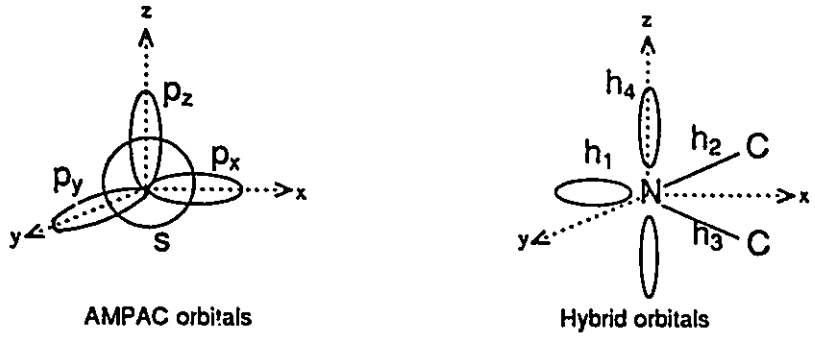

Figure 1.8 *Relationship between AMPAC orbitals and hybrid orbitals.*

The spin densities on the amino-troponeimines were calculated for the hydrogen atoms only since experimental data existed for these atoms[4g,4f]. Since AMPAC computes orbitals expressed according to AMPAC space (Figure 1.8), the orbitals in real space could not be calculated directly and therefore the AMPAC orbitals were converted into

conventional hybrid orbitals in real space (h_1, h_2, h_3 and h_4).

Table 1.2 *Spin density calculations on the allyl radical.*

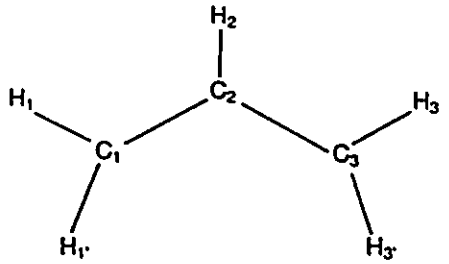

Atom	AMPAC Results			McConnell's Spin Density[68-04] Q_s
	α-electron density P^{α}	β-electron density P^{β}	Spin Density Q_s†	
C_1	0.85087	0.14758	0.3516	0.5694
C_2	0.28303	0.70483	-0.2033	-0.1055
C_3	0.85314	0.14760	0.3528	0.5694
H_1	0.42030	0.46590	-0.0228	
$H_{1'}$	0.42140	0.46590	0.0223	
H_2	0.45423	0.42577	0.0142	
H_3	0.42029	0.46586	-0.0228	
$H_{3'}$	0.42140	0.46590	-0.0222	

† where $Q_s = \frac{1}{2}[P^{\alpha} - P^{\beta}]$.

Given the s, p_x, p_y and p_z orbitals in AMPAC, a basis function, h, on each atom can be defined as:

$$h = OX \qquad (1.22)$$

where X is the atomic basis orbitals in real space and O is the 4x4 matrix relating the two basis sets. For each compound modelled, the final minimized geometry was aligned in the xy-plane as shown in Figure 1.8.

The AMPAC orbitals (s,p_x and p_y) are linear combinations of the hybrid bonding

orbitals (h_1, h_2 and h_3) in real space as shown in Figure 1.8. The p_z orbital in AMPAC space is the same as the hybrid π-orbital h_4 in real space since the π-system of the molecule was aligned in the xy-plane. The relationship of the AMPAC orbitals with the hybrid orbitals can be expressed as a matrix, O:

$$h_1 = \frac{1}{\sqrt{3}}(S + \sqrt{2}P_1) \quad (1.23)$$

$$h_2 = \frac{1}{\sqrt{3}}(S + \sqrt{2}P_2) \quad (1.20)$$

$$h_3 = \frac{1}{\sqrt{3}}(S + \sqrt{2}P_3) \quad (1.25)$$

$$h_4 = P_4 \quad (1.26)$$

where the linear combination of molecular orbitals in AMPAC space that relate to real space are:

$$P_1 = (1,0,0) \quad (1.27)$$

$$P_2 = (-\cos(60°), \cos(30°), 0) \quad (1.28)$$

$$P_3 = (-\cos(60°), -\cos(30°), 0) \quad (1.29)$$

$$P_4 = (0,0,1) \quad (1.30)$$

From this, the matrix can be expressed as:

$$\begin{pmatrix} h_1 \\ h_2 \\ h_3 \\ h_4 \end{pmatrix} = \begin{pmatrix} \frac{1}{\sqrt{3}} & \frac{\sqrt{2}}{\sqrt{3}} & 0 & 0 \\ \frac{1}{\sqrt{3}} & \frac{-1}{\sqrt{6}} & \frac{1}{\sqrt{2}} & 0 \\ \frac{1}{\sqrt{3}} & \frac{-1}{\sqrt{6}} & \frac{-1}{\sqrt{2}} & 0 \\ 0 & 0 & 0 & 1 \end{pmatrix} \begin{pmatrix} S \\ P_x \\ P_y \\ P_z \end{pmatrix} \quad (1.31)$$

From this matrix each hybrid orbital can be expressed in terms of the sp^3 orbitals in AMPAC space:

$$h_1 = \frac{1}{\sqrt{3}}S + \frac{\sqrt{2}}{\sqrt{3}}P_x \quad (1.32)$$

$$h_2 = \frac{1}{\sqrt{3}}S - \frac{1}{\sqrt{6}}P_x + \frac{1}{\sqrt{2}}P_y \quad (1.33)$$

$$h_3 = \frac{1}{\sqrt{3}}S - \frac{1}{\sqrt{6}}P_x - \frac{1}{\sqrt{2}}P_y \quad (1.34)$$

$$h_4 = P_z \quad (1.35)$$

Equation **1.34** yields an expression for the spin density on the lone pair of the ring nitrogen atom (the h_3 hybridized orbital). The spin densities on the ring hydrogens, calculated using AMPAC and those calculated by Eaton[4e,f], for the amino-troponeimines are shown in Table 1.3. AMPAC did not have parameters for nickel and consequently a tin atom was used in the calculations.

The modelled amino-troponeimines are less than half the magnitude of the values found by Eaton possibly because of the use of tin instead of nickel and/or because AMPAC does not include d-orbitals in its calculations. Without including the d-orbital overlap with the π-system of the ring, AMPAC presumably calculates less spin density transmitted out into the ring. The sign of the spin densities calculated are of the opposite sign possibly because of a convention difference used by Eaton's method of spin density calculation[4e,f]. Although the magnitude of the calculated spin densities were not as large as those calculated by Eaton, they could still be used as a model of possible spin density donation from a metal ion out into the ligand.

Table 1.3 *AMPAC Spin Density Calculations on Amino-troponeimines and Amino-imino-azepines Complexed to Tin.*

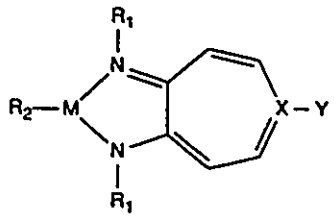

X = C
Y = H

Amino-troponeimine complex

X = N
Y = :

Amino-imino-azepine complex

Compound	R_1	R_2	M	X	Y	Spin Densities		
						Y	H_2	H_3
A	Et	L†	Ni	C	H	0.0429‡	-0.0220‡	0.0589‡
B	Me	L†	Ni	C	H	0.0386‡	-0.0210‡	0.0539‡
C	Me	2H	Sn	C	H	-0.0147	0.0113	-0.0113
D	Me	:	Sn	C	H	-0.0181	0.0133	-0.0183
E	Me	2H	Sn	N	:	-0.0082	0.0109	-0.0136
F	Me	:	Sn	N	:	-0.0148		

† L = symmetric bidentate ligand.
‡ spin densities measured by Eaton *et al.*[44]

The amino-troponeimine calculation which used no substituents on the tin metal generated the most reliable results, therefore the analogous azepine-tin complex was modelled to determine the amount of spin density transmitted out to the nitrogen atom of the azepine ring. The AMPAC calculations for the amino-imino-azepines chelated to tin showed that spin density migrated out into the ring system and onto both the lone pair of the ring nitrogen and the ring hydrogens.

The results in Table 1.3 showed that the spin density was transmitted out to the nitrogen atom but this alone was not enough to ensure that the amino-imino-azepines complexed to a paramagnetic metal would be a useful imaging agent since the system must transmit spin density out to the water molecules. Therefore a water molecule

hydrogen bonded to the amino-imino-azepine complexed to a tin molecule (structure F in Table 1.3) was modelled and the results are shown in Table 1.4. The spin density was calculated to be transmitted from the azepine complex out into the water molecule via the ring nitrogen hydrogen bond as indicated in the Table. The amount of spin density donated was dependent on the proximity of the water molecule to the ring nitrogen as expected. These calculations provided credible evidence for spin density donation from a paramagnetic metal ion out into the π-system of an amino-imino-azepine ring system and ultimately through the ring nitrogen onto hydrogen bonded water molecules indicating that these systems should consequently be useful as MRI contrast agents.

***Table 1.4** Water Molecule Hydrogen-bonded to the Ring Nitrogen on the Azepine-Tin Complex.*

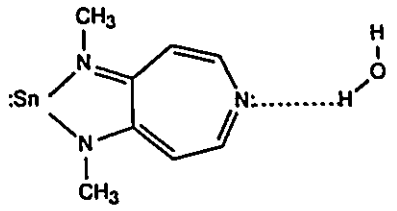

Hydrogen Bond Length H-N (Å)	Spin Density on Hydrogen
1.80	0.000365
1.75	0.000427
1.70	0.000493

1.3 Conclusion

The results of the modelling studies illustrated theoretically that the desired amino-imino-azepines would be useful as paramagnetic ion chelants for magnetic resonance imaging. The spin density calculations predict the spin density from the metal ion would be projected through the π-system of the amino-imino-azepine to the nitrogen atom on the ring. Subsequently, water molecules hydrogen bonded to the nitrogen atom were calculated to experience spin density from the chelant. The objective of the thesis was to develop synthetic routes towards amino-imino-azepines and therefore a review of azepine

chemistry was undertaken to determine the method of choice for synthesis of these systems. After the method was chosen, the reaction system was explored in detail from a synthetic point of view.

Chapter 2

Azepine Synthesis

2.1 Introduction

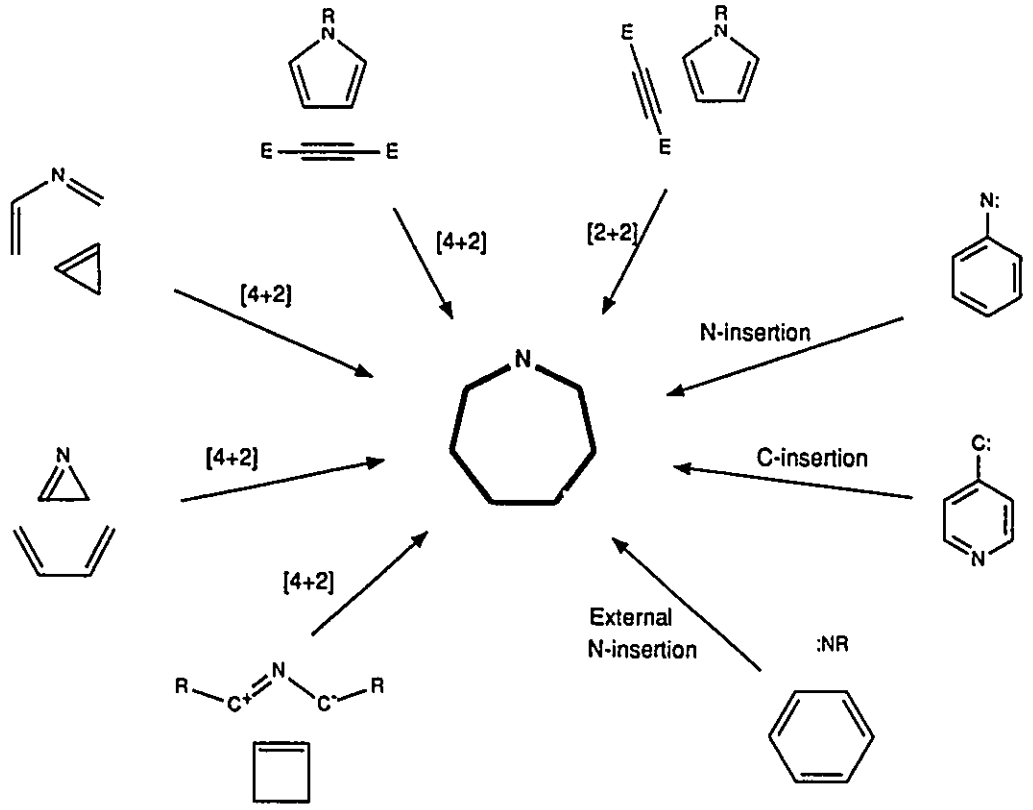

Figure 2.1 Azepine precursors

Azepines are seven-membered heterocycles and have been synthesized through numerous methodologies[6-18]. Research into seven-membered heterocycles emerged in the 1960's, after five- and six-membered heterocycle syntheses had been developed[8c] which

provided the various techniques currently available for the development of seven-membered heterocyclic systems. The reactions can be categorized into two main types: cycloadditions in conjunction with rearrangements[8,15] and direct ring expansion of six membered rings through insertion reactions[9-14,16-18].

The objective of this thesis was to synthesize amino-imino-azepines which are unsaturated seven membered heterocycles containing one nitrogen atom. The amino-imino-azepines are homologs of tropolone systems and it was vital to consider the unsaturation of the ring in the selection of the synthetic route taken. A myriad of azepine synthetic routes have been reported over the past 40 years[8-18]. The principal strategies of synthesizing such unsaturated azepines, together with examples, are presented in the subsequent sections.

2.2 Cycloadditions

A significant amount of effort has been spent on the synthesis of seven-membered heterocycles using pericyclic reactions, much of which has been devoted to azepine synthesis[8c]. Some of the more common routes are through Diels-Alder [4+2][15a-f] and [2+2][15g-k] cycloadditions and through 1,3-dipolar cycloadditions[8c,15l]. These systems have been used with a variety of starting components including the (4+3), (5+2) and (6+1) combinations, where the two numerals express the number of atoms in each system that add to make the seven membered ring heterocycle. Typically the initial cyclization does not produce an azepine directly but relies on a rearrangement of an intermediate formed spontaneously or through a secondary reaction to an azepine framework.

2.2.1 [2+2] Cycloadditions

The formal photochemical [2+2] cycloaddition is a convenient route to (n+2) ring expanded heterocycles[15g-k,8c]. These processes involve the addition of an activated alkyne across an unsaturated double bond in an (n)-heterocycle (shown in Figures 2.2 and 2.3). The resultant cyclobutene intermediate is then ring opened, spontaneously or through acid/base catalysis, to the larger (n+2)-heterocycle.

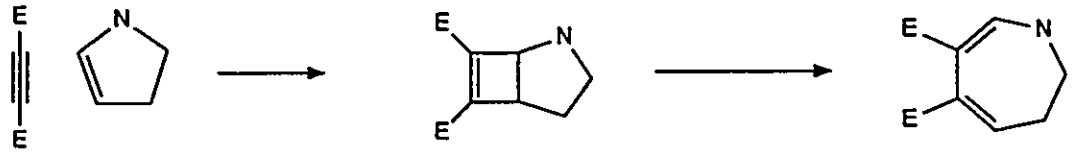

Figure 2.2 General [2+2] Cycloadditions Leading to Azepines.

For example, photolysis of dioxopyrrolines with an appropriate acetylene yields an aza-bicyclo[3.2.0]heptenedione which opens at C_1-C_5 by electrocyclic ring opening or through acid/base catalysis[15j] to the isolated azepine (shown below in Figure 2.3). This particular reaction is significant because a completely unsaturated azepine was furnished in good yield.

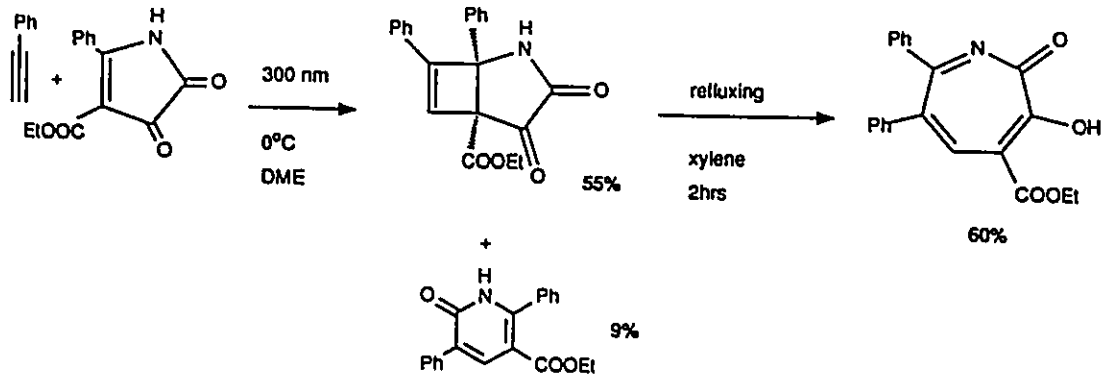

Figure 2.3 Photolysis of Dioxopyrrolines in the Presence of Acetylene to Yield Azepines.

2.2.2 [4+2] Cycloadditions

In a similar fashion to the [2+2] cycloaddition reactions discussed above, thermal [4+2] Diels-Alder cycloadditions have been used in both (2+5) and (3+4) combinations to achieve the desired azepines (shown below in Figure 2.4). The (2+5) combination involved a [4+2] cycloaddition of a pyrrole and an activated acetylene to form an aza-norbornadiene, which upon irradiation rearranged to a quadricyclane derivative which subsequently rearranged thermally to the 1H-dihydroazepine[15c]. The (3+4) combination was facilitated through a [4+2] cycloaddition of azirines with cyclopentadienones which subsequently extruded carbon monoxide to yield azepines in relatively good yield[15a,b]. Alternatively, the (3+4) combination was used through a [4+2] cycloaddition of cyclopropenes and 1,2,4-triazines with the expulsion of nitrogen to yield 4H-dihydroazepines[15c,d].

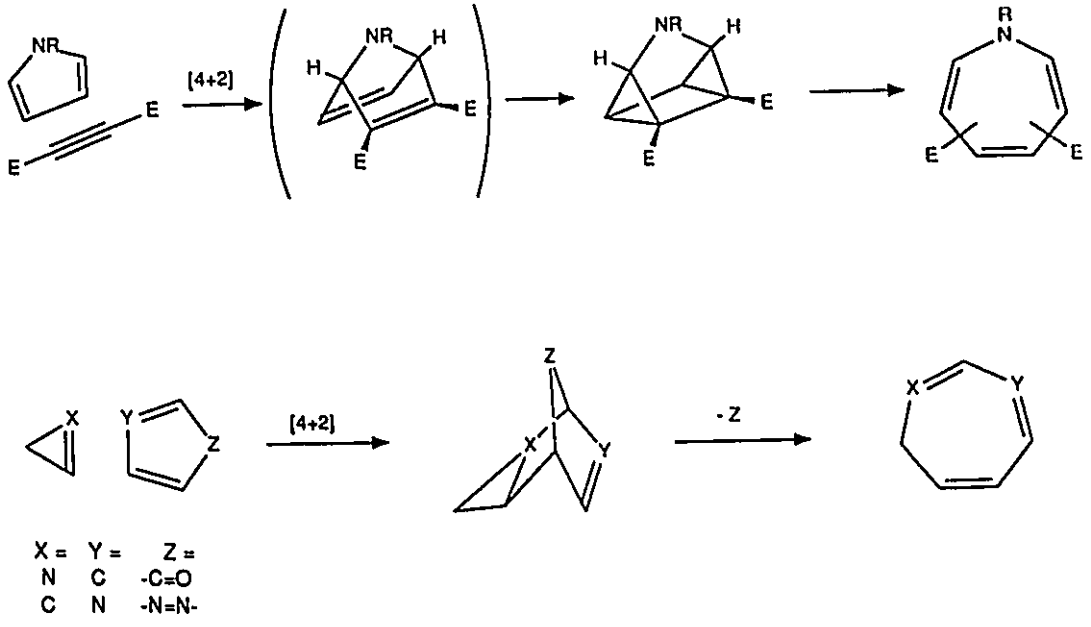

Figure 2.4 General [4+2] Cycloadditions Leading to Azepines.

An example of the (2+5) combination was the reaction of acetylene with tosyl-pyrrole which produced the protected aza-norbornadiene in low yield and, upon irradiation, furnished the 1H-dihydroazepine in a low overall yield of 12%[15c].

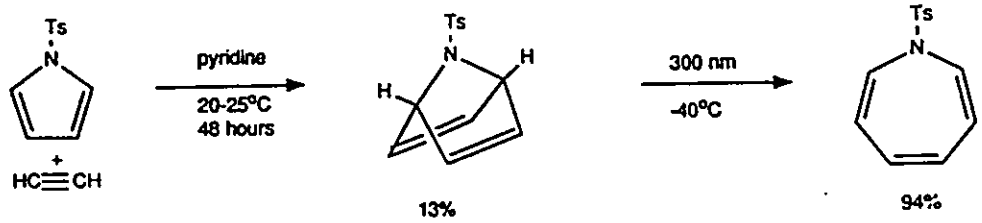

Figure 2.5 Reaction of Acetylenes with Pyrroles to Yield Azepines.

The (3+4) combination case involved the [4+2] cyclization reaction of an unsaturated three membered ring to a diene in the initial step. This was accomplished in two ways. One technique is illustrated below, which involves the reaction of 2-phenyl azirine with 2,5-dimethyl-3,4-diphenyl-cyclopentadienone in refluxing toluene. This sequence produced good yields of the 3H-dihydroazepine[15a,b].

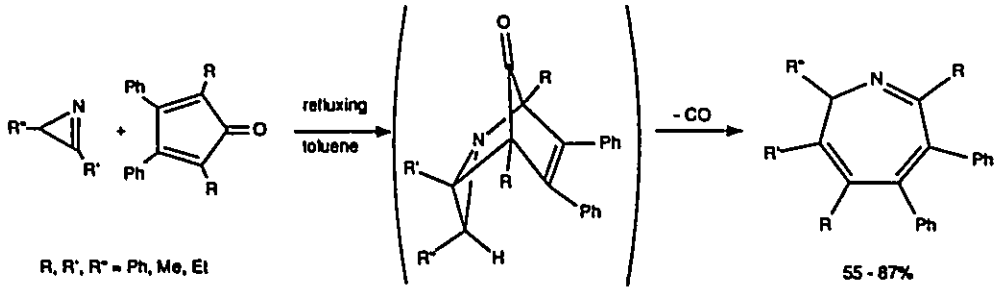

Figure 2.6 Reaction of Azirines with Cyclopentadienones to Yield Azepines.

The alternative strategy, shown in Figure 2.7, involved the reaction of cyclopropene with 1,2,4-triazines yielding 4H-dihydroazepines in relatively good yields[15d].

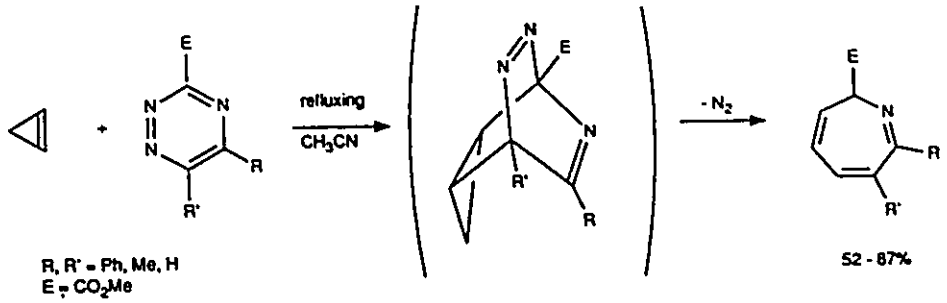

Figure 2.7 Reaction of Cyclopropenes with Triazines to Yield Azepines.

2.2.3 1,3-Dipolar Cycloadditions

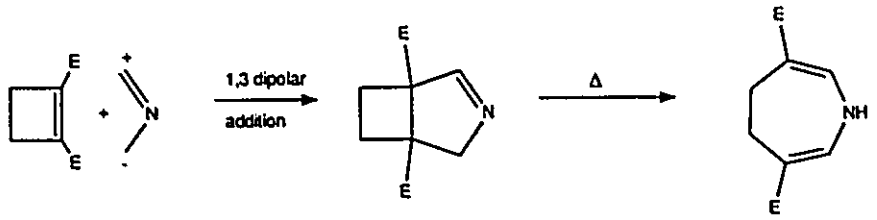

Figure 2.8 General 1,3-Dipolar Cycloadditions Leading to Azepines.

The 1,3-dipolar cycloaddition reactions that resulted in azepine formation involved the addition of ylides across a cyclobutene moiety to form a bicyclic intermediate that ring expanded to a dihydroazepine[8c,15l] (shown in Figures 2.8 and 2.9). An illustration of this technique is shown below where the cycloaddition of 1,2-dicyano-cyclobutene with N-benzyl-chlorobenzonitrile yielded 3,6-dicyano-2,7-diphenyl-1,4,5H-dihydroazepine in a reasonable yield[15l].

These latter cycloaddition reactions are interesting examples but they lend themselves toward specific starting materials that can themselves require elaborate synthesis. In addition, no nitrogen-substituted azepines have been reported in all the

above cycloaddition reactions indicating that cycloaddition reactions may not be a facile avenue towards the synthesis of amino-imino-azepines.

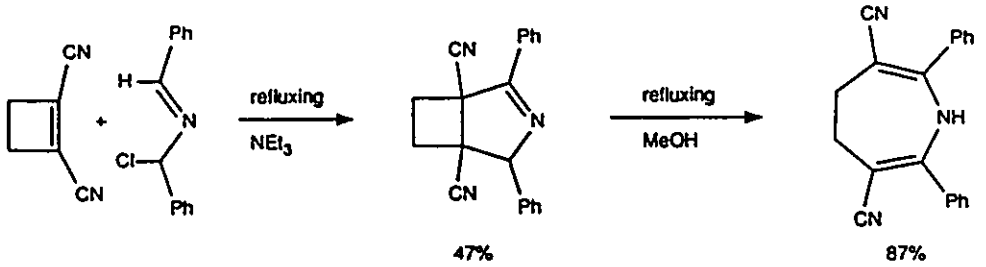

Figure 2.9 1,3-Dipolar Cycloaddition of Ylides and Cyclobutenes to Produce Azepines.

2.3 Ring Expansions Via Insertions

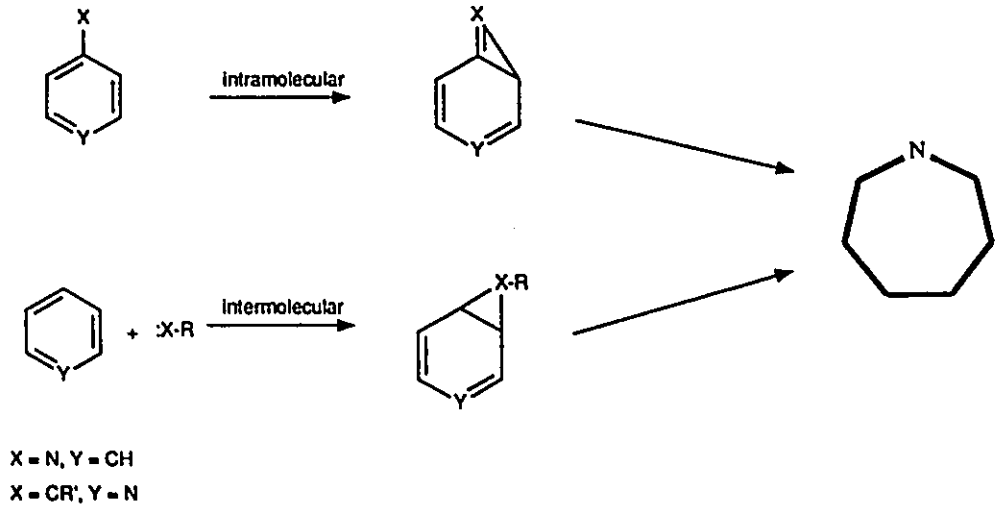

Figure 2.10 General Insertion Reactions Leading to Azepines.

There has been a great deal of work in azepine chemistry utilizing the ring expansion of aryl systems through nitrene insertions on aryl systems and carbenoid insertions on pyridinium species. 3H-Dihydroazepines have been prepared from arylnitrenes derived by physical[9,11] and chemical means[10,13,14] while 1H-dihydroazepines

have been made from reaction of aryl systems with external nitrene[12]. Carbenoid insertions are typically formed chemically by elimination reactions at the carbene precursor atom connected to the aryl system[17,18].

2.3.1 "Carbene" Additions

Photolysis of pyridinium ylides is known to yield azepines[18] and analogously pyridinium salts can ring expand chemically in the presence of strong bases to produce azepines as well[18a]. For example, reaction of 1-benzyl-2,4,6-triphenylpyridinium tetrafluoroborate with sodium hydride in refluxing toluene yielded the 2,4,6,7-tetraphenyl-3H-dihydroazepine in moderate yield[18a] shown in Figure 2.11 below.

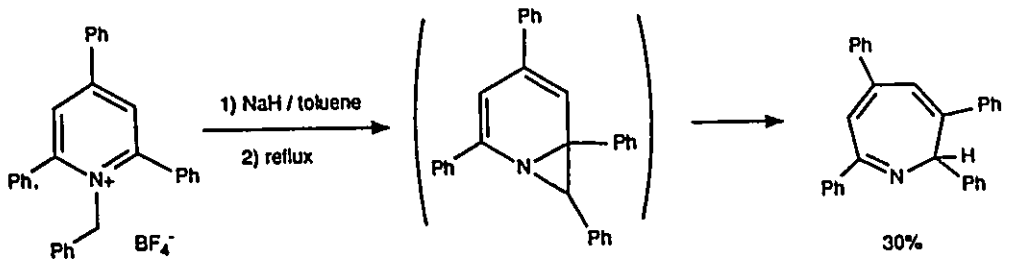

Figure 2.11 *Photolysis of Pyridinium Ylides to Yield Azepines.*

Ring expansions of dihydropyridines through carbene-like insertions are another synthetic route to azepines. Treatment of 4-chloromethyl-1,4-dihydropyridines with strong base affords ring expanded dihydroazepines[17] and, as shown in Figure 2.12, treatment of 4-chloromethyl-1,4-dihydro-2,6-dimethylpyridine-3,5-dicarboxylate with potassium cyanide yielded the 4-cyano-2,7-dimethyl-1H-trihydroazepine-3,6-dicarboxylate in reasonable quantities[17b].

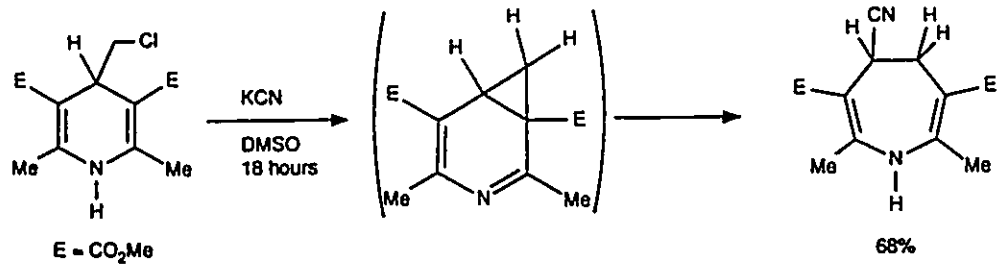

Figure 2.12 Azepines from 4-Chloromethyl-1,4-dihydropyridines.

2.3.2 "Nitrene" Addition

There is a broad range of azepine syntheses that can be grouped into nitrene-like insertions to produce azepines with the simplest nitrenes being formed by the expulsion of nitrogen from aryl azides through their photolysis[9] or thermolysis[11]. The most common chemical method of formation of nitrenes derive from the deoxygenation of nitro- and nitroso-aryl compounds with tervalent phosphorous agents[10]. Some of the more exotic chemical methods of formation are derived from the decomposition of phenyloxaziridines[14a,14b], the thermal α-deoxysilylation of N,O-bis(trimethylsilyl)-N-phenylhydroxylamines[14c], and the reaction of alkyl-substituted quinones with hydrazoic acid (HN_3)[16a]. Two external, or intermolecular, nitrene systems have also been developed, one using a formyl nitrene insertion[12] and the other through addition of chloramines onto phenoxides followed by ring expansion[13].

Arylazides are the most commonly used precursors to azepines because of their relatively ease of synthesis and their reliable generation of azepines. The photolyses of aryl azides have been studied extensively since the early 1960's[9,19] with a typical experiment involving the irradiation of an azide (shown in Figure 2.13) in a nucleophilic solvent, such as an amine or an alcohol, to yield the 3H-dihydroazepines. A co-solvent

is often used if the nucleophile absorbs in the same ultraviolet (UV) region as the azide to maximize the efficiency of the reaction. The reaction is said to proceed initially from an arylnitrene that ring closes to a didehydroazepine intermediate although there is still considerable debate over the actual intermediates involved between the azide and didehydroazepine[9]. The didehydroazepine is then trapped by nucleophiles to form an unstable 1H-dihydroazepine which rearranges to a 3H-dihydroazepine.

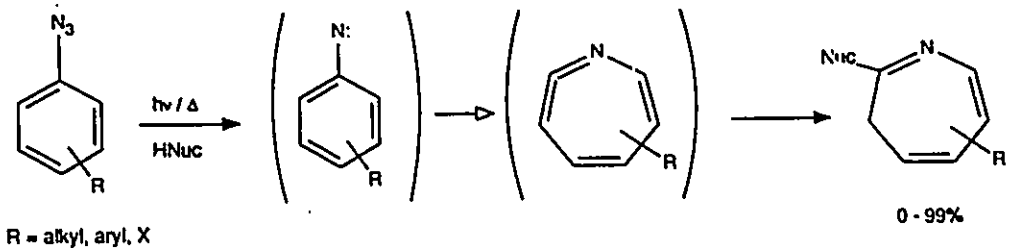

Figure 2.13 *Azepines from the Photolysis or Thermolysis of Arylazides.*

The thermolysis of arylazides parallels the photolysis reaction and has also been used in similar experiments to afford 3H-dihydroazepine[11]. The mechanism is believed to proceed in an analogous manner through a nitrene and didehydroazepine intermediate as in the photolysis of arylazides. This is evidenced by the similarity of products derived from both these reactions[9,11] as shown in Figure 2.13.

The deoxygenation of aryl nitro- and nitroso-compounds with tervalent phosphorous agents is the most common method of generating a nitrene chemically and to form 3H-dihydroazepines[10] in reasonable yields. Typically, treatment of substituted nitrobenzenes with diethyl-methylphosphonite (Figure 2.14) in amine solvents, produced the 3H-dihydroazepine in various yields[10a]. The mechanism has been described as proceeding through a nitrene intermediate as evidenced by the similarity in product distributions from analogous arylazide decompositions[10].

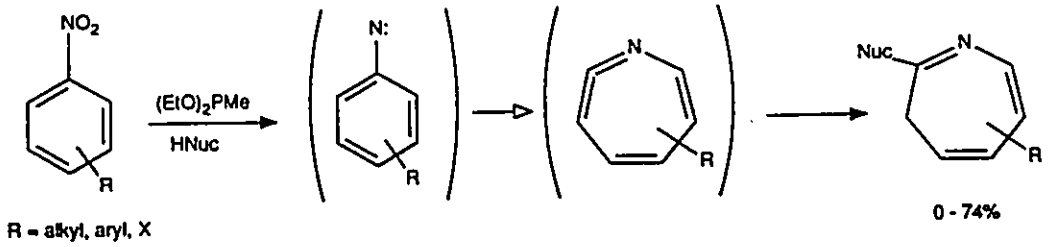

Figure 2.14 *Azepines Via the Deoxygenation of Nitro Aryl Compounds with Tervalent Phosphorous Agents.*

Some more unique methods of arylnitrene formation have been explored although these practices lend themselves to more novel chemistry than to synthetic utility. The thermal elimination of hexamethyldisiloxane from *N,O*-disilylated *N*-phenyl-hydroxylamine produced a high yield of 3H-dihydroazepine[14c] in the presence of amine nucleophiles but unfortunately substituted *N*-phenylhydroxylamines syntheses tend to be quite lengthy and difficult. Another innovative approach was to irradiate 2-phenyloxaziridines[14b] to create arylnitrenes which produce 3H-dihydroazepines, although the practical application of this reaction is very limited because of the difficulty in synthesizing the starting compounds.

The reaction of hydrazoic acid with quinones to yield azepinones is an appealing reaction since the resultant azepine ring system is almost completely unsaturated[16]. The reaction is a modified Schmidt reaction using a quinone instead of a carbonyl compound. For example, reaction of 2,3,5-trimethylquinone with sodium azide in concentrated H_2SO_4 yielded the azepinone in good yield (Figure 2.15). The reaction took place primarily under steric control at the least hindered and more basic carbonyl of the quinone[16b]. The reaction conditions were quite harsh, utilizing concentrated sulphuric acid, and because of this the reaction has been limited to alkyl substituted quinones.

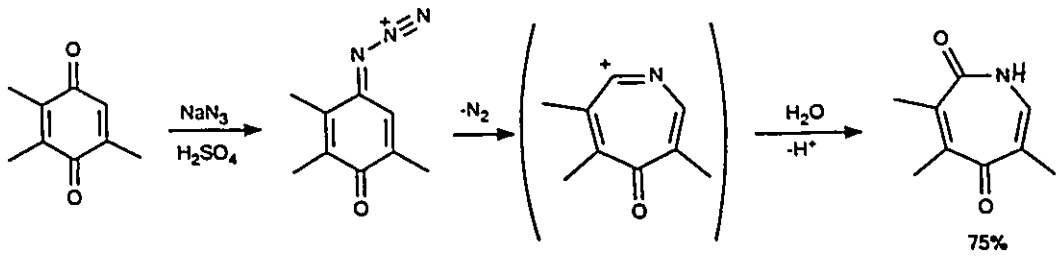

Figure 2.15 Azepines Via Quinones Reacted with Hydrazoic Acid.

External nitrene insertion reactions are concerned with the intermolecular reaction of alkyl azides thermochemically with simple aryl systems and produce 1H-azepines in good yields[12a-f]. For example, photolysis of ethyl azidoformate in benzene afforded *N*-ethoxycarbonylazepine in good yield[12a] (Figure 2.16). The insertion reaction is useful in that the nitrogen can be deprotected in subsequent steps to yield the unstable 1H-dihydroazepine[12b]. Unfortunately substituted *N*-ethoxycarbonylazepines are limited because the selectivity of insertion on substituted aryl systems is unknown and thermal dimerizations and photorearrangements are prevalent[12g-i].

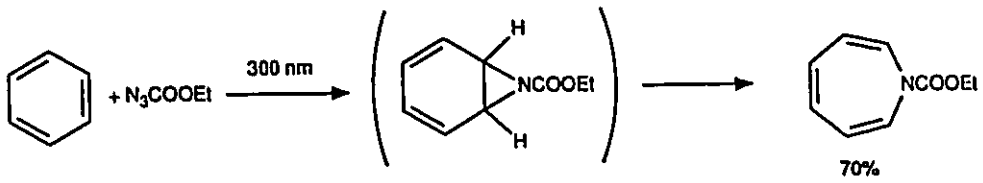

Figure 2.16 External Nitrene Reactions to Yield Azepines.

A better "external nitrene" system is the reaction of 2,6-dialkyl-phenoxides with chloramines to yield 1,3-dihydro-2H-azepin-2-ones in low yields[13]. Reaction of 2,6-dimethylphenol with sodium metal was subsequently heated to 140°C (Figure 2.17). A cold ether solution of chloramine at -70°C was added slowly to yield 1,3-dihydro-3,7-dimethyl-2H-azepin-2-one in reasonable yield[13a].

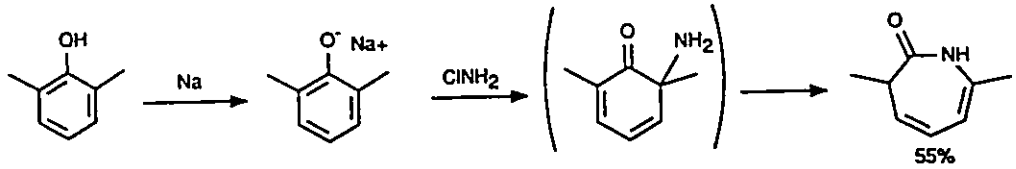

Figure 2.17 Reaction of 2,6-Dialkylphenols with Chloramines to Yield Azepines.

The severity of the reaction conditions and the requirement of the 2,6-dialkyl substituents severely limits the scope of this reaction for substituted azepine synthesis.

2.4 Conclusion

Although considerable research has been devoted to the construction of various synthetic methodologies, the literature reveals a scarcity of work dealing with the synthesis of amino or imino-azepines. In experiments involving the photolysis of arylazides it has been reported that N,N-dimethyl-azido-aniline did not ring expand to yield azepines and that poor yields were also obtained in the photolysis of azido-nitro-benzenes[9a].

The work presented in this thesis explored the synthetic routes in azepine chemistry through the use of the arylnitrene reaction to expand the scope of azepine chemistry into the area of nitrogen substituted systems. Due to the complexity and diversity of credible pathways leading to azepines, only the area of arylnitrene chemistry was explored as a synthetic route towards the synthesis of the amino-imino-azepines. Azepines via nitrene reactions are the most studied and most promising route towards nitrogen substituted azepines with the precursor aryl nitro compounds and arylazides being readily available through reasonable synthetic sequences. The deoxygenation of aryl nitro compounds[10] was the initially proposed reaction explored for the synthesis of the desired azepines. In the event that the deoxygenation reaction of the aryl nitro compounds

failed, the aryl nitro compounds could be easily converted into the corresponding aryl azides which could be subsequently thermolyzed[11] or photolyzed[9] in the presence of nucleophiles to yield 3H-dihydroazepines.

Chapter 3

Azepines Via Phenylnitrenes

3.1 Introduction

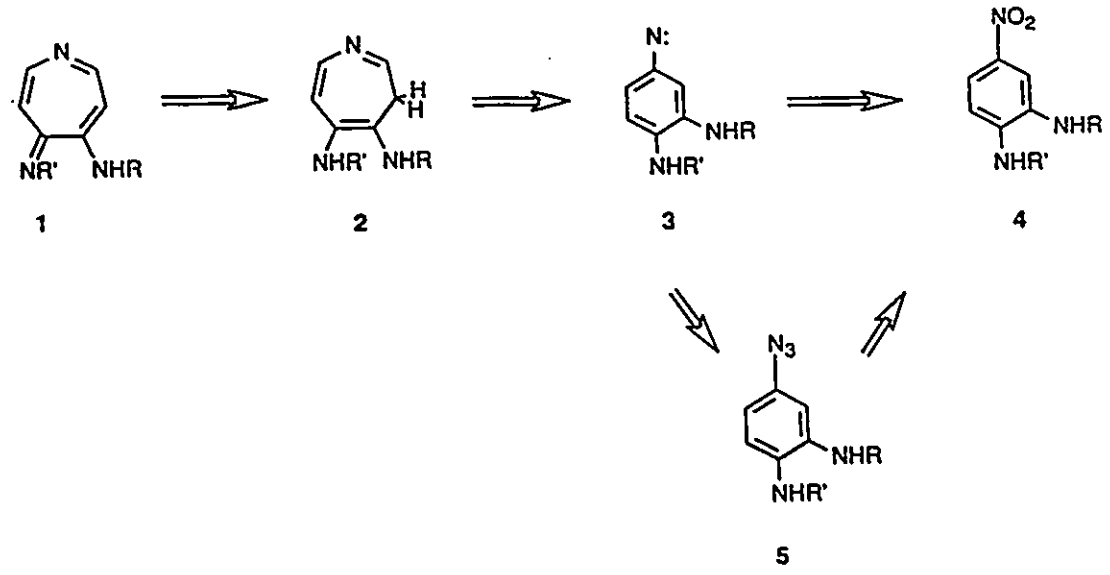

Figure 3.1 *Retro-synthesis of 4-amino-5-imino-azepine.*

The synthesis of 4-amino-5-imino-azepines was attempted through the arylnitrene ring expansion reaction[9-11,19], shown in Figure 3.1 in a retro-synthetic analysis. Deoxygenation of aryl nitro compounds has been reported to proceed through an arylnitrene intermediate[10] to produce ring expanded 3H-dihydroazepines and therefore this system was investigated first. The thermolysis[11] or photolysis[9] of arylazides has also been shown to proceed through an arylnitrene intermediate and these azides could be synthesized from the corresponding aryl nitro compounds in the event that the

deoxygenation of the nitro compounds was unsuccessful. The 3H-dihydroazepines would require two amine substituents at the 4,5-positions (**2**), which after oxidation should yield the 4-amino-5-imino-azepines (**1**). The 3,4-diamino-phenylnitrenes (**3**) could be derived directly from the deoxygenation of the corresponding 3,4-diamino-nitrobenzene (**4**) or from the 3,4-diamino-phenylazide (**5**).

3.2 Deoxygenation of Aryl Nitro Compounds.

The deoxygenation of aryl nitro compounds[10] to yield azepines has historically been associated with the thermal[11] or photochemical[9] reaction of arylazides because of the similarity in the derived products. The deoxygenation reaction was initially attempted over the thermolysis or photolysis of arylazides because the aryl nitro compounds could be synthesized in fewer steps than the corresponding arylazides.

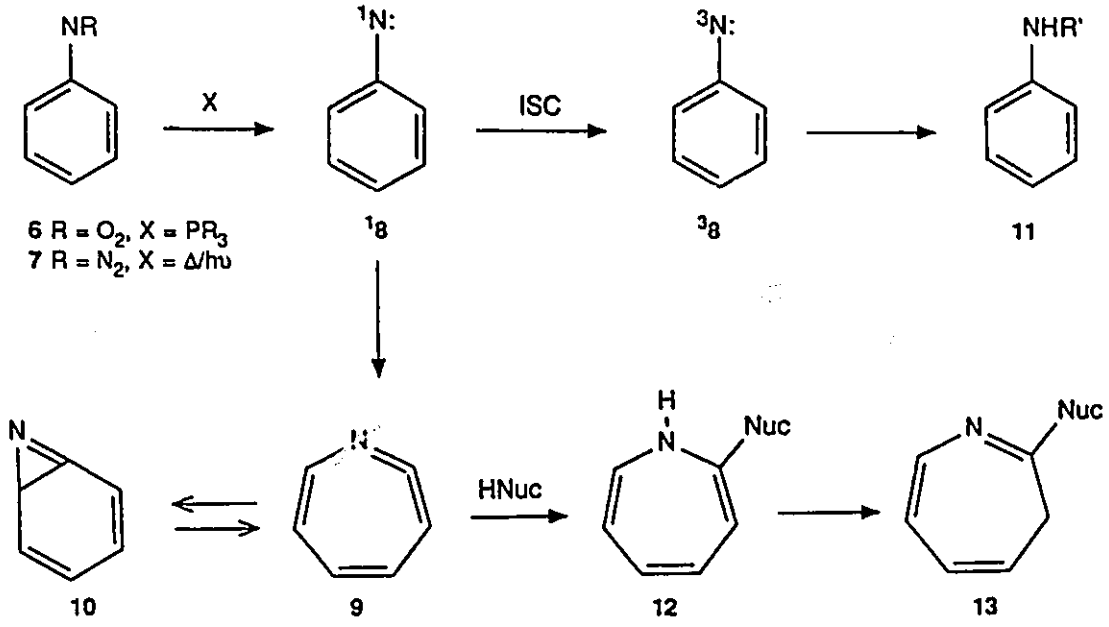

***Figure 3.2** Mechanism of Ring Expansion of Phenylnitrene.*

The arylnitrene ring expansion reaction mechanism to yield 3H-dihydroazepines is outlined in Figure 3.2 for the phenylnitrene system. The nitrene is formed initially in its singlet state (^{1}**8**) which is known to ring expand to yield a didehydroazepine intermediate (**9**) which may or may not be in equilibrium with the azirine intermediate (**10**)[9]. The singlet phenylnitrene intersystem crosses to its triplet state (^{3}**8**) in competition with ring expansion to yield anilines (**11**) through hydrogen abstraction from solvent molecules. The didehydroazepine can be trapped in the presence of nucleophiles, such as amines or alcohols, to yield the unstable 1H-dihydroazepine (**12**) which rearranges to the 3H-dihydroazepine (**13**). In the absence of nucleophiles the nitrenes can also couple to yield azo compounds[9a] and the didehydroazepines can polymerize[9b] (not shown in Figure 3.2).

3.2.1 Synthesis of Aryl Nitro Compounds.

The first attempted synthesis of 3H-dihydroazepines involved the deoxygenation of aryl nitro compounds with tervalent phosphorus reagents[10a,b]. There have been only a few select reports of deoxygenation of substituted nitrobenzenes[10c-e] and the substituents were always electron withdrawing groups. To create an azepine with two amine substituents from a phenylnitrene precursor the amine substituents must be modified to make them more electron withdrawing since amino-phenylnitrenes such as p-N,N-dimethylamino-phenylnitrene does not yield azepines[9a,c]. The amines were converted into amides, which are considerably more electron withdrawing[20], to alter their substituent effect on the phenylnitrene reaction. After the azepines had been synthesized the amines would be deprotected to form the amino-imino-azepines.

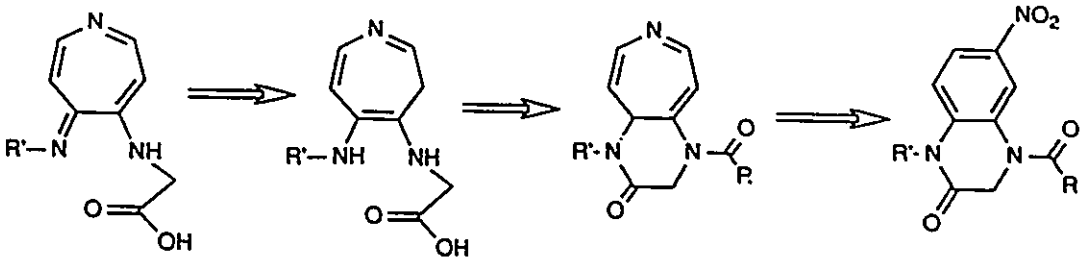

Figure 3.3 *Retro-synthesis of Amino-imino-azepines from 4-Nitro-1,2-dihydroquinoxalinones.*

The 6-nitro-1,2-dihydroquinoxalinone (**17**) system was used to protect the diamino functionality since the bicyclic ring system was easily synthesized and allowed a separate amide to protect the amine in the 4-position (shown in Figure 3.3). The 6-nitro-4-amido-1,2-dihydroquinoxalinone (**17**) was anticipated to yield bicyclic 3H-dihydroazepines (**16**) that, after deprotection (**15**) and oxidation, would yield the desired amino-imino-azepines **14** with a carboxylic acid side chain that would aid in the chelation of a paramagnetic metal ion in the final MRI contrast agent (Chapter 1). Thus the quinoxalinone would act as both a protecting group and an aid for the chelation step.

The 6-nitro-1,2-dihydroquinoxalinones were synthesized from the starting 4-nitro-1,2-phenylenediamine (**18**) as illustrated in Figure 3.4. The diamine **18** was treated with an equivalent of ethylbromoacetate in dimethylformamide (DMF) to yield the 6-nitro-1,2-dihydroquinoxalinone (**19**) in good yield. Compound **19** was treated with an anhydride to protect the remaining 4-amino substituent as the acetamide (**20**) or as the formamide (**21**). Deprotection of the amine protected as the formamide can be facilitated by acid or base hydrolysis[21] while deprotection of the amine protected as the acetamide can be facilitated

by base hydrolysis only[21]. The two protecting groups were explored to determine which was an easier group to use in the overall synthesis. The formamide **21** was treated with sodium hydride and more ethylbromoacetate to yield the 1-(acetic acid ethyl ester)-4-formyl-6-nitro-1,2-dihydroquinoxalinone (**22**) which would eventually contain two carboxylic acid side chains for chelation to a metal on the final ring expanded amino-imino-azepine.

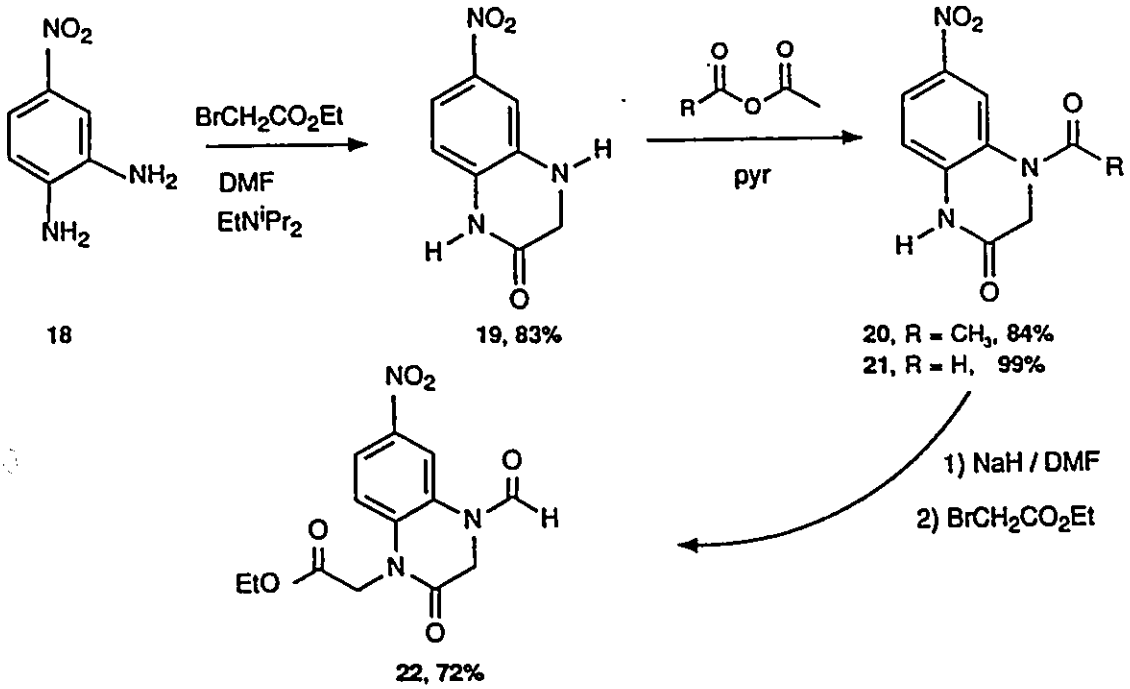

***Figure 3.4** Synthesis of 6-Nitro-4-acetamido-1,2-dihydroquinoxalinones.*

3.2.2 Deoxygenation of Aryl Nitro Compounds with Triethylphosphite.

The deoxygenation reaction was originally explored on nitrobenzene (**6**), using triethylphosphite in refluxing di-*n*-propylamine, as a model system (shown in Figure 3.5), which produced a low yield of 2-di-*n*-propylamino-3*H*-dihydroazepine (**23**). The aryl nitro compounds **20**, **21** and **22** were subsequently deoxygenated under similar conditions (Figure 3.6) but no azepines were evident in the final products. Attempts using different

amine nucleophiles (diethylamine and di-*n*-butylamine) likewise did not yield any azepines. The products were intractable tars that could not be identified by ^{1}H NMR or mass spectrometry even after chromatography using silica gel.

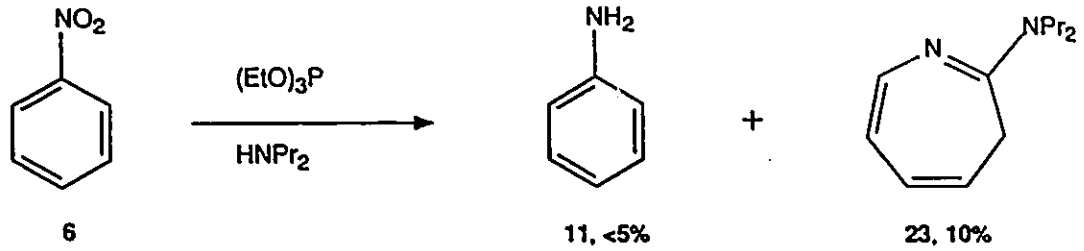

Figure 3.5 Deoxygenation of Nitrobenzene.

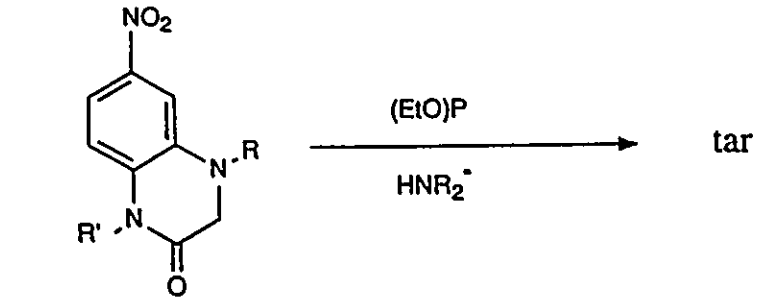

	R	R'
20	$COCH_3$	H
21	CHO	H
22	CHO	CH_2CO_2Et

***Figure 3.6** Attempted Deoxygenation of 6-Nitro-1,2-dihydroquinoxalinones.*

The deoxygenation experiment may have failed because of the presence of the amides on the quinoxalinones which may have reacted with the triethylphosphite. The phosphites have a high affinity for oxygen atoms[10b] and therefore the phosphorous reagents may have attacked the carbonyl groups of the amides. To overcome this problem the nitro groups were converted into their respective azides and the thermolysis[11] and

photolysis[3] of these azides was investigated.

3.3 Thermolysis of 6-Azido-1,2-dihydroquinoxalinones.

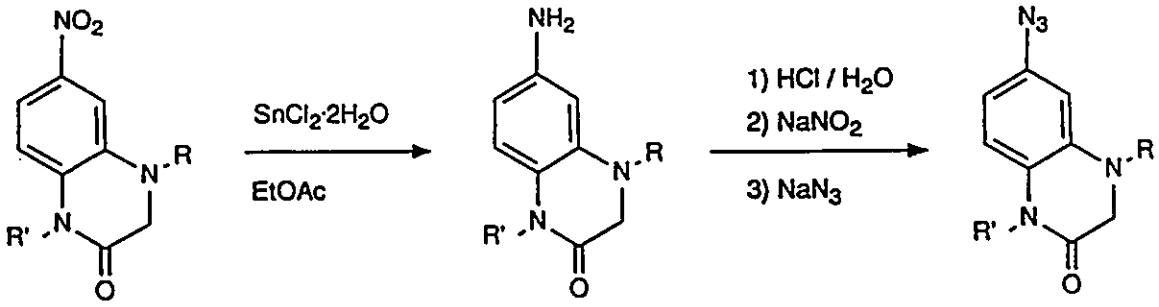

	R	R'		
20	$COCH_3$	H	24, 70%	25, 88%
22	CHO	CH_2CO_2Et	26, 92%	27, 0%

Figure 3.7 Synthesis of 6-Azido-1,2-dihydroquinoxalinones.

The 6-nitro-1,2-dihydroquinoxalinones (**20** and **22**) were reduced to their respective amines (**24** and **26**) by treatment with tin (II) chloride[22a] (shown in Figure 3.7). Diazotization and nucleophilic aromatic substitution of **24** with sodium azide[23] produced the 6-azido-1,2-dihydroquinoxalinone **25**. This and other similar 6-azido-1,2-dihydroquinoxalinones were expected to yield the 3H-dihydroazepines via their thermolysis or photolysis in the presence of alcohols or amines. The 4-formyl-6-nitro-quinoxalinone **22** was reduced to the amine **26** but the acidic conditions required in the diazotization step deprotected the formyl groups and the azide (**27**) could not be synthesized by this method. The formyl group was abandoned at this point as a useful protecting group for the synthesis of the azides.

3.3.1 Thermolysis of the 6-Azido-1,2-dihydroquinoxalinones.

The thermolysis of the azides was attempted before the photolysis reaction because Ohba *et al.*[11a,b] reported that thermolysis of substituted arylazides was superior to photolysis in yielding azepines. Most of the reported thermolyses were carried out in MeOH in sealed ampules at 150 - 170°C[19b,24] and higher yields were reported when thermolyses were done in alcohol over amine solvents[11a].

The azide **25** was thermolyzed in a sealed ampoule, using the procedure similar to that described by Ohba *et al.*[11a] in a high pressure apparatus at 170°C (Figure 3.8). The crude product mixture was analyzed by ^{1}H NMR and mass spectrometry but no azepine products were observed even after chromatography on a silica gel column.

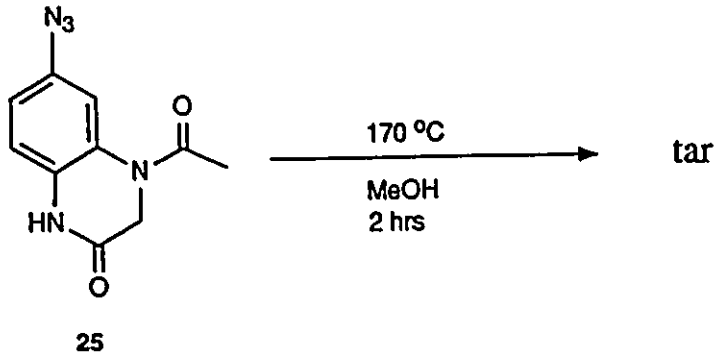

25

Figure 3.8 *Thermolysis of 6-Azido-4-aceto-1,2-dihydroquinoxalinone.*

The disappointing thermolysis reaction of the arylazides may have been because the harsh reaction conditions used caused thermal degradation of the products. The thermolysis reaction was compared to the photolysis reaction by thermolyzing 4-azidoacetophenone (**30**), which is known to yield 3H-dihydroazepines photochemically[9a]. The azide **30** was refluxed in ethanolamine and in a separate experiment in *n*-propanol

however, 30 did not yield any azepines via the thermolysis method. The failure of the deoxygenation and thermolysis reactions indicated the arylnitrene reaction was too complicated to use as a synthetic method of producing substituted azepines without further investigation. Therefore the general arylnitrene reaction was re-investigated from a synthetic point of view to ascertain the subtle nuances of this complex reaction.

3.4 Arylnitrene Chemistry.

3.4.1 Introduction

The photolysis of arylazides to yield arylnitrenes has the luxury of being carried out under a more diverse set of reaction conditions. Parameters such as temperature and excitation wavelength can be altered to dramatically affect the photochemical reactions. The complex mechanism of arylnitrene chemistry was investigated for a series of para-substituted phenylnitrenes reported in the literature and for some synthesized in the laboratory.

As shown earlier in Figure 3.2, the mechanism of arylnitrene ring expansion is complicated and remains under considerable debate. Schuster *et al.*[98] reported that the rate of 5-substituted didehydroazepine trapping with diethylamine is related to the electron withdrawing power of the substituent. The results are illustrated in the graph in Figure 3.9 with the calculated 95% confidence limits of the logarithm of the rate constants shown in dotted lines. The didehydroazepines examined by Schuster *et al.* are shown as plus-signs in the Figure while the Hammett sigma-p values for the acetamido-, amino-, cyano- and nitro-substituents are shown on the line of best fit as shaded triangles. The rates for these substituted didehydroazepines can be estimated by a vertical line from the respective sigma-p value (shaded triangles) to the dotted lines. The rates of trapping the 5-amino-

substituted didehydroazepines (4 x 10^2 to 1 x 10^6 $M^{-1}s^{-1}$) at room temperature were estimated to be similar to that of trapping the 5-methoxy-substituted system (2.5 x 10^4 $M^{-1}s^{-1}$) within the confidence limits. The 5-cyano- and 5-nitro-substituted didehydroazepines were estimated to react much faster with the trapping amine according to the graph (10^8 to 10^{12} $M^{-1}s^{-1}$).

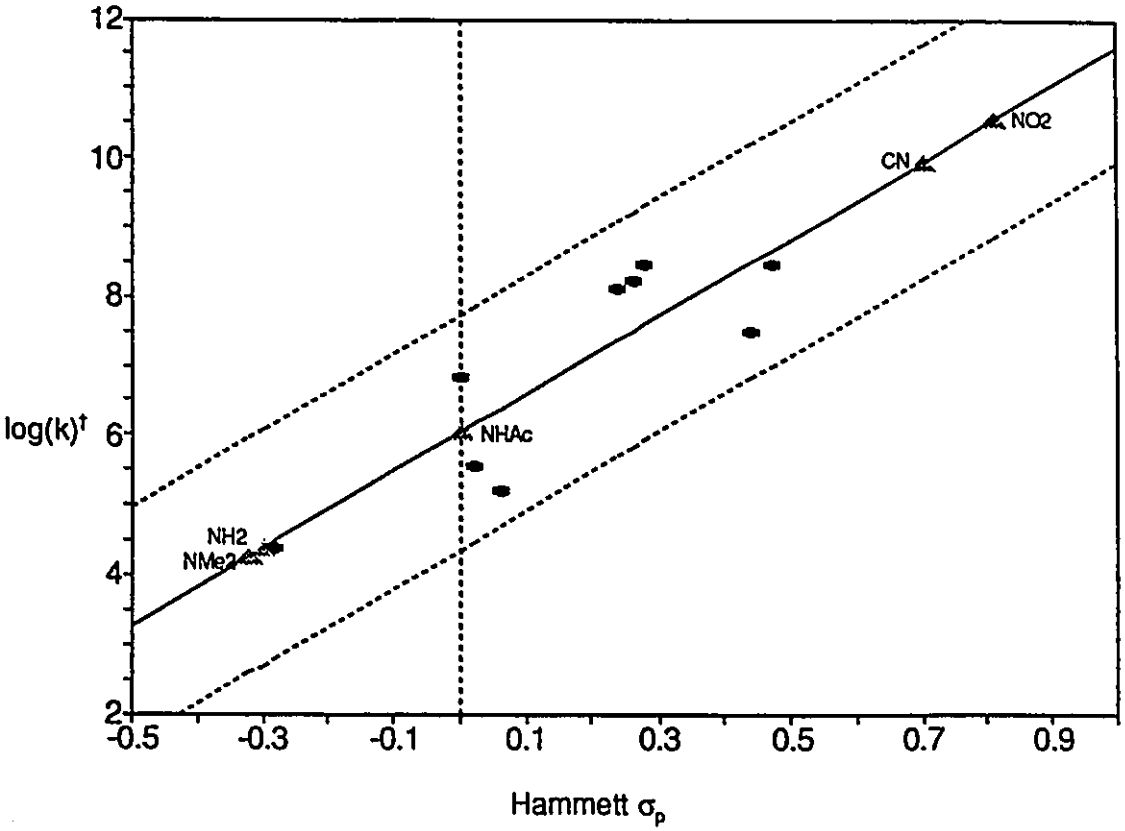

† k = rate of didehydroazepine trapping by $HNEt_2$ in $M^{-1}s^{-1}$ at room temperature

***Figure 3.9** Correlation of Didehydroazepine Trapping and Hammett Sigma Values[20].*

The p-N,N-dimethylamino-phenylazide (**31**) photolysis reaction has been reported not to yield didehydroazepines[9a] nor 3H-dihydroazepines[9a,c] while the p-nitro phenylazide

photolysis was reported to yield didehydroazepines but only low amounts of 3H-dihydroazepines (<3%) were isolated[9a]. The absence of didehydroazepines from the reaction of **31** is not clear from this analysis. Kobayashi *et al.*[9c] found the singlet nitrene derived from **31** rapidly intersystem crossed to the triplet nitrene, preventing the formation of the didehydroazepine. These results suggest two important areas must be considered when the probability of azepine production is investigated: the rate of intersystem crossing and the rate of trapping of the didehydroazepine. The singlet nitrene of **31** was reported to intersystem cross (ISC) rapidly to its triplet state[9c] retarding the production of the didehydroazepine, while the rate of trapping of its didehydroazepine intermediate was estimated to be slow compared to the other didehydroazepines in Figure 3.9. These two combined factors, fast ISC and slow trapping of the didehydroazepine, resulted in the complete exclusion of any azepine products from **31**.

The p-nitro-phenylazide produced a low yield of 3H-dihydroazepine although the didehydroazepine intermediate was predicted to be trapped rapidly by amine nucleophiles. It was not evident from the plot why the reaction yield was so abysmal. The reaction to produce the didehydroazepine intermediate may be inefficient because of enhanced ISC to the triplet state through a charge transfer mechanism as postulated for **31**[9c]. The rates of ISC and didehydroazepine production may be controlled by a number of factors including the relative energies of the intermediates involved, especially if the system is under equilibrating conditions as proposed by Schuster[9a]. With these factors in mind a semi-empirical molecular orbital package contained in the AMPAC computer program was used to help understand the intermediates involved in this complex mechanism in the hope that the important factors behind the ring expansion reaction would become evident.

This would allow a predictive tool to be developed that could be used to design phenylnitrene precursors that would ring expand in a predictable fashion to yield azepines.

3.4.2 AMPAC Modelling of Phenylnitrenes.

The existence of azirine intermediates (for example **10** in Figure 3.2) formed from phenylnitrenes continues to be challenged in the literature[9] and therefore their existence cannot be completely ruled out. Only a few reports in the literature describe the factors involved in the ring expansion reaction of mono-cyclic phenylnitrenes to yield azepines[9a,11a-b,10a]. These and other reports contain contradictions of the exact mechanism, with some reports describing the nitrene as nucleophilic in nature[11a,b], while others describe the nitrene as electron deficient[9d-f]. The AMPAC program was used to calculate the energy differences between the intermediates formed in the phenylnitrene ring expansion reaction to assist in the understanding of this intricate reaction mechanism.

Schuster *et al.*[9a] elegantly showed how the MNDO Hamiltonian[5b], contained in the AMPAC program, calculated the energy states of the intermediates formed from singlet phenylnitrene ^{1}**8** (shown in Figure 3.2). They found the triplet phenylnitrene was the lowest energy intermediate (^{3}**8**) by 21 kcal/mol. The didehydroazepine intermediate **9** was calculated to be 20 kcal/mol lower in energy than ^{1}**8** and 10 kcal/mol lower in energy than the azirine **10**.

The AMPAC program was used to determine the relative energies of the intermediates involved in the ring expansion reaction of a series of reported[9a] para-substituted phenylnitrenes as well as on some para-amido substituted phenylnitrenes prepared in the laboratory. The objective of the modelling experiments was to create

guidelines that could predict phenylnitrene precursors that would have a high probability of ring expanding to yield azepines. Initially the AMPAC program was examined to determine the correct format for modelling the intermediates involved in the reaction since there were many parameters in the program that had to be addressed[6b].

The entire phenylnitrene reaction system was re-examined and modelled using AMPAC to determine if a correlation could be obtained with other measurable parameters. Initial modelling on the phenylnitrene molecule was performed to assess the validity of the program. There have been reports of phenylnitrene molecular modelling studies[9a] and the experimental energy states of phenylnitrene have been determined[5f] so it was possible to relate the calculated AMPAC results to published data. The AMPAC program is equipped with three possible Hamiltonian operators to choose from; AM1[5c], MNDO[5b] and MINDO/3[5m]. The predominant Hamiltonian utilized in the present work was the AM1 model which uses an improved approach towards strain and π-bonding considerations[5c]. Table 3.1 illustrates the effectiveness of AM1 over the other Hamiltonians in calculating the relative energies of the intermediates involved.

Phenylnitrene can exist in either the triplet state, T_0, or in one of two distinct singlet states, S_0 and S_1 (as shown in Table 3.1). Drzaic and Brauman[5f] determined the energies of these states through the photodetachment spectroscopy experiment of the phenylnitrene radical anion. The results indicated that the lowest energy state was the triplet, T_0. Electron spin resonance (ESR) studies[5n] and *ab initio* studies at the 3-21G level by Van-Catledge[5f] on the phenylnitrene system have found similar results. The photodetachment experiment also found two higher energy singlet states, shown in Table 3.1, with the lower energy singlet existing as a biradical.

Table 3.1 Energies of Excited States Calculated by the AMPAC Program.

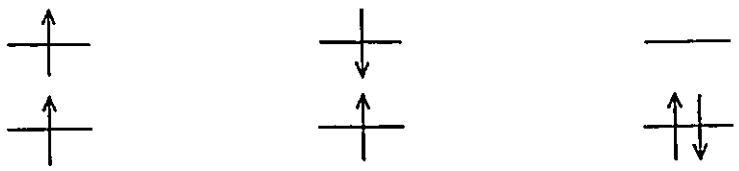

States: T_0 S_0 S_1

Energy of the System (kcal/mol)		Photodetachment Experiment[51] (% error)	AMPAC Program AM1	MNDO	MINDO/3
Absolute	T_0	33.7 (0.9)	105.279	97.397	103.219
	S_0	38.0 (1.1)	108.952		
	S_1	42.5 (1.2)	126.350	120.670	87.595
Relative	T_0	0	0	0	0
	S_0	4.3 (9.3)	3.7		
	S_1	8.8 (5.7)	21.1	23.3	-15.6

Table 3.1 demonstrates the usefulness and the precautions needed when using these semi-empirical programs. Although the absolute energies are not correct, the relative energies are similar to the literature values[51] for the AM1 and MNDO Hamiltonians. The MINDO/3 Hamiltonian completely failed to represent the correct phenylnitrene energy states and therefore it was not used for this system. The AM1 Hamiltonian yielded the best results and, since it was the most improved Hamiltonian offered in AMPAC[51], it was used throughout the remainder of this study.

Table 3.1 also shows the different electronic configurations that the singlet nitrene can adopt. The non-bonding electrons can be confined to a pair of electrons in one orbital, S_1, or they can exist as two electrons in two degenerate orbitals, S_0. The *ab initio* results

by Van-Catledge[5f] indicated the lowest energy singlet state was the biradical S_0 state from the symmetry of the orbitals. Although this was considered the lower energy singlet state, it is most likely not the reacting state yielding ring expanded products. Platz[9d-f] has hypothesized that the singlet state reacts via the insertion of the sigma-electrons into the empty p_y-orbital of the nitrene to generate a didehydroazepine intermediate (see Figure 3.10). Another mechanism involves the insertion of one of the lone pairs of the nitrene into the anti-bonding p_z-orbital of the phenyl ring to yield an azirine intermediate (see Figure 3.11). The azirine then ring expands to the didehydroazepine. Both these mechanisms are discussed in more detail in Chapter 5. In both of these cases the reacting species was considered to be the S_1 state and therefore it was the species modelled.

^{1}8 9

Figure 3.10 Direct Formation of Didehydroazepine from Phenylnitrene.

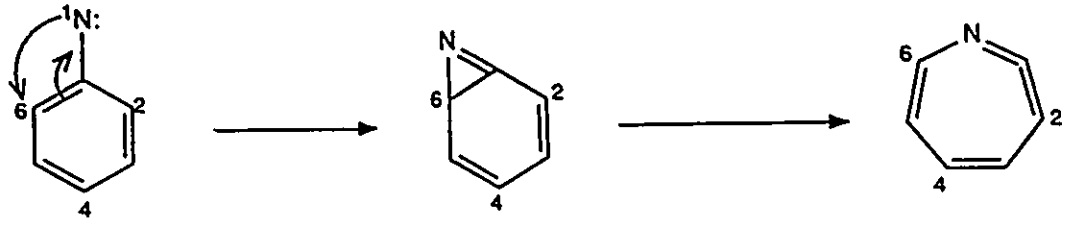

^{1}8 10 9

Figure 3.11 Indirect Formation of Didehydroazepine from Phenylnitrene.

The AMPAC calculated absolute heats of formation in Table 3.1 are much higher than those found by Drzaic and Brauman[5f]. The AMPAC calculated relative energies between the phenylnitrene states was a better reflection of the energy levels between the experimental and theoretical phenylnitrenes. This is obvious from Table 3.1 whereby the absolute energies calculated by AMPAC are two to three times larger than the experimental values.

With the assumption that AM1 can correctly calculate the relative energies of the intermediates involved a series of substituted phenylnitrenes, based on the literature para-substituted phenylnitrenes[9a] and on the phenylnitrenes derived from p-amido-phenylazides synthesized in the laboratory, were modelled using the AMPAC program to calculate relative energies of the possible intermediates involved in the phenylnitrene reaction scheme.

The ring closure of the nitrene to form a didehydroazepine, directly or indirectly through an azirine intermediate, is in competition with intersystem crossing to the triplet nitrene. The rate of intersystem crossing may be dependent on the energy difference between the singlet and triplet states and therefore these energies were calculated for the para-substituted phenylnitrenes. The energy difference between the singlet nitrene and the ring expanded products may also alter the rate of ring expansion relative to intersystem crossing. Therefore, the energies of the azirine and didehydroazepines were also calculated and the AMPAC results are shown in Table 3.2.

Table 3.2 shows the energy differences (ΔH_f) between the triplet phenylnitrene (T_0), azirine (A) and didehydroazepine (D) intermediates (in bold type) relative to their respective singlet phenylnitrene precursors. Although the calculated absolute energies of the substituted intermediates are vastly different, the energy differences between the

singlet and triplet phenylnitrenes was calculated to be very similar (16-22 kcal/mol). The energy differences between the azirine or didehydroazepine intermediates were calculated and were found to vary depending on the substituent.

Table 3.2 AM1 Calculations on the para-Substituted Phenylnitrene Reaction.

Para-Substituent	Heats of Formation (kcal/mol)						
	Singlet Nitrene (S_1)	Triplet Nitrene (T_0)		Azirine (A)		Didehydroazepine (D)	
		Absolute	Relative $\Delta H_f(S_1\text{-}T_0)$	Absolute	Relative $\Delta H_f(S_1\text{-}A)$	Absolute	Relative $\Delta H_f(S_1\text{-}D)$
H	126.343	105.277	21.1	122.970	3.4	103.916	22.4
Cl	119.632	98.583	21.0	116.413	3.2	103.916	7.1
Br	132.832	111.107	21.7	128.430	4.4	125.545	7.4
I	144.693	122.783	21.9	139.664	5.0	136.710	8.0
OCH_3	86.682	66.170	20.5	86.943	-0.3	66.916	19.8
SCH_3	122.678	102.358	20.3	123.397	-0.7	104.217	18.5
CN	160.858	138.601	22.3	155.325	5.5	152.859	8.0
$COCH_3$	92.195	70.104	22.1	86.865	5.3	84.154	8.0
NO_2	135.122	111.781	23.3	127.917	7.2	127.085	8.0
NH_2	116.890	101.032	15.9	122.516	-5.6	103.357	13.5
$N(CH_3)_2$	127.365	111.500	15.9	132.381	-5.0	114.603	12.8
$NHCOCH_3$	86.475	68.208	18.3	87.100	-0.6	82.502	4.0
$NHCOCF_3$	-52.636	-72.441	19.8	-58.870	6.2	-76.974	24.3

3.4.3 Synthesis of Protected para-Amino-phenylazides.

The amino-groups on the phenylazides must be protected with an electron withdrawing substituent to allow the photolysis reaction to occur (as outlined earlier in Section 3.2.1). Two protecting groups were investigated for the para-substituted amino-phenylazide: the acetamido-group and the stronger electron withdrawing trifluoro-acetamido-group. The azides were synthesized from the amido-anilines by diazotization

of the amines, followed by nucleophilic aromatic substitution of the diazonium salt with sodium azide (shown in Figure 3.12). The p-trifluoroacetamido-aniline (**34**) was synthesized from reduction of the p-trifluoroacetamido-nitrobenzene (**33**) with tin (II) chloride and the p-trifluoroacetamido-nitrobenzene was made from reaction of **32** with trifluoroacetic anhydride in THF.

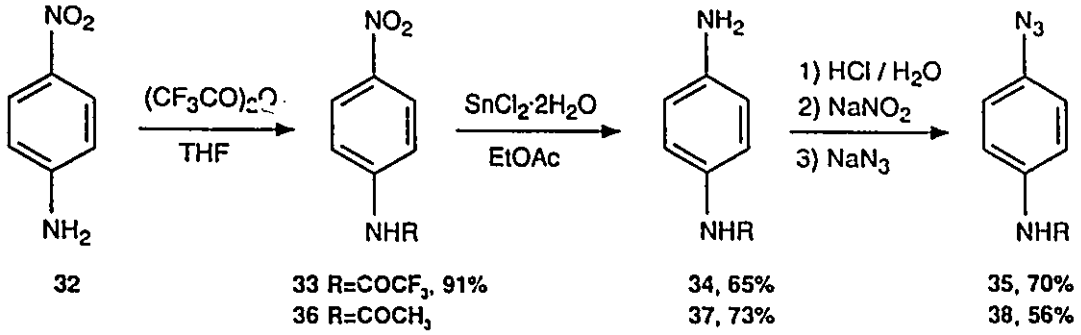

Figure 3.12 Synthesis of para-Amido-phenylazides.

3.4.4 Photolysis of para-Amido-phenylazides

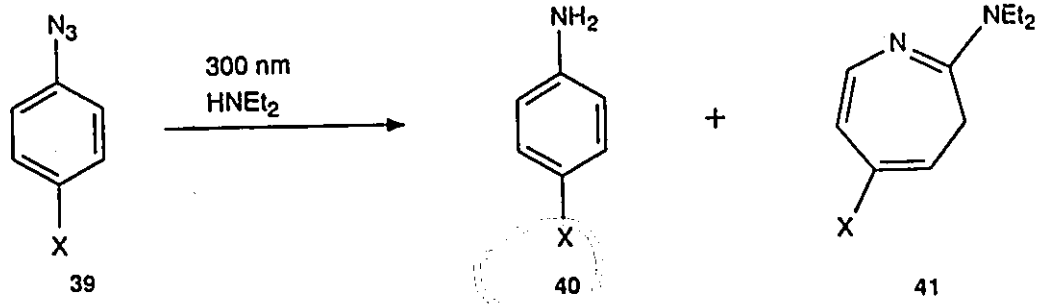

Figure 3.13 Products from the Photolysis of para-Substituted Phenylazides.

The azides **38** and **35** were irradiated in a 2M $HNEt_2/C_6H_{12}$ solution at 300 nm as described by Schuster *et al.*[9a] to yield 5-substituted 2-diethylamino-3H-dihydroazepines and para-substituted anilines (shown in Figure 3.13). The product ratios were determined

by the relative areas of peaks in the ^{1}H NMR. The results found by Schuster *et al.*[9a] and the results from the photolysis of the para-amido phenylazides in the present work are shown in Table 3.3.

***Table 3.3** Products from the Photolysis of Para-substituted Phenylazides.*

Compound	Substituent X	solvent	Product Yield† /%	
			40	41
39a	Cl	C_6H_{12}	0	100
39b	Br		trace	71
39c	I		12	34
39d	OCH_3		30	27
39e	SMe_3		18	51
39f	CN		10	68
39g	$COCH_3$		30	70
39h	NO_2		80	<3
39i	$N(CH_3)_2$		44	0
38	$NHCOCH_3$	C_6H_{12}	major	trace
35	$NHCOCF_3$	C_6H_{12}	24	76
		THF	24	76
		CCl_4	trace	100

† Yields for 39a-I are absolute yields taken from reference 9a except for 38 and 35 which are based on ^{1}H NMR integration.

3.4.5 Discussion

The AMPAC calculations carried out on the phenylazides studied by Schuster *et al.*[9a] (Table 3.2) indicated that, for the systems that yielded azepines (p-Cl, -Br, -I, -OCH_3, -SCH_3, -CN and -$COCH_3$ substituted phenylazides), all the calculated singlet-triplet phenylnitrene energy gaps ΔH_f(ST) were to be found between 20.3 and 22.3 kcal/mol. The p-nitro phenylazide, which yielded very little azepine product (<3%), but did ring expand to the didehydroazepine, as evidenced by the time resolved infrared (IR) detection[9a], was calculated to have a ΔH_f(ST) of 23.3 kcal/mol, larger than the other substituents. The p-N,N-dimethylamino-phenylnitrene did not show any production of didehydroazepine by

time resolved IR detection and its $\Delta H_f(ST)$ was calculated to be 15.9 kcal/mol (a much lower energy gap than that for the other nitrenes investigated) indicating that the lower energy gap may permit more efficient intersystem crossing to the triplet state.

Kobayashi *et al.*[9c] measured the rate of intersystem crossing for p-N,N-dimethylamino-phenylnitrene to be 120 - 145 ps which is exceedingly fast. The efficiency was attributed to a charge-transfer structure which deactivates the singlet ring expansion reaction. The results for the p-acetamido-phenylazide photolysis showed no azepines were formed and its calculated $\Delta H_f(ST)$ was found to be 18.3 kcal/mol, again lower than the norm. The photolysis of the p-trifluoroacetamido-phenylazide, whose calculated $\Delta H_f(ST)$ was found to be 19.8 kcal/mol, yielded azepines and some of the reduced aniline **34**.

The difference in energy between the singlet nitrene and the azirine intermediate or between the singlet nitrene and the didehydroazepine intermediate did not correlate to the observed production of azepines. This independence of the heats of formation of the intermediates indicated the system may be in equilibrium, with the ISC rate determining the fate of the reaction. The AMPAC results indicated a singlet-triplet nitrene energy difference of 20 - 22 kcal/mol was required to drive the reaction to form the didehydroazepine intermediate. Strongly electron withdrawing or electron donating substituents may enhance ISC by stabilizing the singlet nitrene and therefore retarding the singlet ring expansion reaction.

The quinoxalinone systems were investigated using AMPAC to determine the singlet-triplet energy gap and the $\Delta H_f(ST)$ was found to be too small (18.9 kcal/mol for **25**) to allow efficient ring expansion to occur and this may be why the quinoxalinone systems did not produce azepines.

3.5 Comparison of the Deoxygenation of Nitrobenzenes and the Thermolysis and Photolysis of Phenylazides.

In an attempt to compare the deoxygenation reaction to the photolysis reaction, 4-trifluoroacetamido nitrobenzene (**33**) was treated with $(EtO)_3P$ in refluxing $HNEt_2$ and the reaction was monitored for four days by TLC. The expected azepine product 2-diethylamino-5-trifluoroacetamido-3H-dihydroazepine (**42**), which had been synthesized previously through the photolysis of **35** (Table 3.3), was spotted on a TLC plate for reference. No **42** was visible on the TLC after four days and ^1H NMR showed some starting **33** and some of the reduced aniline product **34** (<5%). This experiment showed that deoxygenation of aryl nitro compounds is inferior to photolysis of the analogous arylazide for the formation of azepines.

The attempted thermolysis of p-azido-acetophenone **30** (Section 3.3), which did not yield azepines under the conditions described by Ohba *et al.*[11a], was also inferior to the photolysis of **30**, which did yield azepines[9a].

3.6 Conclusion

The deoxygenation reaction of nitrobenzenes and thermolysis of phenylazides required harsh reaction conditions that may have contributed to the low yields of azepines. In addition, the high temperatures required in both these methods does not permit the investigation of temperature effects on the phenylnitrene reaction. The photolysis of phenylazides, on the other hand, allows for better control over the reaction conditions because the nitrenes can be formed at lower temperatures.

The three methods of phenylnitrene formation to yield azepines were compared to literature results[9-11] and the results of the present work, with the conclusion that the

photolysis of arylazides was the method of choice. The AMPAC program yielded some evidence for the aptitude of a phenylnitrene to ring expand through the calculation of the singlet-triplet phenylnitrene energy gap. Smaller energy gaps resulted in more triplet state products.

The quinoxalinone system was found to be inappropriate for azepine production and another protecting system had to be developed which is discussed in the subsequent Chapters. To develop a model to predict the formation of non-symmetric 3H-dihydroazepines, such as the desired 4,5-substituted-3H-dihydroazepine (shown below), the chemistry of non-symmetric phenylnitrenes had to be investigated.

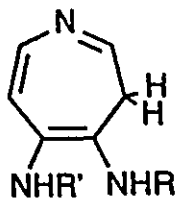

Chapter 4

Photolysis of Non-symmetric Phenylazides

4.1 Introduction

Although there has been a plethora of investigations into arylazide chemistry[9,11], scant work has been conducted into rationalizing and predicting azepine product distributions from non-symmetric phenylnitrenes[9a,g-j,10e,11a-b]. In the ring expansion step that ultimately leads to azepines, the presence of a meta-substituent (shown in Figure 4.1) or an ortho-substituent results in two possible azepine products. The ratio of these two azepine products should be related to the substituent effect on the reactive intermediates involved.

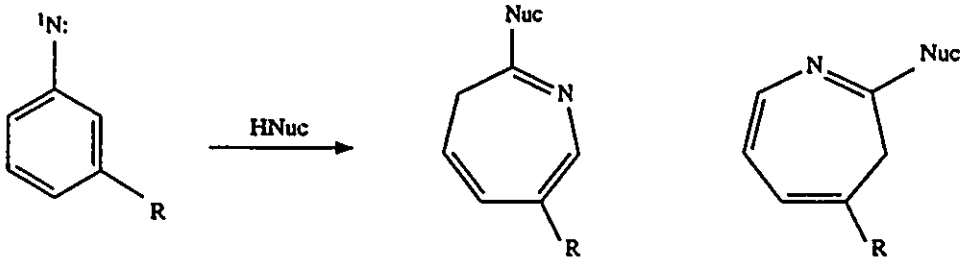

¹43 44 45

Figure 4.1 *Azepine products derived from meta-substituted phenylnitrenes.*

Many reports have been made on non-symmetric arylnitrene reactions but few deal with the factors involved in the azepine product distributions[10e,11a]. Presumably the extremely complex mechanism has been sufficient to quell the additional issue of product

distribution studies. None the less, from a synthetic point of view, how these product distributions arise is extremely important. Consequently, a variety of possible predicting tools were used to aid both in estimating product distributions and to provide insight into the multi-faceted mechanism.

Table 4.1 *Ring Expansion Products for a Series of Meta-substituted Phenylnitrenes.*

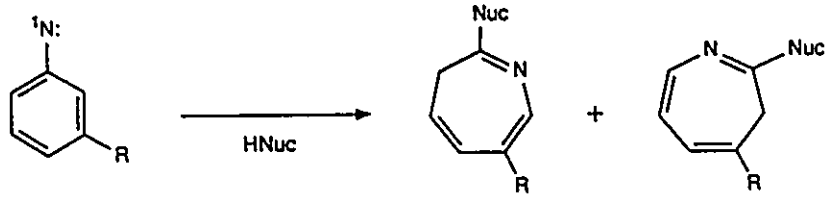

^{1}43 **44** 2-Azepine **45** 6-Azepine

Reference	Meta-Substituent	Method of Nitrene Formation	Ratio of Azepine Products	
			2-Azepine	6-Azepine
de Boer[10e]	Me	Deoxygenation /$(EtO)_2PMe$ /$HNEt_2$	45	55
		Deoxygenation /$EtOPPh_2$ /$HNEt_2$	37	63
		Photolysis /$HNEt_2$ /pyrene	52	48
	OMe	Deoxygenation /$(EtO)_2PMe$ /$HNEt_2$	16	84
		Photolysis /$HNEt_2$ /pyrene	19	81
	Cl	Deoxygenation /$(EtO)_2PMe$ /$HNEt_2$	76	24
		Photolysis /$HNEt_2$ /pyrene	70	30
	Br	Deoxygenation /$(EtO)_2PMe$ /$HNEt_2$	90	10
		Photolysis /$HNEt_2$ /pyrene	90	10
	CO_2Et	Deoxygenation /$(EtO)_2PMe$ /$HNEt_2$	76	24
Ohba[11a]	CO_2Me	Thermolysis /MeOH	64	36
	COMe	"	70	30
	COPh	"	72	28
	NO_2	"	25	75

The limited studies on non-symmetric phenylnitrene reactions have dealt with simple substituents such as alkyl chains[10e], halogens[10e] and a few readily available functional groups[11a]. Even these investigations show the continuing controversy over the

factors which effect the non-symmetric phenylnitrene product distributions. Initial work by deBoer *et al.*[10a] elegantly examined the substituent effect of a small series of meta- and para-substituted phenylnitrenes using both the photolysis of phenylazides and deoxygenation of nitro-benzenes. Ohba[11a] followed with the study of the thermal decomposition of simple meta-substituted phenylazides. Table 4.1 shows the meta-substituted product distributions observed by these groups and provides an effective starting point for product distribution studies conducted during this thesis project.

DeBoer's results showed a general trend whereby electron withdrawing groups at the meta-position favoured ring expansion to the 2-azepine product as illustrated by the chloro, bromo and ethyl ester phenylnitrenes in Table 4.1. The electron donating methoxy phenylnitrene (Table 4.1) favoured production of the 6-azepine product. Peculiarly, Ohba found that the strong electron withdrawing nitro group directed the product formation towards the 6-azepine product, as shown by the thermolysis of 3-nitro-phenylazide, while the less electron withdrawing meta-esters and ketones preferentially produced the 2-azepine products similar to deBoer's results.

These conflicting results illustrate the inadequacy of the literature on predicting product ratios. To compound the problem, the conditions of these reactions were not altered to permit the evaluation of any possible variation in product outcomes. The reactions were also carried out to completion, which permitted both secondary photolysis and possible thermal degradation of the products to occur. Consequently, before examining our more complicated substituted phenylazides, a series of meta-substituted phenylazides were synthesized to verify the reported product distributions[10a,11a] and to determine if the observed azepine product ratios could be predicted and modified in any fashion. For example, reaction conditions such as concentration and temperature were

varied to determine if these affected the observed product ratios.

4.2 Photolysis of Non-symmetric Phenylazides.

The postulated[9,11] intermediates formed from the photolysis of non-symmetric phenylazides were modelled using the AMPAC program to determine if AM1 could reliably predict the observed product ratios. The experimental product distributions were also compared with Hammett substituent parameters since the electron withdrawing ability of a substituent has been shown to affect the product outcome[10e] and since Schuster *et al.*[9n] have shown that the rate of trapping of the didehydroazepine intermediate was dependent on the nature of the attached substituent.

The mechanism of ring expansion is known to involve a didehydroazepine intermediate[9a,k] (Figure 4.2); therefore, the phenylnitrene (**8**) and didehydroazepine (**9**) intermediates were modelled using AMPAC. The azirine intermediates (**10**), which may or may not exist[9l], were also modelled in the event that they may be beneficial as a prediction tool. If the nitrene ring closes to the azirine intermediates reversibly (k_a, $k_{-a} \neq 0$), as shown in Figure 4.2, their relative heats of formation should dictate the observed product ratios. If this process is irreversible ($k_a \neq 0$, $k_{-a} = 0$), the nucleophilic nitrene[11b] should ring close to the more electrophilic carbon. Therefore the charges on the nitrogen atom and the two carbon atoms ortho to the nitrene (C_2 and C_6) were calculated. If the didehydroazepine intermediates are formed reversibly from the singlet phenylnitrene[9a], either through an azirine intermediate (k_a, k'_d and k_{-a}, k'_{-d}) or directly from the phenylnitrene (k_d and k_{-d}), their heats of formation should influence the experimental product ratios. If the phenylnitrene rearranges directly to the didehydroazepine irreversibly (without the involvement of the azirine[9e,k,m,n]) then the longer carbon-carbon bond adjacent to the

nitrene should be more likely to break and to ring expand to the didehydroazepine. Thus the bond lengths of the phenylnitrenes were calculated.

The singlet phenylnitrene can intersystem cross (ISC) to its lower energy triplet state at a rate (k_{ISC}) independent of temperature[9a,o] and therefore ISC could impede azepine production through competitive production of the triplet phenylnitrene. A small singlet-triplet energy gap (outlined in Chapter 3) seemed to facilitate ISC to the lower energy triplet state over ring expansion. This energy gap was calculated for the analogous meta-substituted phenylnitrenes to determine if the yield of azepines was dependent on the singlet-triplet energy gap.

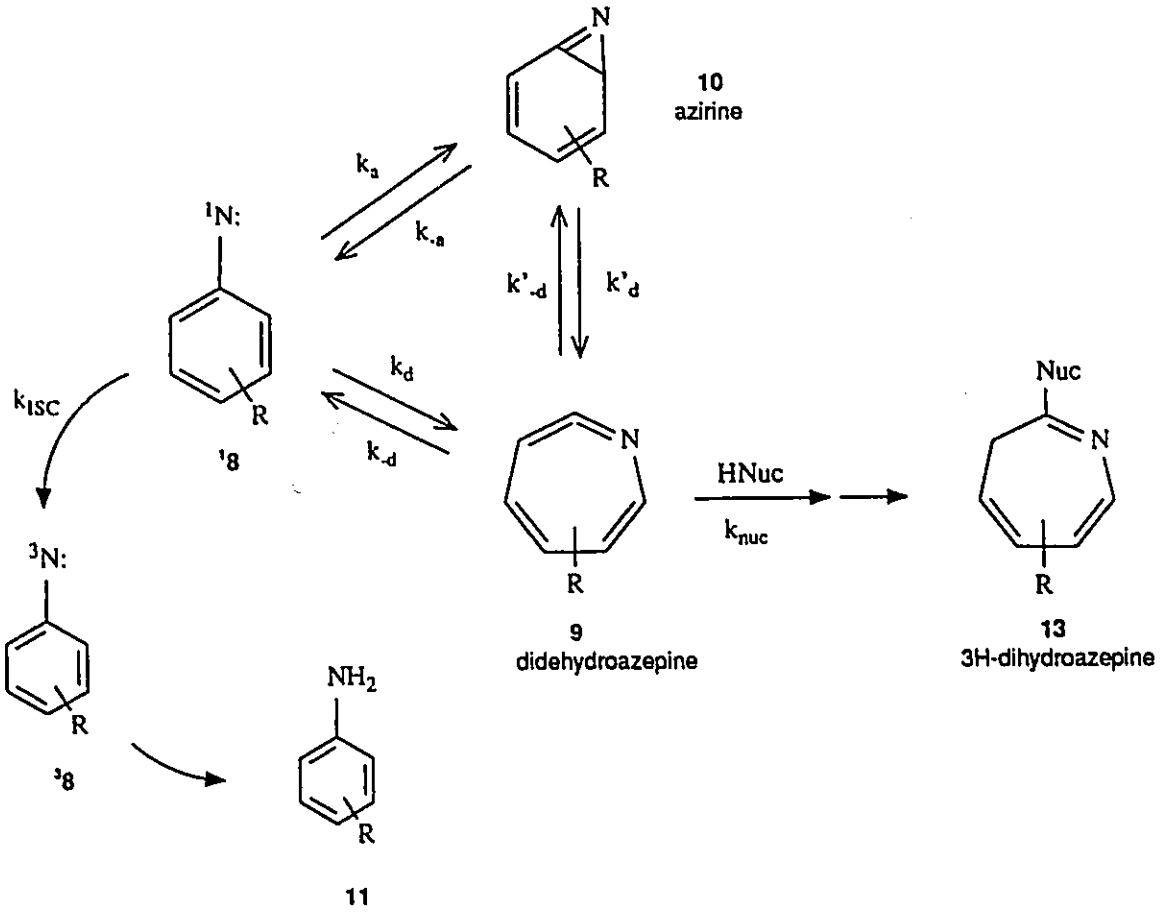

Figure 4.2 Mechanism of arylnitrene closure to produce 3H-dihydroazepines.

4.3 Results

The experimental product yields, shown in Table 4.2, were based on the areas of appropriate ^{1}H NMR signals taken immediately after workup of the crude product. The samples were stored in the freezer wrapped in foil to minimize degradation. Occasionally a sample was checked by ^{1}H NMR to determine if any degradation had occurred although none was observed in all the systems examined over a period of months. The crude reaction mixture was separated using a Chromatotron to isolate the reaction components and the products were identified by ^{1}H NMR and mass spectrometry.

The tables in this Chapter illustrate the relationship of various theoretical values, including semi-empirical calculated values, with the observed experimental azepine product ratios (Tables 4.3 to 4.10). The observed results were compared initially to common Hammett substituent parameters[20] and then to quantities calculated by AMPAC using the AM1 Hamiltonian.

The product mixture from the photolysis of m-iodo-phenylazide was extremely complicated and TLC showed many products were present. Iodine is known to facilitate charge transfer reactions[24] and this was possibly influencing the product distributions. In addition, the photolysis of m-nitro-phenylazide yielded mostly m-nitroaniline and very poor yields of azepines. Nitro groups are also known to induce charge transfer reactions[24]. Because these compounds furnished poor azepine yields, they may proceed through a different and competitive mechanism that would lead to non-general conclusions, therefore they were not used further in the analysis.

The solvent system was confined to THF to allow low temperature photolysis to be performed without requiring a solvent change. As Table 4.2 shows, the solvent can have a dramatic effect on the product distributions. The m-chloro-phenylazide system

illustrated this effectively when more aniline products (Figure 4.3) were formed when the less polar solvent cyclohexane was used instead of THF. In addition, the azepine product ratio was different for each solvent showing the solvent effect on the intermediates formed in the phenylnitrene ring expansion reaction.

A variety of irradiation times were used to determine the conditions needed for low azide conversion to prevent secondary photolysis from occurring since azepines are reported to undergo this process[19a,25]. Fortunately, the results of longer irradiation times in this study did not show significant changes in the product ratios. For example, during the photolysis of m-azido-acetophenone (at either 30°C or -70°C) with varied photolysis periods, similar azepine product ratios were found indicating that secondary photolysis in this case was low (Table 4.2).

The error in measurement of the product yields was estimated to be less than 2% for each integrated peak in the ^{1}H NMR spectrum. This error was deduced by obtaining three separate ^{1}H NMR spectra of a crude sample after workup and integrating each spectrum separately with the difference in the calculated integrals being 1-2% from each other.

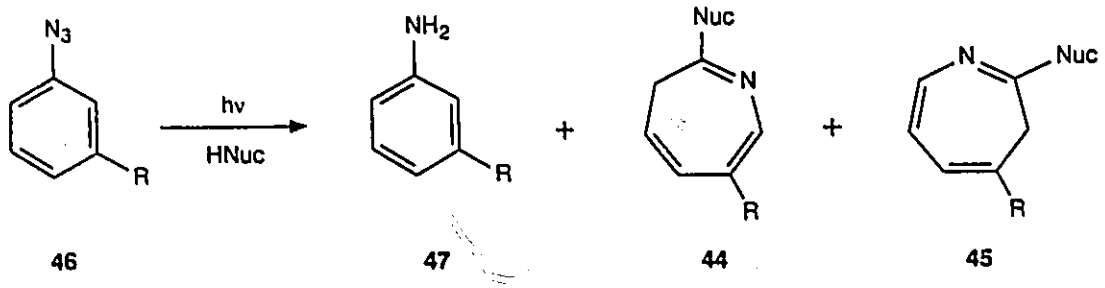

Figure 4.3 Products from the Photolysis of meta-Substituted Phenylazides.

Table 4.2 Experimental Product Yields from the Photolysis of meta-Substituted Phenylazides.

Meta-Substituent	Reaction Conditions				Azepine Yields		Yield $ArNH_2$ 47 /%	Yield ArN_3 46 /%
	Solvent†	Temp. /°C	$[HNEt_2]$ /M	Time /min	44 /%	45 /%		
Cl	CH	30	2	30	23	21	<2	56
	"	"	"	60	28	16	<2	56
	"	"	"	210	64	36	-	-
	THF	"	"	25	49	26	<2	25
	"	"	0.02	60	59	29	<2	12
		-70	2	30	33	15	12	40
Br	CH	30	2	120	32	13	6	46
	THF	"	"	60	53	18	<5	29
	"	"	0.02	55	44	10	15	31
		-70	2	30	20	<2	7	73
CN	CH	30	2	45	10	8	<2	81
	"	"	"	60	18	14	<2	68
	THF	"	"	25	20	18	<2	61
	"	"	0.02	60	28	49	<2	23
		-70	2	30	19	6	6	68
OMe	CH	30	2	20	16	59	<2	25
	THF	"	"	25	15	39	22	24
	"	"	0.02	30	19	59	<2	22
		-70	2	30	4	32	11	53
SMe	CH	30	2	45	23	29	<2	48
	THF	"	"	25	28	36	3	33
	"	"	0.02	60	41	44	<2	16
		-70	2	30	6	19	5	70
COMe	CH	30	2	120	2	46	52	<2
	THF	"	"	20	12	11	36	41
	"	"	"	40	14	12	40	34
	"	"	0.02	30	<2	24	39	37
		-70	2	30	7	5	7	81
	"	"	"	60	7	4	8	81
	"	"	"	90	11	6	4	79
	"	"	"	120	11	6	13	70
$NHCOCF_3$	CH	30	2	30	46	32	<2	22
	THF	"	"	25	31	34	<2	35
	"	"	"	60	17	20	<2	63
	"	"	0.02	25	25	27	<2	48
		-70	2	25	12	36	<2	52
NO_2	CH	30	2.4	30	24	7	69	<2

† CH = 5×10^{-3}M ArN_3 in C_6H_{12} and THF = 5×10^{-3}M ArN_3 in THF

4.4 Discussion

The ratio of the two azepine product yields was compared to common Hammett substituent parameters[20] and to a series of physical constants calculated using the AMPAC program. A regression analysis of the natural logarithm of the product ratio with the physical constants was used in all the comparisons. AMPAC was used to estimate the heats of formation of all the possible intermediates and to calculate the atomic charges and bond lengths on the singlet phenylnitrenes. The calculated results were compared to the observed results in an attempt to provide insight into the mechanism of non-symmetric phenylnitrene ring expansions and to devise a predictive tool for this complex reaction.

4.4.1 Comparison of Observed Product Ratios to Common Hammett Substituent Parameters.

Table 4.3a lists a compilation of Hammett substituent parameters along with the observed product ratios for the photolysis of the meta-substituted phenylazides. No Hammett substituent parameters were available for the trifluoroacetamide substituent and therefore it is absent from the table. A linear regression of each of the Hammett σ-values with the natural logarithm of the observed ratios was calculated to illustrate the extent of the correlation (Table 4.3b). Figure 4.4 shows a sample graphical representation of the relationship between Hammett σ_p-values and the azepine product ratios for the reaction at 30°C using 2M $HNEt_2$.

It is quite evident from Table 4.3b and Figure 4.4 that no correlation exists between the common Hammett σ-values and the meta-substituted phenylnitrene ring expansion reaction to yield one 3H-dihydroazepine over another. The plot shown in Figure 4.4

indicates the line of best fit for the natural logarithm of the ratio of azepine products versus the common Hammett σ_p-values. The correlation of the product distributions with Hammett σ-values was best for the σ_p-values indicating the poor overall correlation between the azepine product distributions and the common Hammett σ-values.

Table 4.3a *Correlation Between Experimental Product Ratios and Linear Free Energy Constants.*

Meta-Substituent	Linear Free Energy Constant[20]				Experimental Azepine Product Ratios ln(44/45)		
	σ_m	σ_p	σ_I	σ_R	30°C 2M $HNEt_2$	30°C 0.02M $HNEt_2$	-70°C 2M $HNEt_2$
H	0	0	0	0	0	0	0
Cl	0.37	0.24	0.46	-0.22	0.621	0.708	0.802
Br	0.37	0.26	0.44	-0.16	1.099	1.449	>3.9
OCH_3	0.10	-0.28	0.27	-0.45	-0.944	-1.152	-2.087
SCH_3	0.14	0.06	0.23	-0.16	-0.241	-0.080	-1.152
CN	0.62	0.70	0.57	0.13	-0.120	-0.080	-1.109
$COCH_3$	0.36	0.47	0.28	0.19	0.122	< -3.9	0.621

Table 4.3b *Linear Regression Between Experimental Product Ratios and LFER Constants.*

LFER Coefficients†		Linear Free Energy Constants			
		σ_m	σ_p	σ_I	σ_R
30°C 2M $HNEt_2$	X-Coeff. (SE) Constant (SE) R	1.22 (1.26) -0.26 (0.65) 0.397	0.89 (0.81) -0.11 (0.64) 0.437	1.19 (1.45) -0.31 (0.67) 0.345	0.72 (1.28) 0.15 (0.69) 0.245
30°C 0.02M $HNEt_2$	X-Coeff. (SE) Constant (SE) R	-0.36 (3.63) -0.41 (1.88) 0.0437	-1.03 (2.35) -0.29 (1.85) 0.193	1.68 (4.03) -1.05 (1.85) 0.184	-3.49 (3.13) -0.84 (1.69) 0.447
-70°C 2M $HNEt_2$	X-Coeff. (SE) Constant (SE) R	5.22 (3.29) -1.00 (1.70) 0.579	3.48 (2.16) -0.26 (1.69) 0.586	4.97 (3.97) -1.13 (1.82) 0.488	3.09 (3.62) 0.76 (1.95) 0.357

† SE = standard error of measurement of the calculated values.

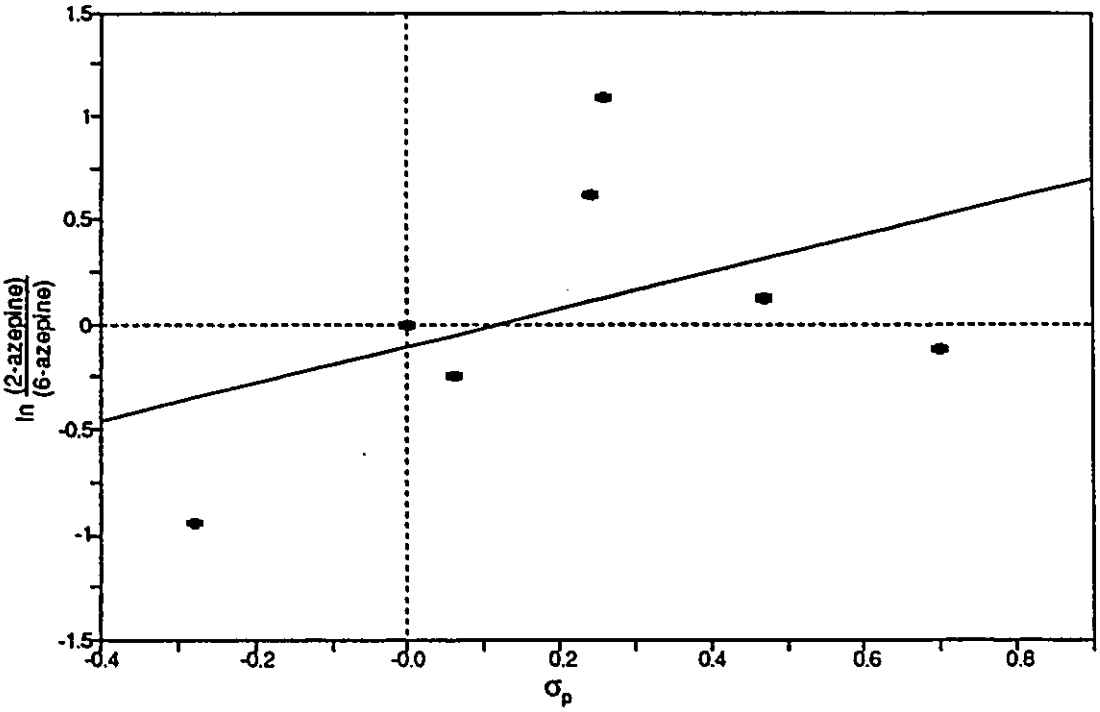

Figure 4.4 Hammett σ_p-Values[20] Versus Azepine Product Ratios at 30°C using 2M $HNEt_2$.

4.4.2 AMPAC Modelling of the Meta-Substituted Phenylnitrene Systems

With the common Hammett σ values showing no clear relationship to the experimental azepine product ratios the system appeared to be as complicated as described by the literature[9-11,19a]. The entire phenylnitrene reaction system was therefore re-examined with the aid of computer modelling to determine if a correlation could be obtained between the experimental results and the theoretical parameters calculated using AMPAC. It was hoped that modelling of the intermediates involved in the ring expansion reaction could be used to predict which azepine product would be formed preferentially from a non-symmetric phenylnitrene.

The intermediates in the meta-substituted phenylazide photolysis were modelled

using the AM1 Hamiltonian. The heats of formation for all the intermediates were calculated to the extent that the gradient normalization of the calculated energy did not change more than 0.01 units (Keyword in AMPAC: GNORM = 0.01), which is 100 times more precise than the default gradient normalization requirement. This precision in the calculation was the optimum gradient to give the smallest change in heats of formation (generally < 0.001 kcal/mol) without lengthy computation time. The atomic charges, the interatomic distances and the eigenvectors for each geometry were computed (Keywords: default, default and VECTORS, respectively). Table 4.5 shows the values calculated for the meta-substituted phenylnitrene systems and Table 4.6 shows the calculated heats of formation for the ensuing azirine and didehydroazepine intermediates formed from the respective singlet phenylnitrene.

Table 4.5 *Meta-Substituted Phenylnitrene Parameters Calculated Using AM1.*

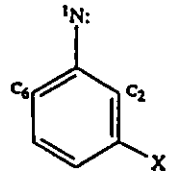

Meta Substituent	Atomic Charge Distribution			Carbon-Carbon Bond Lengths /Å		Heats of Formation /kcal mol⁻¹	
	N	C_2	C_6	C_1-C_2	C_1-C_6	Singlet Nitrene	Triplet Nitrene
H	-0.1911	0.0176	0.0173	1.4420	1.4421	126.343	105.277
Cl	-0.1770	0.0200	0.0191	1.4417	1.4398	120.504	99.303
Br	-0.1775	0.0401	0.0281	1.4424	1.4398	132.152	111.448
I	-0.1793	0.0474	0.0317	1.4428	1.4402	143.274	122.745
OCH_3	-0.1859	-0.0653	0.0004	1.4421	1.4370	89.907	67.713
SCH_3	-0.1869	-0.0055	0.0191	1.4424	1.4385	129.455	108.293
CN	-0.1716	0.0496	0.0343	1.4409	1.4401	159.274	138.324
$COCH_3$	-0.1771	0.0695	0.0341	1.4391	1.4415	90.212	69.616
$NHCOCF_3$	-0.1733	-0.0273	0.0107	1.4390	1.4367	-54.922	-76.361

Table 4.6 Heats of Formation of Intermediates from meta-Substituted Phenylnitrene Ring Closure

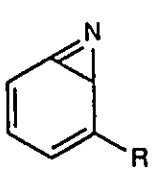

A2

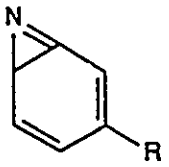

A6

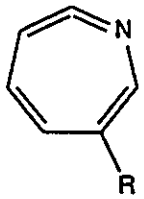

D2

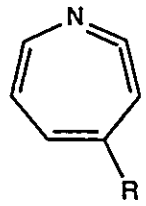

D6

Meta Substituent	Heats of Formation /kcal mol^{-1}					
	Singlet Nitrene ^{1}43	Triplet Nitrene ^{3}43	2-Azirine A2	6-Azirine A6	2-Didehydro-azepine D2	6-Didehydro-azepine D6
H	126.343	105.277	122.970	122.970	103.916	103.916
Cl	120.504	99.303	115.482	116.692	98.065	96.884
Br	132.152	111.448	127.631	128.979	124.148	124.735
OCH_3	89.907	67.713	82.883	85.683	81.080	65.433
SCH_3	129.455	108.293	119.565	122.417	117.563	105.827
CN	159.274	138.324	155.243	156.377	137.091	136.468
$COCH_3$	90.212	69.616	87.133	87.486	68.614	66.842
$NHCOCF_3$	-54.922	-76.361	-61.406	-60.165	-58.755	-62.545

One of the first items that can be noted from Table 4.5 is that all the phenylnitrenes examined had a calculated singlet-triplet energy gap of 20.6 to 22.2 kcal/mol indicating they should have yielded azepines as outlined in Chapter 3. This was observed experimentally (Table 4.2) confirming the use of AMPAC in predicting the probability of azepine production from a particular phenylnitrene system. With this in mind the task of predicting which azepine product would be formed preferentially was undertaken through the use of AMPAC. The physical constants associated with the phenylnitrenes and the intermediates formed from the phenylnitrenes were investigated through the use of AMPAC.

4.4.3 Attempted Correlation of the Experimental Product Ratios with AMPAC Calculated Bond Lengths of the Singlet Phenylnitrene

The phenylnitrene ring expansion mechanism to yield azepines proposed by Platz[9d-f] advocated that the sigma-electrons of the carbon-carbon bond ortho to the nitrene inserted into the empty p-orbital orthogonal to the π-ring system of the nitrene (Figure 4.5). The ring expansion should therefore occur at the weakest sigma-bond which concurrently should be the longer carbon-carbon bond ortho to the nitrene (C_1-C_2 versus C_1-C_6 in Table 4.6). The square of the bond lengths should be proportional to the bond energy. Therefore the difference between the squares of these bond lengths was compared to the natural logarithm of the experimental azepine product ratios. The results are shown in Table 4.6.

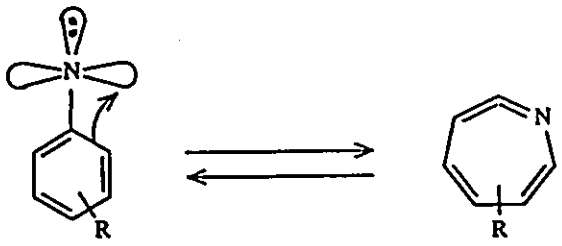

Figure 4.5 *Mechanism of Didehydroazepine Formation Directly from Singlet Phenylnitrene.*

Linear regression analysis of the difference in squares of the AMPAC calculated bond lengths with the experimental azepine product ratios showed a poor correlation (R = 0.325, 0.527 and 0.352 for the 30°C/ 2M $HNEt_2$, 30°C/ 0.02M $HNEt_2$ and -70°C/ 2M $HNEt_2$ reaction conditions, respectively). Figure 4.6 illustrates graphically the correlation for the reaction at 30°C using 2M $HNEt_2$ as an example. It is evident from the plot that the ratio of azepine products observed experimentally did not correlate with the calculated bond lengths of the singlet phenylnitrenes.

Table 4.6 Attempted Correlation of Calculated Bond Lengths with Experimental Azepine Product Ratios.

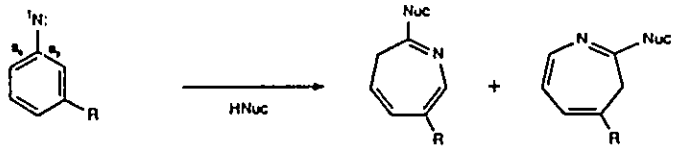

^{1}43 44 45

Meta Substituent	AMPAC Calculated (Bond Length)^2 Difference {favoured product}† $(B_2)^2 - (B_6)^2$ ‡ /$(A)^2$	Experimental Product Ratios			
		Reaction Conditions		ln(44/45)	Azepine formed preferentially♦
		Temperature /°C	[$HNEt_2$] /M		
H	0	-	-	0	-
Cl	0.005360	30	2	0.621	2
		30	0.02	0.708	2
	{2}	-70	2	0.802	2
Br	0.007292	30	2	1.099	2
		30	0.02	1.449	2
	{2}	-70	2	>3.9	2
OCH_3	0.01471	30	2	-0.944	6
		30	0.02	-1.152	6
	{2}	-70	2	-2.087	6
SCH_3	0.01124	30	2	-0.241	6
		30	0.02	-0.080	6
	{2}	-70	2	-1.152	6
CN	0.002190	30	2	-0.120	6
		30	0.02	-0.574	6
	{2}	-70	2	1.154	2
$COCH_3$	-0.006769	30	2	0.122	2
		30	0.02	< -3.9	6
	{6}	-70	2	0.621	2
$NHCOCF_3$	0.006585	30	2	-0.120	6
		30	0.02	-0.080	6
	{2}	-70	2	-1.109	6

† where {2} and {6} refer to the 2-closure and 6-closure products being favoured to yield the 2-azepine and 6-azepine products, respectively.
‡ where B_2 and B_6 are the two ortho carbon-carbon bond lengths.
♦ where "2" and "6" represent more of the 2-azepine and 6-azepine product formed, respectively.

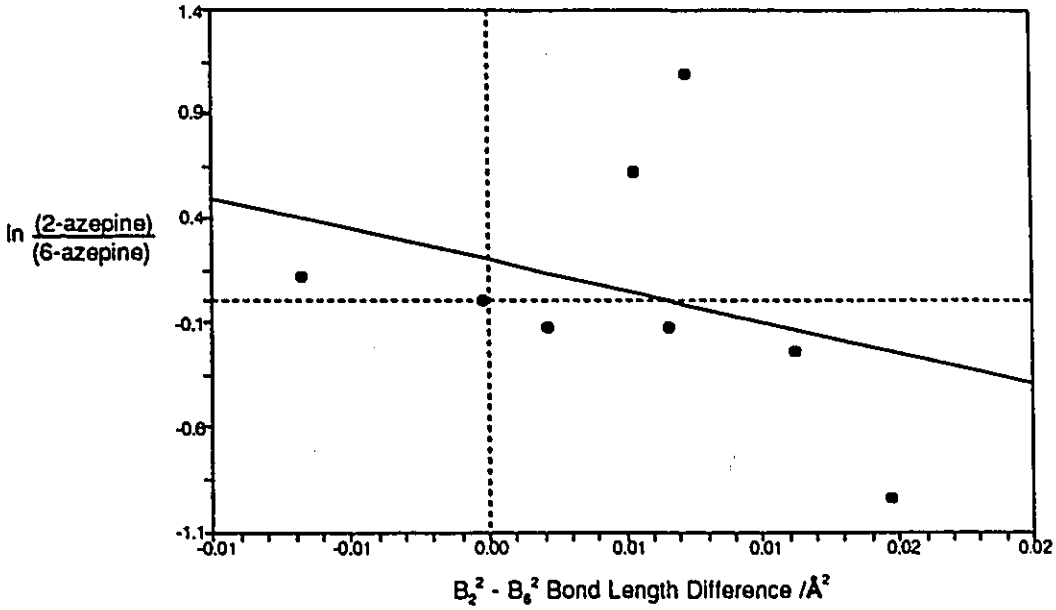

Figure 4.6 *Bond Lengths ortho to the Nitrene Versus Experimental Azepine Product Yields for meta-Substituted Phenylnitrenes*

These results demonstrate that AMPAC failed to reproduce the accurate bond lengths or that the mechanism is not dictated by the strength of the ortho carbon-carbon bonds. If the latter is true, then the mechanism proposed by Platz[9d-f] may not be correct. According to this mechanism the reaction should be operating under equilibrium conditions[9d-f] and therefore, according to the Curtin-Hammett principle, changing the concentration of the nucleophile should not affect the product distribution. When the concentration of diethylamine was lowered from 2 M to 0.02 M the product ratios changed indicating the reaction was not operating under equilibrium conditions and therefore the Curtin-Hammett principle does not apply to these reactions at 30°C. The didehydroazepine may still revert back to the singlet nitrene as proposed by Platz[9d-f] but the reverse reaction must be in competition with trapping of the didehydroazepine to yield azepines.

The rate of formation of the two azepines is dependent on the difference in activation barriers of formation of the didehydroazepines according to this mechanism. This difference should be related to the bond strengths of the carbon-carbon bonds ortho to the nitrene atom. Therefore lowering of the reaction temperature should slow the reactions to produce more azepines derived from breaking of the lower energy carbon-carbon bond. The results calculated using AMPAC indicated only m-$COCH_3$ phenylnitrene should favour production of the 6-azepine product while the remaining meta-substituents should favour production of the 2-azepine product.

When the temperature of the reaction was lowered from 30°C to -70°C, with the diethylamine concentration kept constant at 2 M, the experimental ratios did not follow this prediction. The m-$COCH_3$ phenylnitrene formed more 2-azepine products while the m-OCH_3, m-SCH_3 and m-$NHCOCF_3$ phenylnitrenes formed more 6-azepine products at the lower reaction temperature, all of which are the exact opposite result than what was predicted by the AMPAC calculation. These results along with the poor correlation between the calculated bond lengths and the experimental azepine product yields indicate that it is unlikely the reaction proceeded through this mechanism.

4.4.4 Correlation of Azepine Products with Atomic Charges on the Singlet Phenylnitrene

The phenylnitrene may ring expand via an alternative mechanism involving an azirine intermediate[11c]. This mechanism, which is still under considerable debate[9], entails the nucleophilic attack of the nitrene atom onto the phenyl ring system (shown in Figure 4.7). According to this mechanism, the nucleophilic nitrene[11b] should attack the ortho carbon with the least electron density and therefore the atomic charges on the ortho-

carbons should dictate the azepine product ratios. These atomic charges were calculated and the charge difference between the C_2 and C_6 carbons was compared to the experimental azepine product ratios (shown in Table 4.7).

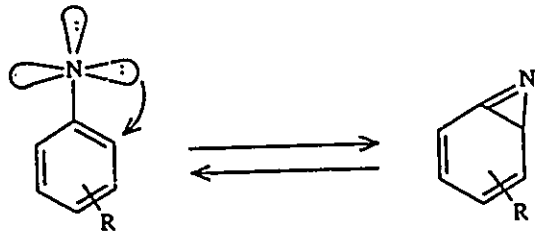

Figure 4.7 *Mechanism of Azirine Formation from Singlet Arylnitrene.*

The calculated charges on the nitrogen atom for all the phenylnitrenes examined were negative. The ortho carbon atoms, on the other hand, generally had a positive charge associated to them. The calculated charge difference results showed a trend between the difference in the atomic charges on each ortho carbon atom (C_2 - C_6) and the observed azepine product distributions. (R = 0.665, 0.213 and 0.737 for the 30°C/ 2M $HNEt_2$, 30°C/ 0.02M $HNEt_2$ and -70°C/ 2M $HNEt_2$ reaction conditions, respectively). This trend is easier to visualize in the plot in Figure 4.8 with the photolysis results at 30°C using 2M $HNEt_2$.

These results imply the reaction mechanism involves an azirine intermediate and that the rate determining step may be the ring closure of the phenylnitrene to an azirine. If this is valid, lowering the temperature of the reaction should yield more of the charge favoured product. From Table 4.7, the charge distributions on the m-OCH_3, m-SCH_3 and m-$NHCOCF_3$ phenylnitrenes indicated the 6-closure products were favoured. When the temperature of the reaction was lowered from 30°C to -70°C more of the 6-closure products were observed experimentally for these systems. Analogously, the m-Cl, m-Br,

Table 4.7 *Correlation Between Atomic Charge Distributions on meta-Substituted Phenylnitrenes and Experimental Azepine Product Ratios.*

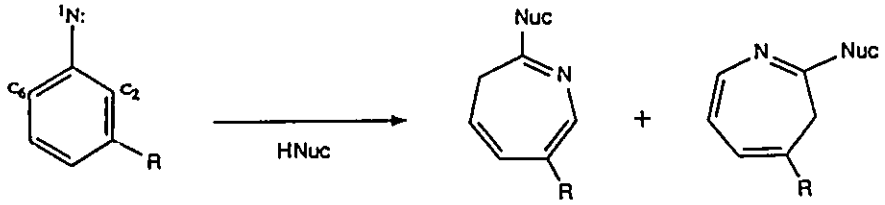

1 43 **44** **45**

Meta Substituent	AMPAC Calculated Charge Difference {favoured product}†	Experimental Product Ratios			
		Reaction Conditions		ln(44/45)	Azepine formed preferentially•
	$C_2 - C_6$‡ /a.u.	Temperature /°C	[$HNEt_2$] /M		
H	0	-	-	0	-
Cl	0.001	30	2	0.621	2
		30	0.02	0.708	2
	{2}	-70	2	0.802	2
Br	0.012	30	2	1.099	2
		30	0.02	1.449	2
	{2}	-70	2	>3.9	2
OCH_3	-0.066	30	2	-0.944	6
		30	0.02	-1.152	6
	{6}	-70	2	-2.087	6
SCH_3	-0.025	30	2	-0.241	6
		30	0.02	-0.080	6
	{6}	-70	2	-1.152	6
CN	0.015	30	2	-0.120	6
		30	0.02	-0.574	6
	{2}	-70	2	1.154	2
$COCH_3$	0.035	30	2	0.122	2
		30	0.02	< -3.9	6
	{2}	-70	2	0.621	2
$NHCOCF_3$	-0.038	30	2	-0.120	6
		30	0.02	-0.080	6
	{6}	-70	2	-1.109	6

† where {2} or {6} refer to the 2-closure or 6-closure product being favoured to yield the 2-azepine or 6-azepine product, respectively.

‡ where N, C_2 and C_6 refer to the atomic charges on the nitrene, C_2 and on C_6, respectively.

• where "2" or "6" represent more of the 2-azepine or 6-azepine product formed, respectively.

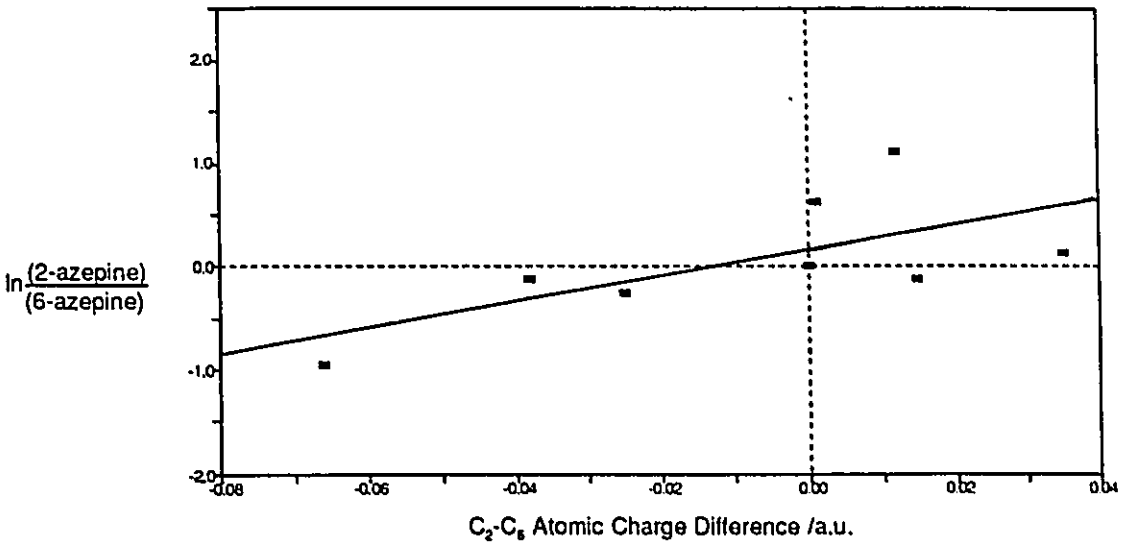

Figure 4.8 Charge Difference on the ortho-Carbons of the Singlet Phenylnitrenes Versus Experimental Azepine Product Ratios.

m-CN and m-$COCH_3$ phenylnitrene charge distributions indicated the 2-closure products were favoured and these systems produced more of the 2-closure products at lower reaction temperatures. The trend at lower nucleophile concentrations (30°C in 0.02M $HNEt_2$) was not as clear possibly because additional factors may have influenced the ratio of azepine products. Factors such as heats of formation of the subsequent intermediates were explored and are discussed in the following section.

4.4.5 Correlation of Observed Azepine Products with Energies of Intermediates Formed

If the ring expansion reaction involving azirine and didehydroazepine intermediates is reversible then the relative heats of formation of the intermediates should influence the product distributions. The discussion in Section 4.4.3 showed that the phenylnitrene intermediates explored in this work were not in equilibrium and that the Curtin-Hammett

principle did not apply to the phenylnitrene reactions discussed here. This was illustrated when, at a constant reaction temperature, the product distributions changed when the concentration of trapping nucleophile was changed. Tables 4.8 and 4.9 show the AMPAC calculated heats of formation of the intermediates involved in the phenylnitrene ring expansion reaction relative to the singlet nitrene along with the experimental azepine product ratios. The energy difference between the intermediates should be directly related to the difference in activation barriers for each intermediate's formation. This is illustrated in Figure 4.9 for a hypothetical ring closure of the R-substituted phenylnitrene to the 6-didehydroazepine (higher ΔH_f) or to the 2-didehydroazepine (lower ΔH_f). The natural logarithm of the product ratios should therefore be directly related to the difference in heats of formation of the intermediates if the intermediates' formation is rate determining.

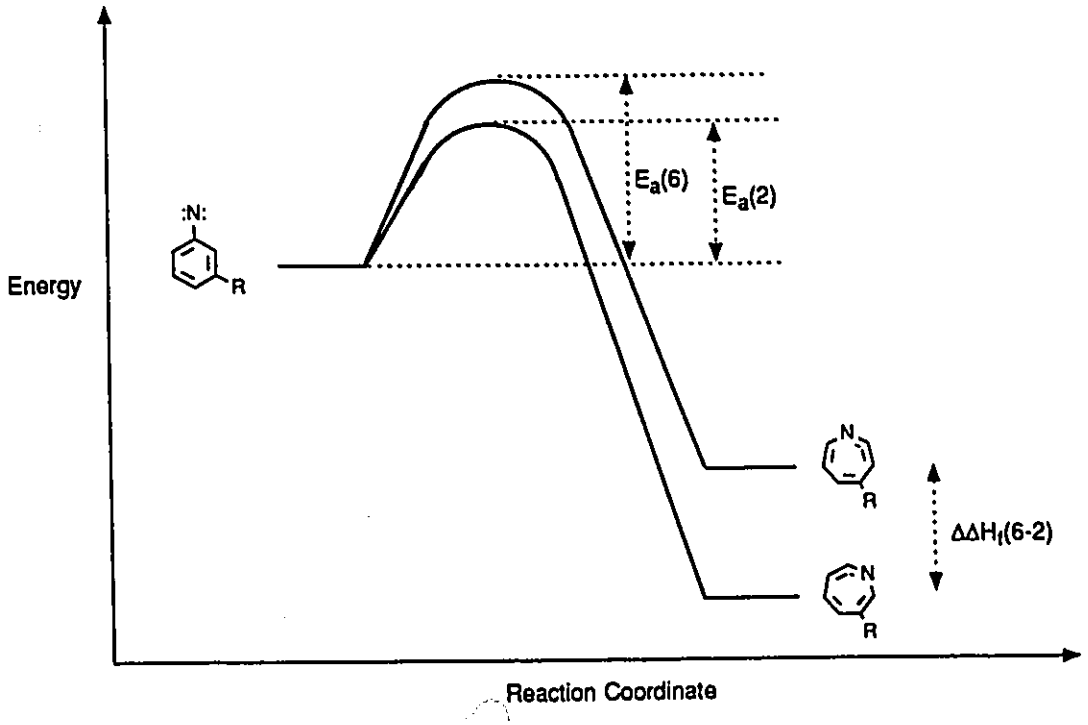

***Figure 4.9** Ring Expansion of a meta-Substituted Phenylnitrene to Didehydroazepines*

The difference in heats of formation between the two azirine or didehydroazepine intermediates was compared to the experimental azepine product ratios. Table 4.8 shows the results for the correlation between the azirine heats of formation differences and the product distributions. Table 4.9 shows the results for the correlation between the didehydroazepine heats of formation differences and the product distributions.

The calculated azirine heats of formation differences inadequately correlated with the experimental azepine product ratios (R = 0.294, 0.205 and 0.133 for the 30°C/ 2M $HNEt_2$, 30°C/ 0.02M $HNEt_2$ and -70°C/ 2M $HNEt_2$ reaction conditions, respectively) and therefore cannot be used as a predictive tool for this reaction. Figure 4.10 illustrates graphically the poor correlation of the difference in azirine heats of formation with the experimental product ratios at 30°C using 2M $HNEt_2$. The results at -70°C using 2M $HNEt_2$ or at 30°C using 0.02M $HNEt_2$ again did not correlate with the azirine heats of formation differences.

These results suggest that the rate determining step does not involve the azirine intermediate or that the azirine intermediates are not involved in the reaction to yield azepines (as suggested by Platz[9e-f]). The azirine intermediates' heats of formation are relatively close in energy to the precursor phenylnitrene suggesting similar activation barriers may exist for the formation of each azirine. This also suggests that the differences in heats of formation of the azirines may not reflect the differences in activation barriers.

***Table 4.8** Azepine Product Distributions Relative to the Heats of Formation of the Azirine Intermediates.*

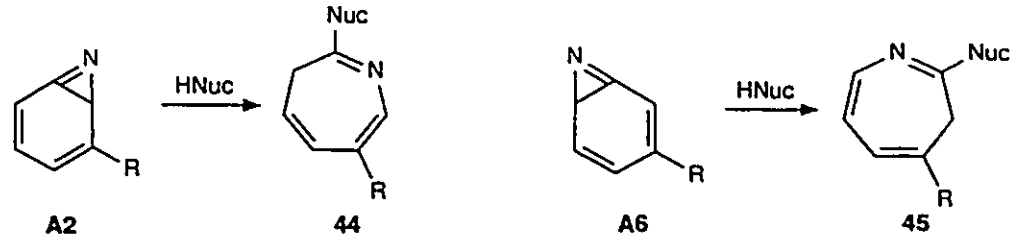

A2 **44** **A6** **45**

Meta Substituent	AMPAC Calculated Azirine Heats of Formation Differences {favoured product}†	Experimental Product Ratios			
		Reaction Conditions		ln(44/45)	Azepine formed preferentially•
	ΔH_f(A6) - ΔH_f(A2)‡ /kcal mol^{-1}	Temperature /°C	[$HNEt_2$] /M		
H	0	-	-	0	-
Cl	1.210	30	2	0.621	2
		30	0.02	0.708	2
	{2}	-70	2	0.802	2
Br	1.348	30	2	1.099	2
		30	0.02	1.449	2
	{2}	-70	2	>3.9	2
OCH_3	2.795	30	2	-0.944	6
		30	0.02	-1.152	6
	{2}	-70	2	-2.087	6
SCH_3	2.852	30	2	-0.241	6
		30	0.02	-0.080	6
	{2}	-70	2	-1.152	6
CN	1.134	30	2	-0.120	6
		30	0.02	-0.574	6
	{2}	-70	2	1.154	2
$COCH_3$	0.353	30	2	0.122	2
		30	0.02	< -3.9	6
	{2}	-70	2	0.621	2
$NHCOCF_3$	1.241	30	2	-0.120	6
		30	0.02	-0.080	6
	{2}	-70	2	-1.109	6

† where {2} or {6} refer to the 2-azirine or 6-azirine product being energetically favoured to yield the 2-azepine or 6-azepine product, respectively.

‡ where ΔH_f(A6 - A2) refers to the heats of formation difference between the 2-azirine and 6-azirine intermediates, respectively.

• where "2" or "6" represent more of the 2-azepine or 6-azepine product formed, respectively.

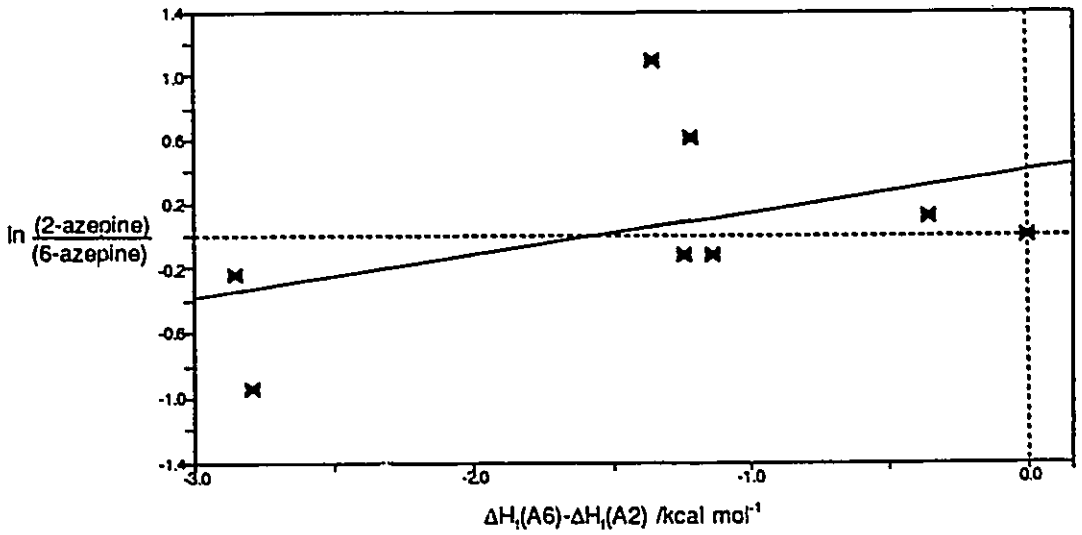

Figure 4.10 *Ratio of Azirine Heat of Formation Versus Experimental Product Ratios at 30°C using 2M $HNEt_2$.*

The calculated energy differences between the two didehydroazepines, on the other hand, did show a correlation with the experimental product ratios (R = 0.775, 0.147 and 0.853 for the 30°C/ 2M $HNEt_2$, 30°C/ 0.02M $HNEt_2$ and -70°C/ 2M $HNEt_2$ reaction conditions, respectively). Figure 4.11 illustrates graphically the trend between the difference in didehydroazepine intermediates' heats of formation and the experimental product ratios. Table 4.9 shows that some of the didehydroazepine intermediates are significantly lower in energy than their precursor singlet phenylnitrene (the m-Cl, m-CN and m-$COCH_3$ substituents all have an energy gap greater than 22 kcal/mol) suggesting the reverse reaction of didehydroazepine to singlet phenylnitrene would be very slow.

Table 4.9 Azepine Product Distributions relative to the Heats of Formation of the Didehydroazepine Intermediates.

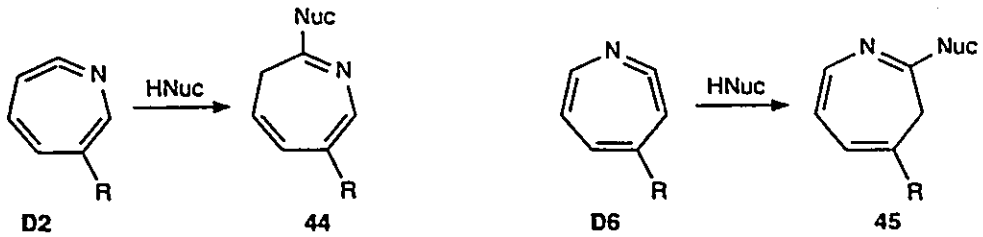

Meta Substituent	AMPAC Calculated Didehydroazepine Heats of Formation Differences {favoured product}†	Experimental Product Ratios			
	ΔH_f(D6) - ΔH_f(D2)‡ /kcal mol^{-1}	Reaction Conditions		ln(44/45)	Azepine formed preferentially♦
		Temperature /°C	[$HNEt_2$] /M		
H	0	-	-	0	-
Cl	-1.181	30	2	0.621	2
		30	0.02	0.708	2
	{6}	-70	2	0.802	2
Br	0.587	30	2	1.099	2
		30	0.02	1.449	2
	{2}	-70	2	>3.9	2
OCH_3	-15.647	30	2	-0.944	6
		30	0.02	-1.152	6
	{6}	-70	2	-2.087	6
SCH_3	-11.736	30	2	-0.241	6
		30	0.02	-0.080	6
	{6}	-70	2	-1.152	6
CN	-0.623	30	2	-0.120	6
		30	0.02	-0.574	6
	{6}	-70	2	1.154	2
$COCH_3$	-2.000	30	2	0.122	2
		30	0.02	< -3.9	6
	{6}	-70	2	0.621	2
$NHCOCF_3$	-3.790	30	2	-0.120	6
		30	0.02	-0.080	6
	{6}	-70	2	-1.109	6

† where {2} or {6} refer to the 2-didehydroazepine or 6-didehydroazepine intermediate being energetically favoured to yield the 2-azepine or 6-azepine product, respectively.

‡ where ΔH_f(D6) - ΔH_f(D2) refer to the difference in heats of formation of the 2-didehydroazepine and 6-didehydroazepine intermediates.

♦ where "2" or "6" represent more of the 2-azepine or 6-azepine product formed, respectively.

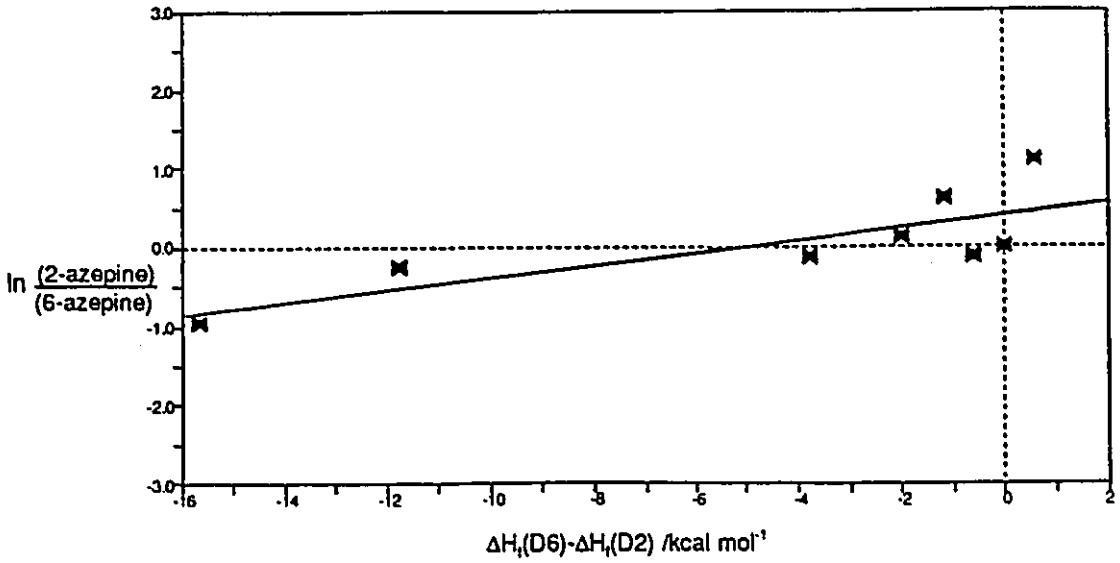

Figure 4.11 Ratio of Didehydroazepine Heats of Formation Versus Experimental Product Ratios at 30°C using 2M $HNEt_2$.

If the didehydroazepines were reverting to their respective singlet phenylnitrenes then lowering of the nucleophile concentration, with the temperature of the reaction remaining constant, should increase the concentration of the lower energy didehydroazepine intermediate. Consequently the azepine product distribution should change to yield more of the trapped didehydroazepine intermediate of lower energy. The results in Table 4.9 shows the AMPAC calculation for the m-Br system favoured trapping of the 2-didehydroazepine. When the $HNEt_2$ concentration was lowered the ratio of the azepine products changed to yield more of the 2-azepine product as predicted. The calculations for the remaining systems predicted the 6-azepine product should be formed preferentially and the m-$COCH_3$, m-OCH_3 and m-CN produced more of the 6-azepine products. The remaining systems, m-Cl, m-SCH_3 and the m-$NHCOCF_3$ substituents,

produced the opposite effect yielding slightly more of the 2-azepine product at lower $HNEt_2$ concentrations. The m-Cl and m-CN systems had large differences between their didehydroazepine intermediates and their precursor phenylnitrenes suggesting the reverse reaction may not have been competitive with the ring expansion reaction even at 0.02M $HNEt_2$. Therefore the 100 fold dilution in trapping amine concentration may not have been sufficient to change the product outcome.

It is obvious from these results that the mechanism is not as easily interpreted as had been hoped. The reason why the product changes were not as pronounced as expected may have been because of secondary factors affecting the reaction such as the charge distribution effects discussed in Section 4.4.4.

4.4.6 Overall Influences on Product Ratios

The photolysis results on the meta-substituted phenylazides showed the dramatic effect both temperature and nucleophile concentration had on the azepine product ratios from non-symmetric phenylnitrenes. The AMPAC results pointed toward an influence of both the atomic charges on the phenylnitrene and the heats of formation of the didehydroazepine intermediates on the experimental azepine product ratios. Table 4.10 shows the combined effect these parameters had on the observed yields.

The results at 30°C using excess diethylamine (2M $HNEt_3$) showed a trend wherein formation of the preferred azepine product was governed by the relative energy difference between the two possible didehydroazepine intermediates. The systems with large differences in didehydroazepine energies, such as the m-OCH_3 and m-SCH_3 substituted phenylnitrenes, preferentially yielded azepines derived from the trapping of the lower energy didehydroazepine intermediate. The heats of formation of the isomeric

Table 4.10 Correlation Between Atomic Charge Densities on the Phenylnitrene, Heats of Formation of the Didehydroazepine and Observed Product Ratios.

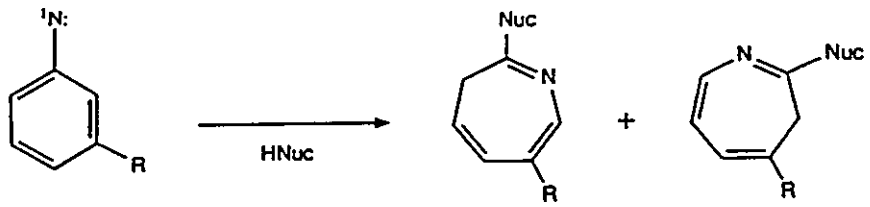

1 43 44 45

Meta Substituent	AMPAC Calculation (favoured product)†		Experimental Product Ratios			
	Charge Difference	Didehydroazepine Difference	Reaction Conditions		ln(44/45)	Azepine formed preferentially♦
	$C_2 - C_6$‡ /a.u.	$\Delta H_f(D6) - \Delta H_f(D2)$★ /kcal mol^{-1}	Temp. /°C	[$HNEt_2$] /M		
Cl	0.001	-1.181	30	2	0.621	2
			30	0.02	0.708	2
	{2}	{6}	-70	2	0.802	2
Br	0.012	0.587	30	2	1.099	2
			30	0.02	1.449	2
	{2}	{2}	-70	2	>3.9	2
OCH_3	-0.066	-15.647	30	2	-0.944	6
			30	0.02	-1.152	6
	{6}	{6}	-70	2	-2.087	6
SCH_3	-0.025	-11.736	30	2	-0.241	6
			30	0.02	-0.080	6
	{6}	{6}	-70	2	-1.152	6
CN	0.015	-0.623	30	2	-0.120	6
			30	0.02	-0.574	6
	{2}	{6}	-70	2	1.154	2
$COCH_3$	0.035	-2.000	30	2	0.122	2
			30	0.02	< -3.9	6
	{2}	{6}	-70	2	0.621	2
$NHCOCF_3$	-0.038	-3.790	30	2	-0.120	6
			30	0.02	-0.080	6
	{6}	{6}	-70	2	-1.109	6

† where {2} or {6} refer to the AMPAC predicted azepine product.
‡ where C_2 and C_6 are the atomic charges on the C_2 and C_6 carbons, respectively.
★ where $\Delta H_f(D2)$ and $\Delta H_f(D6)$ represent the heats of formation of the 2- and 6-didehydroazepine intermediates, respectively.
♦ where "2" or "6" represent more of the 2-azepine or 6-azepine product formed, respectively.

didehydroazepines of the remaining substituted compounds were similar and therefore this factor was probably not influencing these systems. Further, as the concentration of the $HNEt_2$ was decreased from 2M to 0.02M, some of the azepine product ratios dramatically changed to form more of the azepines derived from trapping of the lower energy didehydroazepine intermediate (such as the m-$COCH_3$ and m-OCH_3 substituents) while the remaining systems did not change significantly.

The systems that showed little effect from the calculated differences between didehydroazepine energies were influenced more by the atomic charges on the phenylnitrene. This was evident from the experiment when the temperature was lowered from 30°C to -70°C where the product distribution changed to yield more of the azepine product predicted by the atomic charge distribution (Section 4.4.4).

The meta-substituent study provided some inferences as to the mechanism of phenylnitrene ring expansions to yield azepines. The results presented here suggest the mechanism involves both the azirine and didehydroazepine intermediates. The azirine intermediates, if they exist in phenylnitrene systems, are extremely short lived and have not been observed spectroscopically[9k,n] leading to the belief that they either do not exist[9d-f] or that they rearrange in a few nanoseconds to the didehydroazepine intermediate[9n]. If the azirine intermediates do exist, they probably can ring open back to the singlet phenylnitrene (which has also not been observed spectroscopically[9n]) at room temperature. If ring closure of the phenylnitrene to the azirine became rate determining, by having large concentrations of trapping agent and lowering the reaction temperature, the product distribution should cater to the charge favoured product as was observed with the m-Br phenylnitrene system which produced almost exclusively the 2-azepine product when the reaction temperature was lowered from 30°C to -70°C. This suggests the

reaction involved competition between formation of the didehydroazepine intermediates and re-formation to the singlet phenylnitrene at low amine concentrations at 30°C but not under high amine concentrations at -70°C.

Under reversible reaction conditions (at 30°C using 0.02M $HNEt_2$) the product distributions reflected the differences in the didehydroazepine heats of formation as illustrated in the m-$COCH_3$ phenylnitrene system. For the m-$COCH_3$ system, as the concentration of $HNEt_2$ was lowered from 2M to 0.02M the experimental product distribution changed from mainly the 2-azepine product exclusively the 6-azepine product as predicted by the AMPAC calculation.

4.5 Conclusion

The data yields a better picture into the mechanism of phenylnitrene ring expansions, although not a complete one. The product ratios can be predicted to a limited extent through the modelling of the singlet phenylnitrene and the precursor didehydroazepines. At low temperatures the product distributions change to preferentially yield the azepine product dictated by the closure of the nucleophilic nitrene onto the least electronegative ortho carbon. This trend was observed in all the systems examined at -70°C. Warming of the reaction to 30°C allowed the reverse reaction to compete with trapping and formation of the didehydroazepines. Therefore at 30°C the relative heats of formation of the didehydroazepines dictated the product distributions. Lowering of the trapping agent concentration allowed the reverse reactions to compete more, thus it also allowed the didehydroazepine relative energies to direct the observed product ratios.

Although the AMPAC results did not correlate directly to one specific calculated parameter, two trends were evident for the observed azepine product distributions: the

charges on the two ortho carbons affected the product outcome whereby the nitrene ring closed to the carbon bearing the least electron density and the lower energy didehydroazepine was typically trapped in higher yield than the higher energy didehydroazepine. When the two factors strongly opposed one another (such as in the m-CN case where the charges favoured 2-closure but the didehydroazepine energies favoured the 6-closure) the product ratio was influenced more by the charge distribution at lower temperatures (more of the 2-azepine isolated, ratio of products at 30°C/2M $HNEt_2$ = 0.89 and at -70°C/2M $HNEt_2$ = 3.17). At lower nucleophile concentrations more of the lower energy didehydroazepine product was isolated (more of the 6-azepine isolated, ratio of products at 30°C/2M $HNEt_2$ = 0.89 and at 30°C/0.02M $HNEt_2$ = 0.56). Similar results were found for the m-$COCH_3$ substituted phenylazide system.

With these general rules as a guide, the synthesis of more complicated azepines was attempted so that the photolysis would yield a specific substituted azepine. Each proposed system was modelled in the expectation that the reaction could be driven into preferentially yielding the azepine with substituents at the 4- and 5-positions of the ring. Such a juxtaposition of nitrogens was desired to allow chelation of a metal ion while allowing the metal centre to be as far removed from the ring nitrogen atom as possible to permit strong hydrogen bonding of the nitrogen atom with aqueous solvent molecules (Chapter 1).

Chapter 5

Photolysis of 3,4-Diamido-phenylazides

5.1 Introduction

The structure of substituted, unsaturated azepines presents a dilemma in deciding the best precursor molecule to use as a starting material for their synthesis. By far the simplest synthetic strategy appeared to be the phenylazide ring expansion reaction discussed earlier in Chapters 3 and 4. In order to obtain a 3H-dihydroazepine with the substituents at the 4,5-positions, the precursor phenylazide must possess a 3,4-substitution arrangement. As discussed in Chapter 3, the 4-nitro-quinoxalinone systems, which possessed the required substitution pattern, did not ring expand as envisioned to yield dihydroazepines. Chapters 3 and 4 showed that a singlet-triplet phenylnitrene energy gap, calculated using AMPAC, of 20 - 22 kcal/mol was required to drive the ring expansion reaction to yield azepines. Chapter 4 indicated that the ratio of the two different isolated azepines from a non-symmetric phenylnitrene was dependent on the charge distribution on the phenylnitrene as well as on the energy difference between the two subsequent didehydroazepine intermediates. With these rules in mind the synthesis of more complex 3H-dihydroazepines was undertaken.

The desired amino-imino-azepines required two amines at the 3,4-positions of the phenylazide but amine substituents on phenylnitrenes are too electron-donating to permit ring expansions to occur photolytically[9a]. This was not surprising since simple amino-substituted phenylazides, such as N,N-dimethyl-4-azidoaniline, did not ring expand to

generate azepines as outlined in Chapter 3[9a,c]. For the reaction to proceed, bearing 3,4-nitrogen substituents, the amino groups must first be protected to allow ring expansion to occur and subsequently deprotected to yield the desired azepine products after the 3H-dihydroazepine is formed.

The ideal amine protecting group must be removed relatively easily after the azepine has been formed, remain intact during the photolysis reaction and be acid stable since the diazotization step requires acidic conditions. Ideally, the electronic effect of the protected amino groups would enhance the formation of 3H-dihydroazepines with the substituents ending up in the 4,5-positions. The AMPAC program was used to determine the optimal amine protecting groups and to predict the reaction conditions needed to yield preferentially azepines substituted at the 4,5-positions.

The AMPAC values calculated for the 3,4-substituted phenylnitrenes (Table 5.1) indicated all the compounds investigated had potential for ring expansion to yield the 4,5-disubstituted 3H-dihydroazepines according to their charge distribution pattern on the phenylnitrene precursor. The singlet-triplet phenylnitrene energy gap, calculated using AMPAC, predicted the 3-$NHCOCH_3$-4-$NHCOCF_3$, the 3,4-$(NHCOCF_3)_2$ and the 3,4-$(NHCOCHCl_2)_2$ substituted phenylnitrenes had an energy gap suitable for the production of azepine products. The 3,4-di(trifluoroacetamido)-phenylazide (**48**) and the 3-acetamido-4-trifluoroacetamido-phenylazide (**49**) were chosen as the system to use because the trifluoroacetamido-group is reported to be removed easily through base hydrolysis, is acid stable[21] and was found to be photostable (Chapter 3 and 4). The acetamido-group on **49** was to remain on the azepine in case stabilization of the imino-group on the final amino-imino-azepine was required. These two azides were therefore synthesized and subsequently photolyzed in $HNEt_2$/THF with the conditions of the

photolysis varied to obtain the best yield of 4,5-diamido-substituted-3H-dihydroazepines.

Table 5.1 *Atomic Charges and Heats of Formation of Didehydroazepines Calculated using AMPAC for 3,4-(Substituted-amino)-phenylnitrenes.*

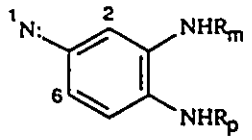

Nitrogen Protecting Groups		AMPAC Results						
		Charges on Singlet Nitrene /a.u.				Heats of Formation of the Phenylnitrenes /kcal mol^{-1}		
R_m	R_p	N:	C_2	C_4	$(C_2 - C_4)^{\dagger}$	$\Delta H_f(^1N:)$	$\Delta H_f(^3N:)$	$\Delta H_{ST}^{\ddagger}$
CHO	CHO	-0.2192	0.0047	0.0408	-0.0361	60.658	42.704	18.0
$COCH_3$	$COCH_3$	-0.2269	0.0028	0.0407	-0.0379	48.665	31.149	17.5
$COCH_3$	$COCF_3$	-0.2003	-0.0001	0.0412	-0.0413	-94.383	-113.458	19.1
$COCCl_3$	$COCCl_3$	-0.2001	0.0139	0.0458	-0.0319	41.190	22.548	18.6
$COCHCl_2$	$COCHCl_2$	-0.2150	0.0080	0.0420	-0.0340	38.260	18.129	20.1
$COCH_2Cl$	$COCH_2Cl$	-0.2084	0.0106	0.0445	-0.0339	36.420	20.182	16.2
$COCF_3$	$COCF_3$	-0.1869	0.0148	0.0482	-0.0334	-237.989	-257.217	19.2

† Charge difference between the C_2 and C_4 carbons.
‡ Singlet-triplet phenylnitrene heats of formation difference.

5.2 Synthesis of 3,4-Diamido-phenylazides.

The 5-azido-2-trifluoroacetamido-acetanilide, a new compound, was synthesized from 4-nitro-1,2-phenylenediamine (**18**) shown in Figure 5.1. The diamine **18** was reacted with slightly more than one equivalent of acetic anhydride to yield 2-acetamido-4-nitro-aniline (**50**) very selectively and without significant acylation of the amine at the 4-position (relative to the nitro-group). The aniline **50** was then reacted with trifluoroacetic anhydride to yield the diacylated product; 5-nitro-2-trifluoroacetamido-acetanilide (**51**). The nitro group was subsequently reduced to the aniline by hydrogenation at 50 psi for 3.5 hours

in a Parr hydrogenator using 10% by weight of 10% palladium-on-carbon. Reduction attempts at lower hydrogen pressures, shorter reaction times or less catalyst produced mixtures of partially reduced **51**. Reduction of **51** using tin (II) chloride was also achieved but the yield was lower (60%) and a much more laborious work-up was required to obtain **52**. The crude aniline was then diazotized in the routine manner using sodium nitrite[23] and then substituted with sodium azide to yield the azide, 5-azido-2-trifluoroacetamido-acetanilide, **49**, in an overall yield of 62%. The azide **49** was characterized by melting point, mass spectrometry, ^{1}H and ^{13}C NMR, UV and IR spectroscopy. The IR spectrum contained the distinctive stretching frequency at 2124 cm^{-1} characteristic of the azido-group.

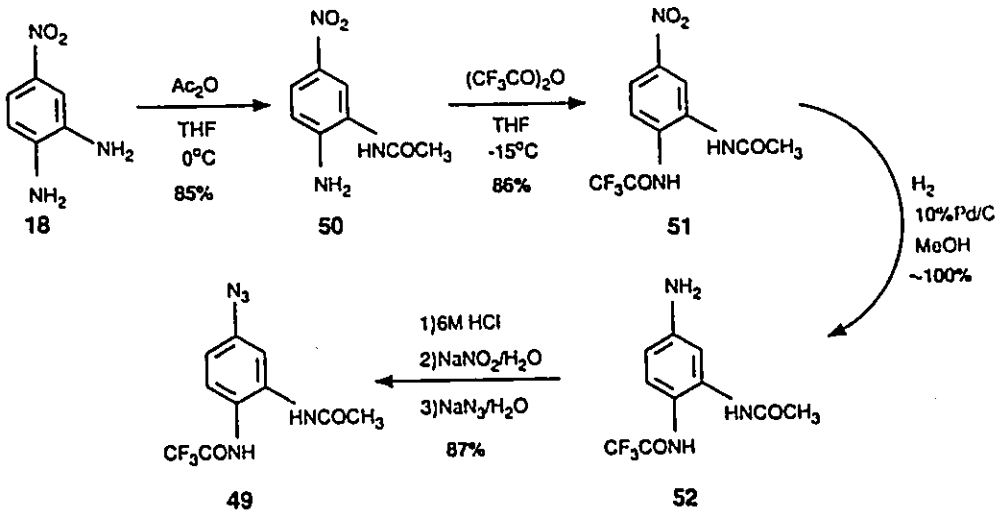

***Figure 5.1** Synthesis of 5-Azido-2-trifluoroacetamido-acetanilide, 49.*

The 3,4-di(trifluoroacetamido)-phenylazide, which was a new compound, was synthesized from the starting diamine **18** shown in Figure 5.2. Compound **18** was treated with excess trifluoroacetic anhydride to yield the disubstituted aryl nitro compound; 3,4-

di(trifluoroacetamido)-nitrobenzene, **53**, which was reduced using tin (II) chloride to the crude 3,4-di(trifluoroacetamido)-aniline, **54**, and subsequently converted into the azide **48** as described above in an overall yield of 18%. The azide **48** was characterized by melting point, mass spectrometry, ^{1}H and ^{13}C NMR, UV and IR spectroscopy. The IR spectrum contained the distinctive stretching frequency at 2133 cm^{-1} characteristic of the azido-group.

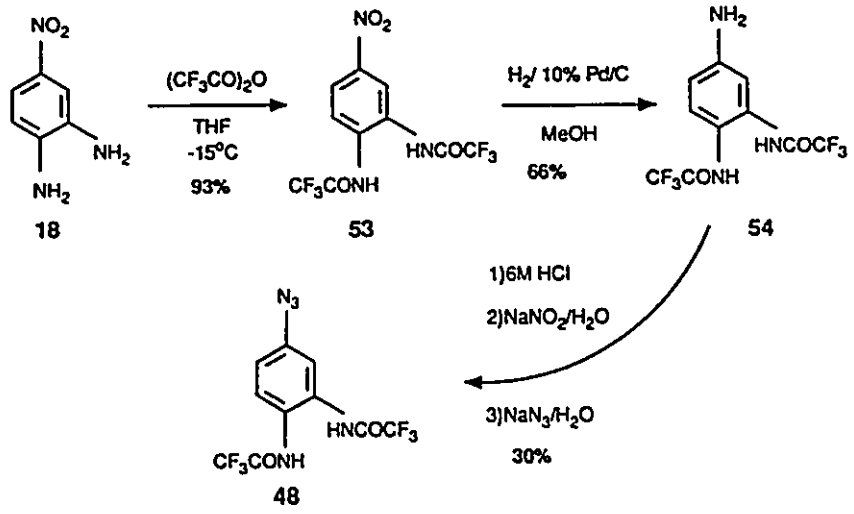

***Figure 5.2** Synthesis of 3,4-Di(trifluoroacetamido)-phenylazide, 48.*

5.3 Photolysis of 5-Azido-2-trifluoroacetamido-acetanilide.

The azide **49** was photolyzed following the general procedure outlined in Chapter 3 using a Rayonet photolysis unit. The products were isolated from preparatory scale reactions (>100 mg **49**) and purified by chromatography using a Chromatotron. The temperature, concentration of **49** and the concentration of the trapping amine were varied to investigate their impact on the observed product distributions. The azide had two UV absorbances in the 200 - 400 nm range, one at 235 nm (ε = 15 800) and the second at

271 nm (ε = 10 500). The 271 nm band tailed into the 300 nm region sufficiently to allow the irradiation using a 300 nm Rayonet bulb.

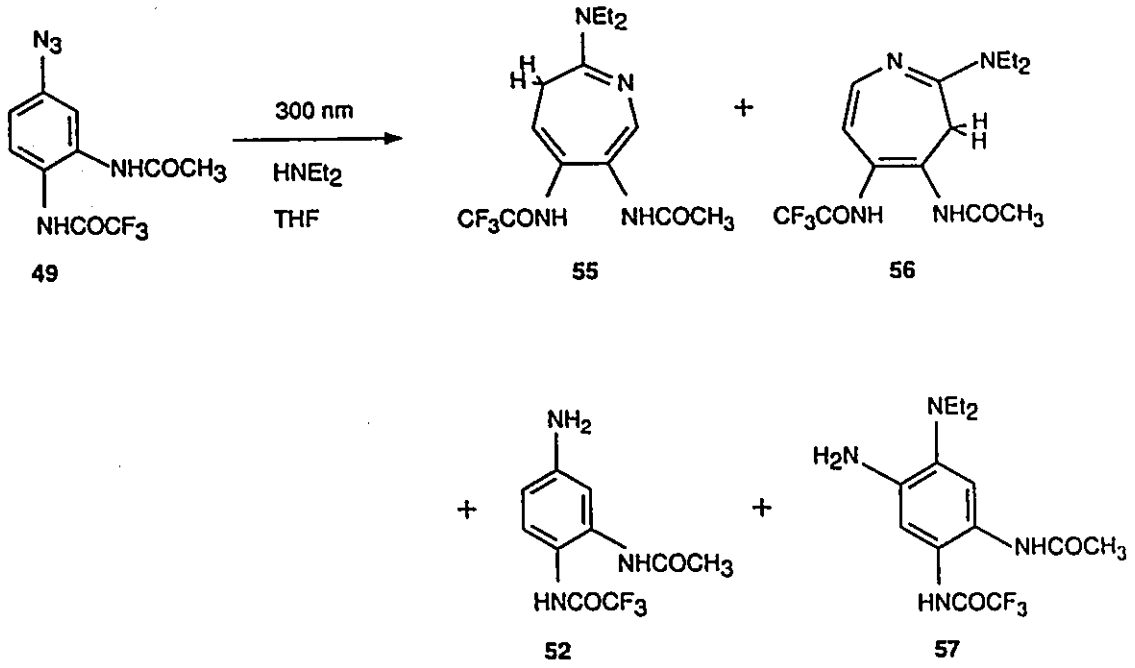

***Figure 5.3** Products from the Photolysis of 49.*

5.3.1 Results

The photolysis results, listed in Tables 5.2 and 5.3, show the overall yield of products and the relative yield of products generated from the photolysis of **49** at 300 nm using a Rayonet photolysis unit. The photolysis of **49** yielded four different products shown in Figure 5.3: the aniline product 3-acetamido-4-trifluoroacetamido-aniline, **52**; two 3H-dihydroazepines, 6-acetamido-2-diethylamino-5-trifluoroacetamido-3H-dihydroazepine, **55**, and 4-acetamido-2-diethylamino-5-trifluoroacetamido-3H-dihydroazepine, **56**; and a

diamine product 4-acetamido-2-diethylamino-5-trifluoroacetamido-aniline, **57**. The product ratios were dependent on the reaction conditions used. The azide concentration, the nucleophile concentration, type of nucleophile (either $HNEt_2$ or HN^iPr_2), temperature and the irradiation times were varied to determine their effect on the product yields.

***Table 5.2** Photolysis of 3-Azido-6-trifluoroacetamido-acetanilide, 49.*

Entry	Photolysis Conditions[a]	[HNuc][b] ($\times 10^{-3}$ M)	Yield of products[d] (%)					
			Azide 49	Aniline 52	2-Diamine 58	6-Diamine 57	2-Azepine 55	6-Azepine 56
1	-80°C, 90 min	2000	0	53	0	47	0	0
2	30°C, 60 min	2000	0	0	0	100	0	0
3	30°C, 20 min	1.8	0	26	0	15	59	0
4	30°C, 30 min	3.55[c]	53	8	0	0	26	11
5	80°C, 30 min 1,4-dioxan	4.36	33	5	0	0	44	19
6a	-70°C, 10 min	5.2	57	3	0	40	0	0
6b	-70°C, 20 min	5.2	39	7	0	54	0	0
6c	-70°C, 40 min	5.2	33	11	0	57	0	0
7a	25°C, 5 min	5.2	56	3	0	24	13	4
7b	25°C, 10 min	5.2	52	3	0	25	15	4
7c	25°C, 30 min	5.2	23	9	0	41	24	4
8a	55°C, 5 min	5.2	53	0	0	15	26	6
8b	55°C, 10 min	5.2	51	5	0	15	24	5
8c	55°C, 30 min	5.2	19	7	0	29	38	7

a) Photolysis in THF in quartz tubes in a 15cm bore Rayonet using 10 300nm bulbs. b) HNuc = $HNEt_2$ unless stated otherwise. c) HNuc = HN^iPr_2. d) by ^1H NMR.

Table 5.3 *Relative Product Yields from the Photolysis of* ***49****.*

Entry	Photolysis Conditions[a]	[HNuc][b] (x 10^{-3} M)	Relative Yield of products[d] /% (Relative yield of singlet products[d] /%)				
			Aniline 52	2-Diamine 58	6-Diamine 57	2-Azepine 55	6-Azepine 56
1	-80°C, 90 min	2000	53	0 (0)	47 (100)	0 (0)	0 (0)
2	30°C, 60 min	2000	0	0 (0)	100 (100)	0 (0)	0 (0)
3	30°C, 20 min	1.8	26	0 (0)	15 (20)	59 (80)	0 (0)
4	30°C, 30 min	3.55[c]	18	0 (0)	0 (0)	58 (69)	24 (31)
5	80°C, 30 min 1,4-dioxan	4.36	7	0 (0)	0 (0)	65 (70)	28 (30)
6a	-70°C, 10 min	5.2	7	0 (0)	93 (100)	0 (0)	0 (0)
6b	-70°C, 20 min	5.2	12	0 (0)	88 (100)	0 (0)	0 (0)
6c	-70°C, 40 min	5.2	16	0 (0)	84 (100)	0 (0)	0 (0)
7a	25°C, 5 min	5.2	7	0 (0)	55 (58)	30 (33)	9 (9)
7b	25°C, 10 min	5.2	6	0 (0)	53 (57)	32 (33)	9 (10)
7c	25°C, 30 min	5.2	12	0 (0)	53 (59)	31 (35)	5 (6)
8a	55°C, 5 min	5.2	0	0 (0)	32 (32)	55 (55)	13 (13)
8b	55°C, 10 min	5.2	10	0 (0)	31 (34)	49 (55)	10 (10)
8c	55°C, 30 min	5.2	9	0 (0)	36 (39)	47 (51)	9 (10)

a) Photolysis in THF in quartz tubes in a 15cm bore Rayonet using 10 300nm bulbs. b) HNuc = $HNEt_2$ unless stated otherwise. c) HNuc = HN^iPr_2. d) by ^1H NMR.

5.3.2 Characterization of Products

The new compounds formed from the photolysis of 49 were characterized by NMR and mass spectrometry. The NMR experiments included ^{1}H, ^{13}C, multiple pulse J-modulated ^{13}C spin echo (commonly called "^{13}C spin-sort") and two dimensional ^{1}H-^{13}C heteronuclear shift correlated experiments[2]. The mass spectrometry relied on high resolution mass spectrometry (HRMS) and the interpretation of the observed fragmentation patterns from the low resolution electron impact (EI) and some ammonia chemical ionization (CI) spectra[26].

The ^{13}C spin-sort NMR experiment[2] gives rise to a ^{13}C NMR spectrum with the phase of the individual carbon signals aligned according to the number of protons that are attached to it. Carbons with an even number of protons are phased opposite to those with an odd number of protons. The carbons with an odd number of protons were conventionally phased positive. The heteronuclear shift correlated NMR experiment shows a correlation between directly bound ^{1}H's and ^{13}C's arising from a polarization transfer of magnetization from the protons to the carbons during a pulse sequence[2]. This experiment is extremely useful in structure elucidation since a complete connectivity map between protons and carbons can be found.

High resolution mass spectrometry (HRMS) of the molecular ion was also critical in determining the molecular formula of the products, but these results had to be interpreted with prudence since structural isomers cannot be differentiated using HRMS. The fragmentation pattern was also useful in assigning structures, since the mass of the lost fragment from a molecule tends to be characteristic of a particular functionality in the structure[26].

4-Acetamido-2-diethylamino-5-trifluoroacetamido-aniline, 57.

Initial ^{1}H NMR spectrum of **57** were not useful in determining its structure since the aromatic region contained only two singlets (H-3 and H-6) and some broad resonances due to the amide N-H's. The ^{13}C of **57** was also not helpful in irrefutably assigning the structure because most of the resonances were found to be quaternary carbons. The ^{13}C spin-sort experiment confirmed this and indicated that there were only two CH's in the structure with chemical shifts of 109.7 and 120.6 ppm which are characteristic of aromatic carbons. The spectrum also showed six quaternary carbons and only one CH_2 carbon; consistent with the aromatic structure of **57**. The lack of a second CH_2 resonance confirmed the compound was not a 2-diethylamino-3H-dihydroazepine structure which would contain two different CH_2 resonances, one from the ring and the other from the diethylamine substituent. To assign the resonances, a heteronuclear shift correlated experiment ("HET-CORR", showing 1-bond ^{1}H-^{13}C coupling) and a long range heteronuclear shift correlated experiment ("LR HET-CORR", showing 2- and 3-bond ^{1}H-^{13}C coupling) were performed and are shown in Figures 5.4a and 5.5a, respectively. The cross-sections from the 2D spectra were particularly useful in showing the weaker correlations and are illustrated in Figures 5.4b and 5.5b.

The simple HET-CORR showed a great deal of information, including the identification of the CH_2 signal which arose from the diethylamine moiety and not from a possible ring CH_2 in a 3H-dihydroazepine. The two singlet protons with resonances at 6.32 and 7.19 ppm in the aromatic region were confirmed to be those of the two CH's in the carbon domain CH-3 and CH-6 (109.5 and 120.2 ppm) but the final assignment between the two could not be substantiated from these data alone. The CH_3 of the amide was confirmed at δ_H = 2.09 and δ_C = 23.3 ppm while that of the diethylamine was at δ_H = 0.93

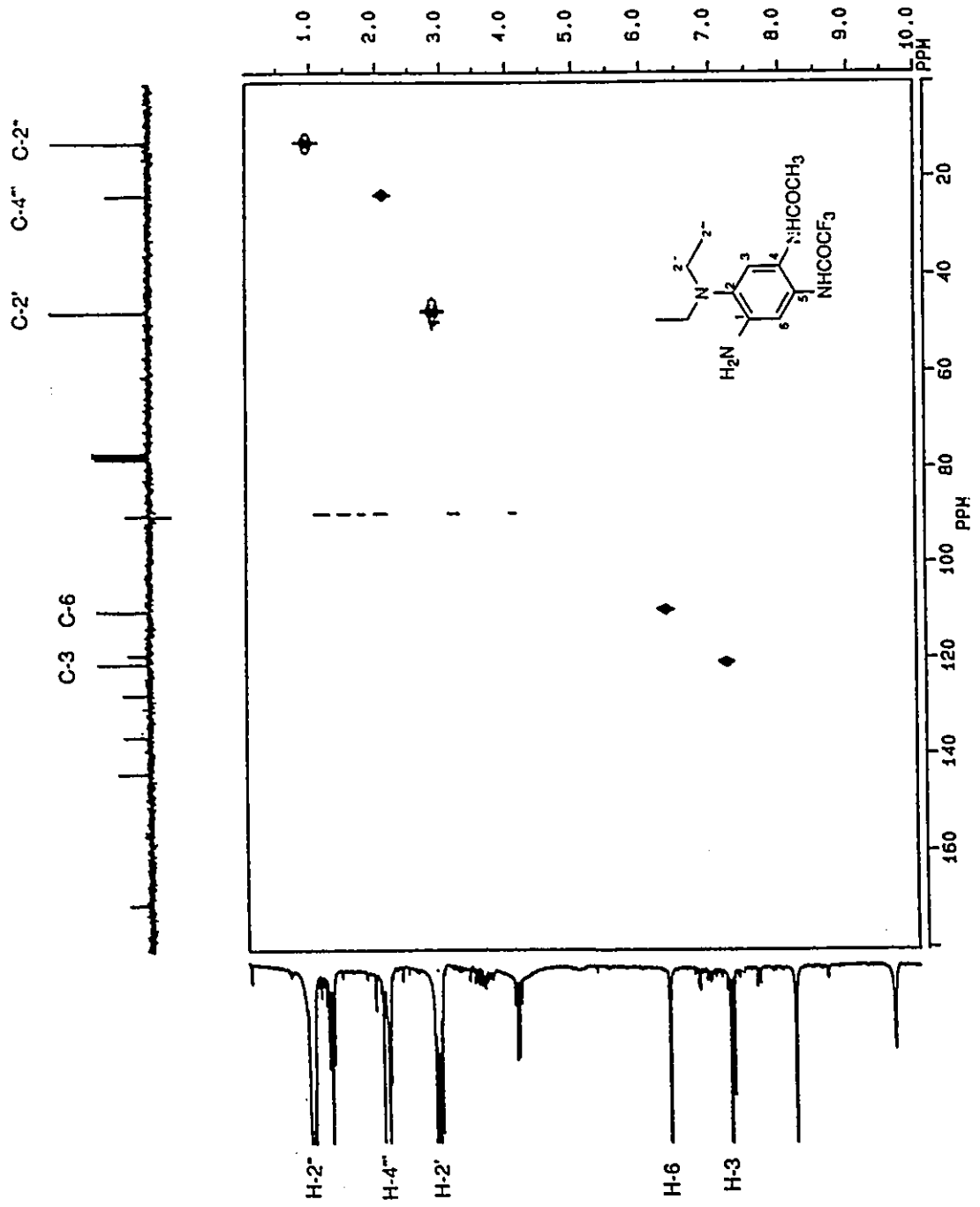

Figure 5.4a ^{1}H - ^{13}C *Heteronuclear Shift Correlated Spectrum of* ***57****.*

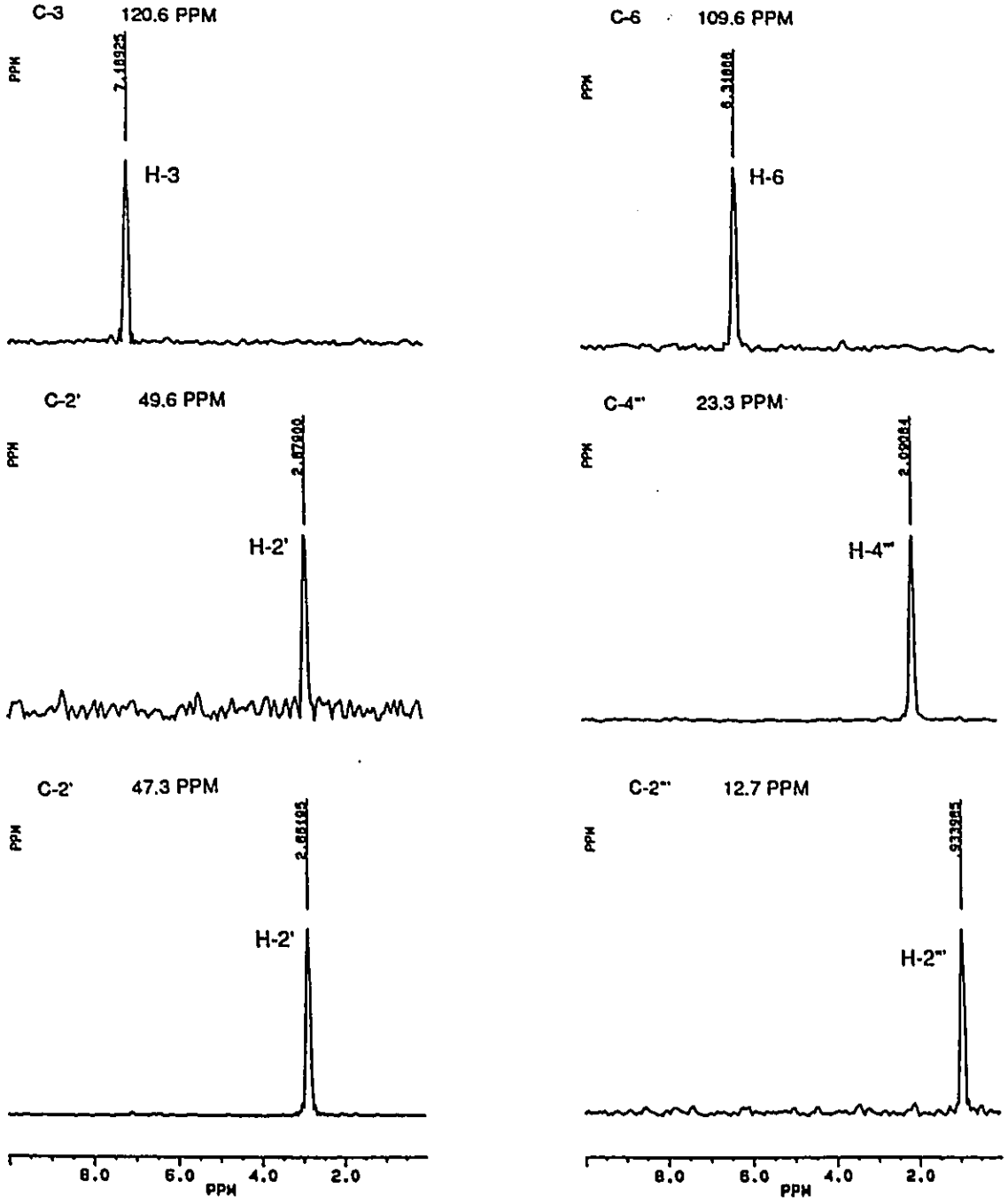

Figure 5.4b ^{1}H - ^{13}C *HET-CORR Cross Sections of* ***57****.*

and δ_C = 12.4 ppm. The quaternary carbons in the HET-CORR did not show any correlation to the protons and therefore the LR HET-CORR experiment was carried out.

The LR HET-CORR, shown in Figure 5.5a along with its plotted cross-sections in Figure 5.5b, revealed a correlation between the quaternary carbon at 170.2 ppm and the proton H-4' (8.08 ppm) of the acetamide and was therefore assigned C-4" (2-bond coupling). The two carbon resonances at 119.2 and 127.7 ppm both correlated to protons H-2' (2.94 ppm) of the diethylamine and a new proton resonance at 3.78 ppm. The new proton resonance was assigned to the amine H-1' proton which exchanges with solvent and therefore is not observed in the standard one-dimensional ^{1}H NMR. The two quaternary carbons were assigned to C-1 (4-bond for H-2' and 2-bond coupling for H-1', respectively) and C-2 (3-bond for H-2' and 3-bond coupling for H-1', respectively). Carbon C-1 was assigned the 119.2 ppm resonance because it correlated to H-1' with the larger intensity while the resonance at 127.7 ppm (C-2) correlated to H-2' with the larger intensity. The quaternary carbon resonance at 120.2 ppm showed a correlation to H-2' (2.94 ppm) and was therefore assigned to carbon C-3 (4-bond W-coupling). The C-4"' (24.9 ppm) resonance of the diethylamine moiety correlated with the proton resonance at 8.08 ppm and therefore this proton was assigned H-4' of the acetamide (3-bond coupling). The final quaternary carbon resonance at 109.5 ppm showed a correlation to proton H-1' (3.79 ppm) and was thus assigned C-6 (3-bond coupling). The remaining CH carbon resonances were assigned as C-5 at 135.4 ppm which correlated to H-1' (3.79 ppm, 4-bond W-coupling) and C-4 at 143.7 ppm which correlated to H-2' (2.94 ppm, 5-bond coupling). The two CH's were assigned in this manner since the opposite arrangement results in a 5-bond and 6-bond coupling assignment.

HRMS found the exact mass to be 332.1470 g/mol which was -1.0 millimass units

(MMU) off from the calculated mass of 332.1460 g/mol, indicating the molecular formula of $C_{14}H_{19}F_3N_4O_2$ was correct. The fragmentation pattern in the electron impact mass spectrum (EI MS) was consistent with loss of CH_3, CH_2CH_3 as the major fragments with some minor fragments also present. The chemical ionization mass spectrum (CI MS) showed the major ion was due to protonation of **57** (m = 333) and very little fragmentation was visible.

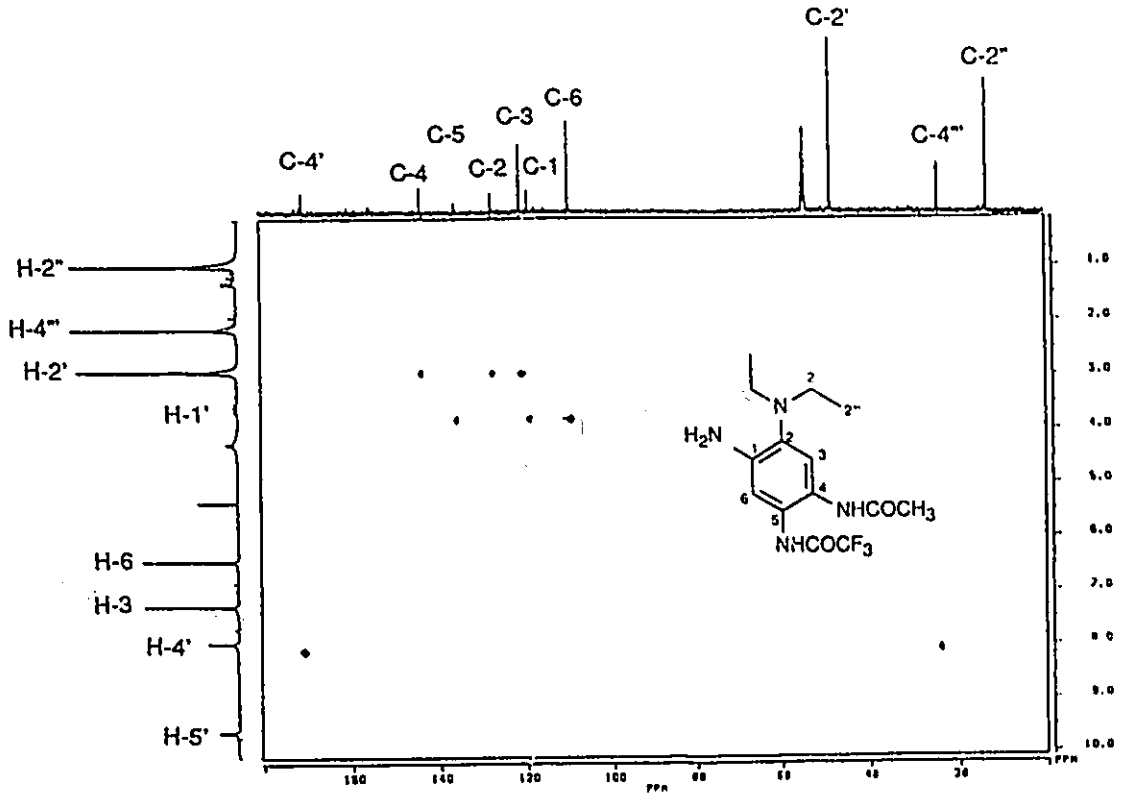

Figure 5.5a *^1H - ^{13}C Long Range HET-CORR of* ***57****.*

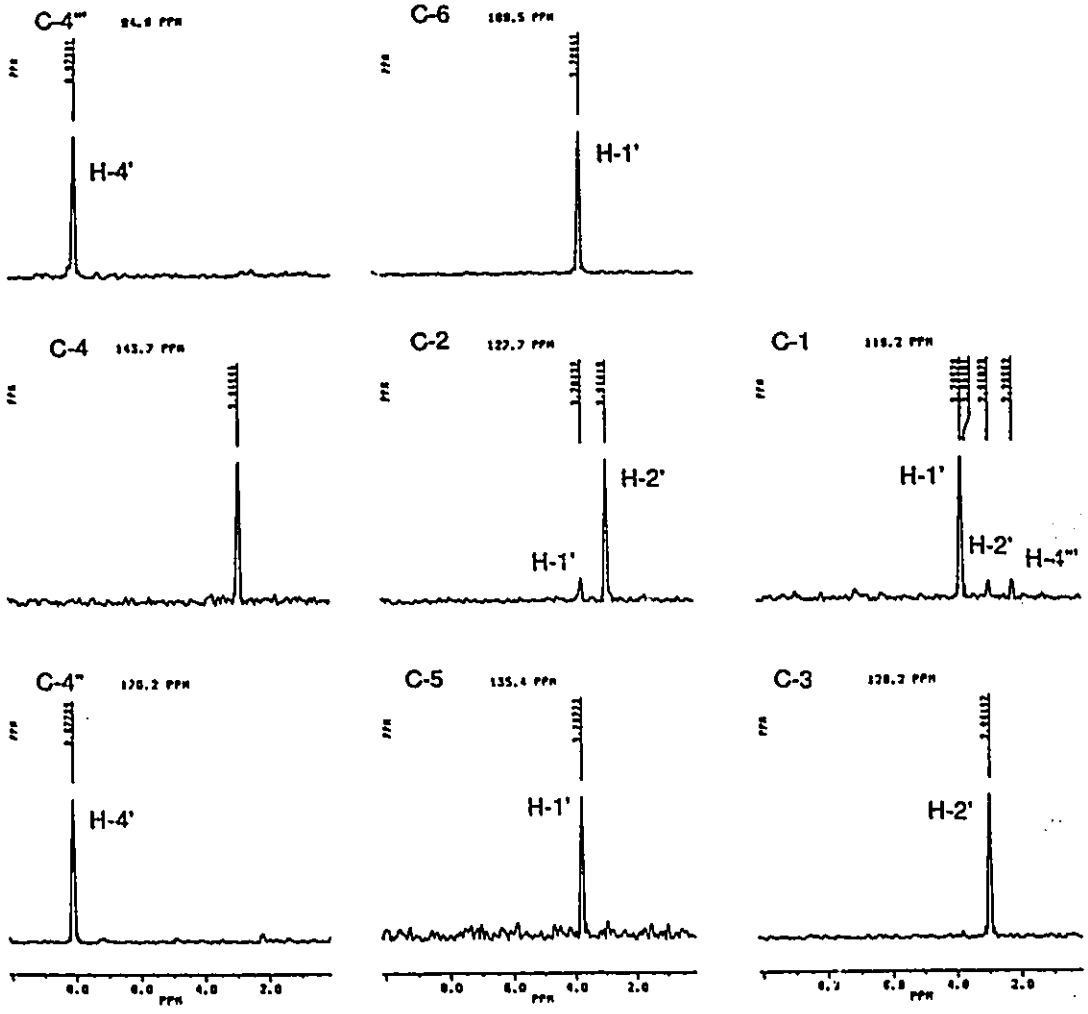

Figure 5.5b *^{1}H - ^{13}C LR HET-CORR Cross Sections of* ***57****.*

6-Acetamido-2-diethylamino-5-trifluoroacetamido-3H-dihydroazepine, 55.

6-Acetamido-2-diethylamino-5-trifluoroacetamido-3H-dihydroazepine, **55**, was identified through its spectroscopic properties and comparison of these with analogous literature values[9a]. The ^{1}H NMR spectrum of **55** showed a triplet (J = 7.9 Hz) at 5.47 ppm characteristic of a ring CH at the 4-position adjacent to a CH_2 in the 3-position and the singlet at 7.11 ppm shift was characteristic of a ring CH at the 7-position of 3H-dihydroazepines[9a]. The ^{1}H NMR also showed the resonances for the diethylamine substituent H-2"' (1.10 ppm) and H-2" (3.41 ppm), the resonances for the acetamide H-6"' (1.77 ppm) and H-6' (7.6 ppm), and the resonance for the trifluoroacetamide H-5' (9.2 ppm). The CH_2 of the ring was not visible in the ^{1}H one dimensional spectrum because the ring was undergoing conformational exchange at an intermediate rate. In addition, and superimposed upon the ring inversions, there were restricted rotations about the amide bonds which created further geometric isomers. The ^{13}C spectrum showed characteristic shifts for all the carbons except for C-2"'. It was considered that the C_2-N_2, bond had restricted rotation at such a rate that the difference between the two resonances of C-2"' resulted in an approximate coalescence of the signals. The ^{13}C also exhibited two distinctive quartets arising from ^{13}C-^{19}F coupling that were attributed to carbons C-5"' (115.8 ppm, J = 287 Hz) and C-5" (155.7 ppm, J = 37 Hz) of the trifluoroacetamido group.

The ^{13}C spin-sort spectrum showed the presence of two CH_2's at 29.4 and 43.4 ppm, one for the diethylamine substituent and the other for the ring CH_2. It also showed two CH_3's (broad) at 12.4 and 22.3 consistent with the diethylamine and acetamide substituents, respectively. The spectrum showed two CH's at 105.9 and 141.0 ppm attributed to the two ring CH's, and four quaternary carbons at 114.4, 132.4, 147.8 and 172.1 ppm consistent with the three ring quaternary carbons and the carbonyl of the

acetamide. The trifluoroacetamide resonances in this spectrum were indistinguishable from baseline noise.

The 2D heteronuclear shift correlated spectrum (Figure 5.6a) showed the appropriate correlations in the 2D contour plot for H-2" (3.41 ppm) and C-2" (43.4 ppm), H-4 (5.47 ppm) and C-4 (105.9), H-6"' (1.77 ppm) and C-6"' (22.3 ppm), and, H-7 (7.11 ppm) and C-7 (141.0 ppm). In addition the contour plot revealed the resonance for carbon C-2"' at 12.4 ppm from its correlation with H-2"' at 1.10 ppm. The 2D contour plot did not show all the coupled CH's and, because it can be difficult to ascertain the correct shifts of both the protons and the carbons from the contour plot, the cross sections in the ^{13}C domain were plotted. Each column shows the 1D proton spectrum of the coupled CH's (Figure 5.6b). These cross sections permitted the extraction of the additional correlation between C-3 at 29.4 ppm and the two proton resonances H-3a at 2.03 ppm and H-3b at 3.31 ppm. Neither of these proton resonances were visible in either the one dimensional ^{1}H NMR spectrum nor the contour plot of the two dimensional NMR spectrum.

The long range HET-CORR of **55** was recorded and is shown in Figure 5.7a and the important cross-sections in Figure 5.7b. The proton resonance at 5.47 ppm (H-4) showed a correlation to only one carbon at 114.4 ppm and therefore this carbon was assigned to C-5 (2-bond coupling). The proton resonance at 7.11 ppm (H-7) showed a correlation to three carbon resonances at 132.4, 141.0 (C-7, 1-bond coupling) and 148.0 ppm. Three possible quaternary carbons that should show such a correlation are: C-6 (2-bond coupling), C-2 (3-bond coupling) and C-5 (3-bond coupling). Since C-5 was already assigned, the two quaternary carbons must be C-2 and C-6. The resonance at 132.4 ppm showed a larger signal-to-noise ratio than that at 148.0 ppm which suggested that the former resonance is the C-6 carbon (2-bond coupling). In addition, the

diethylamine substituent should be more electron donating than the acetamide and therefore the C-6 carbon should be at higher field.

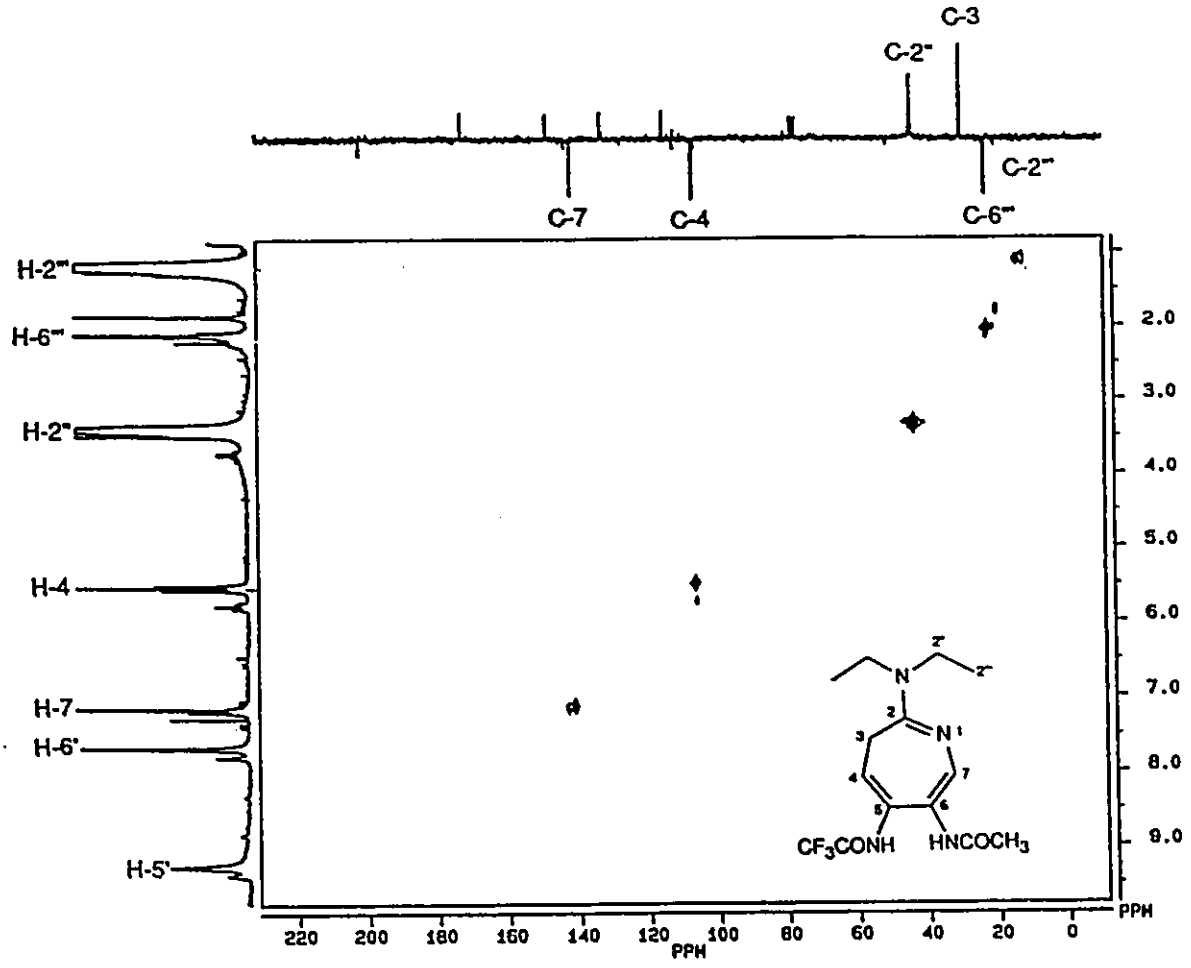

Figure 5.6a ^{1}H - ^{13}C *HET-CORR of 55.*

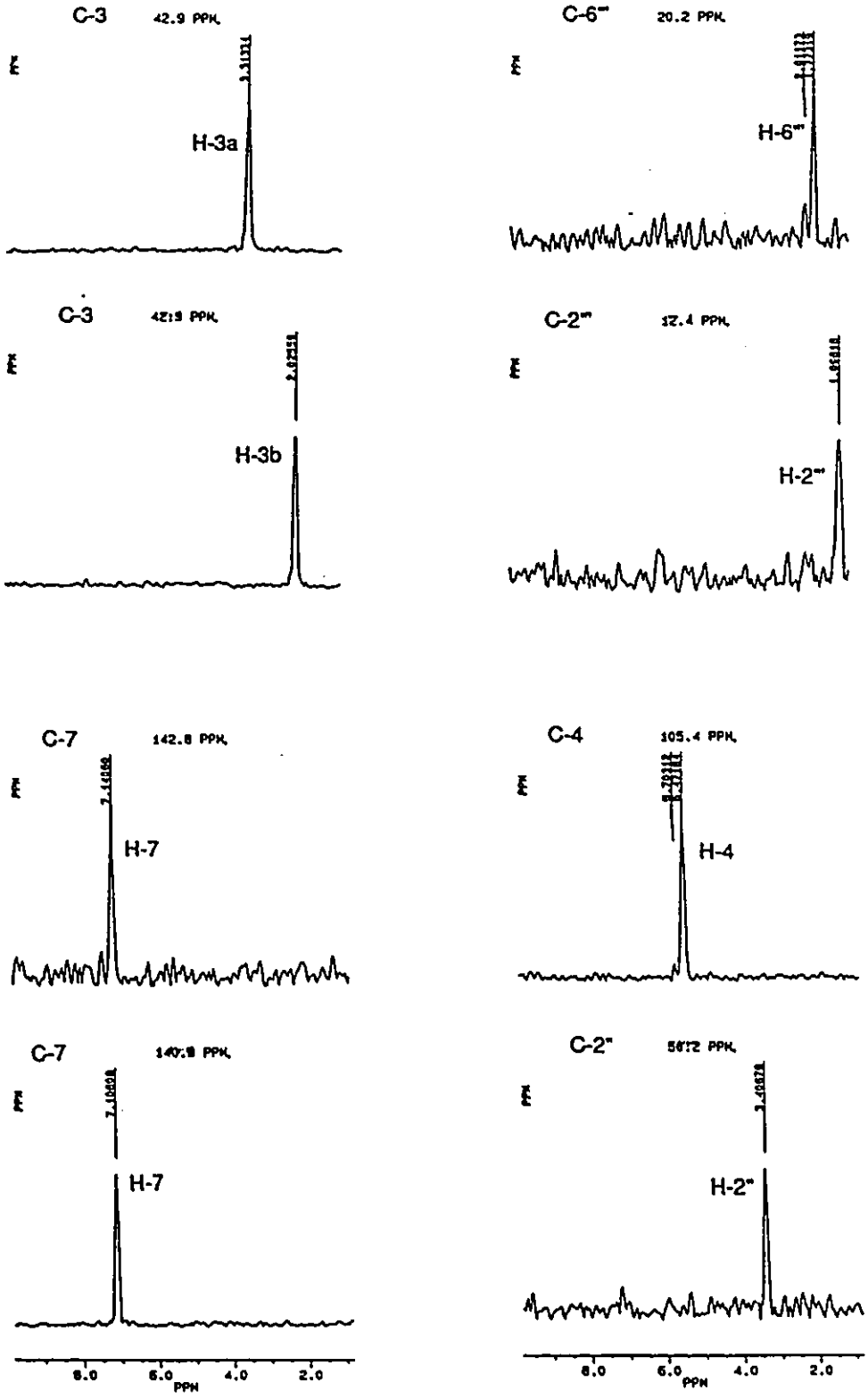

Figure 5.6b ^{1}H - ^{13}C *HET-CORR Cross Sections of* ***55****.*

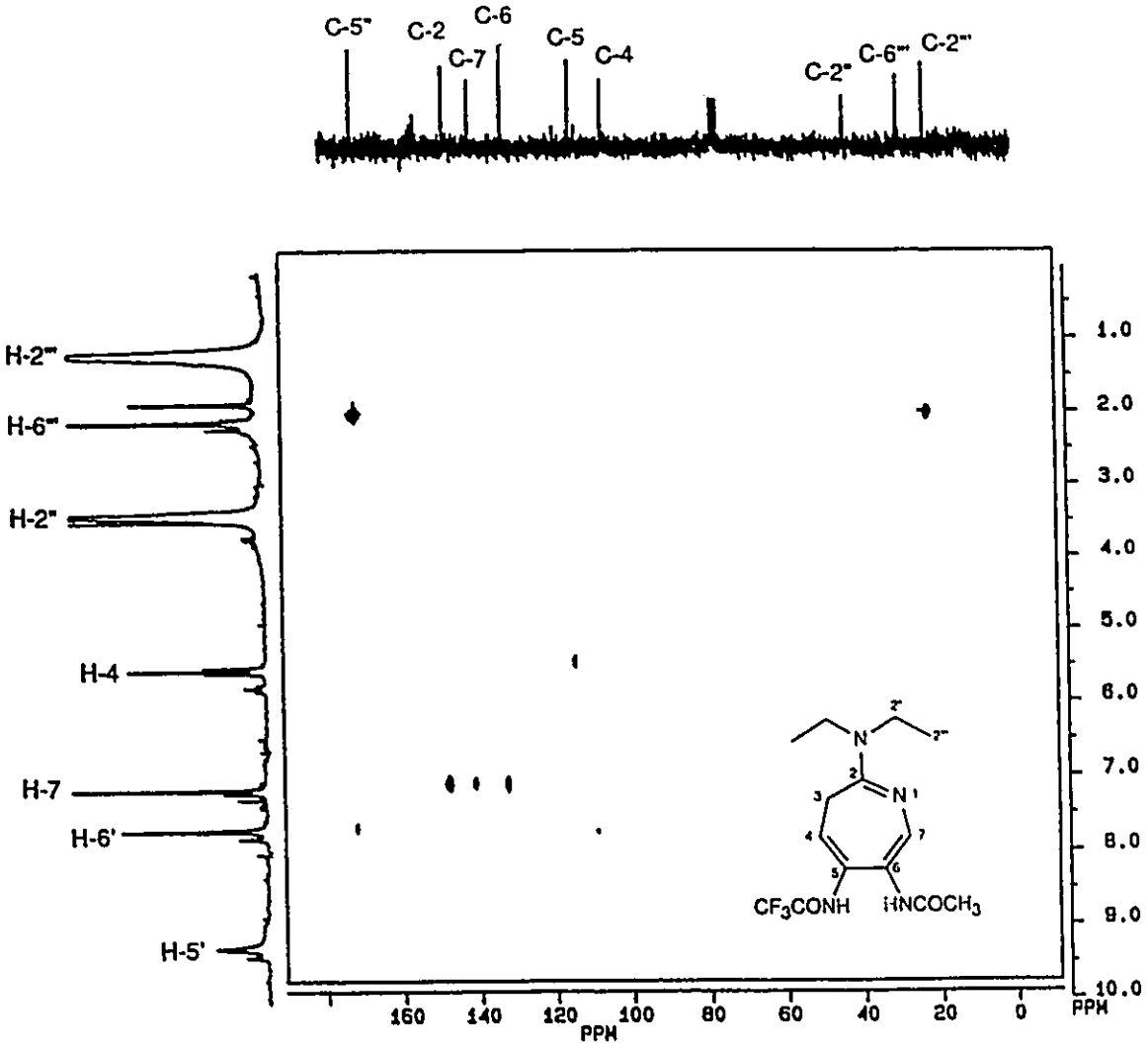

Figure 5.7a ^{1}H - ^{13}C *Long Range HET-CORR of 55.*

HRMS found the exact mass to be 332.1468 g/mol which was -0.8 millimass units off from the calculated mass of 332.1460 g/mol indicating the molecular formula of $C_{14}H_{19}F_3N_4O_2$ was correct. The fragmentation pattern in the EI MS was consistent with the structure of **55** to produce the major fragments $COCH_2$, $NHCOCF_3$ and $HNEt_2$. The CI MS showed one peak attributed to protonation of **55**.

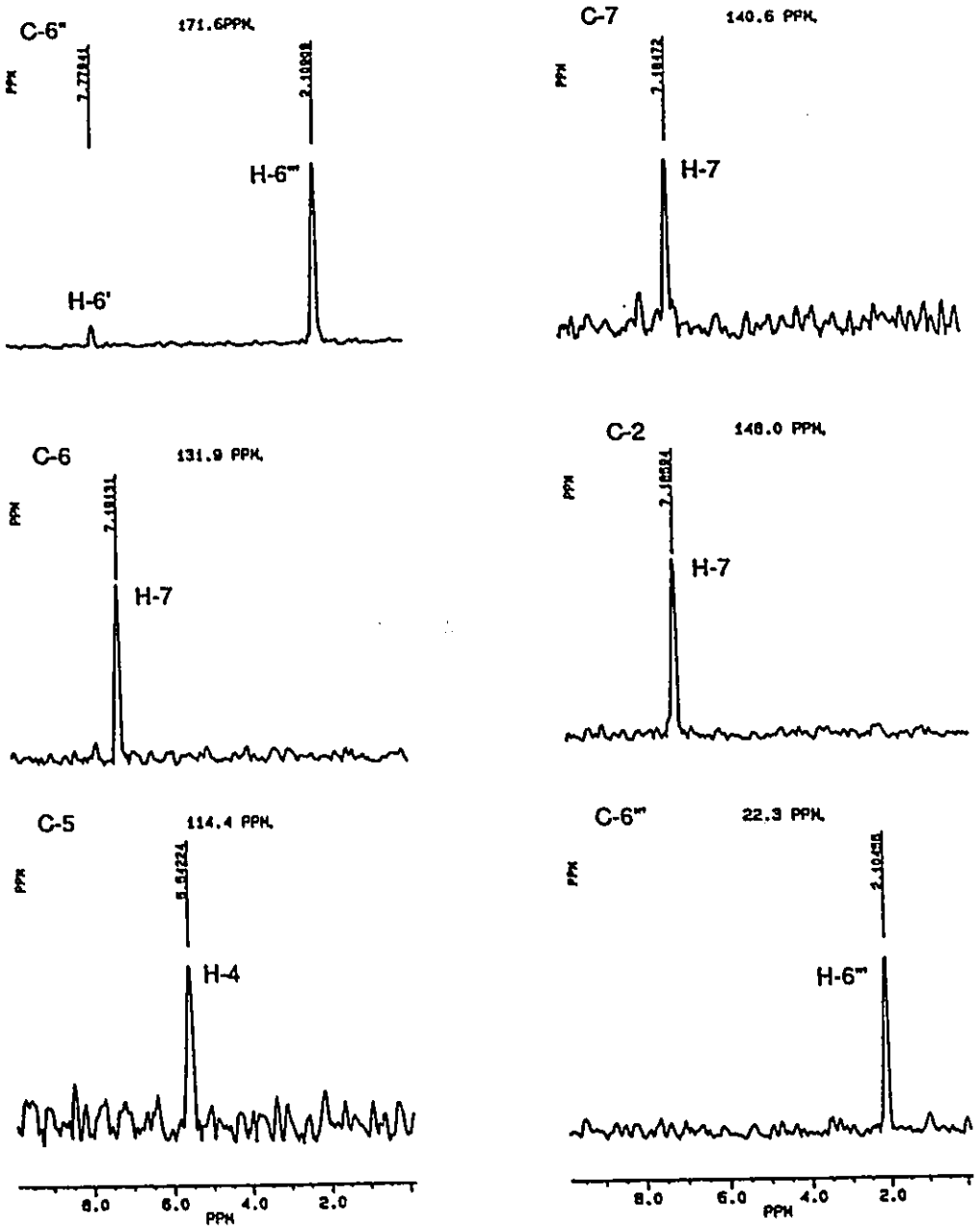

Figure 5.7b ^{1}H - ^{13}C *LR HET-CORR Cross Sections of* ***55****.*

4-Acetamido-2-diethylamino-5-trifluoroacetamido-3H-dihydroazepine, 56.

The 1D ^{1}H NMR spectrum was consistent with the structure of 56 with characteristic shifts of a pair of doublets at 5.80 and 6.93 (J = 8.5 Hz) due to the ring hydrogens, H-6 and H-7, respectively, on a 3H-dihydroazepine. The ^{1}H NMR spectrum also showed the signals for the diethylamine moiety H-2' (1.10 ppm) and H-2" (3.09 ppm), for the acetamide H-4"' (1.73 ppm) and H-4' (8.65 ppm) as well as the resonance for the trifluoroacetamide H-5' (9.5 ppm). The ^{13}C spectrum again showed distinctive couplings due to the ^{13}C-^{19}F couplings on C-5"' (δ = 115.8 ppm, J = 286 Hz) and C-5" (δ = 155.0 ppm, J = 37 Hz) along with signals indicative of the acetamide C=O for C-4" at 169.5 ppm.

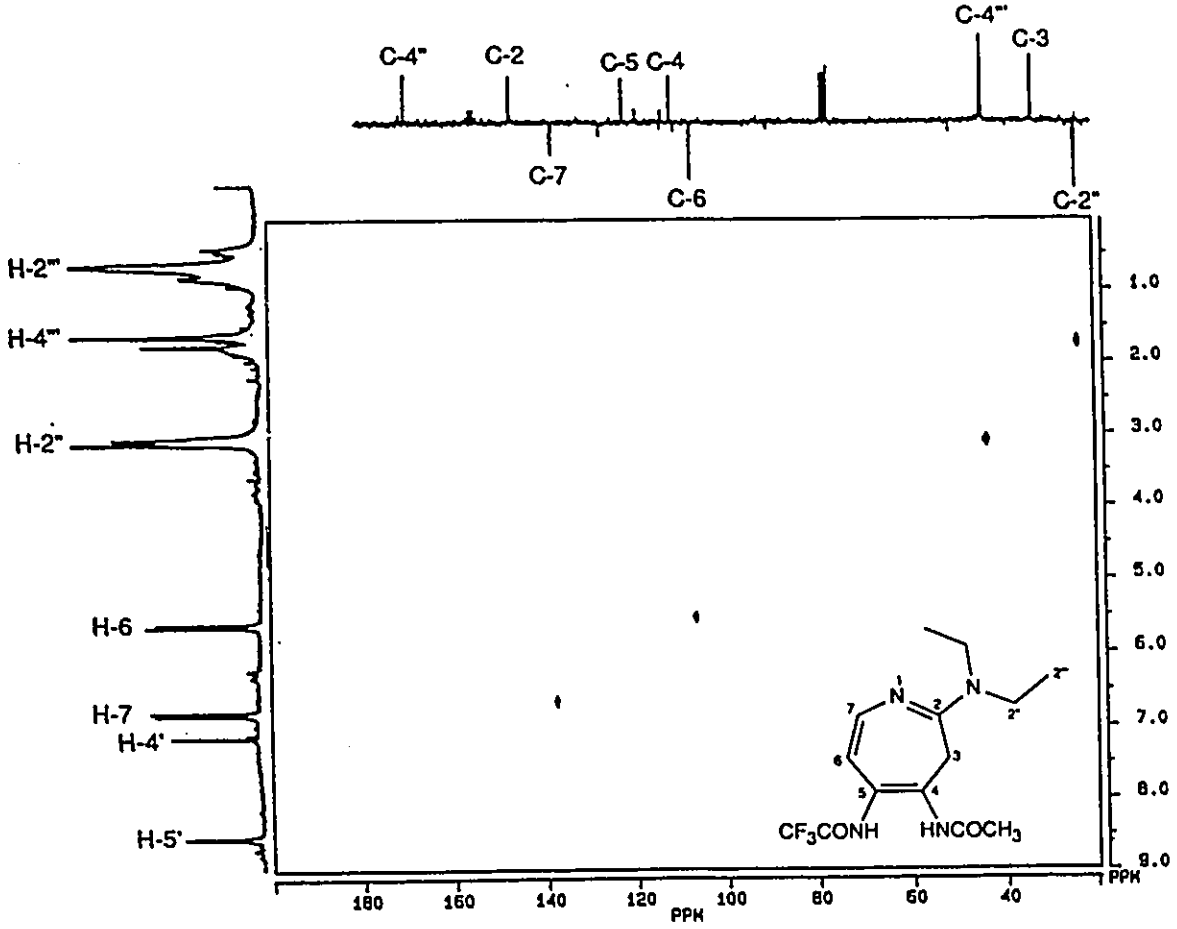

Figure 5.8a ^{1}H - ^{13}C HET-CORR of 56.

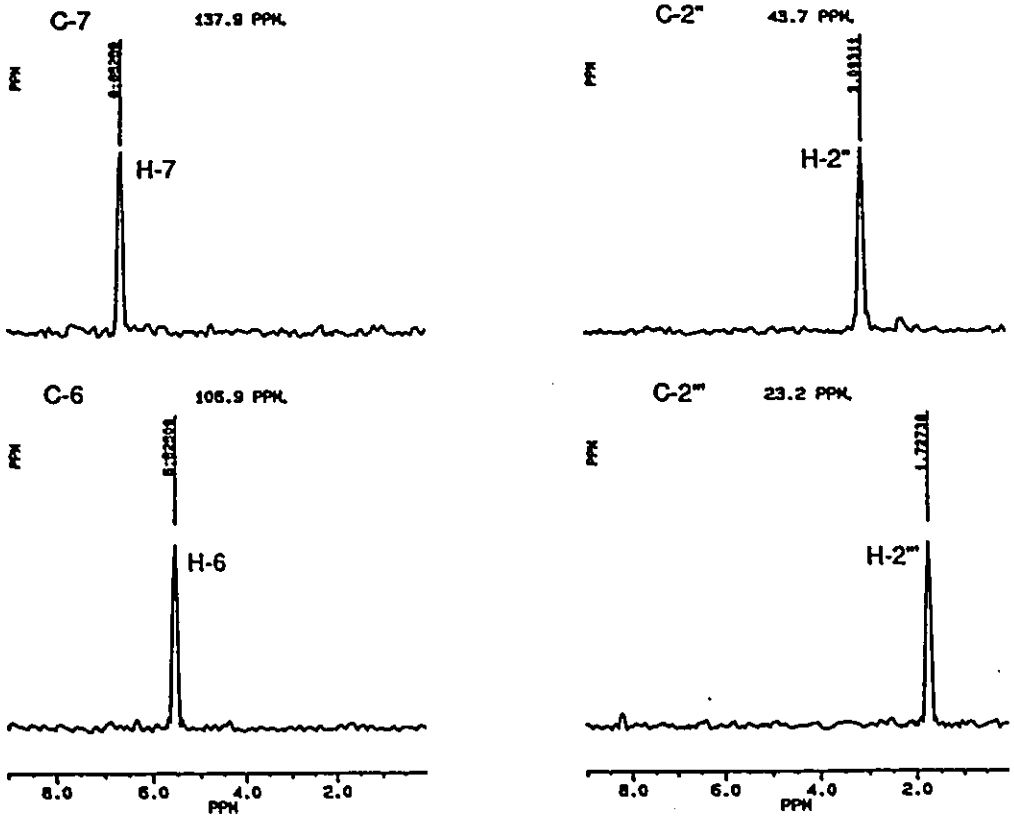

Figure 5.8b ^{1}H - ^{13}C *HET-CORR Cross Sections of* ***56****.*

The heteronuclear shift correlated spectra (Figures 5.8a and 5.8b) showed correlations between CH_2-2", CH_3-2"', CH-6 and CH-7 which indicated the chemical shift for C-2"' was 14.0 ppm. The H-3 shift was not observed in either the one dimensional ^{1}H NMR spectrum nor the two dimensional contour plot in the heteronuclear shift correlated spectrum because of conformational exchange and unfortunately was not seen in the cross-sections because the signal-to-noise ratio was too low.

Using HRMS the exact mass was determined to be 332.1468 g/mol which is -0.8

millimass units off from the calculated mass of 332.1460 g/mol indicating the molecular formula of $C_{14}H_{19}F_3N_4O_2$ was correct. The fragmentation pattern in the EI MS from **56** was consistent with the loss of fragments CH_3, CH_2CH_3, $HCOCH_3$, $NHCOCH_3$ and $HNEt_2$. The CI MS showed one peak attributed to protonation of the azepine **56**.

Summary

The proton and carbon shifts of **55** and **56** are listed in Tables 5.4 and 5.5. The carbon resonances for carbons with the same substituents were found to be very similar. The proton shifts were consistent with literature values[9a].

Table 5.4 *^1H Resonances for the 3H-Dihydroazepines **55** and **56**.*

Azepine	^1H Shifts /ppm									
	Ring Proton					NEt_2		$NHCOCH_3$		$NHCOCF_3$
	H-3	H-4	H-5	H-6	H-7	H-2"	H-2"'	NH	CH_3	NH
55	2.03 3.31	5.47	-†	-†	7.11	3.41	1.10	9.2	1.77	10.5
56	-‡	-†	-†	5.80	6.93	3.09	1.10	8.65	1.73	9.5

† No protons occupied these locations.
‡ The resonances could not be distinguished from baseline noise.

Table 5.5 *^{13}C Resonances for the 3H-Dihydroazepines **55** and **56**.*

Azepine	^{13}C Shifts /ppm											
	Ring Carbon (substituent)						NEt_2		$NHCOCH_3$		$NHCOCF_3$	
	C-2	C-3	C-4	C-5	C-6	C-7	C-2"	C-2"'	CH_3	C=O	CF_3	C=O
55	147.8 (NEt_2)	29.4 (H_2)	105.9 (H)	114.4 (NTf)	132.4 (NAc)	141.0 (H)	43.4	12.4	22.3	172.1	115.8	155.7
56	146.6 (NEt_2)	32.7 (H_2)	111.0 (NAc)	121.6 (NTf)	106.5 (H)	137.5 (H)	43.7	14.0	23.1	169.5	115.8	155.0

5.3.3 Discussion

The azide **49** was initially irradiated at 300 nm in THF at 30°C using 2M $HNEt_2$. The reaction yielded only the diamine product **57** which was inconsistent with literature reports which stated that only bicyclic arylnitrenes form products derived from the trapping of azirine intermediates[9a-o,11]. The product was initially thought to be derived from a Cope type rearrangement of the 1H-dihydroazepine **65** and not through an azirine intermediate (Figure 5.9).

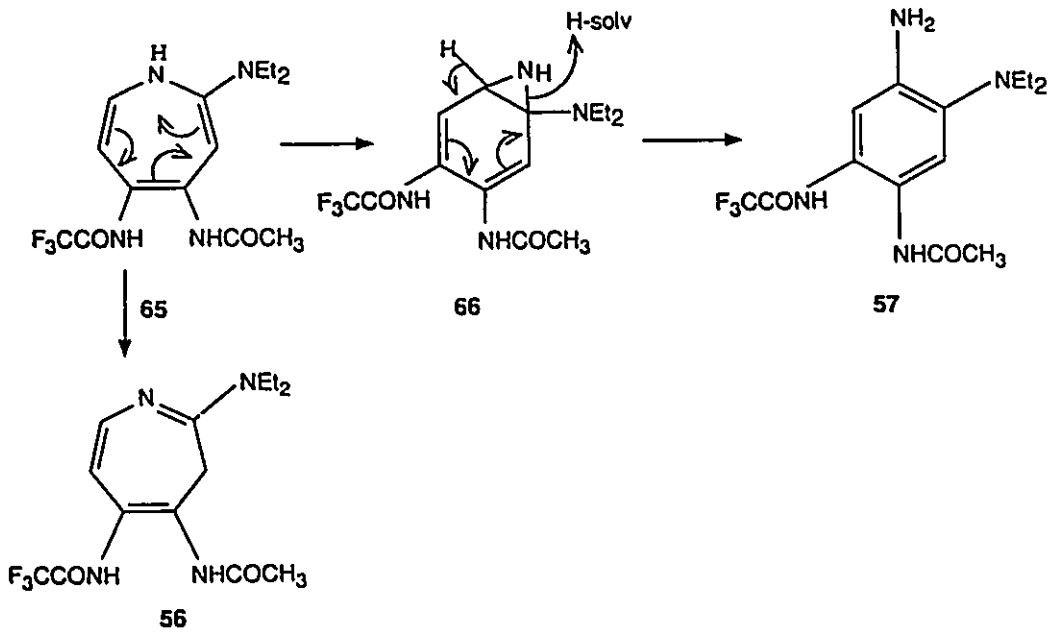

Figure 5.9 *Proposed Rearrangement of the 6-Azepine Product to yield the observed Diamine Product* ***57****.*

The temperature of the photolysis reaction was therefore reduced to -70°C (in the presence of the same concentration of $HNEt_2$) with the intent to slow the rearrangement of the **65** to the aziridine **66** to produce more **56**. The diamine **57** remained the predominant product along with some of the triplet state derived aniline **52** at -70°C and again there was a complete absence of any azepine products. It was concluded that the

aniline product was formed in higher yield at -70°C than at 30°C because intersystem crossing of the singlet to triplet was temperature independent while the rearrangement reaction was temperature dependent[90]. This led to the proposal that the azirine intermediate was the precursor to the diamine since the azirine was trapped with diethylamine analogous to the bicyclic arylnitrene systems.

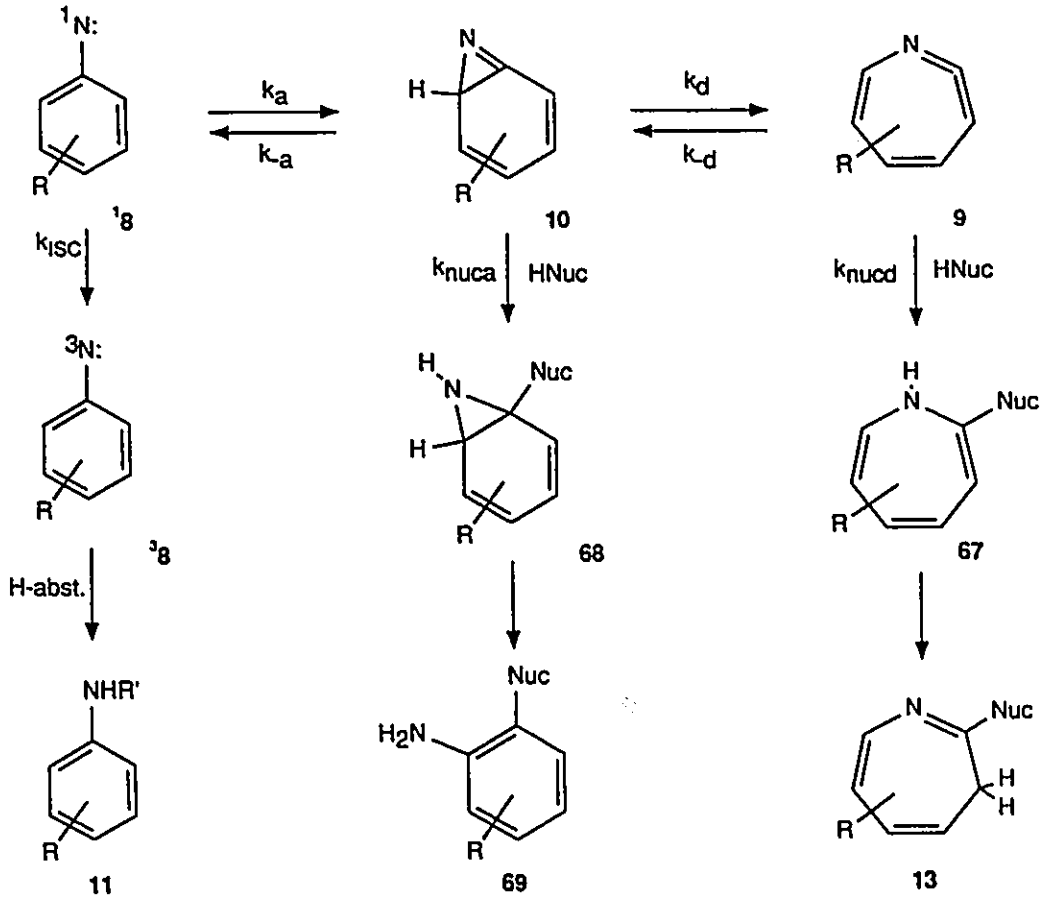

Figure 5.10 *General Mechanism of Phenylnitrene Ring Expansion.*

If the azirine was the precursor to the didehydroazepine then trapping of the azirine with nucleophiles should be in direct competition with its rearrangement to the

didehydroazepine intermediate (Figure 5.10). Therefore lowering of the nucleophile concentration should favour didehydroazepine formation and subsequently increase the yield of 3H-dihydroazepines. Lowering the $HNEt_2$ concentration (Table 5.3, Entries 2 → 7a-c → 3) did result in the formation of more of the 3H-dihydroazepines **55** and **56** which confirmed this hypothesis. However, at low temperatures, such as at -70°C, the diamine product **57** continued to be the only ring closure product even at low $HNEt_2$ concentrations (Entry 6a-c).

The commonly accepted mechanism of phenylnitrene ring expansion to yield 3H-dihydroazepines is shown in Figure 5.11 with the direct formation of the didehydroazepine intermediate[9a,b,d,e,k,n-s] from the singlet phenylnitrene as the initial step. The didehydroazepine is thought to be in equilibrium with the singlet phenylnitrene and can be trapped with nucleophiles to form 1H-dihydroazepines that thermally rearrange to the isolated 3H-isomers. The results for the photolysis of **49** clearly demonstrate that the common mechanism was not operative with the 3,4-diamido-phenylnitrenes.

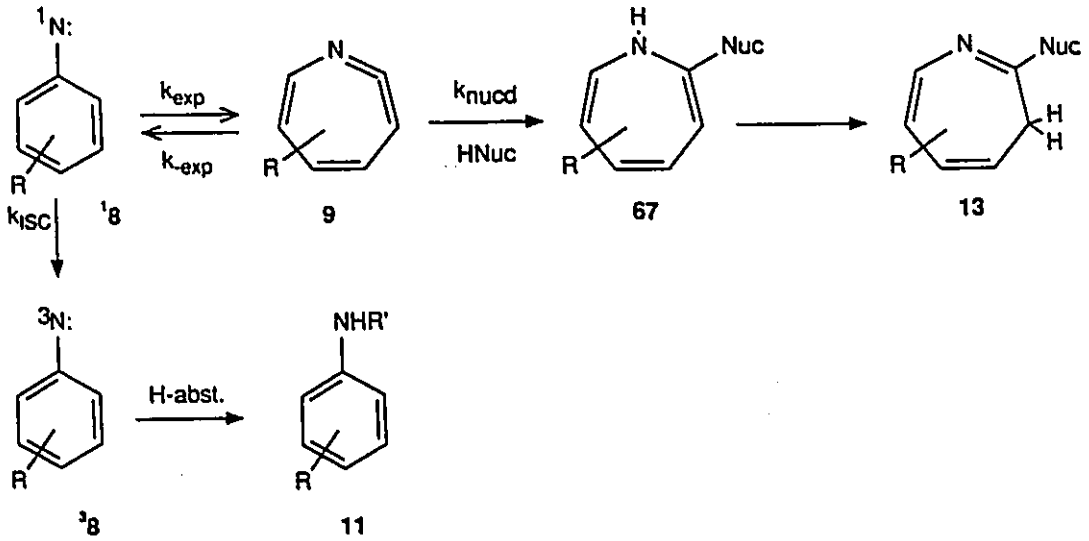

Figure 5.11 Literature Mechanism of Phenylnitrene Ring Expansion.

An alternative mechanism was the independent formation of the two transient intermediates directly from the singlet phenylnitrene. This was ruled out in this case since the rate of formation of each transient would have been independent of the other. The rate of trapping of one intermediate over the other would therefore be independent of nucleophile concentration. In addition, the diamine product is the only product observed at -70°C, even at low concentrations of $HNEt_2$, indicating the azirine is formed *before* the didehydroazepine.

The temperature of the reaction should play an important role in the competitive rearrangements the singlet phenylnitrene could undertake. Lowering of the temperature should favour ISC since ISC is known to be temperature independent[90] while the remaining pathways should proceed at a slower rate because they require thermal activation. The reaction temperature was varied from -70°C to 55°C in the presence of 5.2 mM $HNEt_2$ (Entries 7,8 and 9 in Table 5.3) and showed that as the reaction temperature was increased, more of the trapped didehydroazepine intermediates were formed. This provided evidence for the formation of the didehydroazepine intermediates from the rearrangement of the azirine intermediates.

5.4 Kinetic Evaluation of the Photolysis of 5-Azido-2-trifluoroacetamido-acetanilide.

5.4.1 Introduction

The photolysis of **49** was unquestionably complicated with the formation of products derived from the trapping of azirine and didehydroazepine intermediates. The steady-state kinetics for the ring expansion reaction was determined for the photolysis of **49**. The rearrangement of the singlet phenylnitrene ^{1}**59** to the azirine and

didehydroazepine intermediates was considered reversible.

The azide **49** was irradiated at four different temperatures (-30, 0, 35 and 60°C) in low concentrations of $HNEt_2$ in THF to low conversion of the azide. The four temperatures were chosen to show the effect of temperature on the product distributions while the diethylamine concentrations were kept low (1 to 20 mM) to allow trapping of the didehydroazepine and azirine intermediates. The results are shown in Table 5.6 illustrating the dramatic effect that both temperature and nucleophile concentration have on the observed product ratios.

5.4.2 Kinetic Evaluation of the Intermediates Formed

The rates of each pathway possible from the phenylnitrene ^{1}**59** derived from **49** can be expressed as a series of rate constants and concentrations of intermediates as shown in Figure 5.12. The absolute rates for this system were unobtainable without the use of high speed detection techniques such as laser flash photolysis[19] and therefore only the relative rates were calculated. The singlet phenylnitrene, ^{1}**59**, can rearrange to either of the two azirines, **60** (closure to the 2-position) or **61** (closure to the 6-position), with rate constants k_{2a} and k_{6a} respectively, or ^{1}**59** can intersystem cross to the triplet state ^{3}**59**, with a rate constant of k_{ISC}. The triplet phenylnitrene is then trapped, by hydrogen abstraction[9], to give the isolated aniline product **52**. The azirines can rearrange further to the didehydroazepines (**60** → **62** or **61** → **63**), with rate constants k_{2d} and k_{6d}, respectively; or alternatively they can be trapped by nucleophiles, such as $HNEt_2$, to yield the diamine products **57** and **58**, with rate constants k_{nuc2a} and k_{nuc6a}, respectively. The didehydroazepines, **62** and **63**, can be trapped by nucleophiles, with rate constants k_{2dnuc}

and k_{6dnuc}, to yield the isolated 3H-dihydroazepines **55** and **56**, respectively; rearrange to the triplet phenylnitrene ^{3}**59**[9a]; or, in the absence of nucleophiles, to azo compounds[9n] or polymerize to yield tar[9b]. Rearrangement of the didehydroazepines to ^{3}**59**, azo compounds or tar have been designated here by a combined rate constant k° (or k_2° and k_6°, respectively). All of these rearrangement processes of the highly reactive intermediates have the potential of being reversible, except for intersystem crossing (k_{ISC}), dimerization and polymerization (k_2° and k_6°), and are labelled accordingly in Figure 5.12.

Chapter 4 outlined some of the kinetic data for phenylnitrene ring expansions showing that the azirine heats of formation had no relationship to product distributions and drawing the conclusion that either the singlet phenylnitrene was in equilibrium with the azirines or that the azirines did not exist as intermediates. The results from the photolysis of **49** showed that azirines do indeed exist for these phenylnitrene systems, as evidenced by the product **57** derived from the trapping of the azirine intermediate **61**. Thus the azirines can be considered to be formed from the singlet phenylnitrene. The photolysis results at -70°C indicated that rearrangement of ^{1}**59** to **61** was no longer reversible since trapping of the 6-azirine intermediate **57** was predominant at this temperature regardless of the nucleophile concentration used (3.5 - 2000 mM). The charge distribution on the phenylnitrene ^{1}**59** predicted the 6-azirine intermediate **57** should have been formed preferentially, as was observed at -70°C, confirming the legitimacy of the AMPAC model in predicting the direction of ring closure.

Furthermore, the results presented in Chapter 4 indicated that the didehydroazepines may be formed reversibly from the singlet phenylnitrene, in keeping with the literature[9]. This was illustrated by the influence the difference in heats of formation

of the two didehydroazepines had on the ratio of 3H-dihydroazepine product. This phenomenon could also arise from a lowering of the activation barriers for the ring expansion of the azirines to didehydroazepines for the system that forms the lower energy didehydroazepine.

Table 5.6 Product Distributions from the Kinetic Photolysis of 49.

Temp. /°C	Azide conc. [49] /mM	$[HNEt_2]$ /mM	Ratio of Products by ^1H NMR†			
			49	57	55	56
-30	4.50	16.69	92.9*	6.3*	0.8*	0
		13.34	90.3	7.0	2.7	0
		8.34	90.3	6.4	3.3	0
		6.67	90.0	7.4	2.6	0
		5.00	87.1	7.0	5.9	0
		3.34	91.1*	6.4*	2.5*	0
		1.67	85.4	6.0	8.1	0.5
0	4.50	16.60	78.1	12.0	8.9	0.9
		13.28	79.5	9.5	9.7	1.3
		9.96	82.0	7.5	9.4	1.1
		8.30	81.4	7.0	10.6	1.0
		6.64	77.4	7.5	13.6	1.5
		4.98	75.1	6.4	16.6	1.9
		3.32	78.2	4.1	15.9	1.8
		1.66	84.0	0.9	12.6	2.4
35	4.50	17.09	92.5	3.3	3.5	0.7
		13.67	90.9	3.9	4.2	1.0
		10.25	91.7	3.7	3.6	1.0
		8.55	90.1	4.2	4.2	1.4
		6.84	89.8	4.3	4.5	1.5
		5.13	89.5	4.2	4.5	1.7
		3.42	90.6	4.2	3.4	1.7
		1.71	93.4	3.1	1.8	1.6
60	4.50	16.60	89.5	2.1	5.2	3.2
		13.28	76.9	3.9	13.7	5.4
		9.96	79.6	2.9	12.2	5.2
		8.30	59.6*	2.7*	32.1*	5.6*
		6.64	70.9	3.4	16.4	9.3
		4.98	84.2	2.4	7.5	5.9
		3.32	74.5	4.1	10.7	10.7
		1.66	80.9*	2.1*	5.8*	11.2*

† No 52 or 58 was visible in the ^1H NMR spectra.
* ^1H NMR integrals were not very reliable.

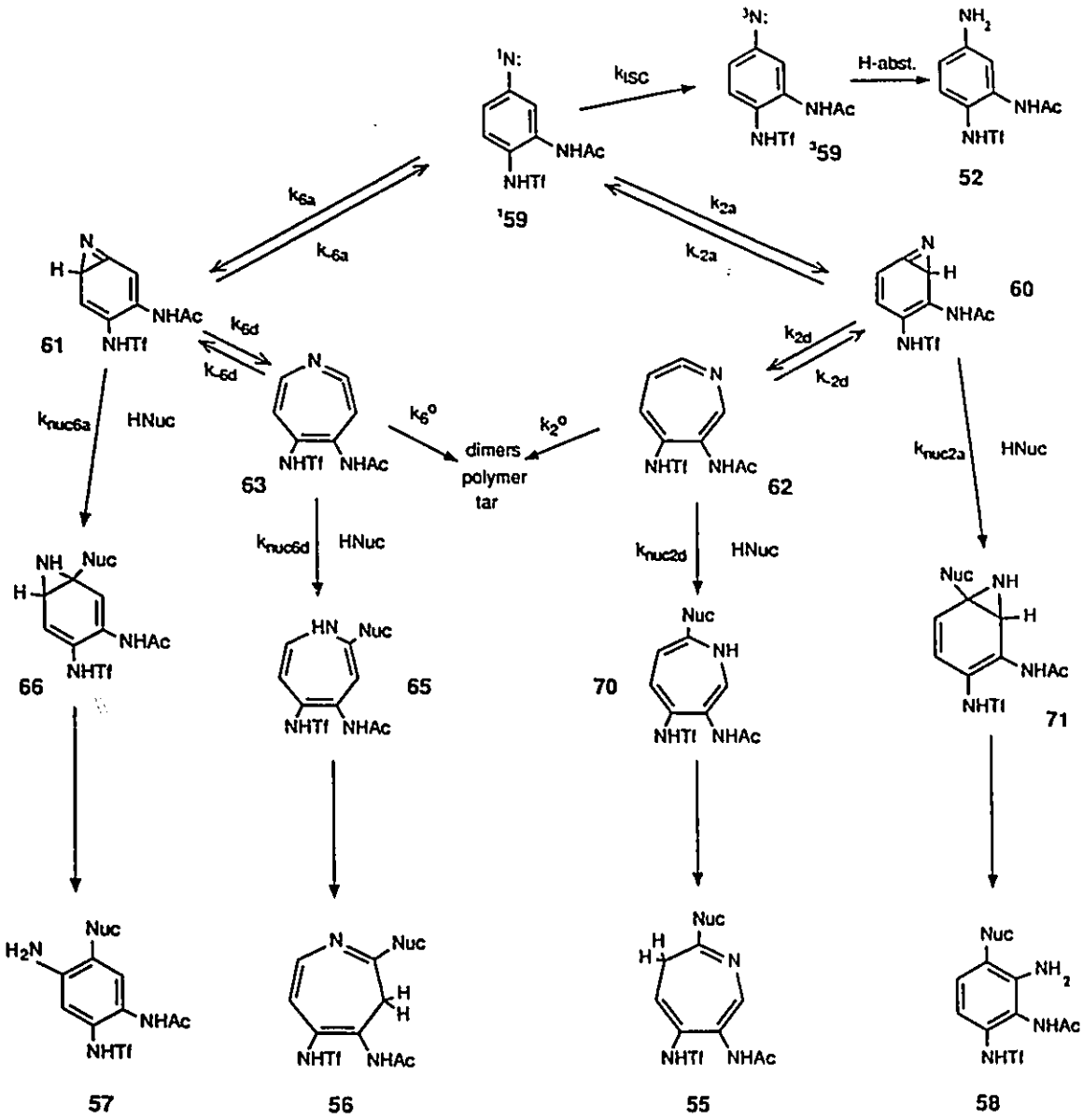

Figure 5.12 Mechanism of Ring Expansion of 49 from the Phenylnitrene 59.

These results indicate that, as a general rule, the singlet phenylnitrene and the azirines may be in equilibrium at and above room temperature and that the didehydroazepines may also be in equilibrium with the azirines. These restrictions were kept in mind when the steady-state analysis (Appendix 1) of the reaction scheme was examined with the reversible steps included. From this the 6-diamine yield over the 6-azepine yield (57/56) can be expressed as a series of rate terms shown below:

$$\frac{[6\text{-}diamine]}{[6\text{-}azepine]} = \frac{k_{nuc6a}[HNuc][6\text{-}azirine](k_{-6d} + k_6^o + k_{nuc6d}[HNuc])}{k_{nuc6d}k_{6d}[HNuc][6\text{-}azirine]}$$

This expression can be simplified to:

$$\frac{[6\text{-}diamine]}{[6\text{-}azepine]} = \frac{k_{nuc6a}(k_{-6d} + k_6^o)}{k_{nuc6d}k_{6d}} + \frac{k_{nuc6a}[HNuc]}{k_{6d}}$$

A plot of the ratio of 6-products (57/56) versus the concentration of nucleophile ([$HNEt_2$]) will have the following slope, intercept; and ratio of intercept to slope:

$$slope = \frac{k_{nuc6a}}{k_{6d}} \qquad intercept = \frac{k_{nuc6a}(k_{-6d} + k_6^o)}{k_{nuc6d}k_{6d}}$$

$$\frac{intercept}{slope} = \frac{k_{-6d} + k_6^o}{k_{nuc6d}}$$

Analogous equations can be derived for the system that yields the 2-products 58 and 55. The 2-closure reaction yielded only one product, the azepine 55. This indicates

that the 2-azirine intermediate **60** rearranged exceedingly fast to the 2-didehydroazepine intermediate **62** (relative to its trapping by amines to yield the 2-diamine product **58**). From this, the reaction of **62** to **60**, if it occurs, must by relatively slow (i.e. $k_{2d} >> k_{-2d}$). The 6-closure reaction did exhibit selection in the reaction to yield either **56** or **57** depending on the reaction conditions used. The 6-closure results are illustrated in the graph in Figure 5.13 and the kinetic data derived are given in Table 5.7.

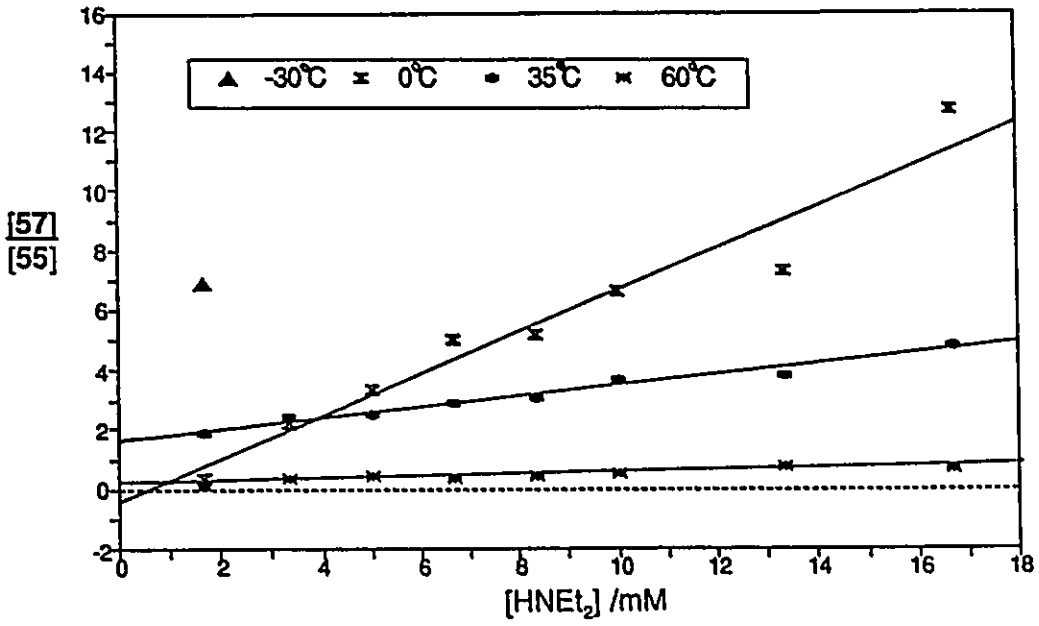

Figure 5.13 *Plot of the Ratio of 6-Closure Products Versus the Trapping Amine Concentration.*

The calculated slopes reveal the rate of trapping of the 6-azirine **61** relative to its rearrangement to the 6-didehydroazepine **63**:

$$\frac{rate(6\text{-}diamine_{trapping})}{rate(6\text{-}diamine_{rearrangement})} = \frac{k_{nuc6a}[HNuc]}{k_{6d}}$$

The intercept divided by the slope yields the rate of rearrangement of the didehydroazepine **63** relative to it being trapped to form the azepine **56**.

$$\frac{rate(6\text{-}dide_{rearrangement})}{rate(6\text{-}dide_{trapping})} = \frac{k_{-6d} + k_6^o}{k_{nuc6d}[HNuc]}$$

Table 5.7 *Kinetic Data Calculated for the Photolysis of* ***49****.*

Temp. /°C	$\frac{k_{nuc6a}}{k_{6d}}$ /M^{-1}	$\frac{k_{nuc6a}(k_{-6d} + k_6^o)}{k_{6d}k_{nuc6d}}$	$\frac{k_{-6d} + k_6^o}{k_{nuc6d}}$ /M
60	31.5 (s=5.7)	0.22 (s=0.76)	0.007 (±0.05)
35	174.1 (s=12.7)	1.67 (s=0.17)	0.010 (±0.04)
0	719.1 (s=71.4)	-0.47 (s=0.95)	-0.001 (±0.003)
-35	>10^4	-	-

The relative rate of trapping of **61** to that of rearrangement of **61** → **63** was found to be low at temperatures above 0°C using low nucleophile concentrations (k_{nuc6a}[HNuc]/k_{6d} ~ 0.03 at 60°C, ~ 0.17 at 30°C and ~ 0.72 at 0°C, for $HNEt_2$ ~ 10^{-3} M). Below -30°C the azirine **61** must be adequately stabilized to be trapped efficiently before rearrangement

to **63** can occur since minimal production of **56** was found above 3 mM concentration of $HNEt_2$ at -30°C and since no production of **56** was evident at -70°C regardless of the diethylamine concentration. At 30°C the ratio of 6-products (**57** : **56**) was highly in favour of production of **57** when the amine concentration was 2 M. This is not surprising since extrapolation of the kinetic data at 35°C for the ratio of products indicates $k_{nuc6a}[HNEt_2]$ = 350 k_{6d}, and therefore the relative yield of 6-azepine, **56**, should be around 0.3% which is too low to be determined by NMR integration.

The rate terms k_2^o and k_6^o represent decay of the didehydroazepines to yield triplet phenylnitrenes or to polymerization of the didehydroazepines. The rearrangement of **63** (to **61** or to polymer) was determined to be negligible at 0°C and 60°C ($\{k_{-6d} + k_6^o\}/k_{nuc6d}$ – 0) indicating the reverse reaction of the 6-didehydroazepine **63** to **61** was slow relative to its trapping with diethylamine. At 35°C the rearrangement of **63** appeared to become competetive with it being trapped ($\{k_{-6d} + k_6^o\}/k_{nuc6d}[HNEt_2]$ = 10 ± 3 when $[HNEt_2] = 10^{-3}$ M). The results at 35°C suggested that **61** and **63** were in equilibrium or that **63** was polymerizing[9b] at low concentrations of diethylamine but not at 60°C. These conflicting results may have arisen because of an impurity in the bulk azide solution that reacted with the intermediates formed for the photolysis reaction at 35°C. The rearrangement of the didehydroazepines to triplet phenylnitrene appeared to be insignificant since no aniline products were observed in the photolysis products for the four temperature ranges investigated.

During the photolysis of **49** above room temperature, as shown in Table 5.3, the yield of aniline product **52** was consistently low when low nucleophile concentrations were used (between 3.5 and 5.2 mM) confirming the low rate of production of triplet

phenylnitrene. At very low concentrations of amine, such as at 1.8 mM in Table 5.3 (Entry #3 in Table 5.3), the yield of **52** increased to 26% indicating the rate of triplet phenylnitrene ^{3}**59** production from didehydroazepine was becoming significant. The production of ^{3}**59** from the didehydroazepines can occur via two modes; directly from the didehydroazepines, indicated here by k°, as described by Schuster *et al.*[9a]; or through the reverse reaction of the didehydroazepine through the azirine and subsequently through the singlet phenylnitrene, indicated by k_{-d} and k_{-a} terms.

If the didehydroazepine intermediates rearrange back to the singlet phenylnitrene, as proposed via the azirine intermediates, then the terms k_2° and k_6° describe the polymerization of the didehydroazepines only. The formation of ^{3}**59** from the didehydroazepine intermediates can arise from the reverse reaction of the intermediates to ^{1}**59**. Further evidence for this comes from the observations of Schuster *et al.*[9a] who described an intermediate, labelled X, between the didehydroazepine intermediate and the triplet phenylnitrene that could not be identified. This is consistent with the reverse reaction of the didehydroazepine intermediate through an azirine intermediate and singlet phenylnitrene to yield the triplet phenylnitrene. Therefore the compound X could be the azirine intermediate or the singlet phenylnitrene.

The 2-azirine intermediate **60** was never trapped to yield the 2-diamine product **58** in all the photolysis reactions explored. One of the reasons why **60** was never trapped may be because it contains a formal double bond between the two bulky amide substituents which should create steric strain destabilizing **60**. When **60** rearranges to the didehydroazepine **62** this strain is partially relieved as the formal double bond rearranges to a formal single bond thus increasing the distance between the two bulky substituents.

This is also consistent with the observed trapping of **61** since its rearrangement requires an increase in steric strain going from **61** → **63** with the formal single bond turning into a formal double bond in **63**. The literature contains many bicyclic arylnitrene examples[9t-w,10d] that conform to the hypothesis of stabilization of the azirines which then allows their trapping. In bicyclic systems the fused aromatic ring stabilizes the formal double bond to maintain aromaticity in the fused ring. Thus, in the bicyclic systems, the favoured products were derived from trapping of the 2-azirine and 6-didehydroazepine intermediates with some trapping of the 2-didehydroazepine intermediate. The literature results as well as those presented here indicate a strong preference for trapping of the stabilized azirine intermediate. This explains why the mono-cyclic phenylnitrenes traditionally do not yield products derived from trapping of the azirine intermediate.

***Table 5.8** Ring C-C Bond Lengths Between the two Amido Groups for the Intermediates formed from **59**.*

	Ring C-C bond length between the two amido groups /Å		
	azirines	didehydroazepines	|difference|
2-products	1.402 (C=C)	1.505 (C-C)	0.103
6-products	1.500 (C-C)	1.401 (C=C)	0.099

To test this hypothesis the bond lengths of the azirines and didehydroazepine intermediates in this system were extracted from the AMPAC minimized geometries (shown in Table 5.8). It is clear from the calculations that the 6-didehydroazepine **63** crowds the two amide substituents closer together by 0.1 angstroms compared to the 6-

azirine **61**. This steric congestion may be the driving force which slows the rate of rearrangement of **61** → **63** enough to permit trapping of **61**. On the other hand, the 2-azirine **60** crowds the two amido groups together by a 0.1 angstroms relative to the 6-didehydroazepine **62**. This steric strain drives the rearrangement **60** → **62** to the point of exclusion of trapping **60**.

5.5 Photolysis of 3,4-Di-(trifluoroacetamido)-phenylazide.

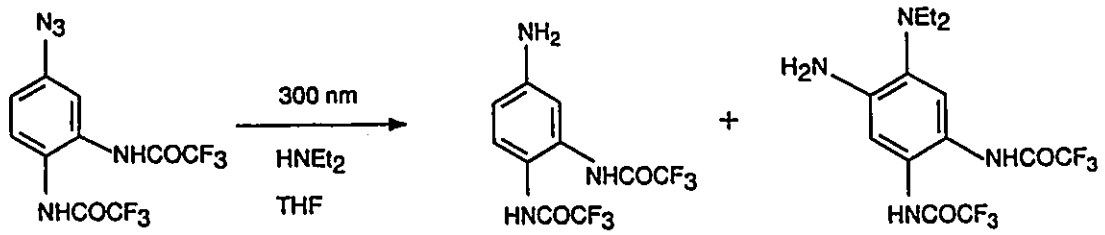

48 **54** **64**

Figure 5.14 *Photolysis Products from the Irradiation of* ***48****.*

Table 5.9 *Photolysis Products from the Irradiation of* ***48****.*

Entry	Photolysis Conditions[a]	[HNuc] (x 10^{-3} M)	HNuc	Yield of products[b] (%)		
				Azide	Aniline	6-Diamine
1	30°C, 45 min	2000	C_6H_{12}	0	46	54
2	30°C, 30 min	5.0	THF	0	20	80

a) Photolysis in THF in quartz tubes in a 15cm bore Rayonet using 10 300nm bulbs.
b) Ratio determined by ^{1}H NMR integrals.

The 3,4-diamido-phenylazide, **48**, was photolyzed as described in the general procedure outlined in Chapter 3 and the products were characterized by ^{1}H NMR and MS.

The results are shown in Table 5.9 with the only product being **64**, the product of trapping the 6-azirine intermediate. The 6-diamine product **64** persisted even at low concentrations of diethylamine indicating the 6-azirine in this case was the only intermediate formed at 30°C. The higher yield of aniline products and lack of 3H-dihydroazepines, compared to that of **49**, implied the rearrangement of the 6-azirine to the 6-didehydroazepine intermediate was less efficient in this case and the reaction may have proceeded reversibly thus increasing the relative rate of intersystem crossing. The azirine and didehydroazepine intermediates were modelled using the AMPAC program and the bond distances between the two amide groups on each molecule were calculated. The ring C-C bond between the amides was consistently 0.1 angstroms shorter for the formal single bonds over the formal double bonds indicating the rearrangement of the 6-azirine was inhibited by the ensuing steric congestion of the two amido groups.

5.6 Conclusion

The photolysis of **49** shows that at temperatures of -70°C or lower, only the 6-diamine product **57** was observed indicating that the system is under kinetic control and that the singlet phenylnitrene rearrangement to the azirine intermediate **61** was irreversible. At -30°C some of the 2-azepine product **55** was observed but the ratio of 2- and 6-closure products (**55** versus **57** + **56**) varied as the concentration of diethylamine was changed. This indicated that the rearrangement of the singlet phenylnitrene to the azirines was reversible. The didehydroazepine intermediates may have been formed reversibly from the azirine intermediates as well. This also indicated that the activation barrier for ring closure of the singlet phenylnitrene ^{1}**59** to the 2-azirine **60** was overcome

and that the rearrangement of **60** → **62** was exceedingly fast such that no trapping of **60** was observed. The rearrangement of **61** → **63** remained slow relative to trapping of **61** with diethylamine. At 35°C and above, all the transient intermediates were formed reversibly with the product distribution determined by the temperature and concentration of the trapping nucleophile.

The general mechanism presented in the literature[9] should be revised to include the azirine intermediate being formed directly from the singlet phenylnitrene. The azirine then rearranges to form the didehydroazepine intermediate. The trapping of the azirine intermediates requires some stabilization of the azirine to permit its trapping as illustrated by the bicyclic arylnitrene ring expansions[9v,x-z,a'] and by the mono-cyclic 3,4-diamido-phenylnitrene ring expansion reactions presented here. The diamido-phenylnitrene results show that the mono-cyclic and bicyclic arylnitrene reactions proceed through the same mechanism. The azirine intermediates formed from most mono-cyclic phenylnitrenes are too short lived to observe or trap because they are not stabilized.

The AMPAC program, using the AM1 Hamiltonian, provides a valuable insight into the mechanism of the phenylnitrene ring expansion reaction. The charge distribution on the phenylnitrene dictates which azepine should be formed preferentially at low temperatures while the ratio of the didehydroazepine heats of formation governs the azepine product ratio at high temperatures.

The phenylnitrene reaction is highly sensitive to both temperature and concentration and type of nucleophile used to the extent that a study of the product ratios observed must take serious consideration of these factors in order to understand the complete mechanism. To this extent, the thermolysis of arylazides at high temperatures resembles high temperature photolysis of arylazides or high temperature deoxygenation

of nitro-aryl compounds. Thus the low temperature work on photolysis of arylazides should not be directly compared to thermolysis or deoxygenation reactions.

Chapter 6

Attempted Synthesis of 4-Amino-5-imino-azepines

6.1 Attempted Synthesis of Amino-imino-azepines from Diamido-3H-dihydroazepines.

6.1.1 Introduction

Chapter 5 discussed the synthesis of 4-acetamido-2-diethylamino-5-trifluoroacetamido-3H-dihydroazepine, **56**, from the photolysis of the precursor 3-acetamido-4-trifluoroacetamido-phenylazide. It was hoped that the trifluoroacetamide protected amino group on **56** could be deprotected and subsequently oxidized to yield a 4-acetamido-5-imino-azepine to be tested as an MRI chelant as outlined in Chapter 1.

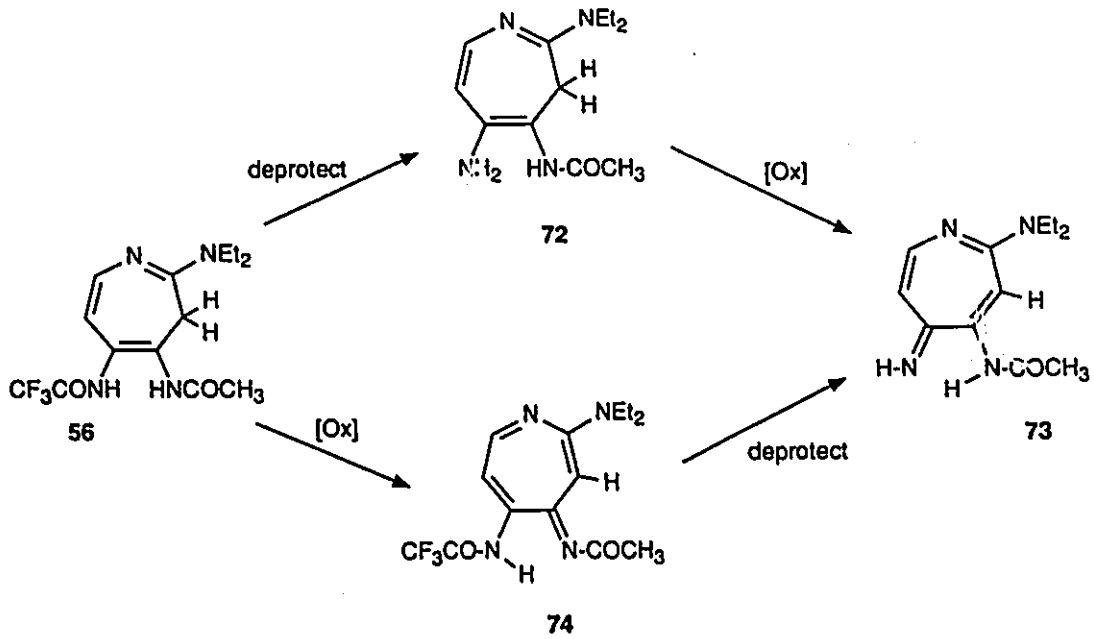

Figure 6.1 *Proposed Synthesis of 4-Acetamido-5-amino-2-diethylamino-azepine.*

There were two routes that were available to convert the 3H-dihydroazepine **56** into the 4-amido-5-imino-azepine **73** (shown in Figure 6.1): one was to initially deprotect the amine group on **56** and subsequently oxidize the resultant 4-acetamido-5-amino-2-diethylamino-3H-dihydroazepine (**72**) to yield **73**; or alternatively, the 3H-dihydroazepine **56** could have been initially oxidized to the 4-acetimido-2-diethylamino-5-trifluoroacetamido-azepine (**74**) followed by deprotection of the amine to yield the desired azepine **73**. The former route was attempted first since the latter proposal involved an unstable acetimido substituent on **74** which may spontaneously reduce to an acetamide (**56**) or degrade via a side reaction.

6.1.2 Deprotection of the Trifluoroacetamide.

The azepines **55** and **56** were not available in great abundance and therefore the deprotection technique was initially tested on a prototype molecule containing a trifluoroacetamido group, 5-nitro-2-trifluoroacetamido-acetanilide (**51**, shown in Figure 6.2). The trifluoroacetamide **51** was refluxed in a saturated potassium carbonate/methanol solution[21b,c] for 5 hours to yield the hydrolysed product, 2-acetamido-4-nitro-aniline (**33**), which was characterized by ^{1}H NMR and by comparison to authentic **33**. The reaction was selective in the deprotection of the trifluoroacetamide while leaving the acetamide intact. This technique seemed to be ideal for the deprotection of **56** since removal of the acetamide was not desired at this point.

A small sample of the 2-closure azepine product, **55**, was therefore treated under similar reaction conditions in an attempt to remove the trifluoroacetyl group to yield the free amine (Figure 6.3). This azepine **55**, which should possess similar chemistry to **56**,

was used to determine if this technique was viable. The reaction of **55** with K_2CO_3/MeOH was monitored by TLC and ^1H NMR but after 5.5 hours at room temperature only **55** was found to be present. The sample was treated again with K_2CO_3/MeOH for 2 days but no change was observed.

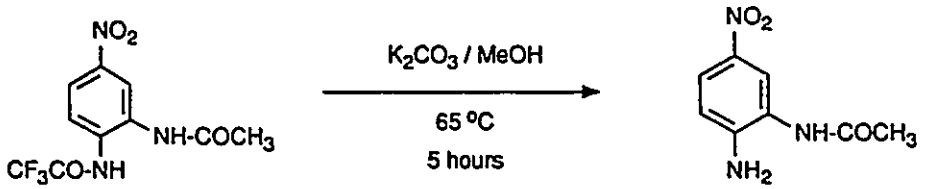

51 **33**

Figure 6.2 *Deprotection of 5-Nitro-2-trifluoroacetamido-acetanilide with K_2CO_3/MeOH.*

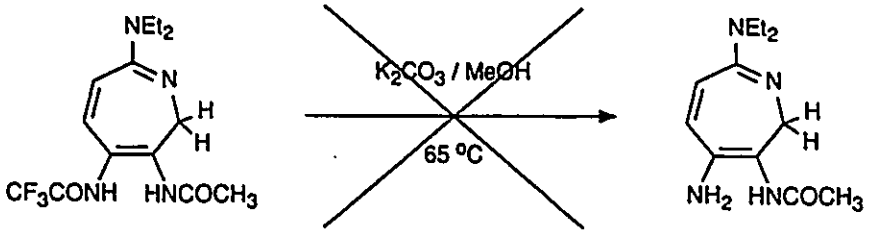

55 **75**

Figure 6.3 *Attempted Deprotection of **55** with K_2CO_3/MeOH.*

The failure of the K_2CO_3/MeOH to deprotect the trifluoroacetamide was attributed to the azepine **55** being less reactive than the prototype **56** (which contained the strongly electron withdrawing nitro substituent). A stronger reagent was required and therefore the saturated ammonia in methanol deprotection technique[21] was attempted.

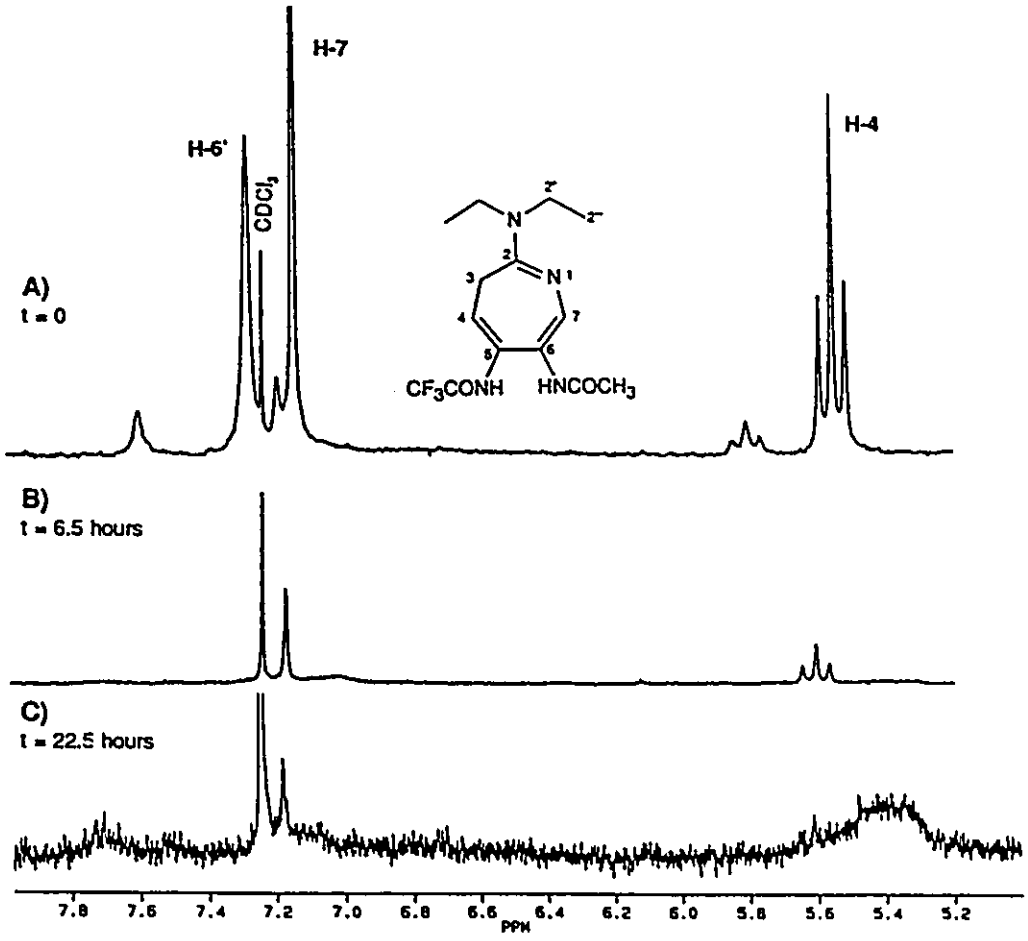

Figure 6.4 Attempted Deprotection of 55 with NH_3/MeOH followed by ^1H NMR.

The 3H-dihydroazepine **55** was treated with a saturated ammonia in methanol solution and the reaction was monitored by ^1H NMR, shown in Figure 6.4 (spectrum A was recorded before any NH_3/MeOH was added) and by TLC. The starting concentration of **55** in the NMR tube was sufficiently concentrated to form micelles of **55** and the ^1H NMR spectrum A shows a doubling of the resonances. After 6.5 hours at room temperature the ^1H NMR showed only the starting azepine **55** (spectrum B). The loss of the doubling of the shifts indicated the concentration of **55** had decreased dramatically. No resonances could be attributed to the 6-acetamido-5-amino-3H-azepine (**75**) in the spectrum. The

azepine was treated for a further 16 hours with NH_3/MeOH but only a small amount of **55** was visible in the ^1H NMR (spectrum C) and still no other products could be ascertained from the spectrum. The loss of signal intensity in the spectrum as time progressed arose from the consumption of **55** through a side reaction, most probably a polymerization as suggested by the broadness of the residual signals. Mass spectral analysis of the final mixture (material with ^1H NMR spectrum C in Figure 6.4) showed a compound with mass 174 g/mol was present which was lower than that of the fully deprotected **55** (195 g/mol). No signal for the trifluoroacetamide deprotected azepine **75** at 236 g/mol was detected. These results indicated that deprotection of the 3H-dihydroazepine was not feasible using strong base hydrolysis conditions.

The 3H-dihydrozepines, such as **76** in Figure 6.5, are reported to rearrange under acidic conditions to yield aniline compounds **77**[25b]. The reaction was stated to proceed through a 1H-dihydroazepine **67** that rearranged to aziridine **68** which subsequently aromatized to the aniline **77.**

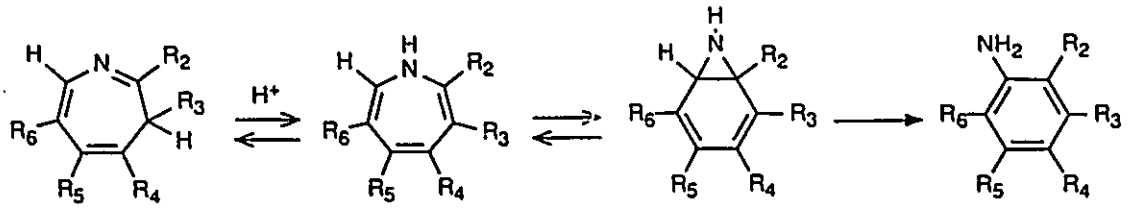

***Figure 6.5** Acid Catalyzed 3H-Dihydroazepine Rearrangement.*

It was possible that the strongly basic conditions used to deprotect the azepines catalyzed a rearrangement before and/or after the azepines were deprotected. The analogous rearranged aniline product from **55** should have been the 2-diamine product

58, which was not observed during the photolysis reaction of 49. The ^{1}H NMR spectrum of the compound produced from 55 could not be assigned because the signal-to-noise ratio was too low (Spectrum C in Figure 6.4). The ^{1}H NMR of 58 should have two doublets in the aromatic region of the spectrum. It was more likely that the azepine ring system degraded to polymer byproducts.

6.1.3 Oxidation of Diamido-3H-dihydroazepines with Iron (III).

To overcome the problem of degradation of the azepine, 56 was treated with a mild oxidizing agent, Fe^{3+}. The iron (III) was chosen for a dual purpose, it was hoped that the azepine would be stabilized through chelation to the iron and that the iron would also oxidize the azepine. The iron (III) was thought to have been able to coordinate to either the amidine of the ring (Figure 6.6) or to the amide substituents.

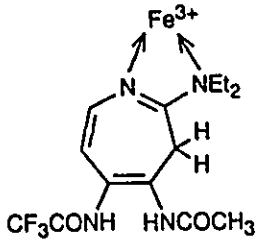

78

***Figure 6.6** Proposed chelation of 56 with Fe^{+3} at the amidine site.*

It was anticipated that after the complex was made and the azepine had been oxidized, the trifluoroacetamide could be deprotected using similar methods discussed above. The iron complex should stabilize the ring system to allow a more facile deprotection of the trifluoroacetamide without as much degradation of the ring system (Figure 6.7).

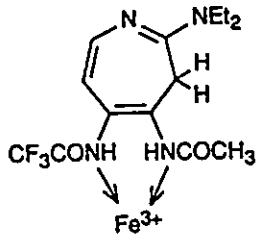

79

Figure 6.7 Proposed chelation of the amido substituents of 56 with Fe^{+3}.

The azepine 56 was dissolved in dry methanol and $FeCl_3$ was added. The reaction was monitored by UV spectroscopy to determine whether the iron chelated to the azepine. A shift in the UV spectrum was expected if the iron chelated to the azepine but unfortunately the UV spectrum of the system did not change over a period of 3 days. This indicated that the iron (III) was not chelated to the azepine and appeared to show no inclination to do so. An alternative strategy was therefore sought such as through a nucleophilic substitution on the azepine ring to yield an amino-imino-azepine.

6.1.4 Summary

The 3H-azepines 55 and 56 appeared to be unstable to deprotection using base hydrolysis and appeared to be stable towards mild oxidants such as iron (III). A stronger oxidant would probably remove both amido substituents[21a] and degrade the resultant azepine and therefore was not attempted. The instability of the 3H-dihydroazepine resulted in the search for another pathway to synthesize the amino-imino-azepines.

6.2 Attempted Synthesis of Amino-imino-azepines Via Nucleophilic Substitution.

6.2.1 Introduction

An alternative route toward the synthesis of an amino-imino-azepine was devised that was analogous to the nucleophilic substitution reaction of tropolones with primary amines to yield amino-troponeimines[28] (Figure 6.8). Lippard's results on the synthesis of amino-troponeimines[28] from tropolones were reported in low overall yields (12-20%) as shown in Figure 6.8. A variety of primary amines were used showing the worthiness of the reaction. Reaction of tropolones with primary amines yielded amino-tropones. Similar products were observed from the reaction of 2-chlorotropone with primary amines. Subsequent treatment of the amino-tropones with Et_3OBF_4 resulted in the formation of ethoxy-troponeimines, which, upon refluxing with another primary amine, yielded the amino-troponeimines.

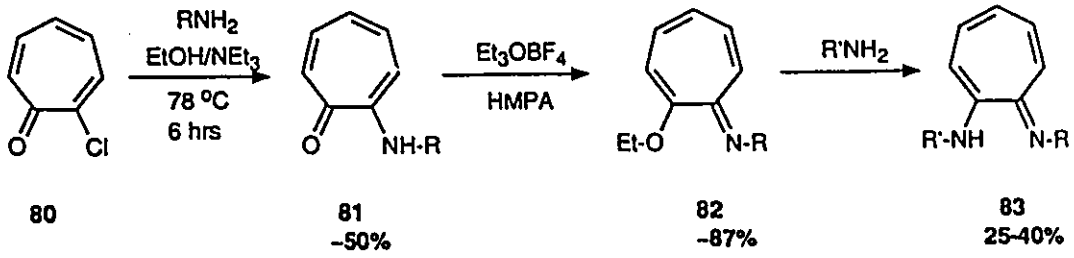

Figure 6.8 Synthesis of Amino-troponeimines from Tropolones.

An analogous experiment was conducted that entailed the reaction of a primary amine with 4-acetamido-5-chloro-3H-dihydroazepine (84). Two possible routes to the amino-imino-azepines (87) from 84 were devised (shown in Figure 6.9): substitution of the chloride with a primary amine (85) followed by oxidation; or oxidation of the acetamide to

the acetimide (86) followed by nucleophilic displacement of the chloride.

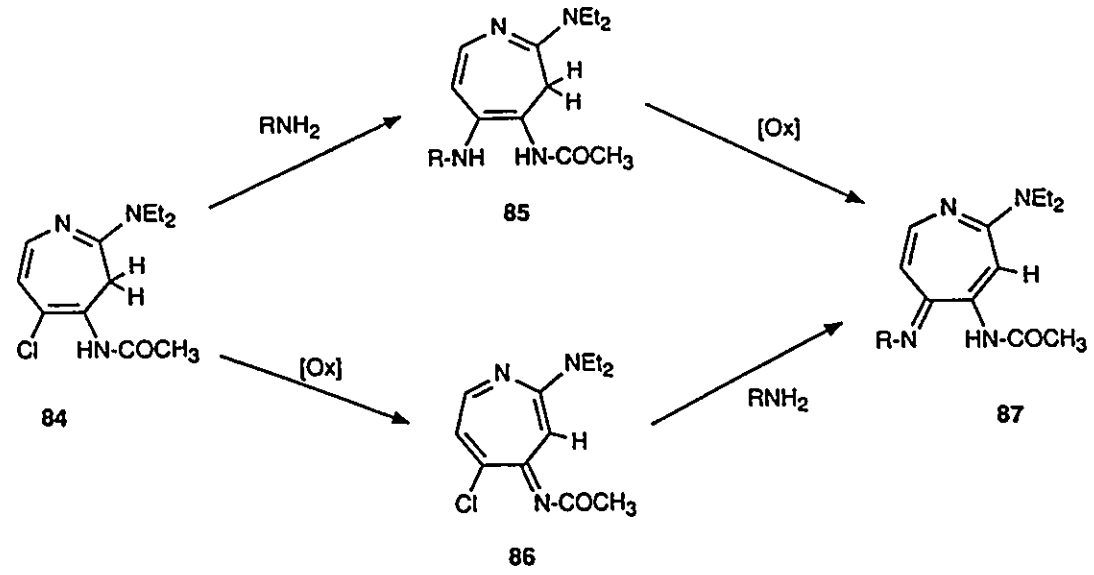

Figure 6.9 Proposed Synthesis of Amino-imino-azepines from 4-Acetamido-5-chloro-2-diethylamino-3H-dihydroazepine.

6.2.2 Synthesis of 4-Acetamido-5-chloro-2-diethylamino-3H-dihydroazepine, 84.

It was anticipated that 3-acetamido-4-chloro-phenylazide **91**, a new compound, would yield the desired azepine **84** based on the AMPAC calculations on the phenylnitrene generated from **91**. The azide was synthesized from 2-chloro-5-nitro-aniline, **88**, in reasonable overall yield (38%) in three steps following the procedure outlined in Chapters 3,4 and 5.

The starting aniline **88** was treated with one equivalent of acetylchloride in THF to yield 2-chloro-5-nitro-acetanilide, **89** (Figure 6.10). Acetyl chloride was used instead of the usual treatment with acetic anhydride (Chapters 3,4 and 5) because the acetic anhydride was not reactive enough at low temperatures (0°C) but at high temperatures (refluxing

THF) diacylation occurred. **89** was reduced using tin (II) chloride to yield the crude 3-acetamido-4-chloro-aniline; the aniline could not be obtained from the standard reduction using H_2/Pd/C because the chloro substituent was simultaneously reduced. Using more mild H_2/Pd/C reduction conditions resulted in the partial reduction of the nitro group to nitroso- and amino-substituents as well as loss of the chloride. The crude aniline, **90**, was immediately converted into the azide **91** by diazotization and displacement with sodium azide as previously described in Chapters 3, 4 and 5.

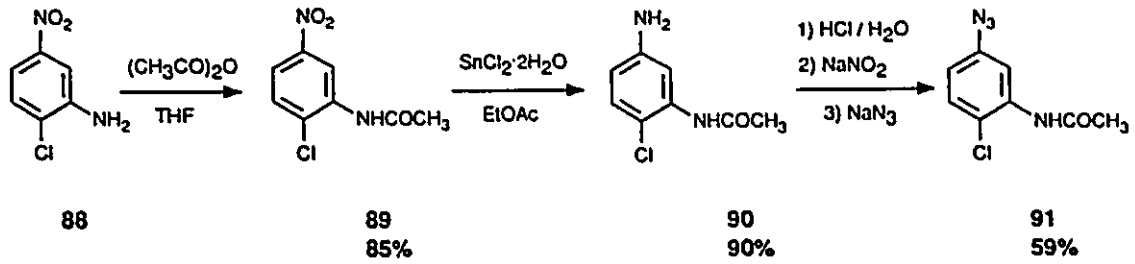

***Figure 6.10** Synthesis of 3-Acetamido-4-chloro-phenylazide, **91**.*

The azide was irradiated in THF in the presence of diethylamine to yield the desired azepine product **84**, as well as the 2-azepine product (6-acetamido-5-chloro-2-diethylamino-3H-dihydroazepine, **92**), the reduced aniline product, **90**, and a possible unknown compound **X**. The yields of each product varied under different reaction conditions shown in Figure 6.11 and Table 6.1. The products were characterized by ^{1}H NMR and mass spectrometry. The ^{1}H and ^{13}C NMR of **84** were confirmed by a ^{1}H-^{13}C heteronuclear shift correlated experiment. Compound **X** was characterized by two singlets in the ^{1}H NMR of the crude product mixture but could not be isolated. The probable structure of **X** is discussed later in this Chapter.

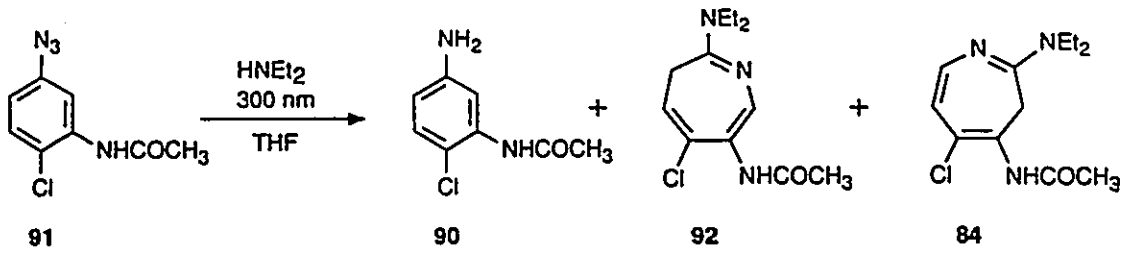

91 90 92 84

Figure 6.11 Photolysis of 91 in $HNEt_2$/THF.

Table 6.1 Photolysis Products from 91 in $HNEt_2$/THF.

Entry	Photolysis Conditions	$[HNEt_2]$ / 10^{-3} M	Yield of products[b] /% (Relative yield of singlet products[b] /%)				Ratio of 2/6 Products
			Azide	Aniline	2-Azepine	6-Azepine	
1	30°C 20 min	1900	23 (-)	11 (-)	44 (67)	22 (33)	2.00
2	-70°C 20 min	1900	77 (-)	5 (-)	14 (79)	4 (21)	3.86
3	30°C 10 min	7.5	49 (-)	0 (-)	23 (44)	28 (56)	0.799

a) Photolysis in THF in quartz tubes in a 15cm bore Rayonet using 10 300nm bulbs.
b) Ratios determined by ^{1}H NMR integrated resonances.

Table 6.1 indicates that at low temperatures and/or at high concentrations of $HNEt_2$ the 2-closure azepine product, **92**, was the favoured product while at low concentrations of $HNEt_2$ the 6-closure azepine product, **84**, was observed in higher yield. The calculated AMPAC charge distribution results on the phenylnitrene derived from **91** indicated the 2-closure should have been preferred (Table 6.2) and the experimental results were in agreement as indicated by the predominance of **92** at -70°C. The AMPAC calculated heats

of formation of the two didehydroazepines indicated the 6-didehydroazepine was the favoured intermediate under equilibrium conditions and therefore raising the temperature and lowering the $HNEt_2$ concentration should favour production of the desired product **84**.

***Table 6.2** AMPAC calculations on the Photolysis of **91**.*

	Charges on Singlet Nitrene			Heats of Formation /kcal			
	N	C_2	C_6	Singlet Nitrene	Triplet Nitrene	Didehydroazepines	
						2	6
absolute	-0.1683	0.0112	-0.0055	84.858	63.131	63.646	58.973
differences	0.0167†			0‡	21.7‡	21.2‡	25.9‡

† Charge difference based on charge on C_2 - charge on C_6.
‡ Heats of formation differences relative to the singlet nitrene.

***Table 6.3** Preparatory Photolysis of **91** in 8 Mm $HNEt_2$/THF at 30°C.*

Photolysis Conditions[a]		Product Yields (Singlet Products)				Ratio of 2/6 Products
		Azide	Aniline	2-Azepine	6-Azepine	
30°C 20 min	Crude[b] /%	52 (-)	0 (-)	29 (60)	19 (40)	1.52
8.0 mM $HNEt_2$	Isolated[c] /mmol	0.313	0	0.155	0.121	
	Isolated /%	46 (-)	0 (0)	23 (56)	18 (44)	1.28

a) Photolysis in THF in quartz tubes in a 15cm bore Rayonet using 10 300nm bulbs.
b) Yields determined by ^1H NMR integrated resonances.
c) Yields determined by mass of isolated products.

A preparatory scale photolysis reaction of **91** was performed using 8 mM $HNEt_2$ in THF and the yields are shown in Table 6.2. The products were isolated by

chromatography (Chromatotron, silica) to yield 30.8 mg of **84**; the products were not purified further. The ratio of 2/6 azepines showed the 2-azepine was formed in higher yield than the 6-isomer. This was not expected from the preliminary photolysis experiment shown in Table 6.1 which indicated the 6-azepine isomer was formed preferentially over the 2-isomer. In the scaled up experiment the light intensity was lower and this may have changed the concentrations of the intermediates and therefore would account for the change in product ratios.

6.2.3 Identification of X.

The ^{1}H NMR of the crude product mixture from the photolysis of **91** showed two singlets in the aromatic region (6.23 and 7.48 ppm) that may be from the 6-diamine product **93** (shown in Figure 6.12). Separation of the crude mixture by silica gel chromatography never yielded fractions with these resonances present and therefore the resonances could not be reliably assigned. In addition, the relative areas of the two singlets were similar indicating they may arise from a single molecule, designated **X**. The 6-diamine product **93** should possess two singlets in this region from the two aromatic protons which should be shifted to higher field because of the electron donating NEt_2 and NH_2 substituents.

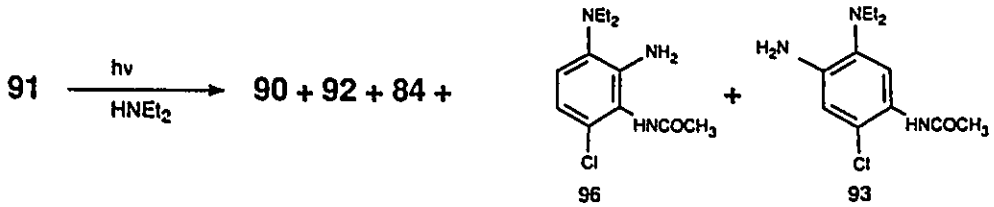

***Figure 6.12** Possible Products from the Photolysis of **91**.*

Evidence against **X** being **93** came from the relative yield of products at various temperatures. The relative yield of **X** was not consistent with it being an intermediate that was trapped before didehydroazepine was formed. If trapping of the 6-azirine to form **93** occurred to form **X**, in competition with rearrangement to the 6-didehydroazepine, then **X** should have been formed preferentially at low temperatures and/or high concentrations of $HNEt_2$ as illustrated in Chapter 5 for the photolysis of **49**. This was not observed and in fact **X** was present in higher yields at low [$HNEt_2$] at 30°C than at high [$HNEt_2$] at -70°C.

Compound **X** could also have been an impurity present in the solvents used or a rearrangement product from one of the azepines. The rearrangement of the azepines requires acid/base catalysis[25]. These products were not observed in the other photolysis reactions examined during the course of this thesis and no strong acids or bases were used during the photolysis reaction nor during work-up of the products. Therefore **X** was unlikely to have been formed from a secondary reaction. It was probable that **X** was an impurity in one of the solvents used such that at the low concentrations of **91** used (5-10 mM), the impurity became visible in the ^{1}H NMR spectrum of the crude products. The possibility that **X** may be the 6-diamine product **93** cannot be ruled out because of the lack of spectroscopic data on a purified sample. Attempts at isolating **X** from the crude reaction mixture by chromatography (Chromatotron, silica) failed.

6.2.4 Attempted Synthesis of the 4-Acetamido-5-imino-2-diethylamino-azepine from 84.

Following the method reported by Lippard *et al.*[28], the 6-azepine **84** was refluxed in *n*-butylamine for 16.5 hours in an attempt to displace the chlorine substituent (Figure 6.13). The ^{1}H NMR spectrum and TLC of the crude reaction product mixture showed only

84 was present. In an attempt to aid the displacement of the chloride ion, silver tetrafluoroborate was added with the intent that AgCl would precipitate and drive the reaction to completion. Unfortunately the ^{1}H NMR spectrum showed 84 as the only identifiable compound present and the spectrum showed the slow degradation of 84 over time and therefore this technique was abandoned.

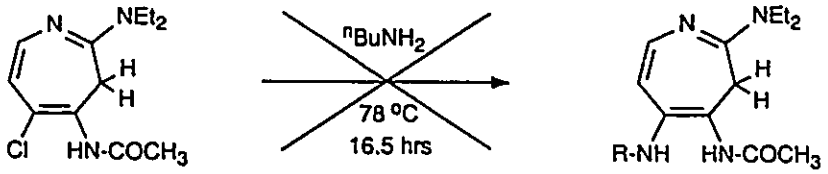

84 85

Figure 6.13 Attempted Displacement of 84 with ^{n}BuNH$_2$.

An alternative route to the imino-azepine was to oxidize 84 to the imido-azepine and subsequently treat the unstable imido-azepine with an amine to yield the desired product. This reaction was carried out on 84 in an NMR tube and followed by ^{1}H NMR spectroscopy (Figure 6.14). The azepine was dissolved into deuterated benzene (spectrum A) and the oxidizing agent 2,3-dichloro-5,6-dicyano-1,4-benzoquinone (DDQ) was added to the mixture. The solution immediately turned black although the ^{1}H NMR spectrum appeared unchanged.

An impurity at 6.13 ppm (I in Figure 6.14) was used as a standard for integration to show the depletion of 84. After 10 minutes 67% of 84 had been depleted (spectrum B) and after 35 minutes no more 84 was visible in the spectrum (C). After a further 2 hours the solution was added to *n*-butylamine and refluxed. TLC of the refluxed solution showed the formation of a second less polar spot and after 2 hours there was no visible change.

The ^{1}H NMR of the crude reaction mixture showed only the starting **84** (Figure 6.15).

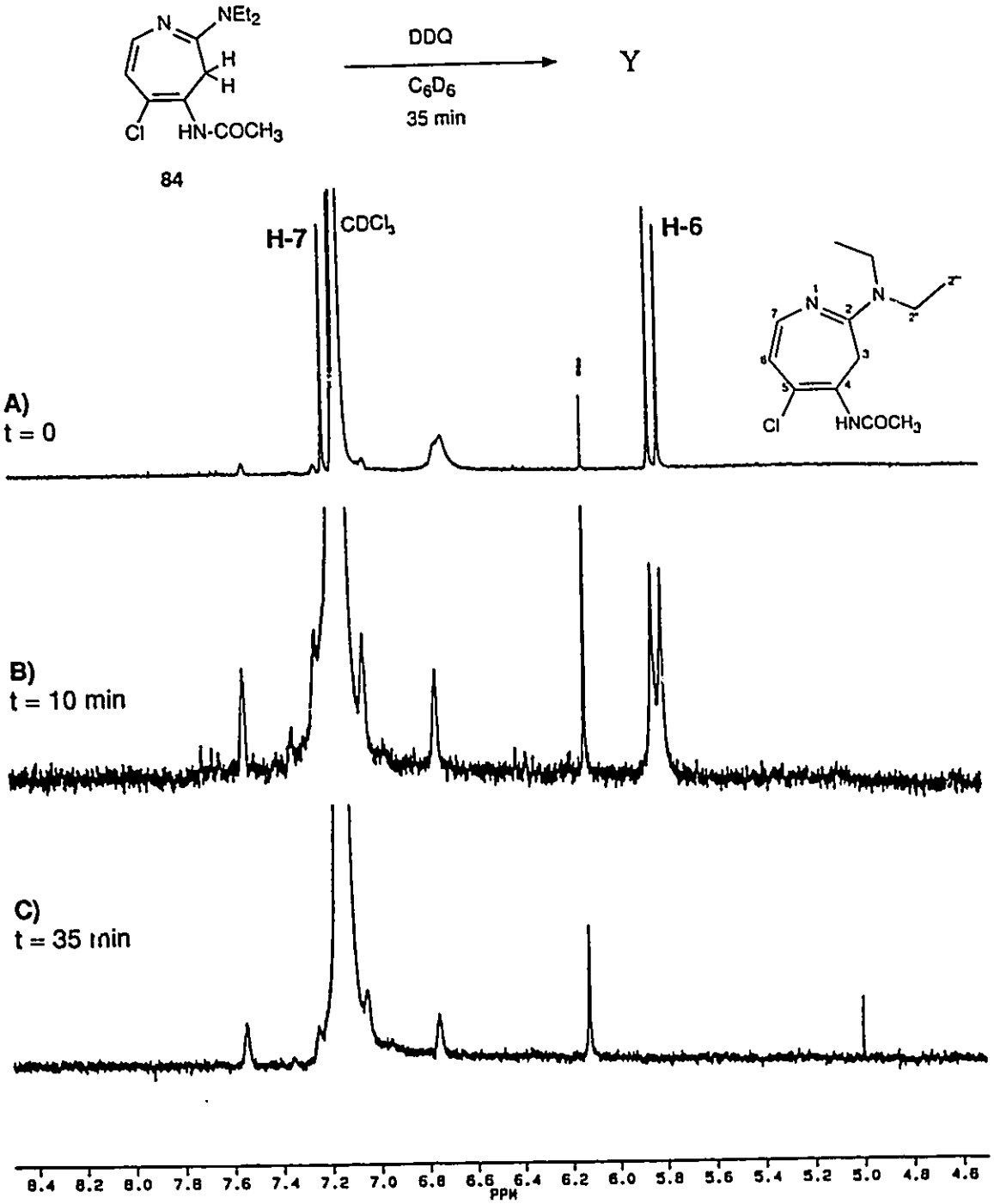

*Figure 6.14 Reaction of **84** with DDQ followed by ^{1}H NMR.*

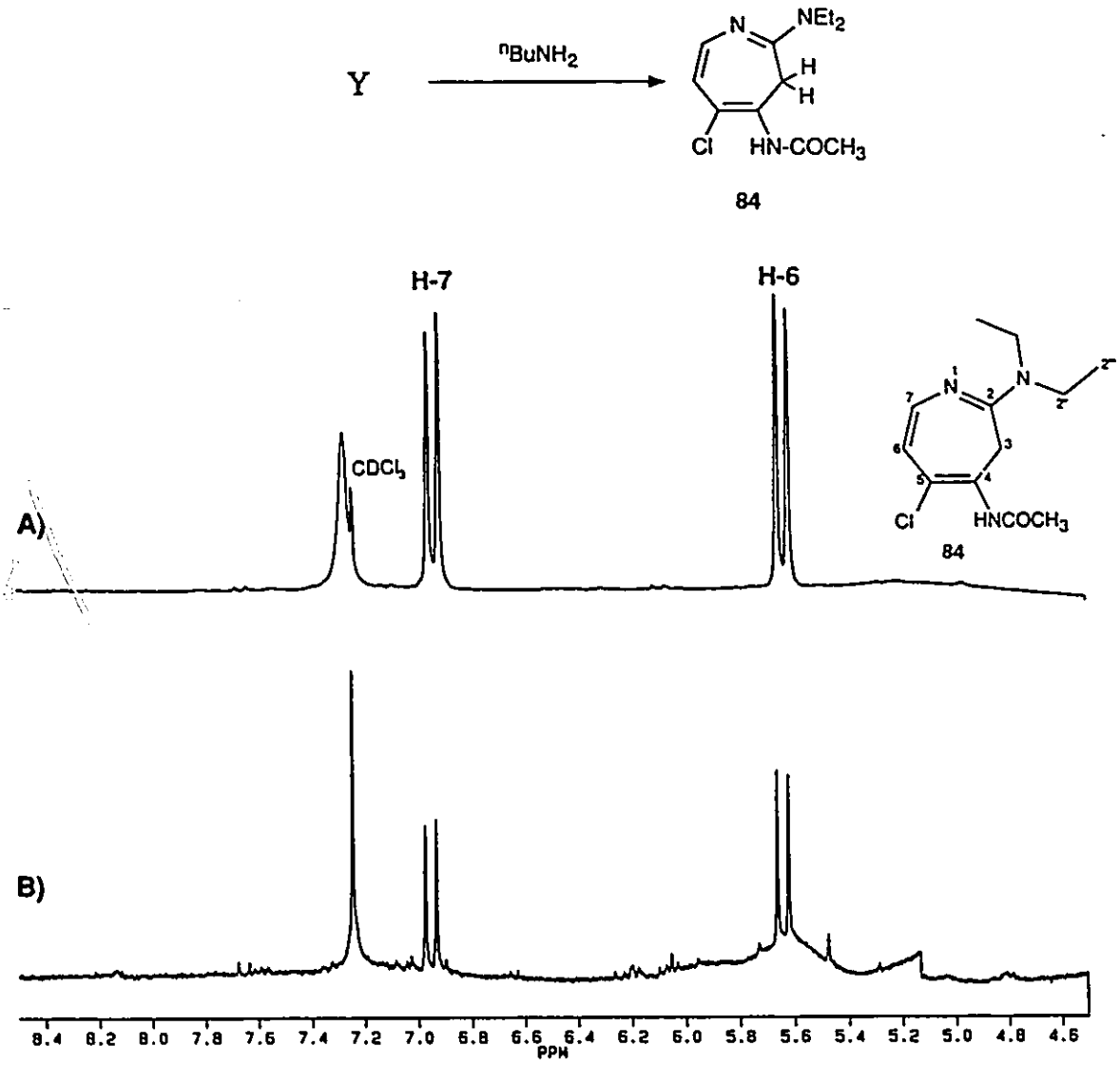

Figure 6.15 Reaction of 84 with DDQ and $^{n}BuNH_2$ followed by ^{1}H NMR.

The new spot observed in the TLC may have been oxidized azepine that subsequently decomposed because of its poor stability. It was unlikely to be the desired acetamido-imino-azepine since the acetamido-imino-azepine would be characterized by

a pair of doublets and a singlet in the aromatic region of the ^{1}H NMR spectrum which was not observed.

6.3 Conclusion

The nucleophilic displacement of the chlorine atom in the 3H-dihydroazepine **84** could not be induced under the conditions described in this thesis. The driving force for displacement of the chlorine atom in the analogous tropolone example[28] occurred because the resultant amino-tropone remains aromatic. The 3H-dihydroazepine **84** does not have the aromatic character necessary for it to undergo facile nucleophilic displacement. The oxidation of the amido-3H-dihydroazepine resulted in an unstable species, possibly the imido-intermediate, that decomposed before displacement with an primary amine occured.

The diamido-3H-dihydroazepines **55** and **56** as well as the amido-chloro-3H-dihydroazepines **92** and **84** were too unstable to permit nucleophilic displacement or oxidation to their respective imido-azepines. The simple displacement reaction attempted with **93** does not imply that it is impossible to achieve this type of reaction, merely that the conditions employed were not satisfactory.

A different synthetic strategy to produce the amino-imino-azepines might be developed to overcome the pitfalls encountered in the attempted reactions discussed above. One possible synthesis would be through the use of a more easily removed amine protecting group, such as a formyl group, that would allow much milder base hydrolysis. To prepare this system, the phenylazide would have to be made under very mild acidic conditions from the aniline precursor to allow the formamide to remain intact.

An alternative method proposed for the synthesis of amino-imino-azepines

(**1**, shown in Figure 6.16) is through a double displacement of an alkoxy-azepinone species similar to Lippard's amino-troponeimines[28]. The azepinone **94** could be synthesized from the photolysis of a 3-alkoxy-4-methoxy-phenylazide **95**.

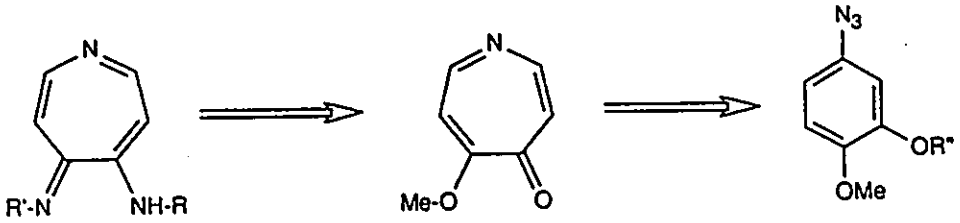

1 **94** **95**

Figure 6.16 *Alternative Retro-synthesis of Amino-imino-azepines from 3,4-dialkoxy-phenylazides.*

Overall Conclusion

The work presented illustrates a methodology towards the synthesis of substituted azepines guided by semi-empirical molecular orbital calculations. The ring expansion reaction of non-symmetric phenylnitrenes was studied to determine which factors influenced the azepine product ratios. The work showed that the temperature of the reaction and the concentration of the nucleophile used dramatically affected the product outcome. For this reason the thermolysis of arylazides and deoxygenation of aryl nitro compounds resembles the high temperature photolysis of arylazides. The low temperature photolysis of non-symmetric phenylazides represents a different regime in phenylnitrene chemistry because the interconversion of reactive intermediates is slowed. The concentration, or the nature of the nucleophile, also had a dramatic effect on the product outcome. Using low concentrations of nucleophile or using less reactive nucleophiles permited the interconversion of the reactive intermediates to take place.

The ring expansion reaction for substituted phenylnitrenes was modelled using a semi-empirical molecular orbital calculation (AMPAC). The AMPAC results for a series of meta- and para-substituted phenylnitrenes indicated a small singlet-triplet phenylnitrene energy gap (<20 kcal/mol) hindered the singlet state ring expansion reaction. The AMPAC results for the meta-substituted phenylnitrene ring expansion yielded a set of rules to aid in the prediction of which azepine product would be formed preferentially. The rules state that the charge density on the singlet phenylnitrene influenced the ratio of azepine

products at low temperatures using high concentrations of nucleophile while the difference in heats of formation between the didehydroazepine intermediates influenced the azepine product ratio at high temperatures in the presence of low concentrations of nucleophile. The AMPAC calculations were used to predict phenylnitrene precursors that would yield highly substituted 3H-dihydroazepines.

The meta-substituted phenylnitrene ring expansion reaction suggested, from the charge density calculation, that an azirine intermediate may have been involved in the reaction for mono-cyclic phenylnitrenes. The photolysis of the 3,4-diamido-phenylazides yielded proof that the azirine intermediate existed for mono-cyclic phenylnitrenes as observed for bicyclic arylnitrenes[9v,x-z,a']. These results indicated a common mechanism for both systems involving azirine and didehydroazepine intermediates. Kinetic data obtained from the photolysis of the 3,4-diamido-phenylazides showed that the azirine intermediate was formed directly from the singlet phenylnitrene. It also showed that the didehydroazepine intermediate was formed from the azirine intermediate and not directly from the singlet phenylnitrene.

Although the desired amino-imino-azepines were not synthesized, the work presented allows for a more extensive understanding of phenylnitrene chemistry. This was necessary to develop further the chemistry of more substituted azepines. Future synthetic work in azepine chemistry via phenylnitrenes can now be assisted through the use of the computer calculations outlined.

Chapter 7

EXPERIMENTAL

7.1 Apparatus and Materials

7.1.1 Materials.

All starting materials and reagents were purchased from the Aldrich Chemical Company or BDH Chemicals. The flash silica gel was Merck, grade 60, with a mesh size of 230-400, 60Å. The Chromatotron plates were prepared according to the manufacturers directions using Merck silica gel, TLC grade with a gypsum binder and fluorescent indicator.

Photolysis solvents were freshly distilled under dry nitrogen the day of the photolysis. The nitrogen was dried over indicating drierite ($CaSO_4$) and exited through an oil bubbler. THF and 1,4-dioxan were distilled from sodium benzophenone ketyl as an indicator. Methanol was distilled from magnesium turnings. Diethylamine ($HNEt_2$) was distilled from potassium hydroxide pellets using a fractionating column with the first few millilitres being discarded and the di-isopropylamine (HN^iPr_2) was distilled in a similar fashion. The cyclohexane used was HPLC grade and was not purified further.

7.1.2 General Methods.

Melting points were obtained using a Gallenkamp electrothermal melting point apparatus and are corrected.

Infrared (IR) spectra were recorded on a Perkin-Elmer 283 grating

spectrophotometer or on a BIO-RAD FTS-40 FT-IR spectrophotometer.

Ultraviolet (UV) spectra were recorded on a Hewlet Packard UV spectrometer (model 8451) or on a Perkin-Elmer Lambda 9 spectrometer using HPLC grade C_6H_{12} or freshly distilled THF as solvents.

Mass spectra were recorded on a ZAB-E or VG spectrometer. Electron Impact (EI) and Chemical Ionization (CI) samples were admitted into the mass spectrometer via a glass capillary with solid samples dissolved in MeOH. The CI used ammonia ions for all CI spectra reported.

7.1.3 Nuclear Magnetic Resonance (NMR)

The NMR spectra were acquired on three different instruments; a Varian EM 390, a Bruker AC-200 or on a Bruker AM-500.

The standard NMR spectra were obtained by dissolving the desired compound in a deuterated solvent such as deuterated chloroform ($CDCl_3$) or deuterated dimethyl-sulphoxide (DMSO-d_6). The chemical shifts are reported in parts per million (ppm) using the residual solvent signals at 7.24 (singlet) and 77 ppm (triplet) for $CDCl_3$; and 2.49 (pentet) and 39.5 ppm (heptet) for DMSO-d_6 for the ^1H and ^{13}C spectra, respectively.

All structure elucidation NMR spectra were recorded on the Bruker AC-200 spectrometer unless otherwise stated. Proton spectra were acquired at 200 MHz using a 5 mm multiple frequency ^1H - ^{13}C probe. Routine spectra were obtained in 32 scans in 16K data points over a 1.600 to 2.400 kHz spectral width. Sample temperature was maintained at 30°C by a Bruker BVT-1000 variable temperature unit. The free induction decay (FID) was zero-filled to 32K before Fourier transformation and processed using exponential multiplication (line broadening (LB) = 0.11 to 0.15 Hz). ^1H NMR spectra for

kinetic data were recorded using 128 scans in 16K data points over a 1.600 kHz spectral width. The FID's were zero-filled to 32K before exponential multiplication (LB = 0.11 Hz). Repetitive proton spectra on larger samples were recorded on a Varian EM-390 continuous wave spectrometer operating at 90 MHz. The 90-MHz ^1H chemical shifts are reported relative to tetramethylsilane (TMS) as an internal standard at 0 ppm.

Carbon-13 NMR spectra were recorded on a Bruker AC-200 at 50.323 MHz using a 5 mm multiple frequency ^1H - ^{13}C probe. The spectra were acquired over a 10.0 KHz spectral width in 16K data points. Single pulse spectra were obtained with a ^{13}C pulse width of 3.2 μs (35° flip angle) and no relaxation delay was used. The FID's were zero-filled to 32K before Fourier transformation and processed using exponential multiplication (LB = 1.0 to 1.5 Hz). Carbon 1-dimensional spectral editing was achieved using standard J-modulated spin-sort or DEPT pulse sequences[2a].

The ^{13}C - ^1H chemical shift correlation spectra were acquired using the standard pulse sequence[2a] incorporating the BIRD pulse during the evolution period for ^1H - ^1H decoupling in F1. The spectra in F2 (carbon) were recorded over a spectral width of 9.090 KHz in 2K data points. The 256 FID's in F1 (proton) were obtained over a ^1H spectral width of 1.800 KHz. The fixed delays in the pulse sequence were a 0.0 s relaxation delay, BIRD pulse and polarization transfer delays ($1/2J_{CH}$ where a standard J_{CH} = 140 Hz) of 3.571 ms, and a refocussing delay ($1/4J_{CH}$) of 1.786 ms. The ^{13}C 90° pulse width was 5.40 μs while the ^1H 90° pulse width through the decoupler channel was 8.20 μs. The data were processed using exponential multiplication (LB = 9 Hz) in F2 and unshifted sine bell in F1.

The long range ^{13}C - ^1H chemical shift correlation spectra were acquired using the standard pulse sequence[2a] incorporating the BIRD pulse during the evolution period for

^1H - ^1H decoupling in F1. The spectra in F2 (carbon) were recorded over a spectral width of 10.0 KHz in 2K data points. The 256 FID's in F1 (proton) were obtained over a ^1H spectral width of 1.500 KHz. The fixed delays in the pulse sequence were a 0.0 s relaxation delay, BIRD pulse and polarization transfer delays ($1/2J_{CH}$, J_{CH} = 10 Hz) of 50 ms, and a refocussing delay ($1/4J_{CH}$) of 25 ms. The ^{13}C 90° pulse width was 5.40 µs while the ^1H 90° pulse width through the decoupler channel was 8.20 µs. The data were processed using exponential multiplication (LB = 9 Hz) in F2 and unshifted sine bell in F1. A 2048 x 256 data matrix was obtained.

All NMR spectra use the following numbering system for structure identification:

Substituted aryl systems:

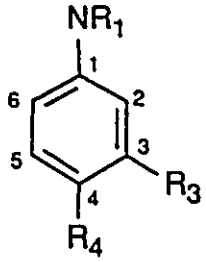

1,2-Dihydroquinoxalinones:

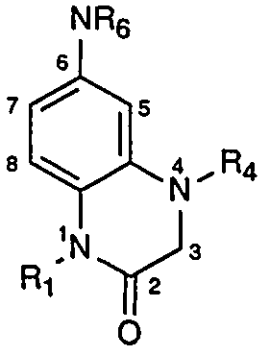

3H-Dihydroazepines:

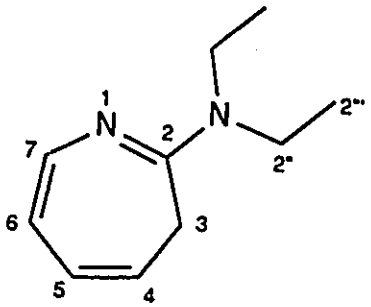

7.1.4 Photolysis Units

Three different photolysis units were routinely used throughout this project. Two standard Rayonet reactor units were used, one having a 10 cm bore and the other a 20 cm bore. The 10 cm bore reactor contained ten 300 nm Rayonet bulbs and was used for the photolysis of all meta-substituted aryl azides and on all initial azide photolyses. This reactor was also used during the preparatory photolysis of aryl azides at room temperature. A second 20 cm bore Rayonet reactor was used during the preparatory photolysis of **49** at 65°C using ten 300 nm rayonet bulbs. The third reactor unit was used during the kinetic photolyses of **49** and consisted of a single 300 nm rayonet bulb mounted abreast to a 5L pyrex bath (3 mm pyrex) filled with either water or methanol. A "carousel" was used to rotate the individual pyrex tubes to ensure uniform light intensities during each experiment for each sample.

7.1.5 Computer Modelling

The structures were drawn and viewed using the computer program PCMODEL[6a], version 4.0, on a IBM Personal System/2 computer (model 70 486 or model 55 SX). The geometries were initially minimized using PCMODEL before further minimization. A semi-empirical molecular orbital package, AMPAC[6b], was used to calculate the minimum energy geometric and electronic structures of a given compound. The AMPAC program was used on an IBM Power Station 530 using a UNIX based IBM AIX Version 3 for RISC System/6000 or the AMPAC386 program (a modified AMPAC program for use on 386 or higher computers) was used on an IBM PS/2 model 70.

7.2 Synthesis of Aryl-Nitro Compounds

All new aryl nitro compounds were characterized by mp, ^{1}H NMR and HRMS. The known compounds were compared to literature mp values.

6-Nitro-1,2-dihydroquinoxalinone (19)

The procedure was an adaption of the work of Perkin and Riley[29]. 4-Nitro-1,2-phenylenediamine (**18**, 25.010 g, 163 mmol) was added to a solution of DMF (300 mL) and di-*n*-propyl-ethylamine (30 mL, 172 mmol) in a 1 litre 3-neck round bottom flask fitted with a condenser. Ethylbromoacetate (21 mL, 189 mmol) was added to the stirred solution. The solution was heated to 80°C for 72 hours. Hot H_2O was added to the hot solution until a precipitate began to form. The solution was cooled slowly to 0°C and the precipitate was filtered and washed with cold H_2O. The solid was recrystallized from MeOH/H_2O to give **19** as a fluffy reddish-brown solid, (26.01 g, 135 mmol, 83%).

Compound **19** showed:

mp = 220 - 224 °C.

R_f (10%MeOH/$CHCl_3$) = 0.67 {**18** R_f = 0.61)

^{1}H NMR (90 MHz, DMSO-d_6) δ 3.90 (H-3, 2H, s), 6.60 (H-4, 1H, br), 6.85 (H-8, 1H, d, J=9Hz), 7.50 (H-5 and H-7, 2H, m), 10.80 (H-1, 1H, br).

MS (EI) [RI%] found: 193 $(M)^{+\cdot}$ [100%], 164 $(M\text{-}HNCH_2)^{+\cdot}$ [64%], 147 $(M\text{-}NO_2)^{+\cdot}$ [17%], 118 $(M\text{-}75)^+$ [58%].

HRMS (EI) found exact mass = 193.0479 g/mol

calcd. mass ($C_8H_7N_3O_3$) = 193.0487 g/mol (0.8 mmu)

4-Aceto-6-nitro-1,2-dihydroquinoxalinone (20)

Compound **19** (14.248 g, 73.82 mmol) was dissolved in 200 mL of pyridine (2.47 mol) in a 1 litre 3-neck round bottom flask cooled in an ice bath. Acetic anhydride (15 mL, 158 mmol) was added slowly to the stirred solution over a period of 5 minutes. The solution was heated to 80°C for 14 hours and then cooled to room temperature. The solvents were evaporated at reduced pressure to give an oil. The oil was recrystallized from MeOH/H_2O to give **20** (14.65 g, 62.3 mmol, 84%), a new compound, as a bright yellow solid.

Compound **20** showed:

mp = 208 - 211 °C.

^{1}H NMR (90 MHz, DMSO-d_6) δ 2.25 (H-4", 3H, s), 4.45 (H-3, 2H, s), 7.20 (H-8, 1H, d, J=9Hz), 8.00 (H-7, 1H, dd, J=9, 3Hz), 8.55 (H-5, 1H, d, J=3Hz), 11.30 (H-1, 1H, br).

MS (EI) [RI%] found: 235 $(M)^{+\cdot}$ [25%], 193 $(M-H_2CCO)^{+\cdot}$ [100%], 164 $(M-71)^{+}$ [43%].

HRMS (EI) found exact mass = 235.0601 g/mol

calcd. mass ($C_{10}H_9N_3O_4$) = 235.0593 g/mol (-0.8 mmu)

4-Formyl-6-nitro-1,2-dihydroquinoxalinone (21)

Formic acid (98%, 50 mL, 1.3 mol) was added to acetic anhydride (65 mL, 0.689 mol) in a 200 mL round bottom flask at 0°C. Pyridine (40 mL, 0.494 mol) was added slowly to the cooled solution. Compound **19** (4.1231 g, 21.36 mmol) was added to the mixed anhydride solution. The solution was warmed to room temperature and after 3 hours the solvents were evaporated at reduced pressure. The solid was dried on a

vacuum pump for 3 hours to give a light brown solid, **21** (4.6823 g, 21.19 mmol, 99%), a new compound.

Compound **21** showed:

mp = 231 - 236°C.

R_f (5%MeOH/$CHCl_3$) = 0.23 {**18** R_f = 0.18}

^1H NMR (90 MHz, DMSO-d_6) δ 4.40 (H-3, 2H, s), 7.10 (H-8, 1H, d, J=9Hz), 8.00 (H-7, 1H, dd, J=9, 3Hz), 8.30 (H-5, 1H, d, J=3Hz), 8.75 (H-1, 1H, br), 11.30 (H-4", 1H, br).

MS (EI) [RI%] found: 221 $(M)^{+\cdot}$ [85%], 192 $(M\text{-}CHO)^+$ [18%], 177 $(M\text{-}NH_2CHO)^{+\cdot}$ [37%], 164 $(M\text{-}NCHOCH_2)^+$ [84%].

HRMS (EI) found exact mass = 221.0426 g/mol

calcd. mass ($C_9H_7N_3O_4$) = 221.0437 g/mol (1.1 mmu)

1-(Acetic acid ethyl ester)-4-formyl-6-nitro-1,2-dihydroquinoxalinone (22)

Sodium hydride (60% in mineral oil, 76.5 mg, 1.91 mmol) was washed with dry light petroleum ether (3 x 5 mL) in a 30 mL round bottom flask fitted with a septum cap and under an N_2 atmosphere. 5 mL of dry DMF was added and then **21** (324.9 mg, 1.47 mmol) in 5mL dry DMF. The solution was cooled to 0°C and after 10 minutes ethyl bromoacetate (800 µl, 7.21 mmol) was added dropwise with stirring. The solution was warmed to room temperature, stirred for 60 minutes and evaporated at reduced pressure to give an oil. The oil was dissolved in 20 mL H_2O and extracted into ethyl acetate (3 x 20 mL). The organic layers were combined, evaporated at reduced pressure and the crude product was recrystallized from EtOH/H_2O to afford **22** (323.4 mg, 1.053 mmol, 72%), a new compound, as an orange solid.

Compound **22** showed:

mp = 147 - 149°C.

^{1}H NMR (90 MHz, $CDCl_3$) δ 1.30 (H-1"", 3H, t, J=7Hz), 4.25 (H-1"', 2H, q, J=7Hz), 4.60 (H-3, 2H, s), 4.70 (H-1', 2H, s), 6.95 (H-8, 1H, d, J=10Hz), 8.15 (H-5 and H-6, 2H, m), 8.70 (H-4", 1H, s).

MS (EI) [RI%] found: 307 $(M)^{+\cdot}$ [65%], 277 $(M\text{-}O_2\text{+}2H)^{+\cdot}$ [65%], 178 $(M\text{-}129)^+$ [100%].

1-(Acetic acid ethyl ester)-6-nitro-1,2-dihydroquinoxalinone (97)

The procedure used was similar to that used in the synthesis of **22**. Compound **19** (126.0 mg, 0.653 mmol) was used along with excess ethyl acetate (256 mg, 1.53 mmol, 2.3 equivalents). The oily product obtained was recrystallized from DMF/H_2O to give **97** (73.6 mg, 0.264 mmol, 40%), a new compound, as an orange/brown solid.

Compound **97** showed:

mp = 143 - 149°C.

R_f (10%MeOH/CH_2Cl_2) = 0.76 {**19** R_f = 0.51}

^{1}H NMR (90 MHz, DMSO-d_6) δ 1.20 (H-1"", H, t, J=7Hz), 4.00 (H-3, 2H, s), 4.15 (H-1"', 2H, q, J=7Hz), 4.80 (H-1', 2H, s), 6.75 (H-4, 1H, br), 7.08 (H-8, 1H, d, J=9Hz), 7.55 (H-7, 1H, dd, J=9, 2Hz), 7.60 (H-5, 1H, d, J=2Hz).

MS (EI) [RI%] found: 365 $(M\text{+}CHCO_2Et)^{+\cdot}$ [15%], 292 [20%], 279 $(M)^{+\cdot}$ [75%], 264 $(M\text{-}CH_2)^+$ [12%], 250 $(M\text{-}CH_2CH_3)^+$ [13%], 192 $(M\text{-}CHCO_2Et)^+$ [50%], 178 $(M\text{-}NCH_2CO_2Et)^+$ [100%].

HRMS (EI) found exact mass = 279.0849 g/mol

calcd. mass ($C_{12}H_{13}N_3O_5$) = 279.0855 g/mol (0.6 mmu)

1,4-Di-(acetic acid ethyl ester)-6-nitro-1,2-dihydroquinoxalinone (98)

The procedure used was similar to that used in the synthesis of **22**. Diisopropyl-ethylamine (482 µl, 2.767 mmol) was added with the ethyl bromoacetate (3.0 mL, 27.1 mmol) to the solution of NaH (132.8 mg, 3.32 mmol) and **19** (534.0 mg, 2.767 mmol) to afford **98** (734.8 mg, 2.01 mmol, 77%), a new compound, as a brown solid.

Compound **98** showed:

mp = 132 - 139°C.

R_f (10%MeOH/CH_2Cl_2) = 0.65 {**19** R_f = 0.55}

^{1}H NMR (90 MHz, $CDCl_3$) δ 1.30 (H-1"", 3H, t, J=6Hz), 1.32 (H-4"", 3H, t, J=6Hz), 4.10 (H-3, 2H, s), 4.20 (H-4', 2H, s), 4.25 (H-1"', 2H, q, J=6Hz), 4.27 (H-4"', 2H, q, J=6Hz), 4.70 (H-1', 2H, s), 6.75 (H-8, 1H, d, J=9Hz), 7.40 (H-5, 1H, d, J=2Hz), 7.85 (H-7, 1H, dd, J=9, 2Hz).

MS (EI) [RI%] found: 365 $(M)^{+\cdot}$ [78%], 320 $(M\text{-}OEt)^+$ [8%], 292 $(M\text{-}CH_2CO_2Et)^+$ [100%], 278 $(M\text{-}NCH_2CO_2Et)^{+\cdot}$ [55%].

MS (+NH_3 CI) [RI%] found: 383 $(M+NH_4)^+$ [55%], 365 $(M)^{+\cdot}$ [19%], 292 $(M\text{-}CH_2CO_2Et)^+$ [7%], 264 $(M\text{-}101)^+$ [6%].

HRMS (EI) found exact mass = 365.1211 g/mol

calcd. mass ($C_{16}H_{19}N_3O_7$) = 365.1223 g/mol (1.2 mmu)

4-(Acetic acid ethyl ester)-6-nitro-1,2-dihydroquinoxalinone (99)

Compound **18** (25.042 g, 163.5 mmol) was dissolved in a solution of ethyl bromoacetate(90 mL, 811.6 mmol) and DMF (200 mL) in a 1 litre round bottom flask fitted

with a condenser. The solution was refluxed for 16 hours, transferred to a 2 litre beaker and 200 mL hot H_2O was added. The solution was cooled slowly to 0°C and the precipitate was filtered and washed with cold water to give a greenish/brown solid, **99** (37.81 g, 135.5 mmol, 83%).

Compound **99** showed:

mp = 153 - 157°C.

R_f (10%MeOH/CH_2Cl_2) = 0.58 {**18** R_f = 0.42}

^{1}H NMR (90 MHz, DMSO-d_6) δ 1.20 (H-4"", 3H, t, J=9Hz), 4.00 (H-3, 2H, s), 4.18 (H-4"', 2H, q, J=9Hz), 4.30 (H-4', 2H, s), 6.95 (H-8, 1H, d, J=8Hz), 7.32 (H-5, 1H, d, J=2Hz), 7.70 (H-7, 1H, dd, J=8, 2Hz), 11.10 (H-1, 1H, br).

MS (EI) [RI%] found: 279 $(M)^{+\cdot}$ [9%], 206 $(M-73)^{+\cdot}$ [16%], 131 $(M-148)^{+}$ [100%].

HRMS (EI) found exact mass = 279.0849 g/mol

calcd. mass ($C_{12}H_{13}N_3O_5$) = 279.0855 g/mol (0.6 mmu)

2-Acetamido-4-nitroaniline (50)

4-Nitro-1,2-phenylenediamine, **18** (10.594 g, 69.18 mmol), was dissolved in 42 mL THF and cooled to 0°C. Acetic anhydride (8.0 mL, 8.66 g, 84 mmol, 1.21 equivalents) was added dropwise with stirring and the solution was allowed to warm to room temperature. The reaction was quenched after 10 hours by the addition of 10 mL H_2O. The solution was evaporated at reduced pressure to a greenish/yellow slurry. The product was dissolved in 300 mL hot MeOH, treated with charcoal and filtered. Warm H_2O was added until a precipitate started to form. The solution was cooled to 0°C and the precipitate was filtered and washed with cold H_2O to give **50** (11.523 g, 59.1 mmol, 85%) as a bright yellow solid.

Compound **50** showed:

mp = 204 - 205°C (lit.[30] mp = 204 - 205°C).

^{1}H NMR (DMSO-d_6) δ 2.02 (H-3", 3H, s), 6.40 (H-4', 2H, br), 6.70 (H-5, 1H, d, J=9Hz), 7.78 (H-6, 1H, dd, J=9, 3Hz), 8.20 (H-2, 1H, d, J=3Hz), 9.15 (H-3', 1H, br).

MS (EI) [RI%] found: 195 $(M)^{+\cdot}$ [64%], 178 $(M\text{-}OH)^+$ [14%], 153 $(M\text{-}CH_2CO)^{+\cdot}$ [100%], 136 $(M\text{-}NH_3\text{-}CH_2CO)^+$ [15%].

HRMS (EI) found exact mass = 195.0645 g/mol

calcd. mass ($C_8H_9N_3O_3$) = 195.0644 g/mol (-0.1 mmu)

Alternate synthesis of 20

Compound **50** (1.233 g, 6.323 mmol) in 40 mL dry DMF was added to a solution of NaH (305.9 mg, 7.648 mmol) in 10 mL dry DMF at -15°C. After 30 minutes, ethyl bromoacetate (850 µl, 7.665 mmol) was added, the cold bath was removed and the solution was stirred for 10 hours. The solvents were removed by evaporation at reduced pressure and the product was recrystallized from MeOH/H_2O to yield **20** (315.0 mg, 1.34 mmol, 21%) as a yellow solid.

Compound **50** showed a mp (202 - 206°C) and ^{1}H NMR spectrum consistent with **50** synthesized above.

3-Nitro-trifluoroacetamido-benzene (100)

3-Nitroaniline (**101**, 1.2037 g, 8.540 mmol) was dissolved in 10 mL of dry THF in a 35 mL round bottom flask under N_2 at -15°C. Trifluoroacetic anhydride (3.0 ml, 21 mmol) was added dropwise to the stirred solution. The solution was warmed to room temperature

and, after 60 minutes, 10 mL H_2O was added. The solution was concentrated to 15 mL and MeOH (10ml) was added. The solution was cooled to 0°C and the precipitate was filtered and washed with cold H_2O to afford **100** (1.6552 g, 7.074 mmol, 83%) as cream coloured needles.

Compound **100** showed:

mp = 94 - 94.5°C (lit.[31] mp = 87°C).

^{1}H NMR ($CDCl_3$) δ 7.13 (H-5, 1H, dd, J=7, 7Hz), 8.13 (H-4, H-6, 2H, m), 8.50 (H-2, 1H, dd, J=2, 2Hz).

MS (EI) [RI%] found: 234 $(M)^{+\cdot}$ [100%], 215 $(M-F)^+$ [8%], 188 $(M-NO_2)^+$ [17%], 165 $(M-CF_3)^+$ [39%], 137 $(M-COCF_3)^+$ [14%].

4-Nitro-trifluoroacetamido-benzene (33)

Compound **33** (1.776 g, 7.589 mmol, 91%) was synthesized from **32** (1.1518 g, 8.34 mmol) using the same procedure used in the synthesis of **100**. Compound **33** was a yellow crystalline solid and showed:

mp = 153 - 154°C (lit.[31] mp = 150°C).

R_f (10%MeOH/$CHCl_3$) = 0.57 {**101** R_f = 0.47}

R_f (5%MeOH/CH_2Cl_2) = 0.67 {**101** R_f = 0.27}

^{1}H NMR ($CDCl_3$) δ 7.77 (H-3, 2H, d, J=10 Hz), 8.19 (H-4', 1H, br), 8.32 (H-2, 2H, d, J=10 Hz).

^{13}C NMR ($CDCl_3$) δ 120.5 (C-3, **C**H), 124.6 (C-2, **C**H), 142.3 (C-4, **C**), 144.4 (C-1, **C**).

MS (EI) [RI%] found: 234 $(M)^{+\cdot}$ [100%], 218 $(M-O)^+$ [9%], 204 $(M-30)^{+\cdot}$ [18%], 188 $(M-NO_2)^+$ [10%], 165 $(M-CF_3)^+$ [26%].

5-Nitro-2-trifluoroacetamido-acetanilide (51)

Compound **50** (1.1400 g, 5.846 mmol) was dissolved in 15 mL dry THF in a dry 35 mL round bottomed flask (RBF) with a septum attached under N_2 and stirred with a magnetic stirrer. The solution was cooled to -15°C using a salt/ice bath. Trifluoroacetic anhydride (2.0 ml, 3.0 g, 14.2 mmol) was added dropwise to the stirred solution. The solution was allowed to warm to room temperature. After one hour 10 mL of water was added to quench the remaining anhydride. The solution was evaporated under reduced pressure to give a pale yellow solid. The solid was recrystallized from MeOH/H_2O to give pale yellow crystals, **51**, in 86% yield (1.468 g, 5.044 mmol).

Compound **51** showed:

mp = 203 - 204 °C

R_f (5%MeOH/$CHCl_3$) = 0.31

^{1}H NMR (DMSO-d_6) δ 2.10 (H-3", 3H, s), 7.70 (H-5, 1H, d, J=8.9 Hz), 8.04 (H-6, 1H, dd, J=8.9, 2.6 Hz), 8.58 (H-2, 1H, d, J=2.6 Hz), 9.97 (H-3', 1H, br), 11.12 (H-4', 1H, br).

^{1}H NMR ($CDCl_3$) δ 22.6 (C-3", **C**H_3), 119.9 (C-5, **C**H), 120.8 (C-6, **C**H), 125.3 (C-2, **C**H), 131.0 (C-3, **C**), 133.9 (C-4, **C**), 145 (C-1, **C**), 171.7 (C-3", **C**=O).

MS (EI) [RI%] found: 292 $(M+1)^+$ [9%], 291 $(M)^{+\cdot}$ [7%], 249 $(M-COCH_2)^{+\cdot}$ [44%], 180 $(M-NCOCF_3)^{+\cdot}$ [100%], 134 $(M-157)^+$ [28%], 105 $(M-186)^+$ [42%].

MS (CI) [RI%] found: 309 $(M+NH_4)^+$ [100%], 279 $(M+NH_4-COCH_2)^+$ [42%], 262 $(M-Et)^+$ [13%].

HRMS (EI) found exact mass = 291.0469 g/mol

calcd. mass ($C_{10}H_8F_3N_3O_4$) = 291.0467 g/mol (-0.2 mmu)

4-Nitro-1,2-di(trifluoroacetamido)-benzene (53)

4-Nitro-1,2-phenylenediamine, **18**, (5.035 g, 32.88 mmol) was reacted with trifluoroacetic anhydride (12 ml, 17.8 g, 85 mmol, 2.6 equivalents) in cold THF (-15°C) for 1 hour as described previously for compound **100** to yield crude **53**. The solid was recrystallized from MeOH/H_2O to give **53** in 93% yield (10.5883 g, 30.69 mmol).

Compound **53** showed:

^{1}H NMR ($CDCl_3$) δ 7.86 (H-5, 1H, d, J=8.9 Hz), 8.27 (H-6, 1H, dd, J=8.9, 2.5 Hz), 8.40 (H-2, 1H, d, J=2.5 Hz), 8.79 (H-3', 1H, br), 8.87 (H-4', 1H, br).

MS (EI) [RI%] found: 345 $(M)^{+\cdot}$ [32%], 276 $(M\text{-}CF_3)^+$ [100%], 258 $(M\text{-}87)^+$ [17%].

7.3 Deoxygenation Attempts on Aryl-Nitro Compounds

Deoxygenation of Nitrobenzene to Yield 2-(Di-*n*-propyl)amino-3H-azepine (23)

The procedure of Cadogan[10a] was used. Nitrobenzene (**6**, 300 µl, 359 mg, 2.91 mmol) was treated with triethylphosphite (870 µl, 843 mg, 5.08 mmol, 1.7 equivalents) in $^n Pr_2NH$ (4 ml, 2.95 g, 29.2 mmol, 10 equivalents) at 90°C for 4 days. TLC showed three products were present; R_f (5%MeOH/CH_2Cl_2) = 0.87, 0.30, 0.19. The least polar component was the starting nitrobenzene, **6**. The crude product was distilled in a bulb-to-bulb distillation apparatus under reduced pressure. The first component to distill was the nitrobenzene (bp = 75°C/5 mm Hg). The second component contained the three components together (bp = 95-100°C /5 mm Hg). The second component was chromatographed on silica (1x25 cm, 5% MeOH/CH_2Cl_2 for the first fraction, 25% MeOH/CH_2Cl_2 for the remaining fractions. The second fraction (R_f = 0.30) contained the

reduced product, aniline. The third fraction (R_f = 0.19) contained the azepine and some $(EtO)_3P$ (total mass = 54.2 mg, yield of azepine = 10%). Compound **23** was a dark brown oil whose ^1H NMR spectrum agreed with the literature[10g].

Compound **23** showed:

^1H NMR ($CDCl_3$) δ 0.9 (H-2"", 6H, t, J=7Hz), 1.6 (H-2"', 4H, tq, J=7, 7Hz), 2.75 (H-3, 2H, d, J=8Hz), 3.35 (H-2", 4H, t, J=7Hz), 5.15 (H-4, 1H, dt, J=8, 8Hz), 5.8 (H-5, 1H, dd, J=8, 3Hz), 6.32 (H-6, 1H, dd, J=3, 8Hz), 7.1 (H-7, 1H, d, J=8Hz).

Reaction of 6-Nitro-1,2-dihydroquinoxalinones (18, 19 and 98), nitroanilines (32 and 102) and nitroacetanilides (36) with Triethylphosphite.

The procedure outlined above for the deoxygenation of nitrobenzene was used in an attempt to yield azepines from 6-nitro-1,2-dihydroquinoxalinones **18**, **19** and **89**, nitroanilines **32** and **102**, and nitroacetanilide **36**. No azepines were isolated from the product mixtures for each of the examined systems.

Reaction of 4-Nitro-trifluoroacetamido-benzene (33) with Triethylphosphite in Diethylamine.

The general procedure of Cadogan[10a] was used. The nitro-compound (251.0 mg, 1.073 mmol, 0.065 M) was dissolved in triethylphosphite (1.5 ml, 1.45 g, 8.76 mmol, 0.53 M) and diethylamine (15 ml, 10.6 g, 145 mmol, 8.8 M). The solution was refluxed under nitrogen for 4 days. TLC showed the starting azide as the major product (R_f (10% MeOH/$CHCl_3$) = 0.74). Some aniline was also observed (R_f (10% MeOH/$CHCl_3$) = 0.44). Both TLC and ^1H NMR did not show any appreciable azepine formation.

7.4 Synthesis of Arylazides

7.4.1 General Method

The arylazides were prepared from their corresponding aniline precursors through diazotization and nucleophilic substitution with sodium azide[23]. The precursor anilines were either purchased or made from the reduction of the former aryl-nitro compounds. The aryl-nitro compounds were reduced using either tin (II) chloride[22a] ($SnCl_2 \cdot 2H_2O$) or by hydrogenation using hydrogen with 10% palladium on carbon[22b] (Pd/C) in a Parr hydrogenator. The tin reduction involved refluxing the nitroaryl compound in 5 equivalents of $SnCl_2 \cdot 2H_2O$ in ethylacetate (EtOAc) for an hour. The solution was neutralized with base and the aniline was extracted into EtOAc. The standard hydrogenation involved using 5% by weight of 10% Pd/C relative to the nitroaryl compound and hydrogenating the dilute MeOH solution under 30 psi of H_2 for an hour. The solution was filtered through Celite to recover the Pd/C. The crude aniline products were usually converted immediately to the azides without further purification.

To synthesize the azides, the desired precursor aniline was dissolved in 4.3M hydrochloric acid and cooled to 0 C after which sodium nitrite dissolved in a minimal amount of water was added dropwise to the cold aniline solution. After 45 minutes the solution was treated with activated charcoal and filtered into a large beaker. The solution was stirred vigorously at 0 C and sodium azide, dissolved in a minimum volume of water, was added dropwise. The solution was allowed to react for 1 hour and then filtered. The crude azide was recrystallized from $MeOH/H_2O$.

7.4.2 Para-substituted Phenylazides

4-Azido-nitrobenzene (103)

The procedure described by Mallory[23b] was used. 4-Nitroaniline (**32**, 2.000 g, 14.48 mmol, 1.21 M) was dissolved in 4.32M HCl (10 ml) at 0°C. Sodium nitrite (1.138 g, 16.0 mmol, 1.33 M) in a minimum volume of H_2O (~2 ml), was added dropwise with stirring. After 60 minutes the solution was treated with activated charcoal and filtered into a large beaker. Sodium azide (1.052 g, 16.2 mmol) in H_2O was added dropwise with vigorous stirring. The solution was kept cool and stirred occasionally over the next 60 minutes. The precipitate was filtered and washed with cold H_2O to give **32**. The solid was recrystallized from MeOH/H_2O in 95% yield as an orange solid and the melting point and ^1H NMR agreed with the literature[38].

Compound **32** showed:

mp = 71 - 72°C (lit.[38] mp = 75°C).

R_f (1% MeOH/15% EtOAc/hexanes) = 0.56

^1H NMR (DMSO-d_6) δ 7.20 (H-2, 2H, d, J=9Hz), 8.35 (H-3, 2H, d, J=9Hz).

4-Amino-acetanilide (104)

The general $SnCl_2 \cdot 2H_2O$ procedure was used[22a] to reduce 4-nitro-acetanilide, **36**, to **104** in 73% yield. Compound **36** (1.028 g, 5.709 mmol, 0.476 M) was added to a slurry of $SnCl_2 \cdot 2H_2O$ (6.453 g, 28.6 mmol, 2.38 M, 5 equivalents) in 12 mL EtOAc in a round bottom flask fitted with a condenser. The solution was refluxed for 1.5 hours, cooled to room temperature then poured on crushed ice. The solution was neutralized with 2M NaOH. It was then continuously extracted with 200 mL EtOAc for 10 hours. The organic

layer was separated, warmed, treated with charcoal and filtered. The filtrate was evaporated and dried on a vacuum pump to give **104**, (626.7 mg, 4.178 mmol, 73%), as a beige solid.

Compound **104** showed:

mp = 166 - 169°C (lit.[32] mp = 165 - 168°C).

^{1}H NMR (DMSO-d_6) δ 1.95 (H-4''', 3H, s), 4.80 (H-1', 2H, br), 6.50 (H-2, 2H, d, J=9Hz), 7.20 (H-3, 2H, d, J=9Hz), 9.55 (H-4', 1H, br).

4-Azido-acetanilide (38)

Compound **38** was synthesized from **104** in 56% yield by the general procedure. Compound **104** (471.5 mg, 3.143 mmol, 0.524 M), sodium nitrite (243.5 mg, 3.494 mmol, 0.582 M) and sodium azide (220.3 mg, 3.355 mmol) gave **38** as cream coloured crystals in 56% yield (308.2 mg, 1.751 mmol).

Compound **38** showed:

mp = 112 - 115°C.

R_f (1% MeOH/15% EtOAc/hexanes) = 0.04

R_f (1% MeOH/50% EtOAc/hexanes) = 0.32

UV in C_6H_{12} (c=5x10^{-5}M) found λ (A) = 214 (0.74), 276 (1.40).

^{1}H NMR ($CDCl_3$) δ 2.20 (H-4'', 3H, s), 6.95 (H-2, 2H, d, J=9Hz), 7.45 (H-3, 2H, d, J=9Hz).

MS (EI) [RI%] found: 176 $(M)^{+\cdot}$ [7%], 148 $(M\text{-}N_2)^{+\cdot}$ [18%], 106 $(M\text{-}N_2\text{-}COH_2)$ [100%], 79 $(M\text{-}73)^+$ [37%].

HRMS (EI) exact mass found = 176.0700 g/mol

calcd. mass ($C_8H_8N_4O$) = 176.0698 g/mol (-0.2 MMU)

4-Azido-acetophenone (30)

Compound **30** was synthesized from p-amino-acetophenone, **105**, (2.5296 g, 18.71 mmol) in 96% yield (2.8898 g, 17.95 mmol) by the general procedure as a cream coloured solid which agreed with literature characterizations[11a].

Compound **30** showed:

mp = 43 - 43.5°C (lit.[11a] mp = 44°C).

4-Trifluoroacetamido-aniline (34)

Compound **33** (1.3807 g, 5.900 mmol) was reduced by the $SnCl_2 \cdot 2H_2O$ procedure as described above to give **34** in 65% yield (777.1 mg, 3.809 mmol).

Compound **34** showed:

^1H NMR ($CDCl_3$) δ 6.68 (H-2, 2H, d, J=8.9 Hz), 7.34 (H-3, 2H, d, J=8.9 Hz).

MS (EI) [RI%] found: 204 $(M)^{+\cdot}$ [71%], 185 $(M\text{-}F)^+$ [3%], 134 $(M\text{-}HCF_3)^{+\cdot}$ [9%], 107 $(M\text{-}COCF_3)^+$ [100%].

4-Azido-trifluoroacetamido-benzene (35)

Compound **34** (660.8 mg, 3.239 mmol) was transformed to the azide as described above to yield **35** in 70% yield (523.5 mg, 2.276 mmol).

Compound **35** showed:

R_f (1% MeOH/15% EtOAc/hexanes) = 0.32

UV in C_6H_{12} ($c=10^{-4}M$) found λ (A) = 216 (1.23), 272 (2.07), 278 (2.05).

IR υ /cm^{-1} = 3316.7 (s) [NH amide stretching], 3150-3200 (m) [CH aromatic stretching], 2119.7 (s) [N_3 stretching], 1702.6 (s) [C=O amide stretching], 1508.1 (m) [NH

amide bending], 1282.8-1155.6 (m) [CF stretching], 832.5 (s) [1,4-substituted benzene].

^{1}H NMR ($CDCl_3$) δ 7.03 (H-2, 2H, d, J=8.9 Hz), 7.55 (H-3, 2H, d, J=8.9 Hz), 7.88 (H-4', 1H, br).

MS (EI) [RI%] found: 230 $(M)^{+\cdot}$ [14%], 202 $(M-N_2)^{+\cdot}$ [100%], 133 $(M-CF_3)^{+\cdot}$ [42%], 105 $(M-N_2-COCF_3)^+$ [72%].

7.4.3 Meta-substituted Phenylazides

3-Azido-chlorobenzene (46a)

3-Azido-chlorobenzene was synthesized from 3-chloro-aniline, **47a**, (5.0 ml, 6.03 g, 47.3 mmol) using the general method. The crude azide oil was distilled under reduced pressure (CAUTION: Distillation of azides have the potential to explode. A shield was used in all distillations). The yield of pure azide was 72% (5.239g, 34.11 mmol) and agreed with the literature reports[33].

Compound **46a** showed:

bp = 37°C/0.6 mm Hg (lit.[33] bp = 36 - 37°C/1 mm Hg).

R_f (1% MeOH/15% EtOAc/hexanes) = 0.81

UV in C_6H_{12} ($c=10^{-4}$M) found λ (A) = 214 (1.40), 248 (1.29).

^{1}H NMR ($CDCl_3$) δ 6.84 (H-6, 1H, ddd, J=7.9, 2.1, 1.0 Hz), 6.94 (H-2, 1H, dd, J=2.1, 1.9 Hz), 7.05 (H-4, 1H, ddd, J=8.0, 1.9, 1.0 Hz), 7.20 (H-5, 1H, dd, J=8.0, 7.9 Hz).

^{13}C NMR ($CDCl_3$) δ 117.0 (C-6, **C**H), 119.2 (C-2, **C**H), 124.9 (C-4, **C**H), 130.4 (C-5, **C**H), 135.3 (C-3, **C**), 141.3 (C-1, **C**).

3-Azido-bromobenzene (46b)

3-Azido-bromobenzene was synthesized from 3-bromo-aniline, **47b**, (3.0 ml, 4.74 g, 27.6 mmol) as outlined above. The crude oil was distilled under reduced pressure in 76% yield (4.164 g, 21.0 mmol).

Compound **46a** showed:

bp = 79°C/2.0 mm Hg (lit.[34] bp = 63 - 65°C/0.7 mm Hg).

R_f (1% MeOH/15% EtOAc/hexanes) = 0.79

UV in C_6H_{12} (c=10^{-4}M) found λ (A) = 208 (0.52), 248 (0.27).

^{1}H NMR ($CDCl_3$) δ 6.99 (H-6, 1H, ddd, J=7.6, 2.1, 1.5 Hz), 7.21 (H-2, 1H, dd, J=2.1, 1.8 Hz), 7.24 (H-5, 1H, dd, J=8.0, 7.6 Hz), 7.31 (H-4, 1H, ddd, J=8.0, 1.8, 1.5 Hz).

^{13}C NMR ($CDCl_3$) δ 117.7 (C-6, **C**H), 122.1 (C-2, **C**H), 123.2 (C-3, **C**), 127.9 (C-4, **C**H), 130.8 (C-5, **C**H), 141.5 (C-1, **C**).

3-Azido-iodobenzene (46h)

3-Azido-iodobenzene was synthesized from 3-iodo-aniline, **47h**, (2.226 g, 10.16 mmol) as described above. The crude oil was distilled under reduced pressure in 68% yield (1.692 g, 6.91 mmol).

Compound **46h** showed:

bp = 64 - 66°C/0.2 mm Hg (lit.[35] bp = 82 - 83°C/0.85 mm Hg).

R_f (1% MeOH/15% EtOAc/hexanes) = 0.76

UV in C_6H_{12} (c=10^{-4}M) found λ (A) = 230 (1.85), 250 (1.16).

^{1}H NMR ($CDCl_3$) δ 6.92 (H-6, 1H, ddd, J=8.1, 1.7, 1.4 Hz), 7.04 (H-5, 1H, dd, J=8.1, 8.1 Hz), 7.35 (H-2, 1H, dd, J=1.8, 1.7 Hz), 7.44 (H-4, 1H, ddd, J=7.6, 1.8, 1.4 Hz).

^{13}C NMR ($CDCl_3$) δ 94.6 (C-3, **C**), 118.3 (C-6, **C**H), 127.9 (C-2, **C**H), 131.0 (C-5, **C**H), 133.9 (C-4, **C**H), 141.3 (C-1, **C**).

3-Azido-acetophenone (46f)

3-Azidoacetophenone was prepared from 3-amino-acetophenone, **47f**, (6.954 g, 49.90 mmol) as described above. The crude azide oil was distilled under reduced pressure in 49% yield (3.920 g, 24.34 mmol) whose ^1H NMR matched the literature[11a]. Compound **46f** showed:

bp = 75 - 76°C/0.2 mm Hg.

R_f (1% MeOH/15% EtOAc/hexanes) = 0.45

UV in C_6H_{12} ($c=10^{-4}M$) found λ (A) = 228 (1.85), 234 (1.93), 302 (0.23).

^1H NMR ($CDCl_3$) δ 2.55 (H-3", 3H, s), 7.16 (H-6, 1H, ddd, J=8.0, 2.0, 1.3 Hz), 7.41 (H-5, 1H, dd, J=8.0, 7.7 Hz), 7.55 (H-2, 1H, dd, J=2.0, 1.7 Hz), 7.67 (H-4, 1H, ddd, J=7.7, 1.7, 1.3 Hz).

^{13}C NMR ($CDCl_3$) δ 26.7 (C-3", CH_3), 118.4 (C-2, **C**H), 123.4 (C-4, **C**H), 124.8 (C-6, **C**H), 130.0 (C-5, **C**H), 138.6 (C-3, **C**), 142.1 (C-1, **C**), 197.1 (C-3', **C**=O).

MS (EI) [RI%] found: 161 $(M)^{+\cdot}$ [37%], 133 $(M-N_2)^{+\cdot}$ [100%], 90 $(M-N_2-COCH_3)^{+\cdot}$ [20%].

MS (CI) [RI%] found: 179 $(M+NH_4)^+$ [100%], 162 $(M+H)^+$ [9%], 153 $(M-N_2+2H+NH_4)^+$ [97%], 136 $(M-N_2+3H)^+$ [26%].

3-Azido-benzonitrile (46c)

3-Azido-benzonitrile was synthesized from 3-amino-benzonitrile (**47c**, 2.055 g, 17.22 mmol) as described above. The yield of purified azide after recrystallization

(MeOH/H_2O) was 93% (2.315 g, 16.08 mmol). The cream coloured needles were dried over P_2O_5 overnight.

Compound **46c** showed:

mp = 53 - 55°C (lit.[36] mp = 55 - 56.5°C)

R_f (1% MeOH/15% EtOAc/hexanes) = 0.47

UV in C_6H_{12} (c=10^{-4}M) found λ (A) = 222 (1.65), 250 (1.37), 292 (0.21).

^{1}H NMR ($CDCl_3$) δ 7.21 - 7.26 (H-6, H-2, 2H, m), 7.38 - 7.50 (H-5, H-4, 2H, m).

^{13}C NMR ($CDCl_3$) δ 113.9 (C-3, **C**), 122.3 (C-2, **C**H), 123.3 (C-6, **C**H), 128.3 (C-4, **C**H), 130.6 (C-5, **C**H), 141.5 (C-1, **C**).

3-Azido-anisole (46d)

m-Anisidine was purified by distillation under reduced pressure in a microboiling apparatus to give a clear colourless liquid, **47d**.

Compound **47d** showed:

bp = 95°C/2.5 mm Hg (lit.[32] bp = 251°C/760 mm Hg).

^{1}H NMR ($CDCl_3$) δ 6.22 - 6.34 (H-6, H-4, H-2, 3H, m), 7.05 (H-5, 1H, dd, J=8.0, 8.0 Hz).

3-Azido-anisole was synthesized from m-anisidine (**47d**, 3.095 g, 25.13 mmol) as described above. The crude azide **46d** was distilled under reduced pressure in 62% yield (2.3139 g, 15.53 mmol).

Compound **46d** showed:

bp = 50°C/0.15 mm Hg (lit.[37] bp = 56 - 57°C/1 mm Hg).

R_f (1% MeOH/15% EtOAc/hexanes) = 0.74

UV in C_6H_{12} (c=10^{-4}M) found λ (A) = 218 (1.44), 248 (0.75), 284 (0.26).

^{1}H NMR ($CDCl_3$) δ 3.79 (H-3', 3H, s), 6.54 (H-2, 1H, dd, J=2.2, 2.2 Hz), 6.65 (H-6, H-4, 2H, m), 7.24 (H-5, 1H, dd, J=8.2, 8.0 Hz).

^{13}C NMR ($CDCl_3$) δ 56.0 (C-3', CH_3), 104.9 (C-2, CH), 110.6 (C-4, CH), 111.2 (C-6, CH), 130.4 (C-5, CH), 141.2 (C-1, C), 160.8 (C-3, C).

3-Azido-methylmercaptobenzene (46e)

3-Azido-methylmercaptobenzene was synthesized from 3-methylmercapto-aniline (**47e**, 3.201 g, 22.99 mmol) as described above. The crude azide oil was distilled under reduced pressure in 56% yield (2.1272 g, 12.89 mmol).

Compound **46e** showed:

bp = 79 - 80°C/0.3 mm Hg.

R_f (1% MeOH/15% EtOAc/hexanes) = 0.74

UV in C_6H_{12} (c=10^{-5}M) found λ (A) = 250 (0.24), 300 (0.02).

^{1}H NMR ($CDCl_3$) δ 2.45 (H-3', 3H, s), 6.76 (H-6, 1H, ddd, J=7.9, 2.1, 0.8 Hz), 6.84 (H-2, 1H, dd, J=2.1, 1.8 Hz), 6.97 (H-4, 1H, ddd, J=7.9, 1.8, 0.8 Hz), 7.22 (H-5, 1H, dd, J=7.9, 7.9 Hz).

MS (EI) [RI%] found: 165 $(M)^{+\cdot}$ [50%], 137 $(M-N_2)^{+\cdot}$ [32%], 136 $(M-N_2-H)^+$ [25%], 122 $(M-N_2-CH_3)^+$ [100%].

MS (CI) [RI%] found: 165 $(M)^{+\cdot}$ [8%], 140 $(M-N_2+3H)^+$ [100%], 122 $(M-N_2-CH_3)^+$ [12%].

3-Azido-nitrobenzene (46l)

3-Azido-nitrobenzene was synthesized from 3-nitro-aniline, (**101**, 5.235 g, 37.90

mmol) as described above. The crude azide solid was recrystallized from MeOH/H_2O in 98% yield (5.833 g, 35.57 mmol).

Compound **46i** showed:

mp = 54 - 55.5°C (lit.[11a] mp = 54 - 55°C)

R_f (1% MeOH/15% EtOAc/hexanes) = 0.54

UV in C_6H_{12} (c=10^{-4}M) found λ (A) = 208 (0.75), 242 (1.91), 318 (0.18).

^{1}H NMR ($CDCl_3$) δ 7.32 (H-6, 1H, m), 7.51 (H-5, 1H, dd, J=8.1, 8.1 Hz), 7.86 (H-2, 1H, m), 7.97 (H-4, 1H, m).

3-Trifluoroacetamido-aniline (47g)

Compound **100** (449.8 mg, 1.922 mmol) was added to a solution of $SnCl_2 \cdot H_2O$ (2.201 g, 9.755 mmol) and 5 mL EtOH in a 20 mL round bottom flask fitted with a condenser. The solution was heated to 65°C with stirring for 60 minutes. The product was worked up as shown in the synthesis of **24** to give **47g** (160.7 mg, 0.788 mmol, 41%) as a cream coloured solid.

Compound **47g** showed:

^{1}H NMR ($CDCl_3$) δ 3.70 (H-1', 2H, br), 6.51 (H-6, 1H, dd, J=8.0, 1.6 Hz), 6.71 (H-4, 1H, dd, J=8.0, 1.5 Hz), 7.10 (H-2, 1H, dd, J=1.6, 1.5Hz), 7.12 (H-5, 1H, dd, J=8.0, 8.0 Hz), 7.72 (H-3', 1H, br).

MS (EI) [RI%] found: 204 $(M)^{+\cdot}$ [100%], 135 $(M\text{-}CF_3)^+$ [46%], 107 $(M\text{-}COCF_3)^+$ [12%], 92 $(M\text{-}NHCOCF_3)^+$ [82%].

3-Azido-trifluoroacetamido-benzene (46g)

Compound **46g** was synthesized from **47g** (82%) using the procedure used to synthesize **24**. Compound **46g** was a cream coloured solid.

Compound **46g** showed:

mp = 90 - 91°C.

R_f (1% MeOH/15% EtOAc/hexanes) = 0.35

UV in C_6H_{12} ($c=6.7\times10^{-5}$M) found λ (A) = 240 (1.35).

IR υ /cm^{-1} = 3308.3 (s) [NH amide stretching], 3050-3200 (m) [CH aromatic stretching], 2113.6 (s) [N_3 stretching], 1705.8 (s) [C=O amide stretching], 1605.0 (m) [NH amide bending], 1341.7-1158.8 (m) [CF stretching], 844.4 (m) and 790.4 (s) [1,3-substituted benzene].

^{1}H NMR ($CDCl_3$) δ 6.91 (H-6, 1H, ddd, J=7.8, 2.2, 1.4 Hz), 7.22-7.41 (H-2, H-4, H-5, 3H, m), 7.90 (H-3', 1H, br).

MS (EI) [RI%] found: 230 $(M)^{+\cdot}$ [47%], 202 $(M-N_2)^{+\cdot}$ [100%], 175 $(M-55)^+$ [86%].

7.4.4 Disubstituted Aryl Azides

4-Aceto-6-amino-1,2-dihydroquinoxalinone (24)

The general $SnCl_2{\cdot}2H_2O$ procedure was used[22a]. Compound **20** (12.461 g, 53.03 mmol) was refluxed with $SnCl_2{\cdot}2H_2O$ (73.11 g, 324.0 mmol) in 350 mL EtOAc for 5 hours to yield **24**, (7.6374 g, 37.3 mmol, 70.3%), as a brown solid.

Compound **24** showed:

mp = 154 - 157°C.

^{1}H NMR (90 MHz, DMSO-d_6) δ 2.10 (H-4', 3H, s), 4.20 (H-3, 2H, s), 4.90 (H-6', 2H, br), 6.40 (H-7, 1H, dd, J=9, 2Hz), 6.65 (H-5, 1H, d, J=2Hz), 6.70 (H-8, 1H, d, J=9Hz), 10.30 (H-1, 1H, br).

MS (EI) [RI%] found: 205 $(M)^{+\cdot}$ [68%], 163 $(M\text{-}CH_2CO)^{+\cdot}$ [47%], 134 $(M\text{-}CH_2NCOCH_3)^{+\cdot}$ [100%].

4-Aceto-6-azido-1,2-dihydroquinoxalinone (24)

The general procedure[23b] was used. Compound **24** (1.496 g, 7.30 mmol) was treated sequentially with sodium nitrite (560.4 mg, 7.88 mmol) then with sodium azide (524.8 mg, 6.41 mmol) to give tan coloured crystals, **24**, (1.4809 g, 6.41 mmol, 88%). Compound **24** showed:

^{1}H NMR (90 MHz, DMSO-d_6) δ 2.20 (H-4', 3H, s), 4.30 (H-3, 2H, s), 7.00 (H-7 and H-8, 2H, m), 7.32 (H-5, 1H, s), 10.85 (H-1, 1H, br).

MS (EI) [RI%] found: 231 $(M)^{+\cdot}$ [27%], 203 $(M\text{-}N_2)^{+\cdot}$ [100%], 174 $(M\text{-}NCOCH_3)^{+\cdot}$ [13%].

6-Amino-1-(acetic acid ethyl ester)-4-formyl-1,2-dihydroquinoxalinone (25)

The general $SnCl_2{\cdot}2H_2O$ procedure was used. **22** (263.7 mg, 0.8590 mmol, 0.172 M) was refluxed in EtOAc along with $SnCl_2{\cdot}2H_2O$ (982.5 mg, 4.35 mmol, 0.871 M, 5.1 equivalents) for 90 minutes. The solution was extracted with 3x40 mL EtOAc, the organic layers were combined, washed with 2x15 mL saturated NaCl solution, treated with activated charcoal and then filtered through celite under reduced pressure. The solvent was removed under reduced pressure to yield **25**, (218.6 mg, 0.789 mmol, 92%), as a brown solid.

Compound **25** showed:

^{1}H NMR (90 MHz, DMSO-d_6) δ 1.20 (H-1"", 3H, t, J=6Hz), 3.50 (H-6', 2H, br), 4.15 (H-1"', 2H, q, J=6Hz), 4.40 (H-3, 2H, s), 4.50 (H-1', 2H, s), 6.00 (H-7, 1H, dd, J=10, 2Hz), 6.30-6.50 (H-5 and H-8, 2H, m), 8.50 (H-4", 1H, s).

MS (EI) [RI%] found: 277 $(M)^{+\cdot}$ [92%], 249 $(M-CO)^{+\cdot}$ [100%].

Attempted synthesis of 6-azido-1-(acetic acid ethyl ester)-4-formyl-1,2-dihydroquinoxalinone (26)

Compound **25** (85.4 mg, 0.308 mmol) was added to a solution of HCl (560 µl) in H_2O (2.0 ml) at 0°C. $NaNO_2$ (24.5 mg, 0.355 mmol in 1 mL H_2O) was added dropwise to the stirred solution. After 2 hours the solution was transferred to a beaker and NaN_3 (21.2 mg, 0.326 mmol in 1 mL H_2O) was added dropwise with vigorous stirring. After a further 2 hours the solution was filtered and washed with cold H_2O. The solid was dissolved in warm EtOH, treated with charcoal, filtered and evaporated to an oil. The oily residue (22.1 mg) contained two products by TLC (10% MeOH in CH_2Cl_2, Rf = 0.8 and 0.7). Both products showed an absorption in the IR for an azide, (IR υ = 2100). Neither product could be identified by NMR or mass spectrometry. The formyl group most likely was removed during the harsh acidic conditions of the diazotization.

6-Amino-4-(acetic acid ethyl ester)-1,2-dihydroquinoxalinone (106)

The general $SnCl_2{\cdot}2H_2O$ procedure[22a] was used. **99** (1.304 g, 4.675 mmol, 0.156 M) was refluxed with $SnCl_2{\cdot}2H_2O$ (7.756 g, 34.4 mmol, 1.15 M, 7.4 equivalents) in EtOAc (30.0 ml) and refluxed for 2.5 hours. The solution was poured on ice, neutralized with 1M NaOH and then extracted with 4x200 mL EtOAc. The combined organics were evaporated

under reduced pressure to 300 ml, extracted with 3x15 mL brine, dried using anhydrous $NaSO_4$ and then filtered. The solvent was removed under reduced pressure to yield **106** (1.003 g, 4.03 mmol, 86%).

Compound **106** showed:

^{1}H NMR (90 MHz, $CDCl_3$) δ 1.30 (H-4"", 3H, t, J=6Hz), 3.50 (H-6', 2H, br), 3.90 (H-3, 2H, s), 4.00 (H-4', 2H, s), 4.22 (H-4"', 2H, q, J=6Hz), 5.85 (H-5, 1H, d, J=2Hz), 6.10 (H-7, 1H, dd, J=8, 2Hz), 6.52 (H-8, 1H, d, J=8Hz), 8.15 (H-1, 1H, br).

MS (EI) [RI%] found: 249 $(M)^{+\cdot}$ [90%], 176 $(M\text{-}CO_2Et)^+$ [100%].

6-Azido-4-(acetic acid ethyl ester)-1,2-dihydroquinoxalinone (107)

Compound **107** was synthesized from **106** using the general procedure[23a]. Compound **106** (617.5 mg, 2.48 mmol) was dissolved in 2.4M HCl at 0°C. $NaNO_2$ (2.05 mg, 2.97 mmol) in 1 mL H_2O was added dropwise with stirring. After 1 hour, the solution was filtered and the filtrate was transferred to a 250 mL beaker at 0°C. NaN_3 (169.0 mg, 2.60 mmol) in 1 mL H_2O was added dropwise with vigorous stirring and a precipitate formed. The solution was allowed to react for 12 hours at 4°C. The solution was extracted into $CHCl_3$ (3x25 ml). The combined organics were evaporated under reduced pressure. The solid was recrystallized from EtOH/H_2O to yield a tan coloured solid, **107** (593.2 mg, 2.157 mmol, 87%).

Compound **107** showed:

mp = 154°C (decomp.).

^{1}H NMR (90 MHz, DMSO-d_6) δ 1.0 (H-4"", 3H, t, J=7Hz), 3.6-4.1 (H-3, H-4' and H-4"', 6H, m), 6-7 (H-5, H-7 and H-8, 3H, m), 10.4 (H-1, 1H, br).

MS (EI) [RI%] found: 275 $(M)^{+\cdot}$ [47%], 247 $(M-N_2)^{+\cdot}$ [78%], 219 $(M-CH_2CON)^{+}$ [58%], 85 $(M-190)^{+}$ [100%].

3-Acetamido-4-trifluoroacetamido-aniline (52) Via $SnCl_2 \cdot 2H_2O$.

Compound **51** was reduced using the general $SnCl_2.2H_2O$ procedure[22a]. **51** (1.2328 g, 4.2364 mmol, 4.24 M) and $SnCl_2 \cdot 2H_2O$ (4.781 g, 21.19 mmol, 2.12 M, 5 equivalent) was dissolved in EtOAc (10 ml). The solution was refluxed for 2 hours, worked up as described above to afford **52** as an orange/brown solid (733.9 mg, 2.796 mmol, 66%). Compound **52** showed:

R_f (5% MeOH/$CHCl_3$) = 0.03 {**51** R_f = 0.31}.

^{1}H NMR ($CDCl_3$) δ 2.14 (H-3", 3H, s), 3.10 (H-1', 2H, br), 6.31 (H-2, 1H, d, J=2.5 Hz), 6.53 (H-6, 1H, dd, J=8.6, 2.5 Hz), 7.30 (H-5, 1H, , 7.77 (H-3', 1H, br), 9.50 (H-4', 1H, br).

^{13}C NMR ($CDCl_3$/10% MeOH) δ 22.3 (C-3"', **C**H_3), 110.0 (C-2, **C**H), 113.0 (C-6, **C**H), 118.3 (C-4, **C**), 125.0 (C-4"', **C**F_3, q, J_{CF}=130Hz), 126.1 (C-5, **C**H), 131.3 (C-3, **C**), 146.3 (C-1, **C**), 155.4 (C-4", **C**=O, q, J_{CF}=49 Hz), 170.8 (C-3", **C**=O).

3-Acetamido-4-trifluoroacetamido-aniline (52) Via H_2 Pd/C.

Compound **51** (298.9 mg, 1.027 mmol, 0.0342 M) was dissolved in 30 mL MeOH in a Parr flask[22b]. 10%Pd/C (34.9 mg, 12% by weight) was added and the solution was hydrogenated (H_2) at 50 psi for 2.5 hours. The solution was filtered through celite and the celite was washed with 150 mL MeOH. The MeOH was evaporated at reduced pressure to yield crude **52** (273.5 mg, ~1.048 mmol, ~100%). The crude amine was not purified

further.

Compound **52** showed:

R_f (5% MeOH/$CHCl_3$) = 0.03 {**51** R_f = 0.31}.

^{1}H NMR ($CDCl_3$) δ 2.14 (H-3", 3H, s), 3.10 (H-1', 2H, br), 6.31 (H-2, 1H, d, J=2.5 Hz), 6.53 (H-6, 1H, dd, J=8.6, 2.5 Hz), 7.30 (H-5, 1H, d, J=8.6 Hz), 7.77 (H-3', 1H, br), 9.50 (H-4', 1H, br).

5-Azido-2-trifluoroacetamido-acetanilide (49)

Compound **52** (366.0 mg, 1.402 mmol) was dissolved in 2 mL HCl and 1 mL H_2O. $NaNO_2$ (96.6 mg, 1.36 mmol) in 1 mL H_2O was added dropwise with stirring at 0°C. After 45 minutes, the solution was treated with activated charcoal, filtered and stirred at 0°C. The solution was treated with NaN_3 (83.4 mg, 1.27 mmol, 1.2 equivalent) as in the general procedure. The solid was recrystallized from MeOH/H_2O to give **49** as yellow needles (348.6 mg, 1.21 mmol, 87%).

Compound **49** showed:

mp = 167 - 170 °C (decomp.)

R_f (1%MeOH/15%EtOAc/hexanes) = 0.44 {**52** R_f = 0.03}

UV (c=6.3x10^{-5}M) found λ (A) = 235 (0.996), 271 (0.663).

IR υ /cm^{-1} = 3266.9 (s) [NH amide stretching], 2123.7 (s) [N_3 stretching], 1739.4 (s) [C=O(CF_3) stretching], 1655.4 (s) [C=O(CH_3) stretching], 1530.3 (m) and 1433.2 (m) [NH amide bending], 1373.1-1155.8 (m) [CF stretching].

^{1}H NMR ($CDCl_3$) δ 2.24 (H-3", 3H, s), 6.74 (H-2, 1H, d, J=2.5 Hz), 6.98 (H-6, 1H, dd, J=8.7, 2.5 Hz), 7.54 (H-3', 1H, br), 7.70 (H-5, 1H, d, J = 8.7 Hz),

9.62 (H-4', 1H, br).

^{13}C NMR ($CDCl_3$) δ 22.8 (C-3''', **C**H_3), 114.8 (C-2, **C**H), 115.8 (C-4''', **C**F_3, q, J_{CF} = 286 Hz), 116.7 (C-6, **C**H), 124.9 (C-4, **C**), 126.7 (C-5, **C**H), 132.0 (C-3, **C**), 138.9 (C-1, **C**), 155.8 (C-4'', **C**=O, q, J_{CF} = 32 Hz), 171.1 (C-3'', **C**=O).

MS (EI) [RI%] found: 288 $(M+H)^+$ [17%], 287 $(M)^{+\cdot}$ [16%], 259 $(M-N_2)^{+\cdot}$ [77%], 217 $(M-HCF_3)^{+\cdot}$ [58%], 190 $(M-COCF_3)^{+\cdot}$ [16%], 162 $(M-N_2-COCF_3)^+$ [100%], 148 $(M-N_2-NCOCF_3)^{+\cdot}$ [43%].

MS (CI) [RI%] found: 305 $(M+NH_4)^+$ [100%], 288 $(M+H)^+$ [17%], 279 $(M+NH_4+2H-N_2)^+$ [96%].

HRMS (EI) found exact mass = 287.0619 g/mol

calcd.($C_{10}H_8F_3N_5O_2$) = 287.0630 g/mol (MMU = 1.1).

Alternate Synthesis of 5-Azido-2-trifluoroacetamido-acetanilide (49)

Compound **51** (2.0244 g, 6.957 mmol) was dissolved in 190 mL MeOH and 10 mL H_2O in a Parr flask. 10%Pd/C (2.023 mg, 10% by weight) was added and the solution was hydrogenated (H_2) at 50 psi for 3.5 hours. The solution was filtered through celite and the celite was washed with 150 mL MeOH. The MeOH was evaporated at reduced pressure to yield crude **52**. The crude solid was dissolved in 8 mL 6M HCl. $NaNO_2$ (600.1 mg, 8.436 mmol, 1.2 equivalents) in 1 mL H_2O was added dropwise with stirring at 0°C. After 45 minutes, the solution was treated with activated charcoal, filtered and stirred at 0°C. The solution was treated with NaN_3 (513.0 mg, 7.812 mmol, 1.12 equivalents) as in the general procedure. The solid was recrystallized from MeOH/H_2O to give **49** as yellow needles (1.1975 g, 4.1724 mmol, 60%). The mother liquor was evaporated at reduced

pressure and recrystallized using MeOH/H_2O to yield a second crop of **49** (353.0 mg, 1.23 mmol, 18%) for a total yield of 78%.

Compound **49** showed:

mp = 168 - 170 °C (decomp.)

R_f (1%MeOH/15%EtOAc/hexanes) = 0.44

3,4-di(Trifluoroacetamido)-aniline (54)

Compound **53** (2.001 g, 5.8 mmol) was reduced as described above using the $SnCl_2.2H_2O$ procedure[22a] to give crude **54**. The solid was recrystallized from MeOH/H_2O in 66% yield (1.193 g, 3.788 mmol).

Compound **54** showed:

^{1}H NMR ($CDCl_3$) δ 3.90 (H-1', 2H, br), 6.60 (H-6, 1H, dd, J=8.7, 2.5 Hz), 6.80 (H-2, 1H, d, J=2.5 Hz), 7.11 (H-5, 1H, d, J=8.7 Hz), 8.31 (H-4', 1H, br), 8.68 (H-3', 1H, br).

MS (EI) [RI%] found: 316 $(M+H)^+$ [55%], 315 $(M)^{+\cdot}$ [67%], 246 $(M-CF_3)^+$ [7%], 218 $(M-COCF_3)^+$ [13%], 202 $(M-H_2NCOCF_3)^{+\cdot}$ [71%], 201 $(M-HNCOCF_3)^+$ [100%], 181 (M-134)$^+$ [39%], 149 $(M-COCF_3-CF_3)^+$ [83%].

MS (CI) [RI%] found: 333 $(M+NH_4)^+$ [78%], 315 $(M)^{+\cdot}$ [13%], 202 $(M-H_2NCOCF_3)^{+\cdot}$ [100%].

HRMS (EI) found exact mass = 315.04320 g/mol

Calcd. mass ($C_{10}H_7F_6N_3O_2$) = 315.04424 g/mol (1.04 mmu).

4-Azido-1,2-di(trifluoroacetamido)-benzene (48)

The azide, **48**, was synthesized from the respective aniline, **54**, (471.4 mg, 1.497 mmol) in the above described manner in 30% yield (149.0 mg, 0.437 mmol) as light

orange/red needles after recrystallization from MeOH/H_2O.

Compound **48** showed:

mp = 108.5 - 109°C

R_f (1% MeOH/15% EtOAc/hexanes) = 0.16

UV (c=4x10^{-4}M) found λ (A) = 265 (1.75), 292 (1.09).

IR υ /cm^{-1} = 3387.2 (s) [NH amide stretching], 3212.0-3047.4 (m) [CH aromatic stretching], 2133.2 (s) [N_3 stretching], 1739.8 and 1705.5 (s) [C=O stretching], 1604.7 (m) and 1541.2 (m) [NH amide bending], 1300-1150 (m) [CF stretching].

^{1}H NMR ($CDCl_3$) δ 7.03 (H-6, 1H, dd, J=8.6, 2.4 Hz), 7.16 (H-2, 1H, d, J=2.4 Hz), 7.41 (H-5, 1H, d, J=8.6 Hz), 8.48 (H-4', 1H, br), 8.65 (H-3', 1H, br).

^{13}C NMR ($CDCl_3$) δ 116.1 (C-2, **C**H), 118.1 (C-6, **C**H), 125.1 (C-4, **C**), 127.3 (C-5, **C**H), 130.2 (C-3, **C**), 139.8 (C-1, **C**), 156.5 (C-3", **C**OCF_3, q, J_{CF}=46 Hz), 170.5 (C-4", **C**OCF_3, q, J_{CF}=46 Hz).

MS (EI) [RI%] found: 341 $(M)^{+\cdot}$ [8%], 313 $(M-N_2)^+$ [21%], 216 $(M-99)^+$ [100%].

MS (CI) [RI%] found: 359 $(M+NH_4)^+$ [100%], 342 $(M+H)^+$ [4%], 341 $(M)^{+\cdot}$ [10%], 333 $(M+NH_4-N_2)^+$ [17%], 314 $(M+H-N_2)^{+\cdot}$ [12%], 313 $(M-N_2)^{+\cdot}$ [25%], 216 $(M-125)^+$ [100%].

HRMS (EI) found exact mass = 341.0355 g/mol

calcd. mass ($C_{10}H_5F_6N_5O_2$) = 341.0347 g/mol (0.8 mmu)

Synthesis of 2-Chloro-5-nitro-acetanilide (89)

2-Chloro-5-nitro-aniline (**108**, 1.007 g, 5.80 mmol) was dissolved in 25 mL THF and cooled to -30°C. Acetylchloride (5 ml, 5.5 g, 70.3 mmol, 12 equivalents) was added

dropwise with stirring. TLC after 30 minutes showed no more starting **108** and then 10 mL of H_2O was added. The solution was allowed to warm to room temperature and the solvents were removed by evaporation under reduced pressure. The solid was recrystallized to yield **89** as beige crystals (1.057 g, 4.93 mmol, 85%).

Compound **89** showed:

mp = 157 - 158°C (lit.[5a] mp = 156°C)

R_f (1% MeOH/15% EtOAc/hexanes) = 0.05

R_f (1% MeOH/50% EtOAc/hexanes) = 0.54

^{1}H NMR (DMSO-d_6) δ 2.15 (H-3"', 3H, s), 7.77 (H-5, 1H, d, J=8.9), 7.97 (H-6, 1H, dd, J=2.7, 8.9), 8.73 (H-2, 1H, d, J=2.7), 9.82 (H-3', 1H, br).

^{13}C NMR (DMSO-d_6) δ 23.5 (C-3"', **C**H_3), 119.1 (C-2, **C**H), 119.9 (C-6, **C**H), 130.6 (C-5, **C**H), 131.7 (C-4, **C**), 136.1 (C-3, **C**), 146.2 (C-1, **C**), 169.3 (C-3", **C**=O).

Synthesis of 3-Acetamido-4-chloro-aniline (90)

2-Chloro-5-nitro-acetanilide (**89**, 353.5 mg, 1.648 mmol) was reduced using the tin(II)chloride procedure (1.913 g $SnCl_2 \cdot 2H_2O$, 8.48 mmol in 6 mL EtOAc). The crude aniline was not purified further (**90**, 273.1 mg, ~1.48 mmol, ~90%).

Compound **90** showed:

R_f (1% MeOH/15% EtOAc/hexanes) = 0.012

R_f (1% MeOH/50% EtOAc/hexanes) = 0.27

^{1}H NMR (DMSO-d_6) δ 2.02 (H-3"', 3H, br), 5.46 (H-1', 2H, br), 6.36 (H-6, 1H, dd, J=2.7, 8.6), 6.98 (H-2, 1H, d, J=2.7), 7.03 (H-5, 1H, d, J=8.6).

MS (EI) [RI%] found: 186 ($M\{^{37}Cl\})^{+\cdot}$ [8%], 184 ($M\{^{35}Cl\})^{+\cdot}$ [34%], 149 $(M\text{-}Cl)^{+\cdot}$ [100%], 144 ($M\{^{37}Cl\}\text{-}CH_2CO)^{+\cdot}$ [27%], 142 ($M\{^{35}Cl\}\text{-}CH_2CO)^{+\cdot}$ [83%], 114 ($M\{^{35}Cl\}$-70) [12%].

HRMS (EI) found exact mass = 184.03954 g/mol

calcd. mass ($C_8H_9ClN_2O$) = 184.04034 g/mol (MMU = 0.8)

Synthesis of 5-Azido-2-chloro-acetanilide (91)

The crude **90** (273.1 mg, 1.480 mmol) was converted into the azide **91** (184.5 mg, 0.876 mmol, 59% or 45% from **89**) by the general procedure.

Compound **91** showed:

mp = 131.0 - 131.5°C

R_f (1% MeOH/15% EtOAc/hexanes) = 0.17

UV ($c=1.5\times10^{-4}$M) found λ (A) = 232 (1.009), 262 (0.710), 290 (0.135).

IR υ /cm^{-1} = 3250.4 (s) [NH amide stretching], 3100-3000 (m) [CH aromatic stretching], 2119.5 (s) [N_3 stretching], 1664.8 (s) [C=O stretching], 1578.1 (m) [NH bending], 804.7-620.3 (m) [C-Cl bending].

^{1}H NMR ($CDCl_3$) δ 2.23 (H-3‴, 3H, s), 6.68 (H-6, 1H, dd, J=2.7, 8.6), 7.29 (H-5, d, J=8.6), 7.60 (H-3', 1H, br), 8.19 (H-2, 1H, d, J=2.7).

^{13}C NMR ($CDCl_3$) δ 24.8 (C-3‴, **C**H_3), 111.9 (C-2, **C**H), 115.0 (C-6, **C**H), 119.5 (C-4, **C**), 129.7 (C-5, **C**H), 135.6 (C-1, **C**), 139.9 (C-3, **C**), 168.3 (C-3", **C**=O).

MS (EI) [RI%] found: 212 ($M\{^{37}Cl\})^{+\cdot}$ [15%], 210 ($M\{^{35}Cl\})^{+\cdot}$ [47%], 184 ($M\{^{37}Cl\}\text{-}N_2)^{+\cdot}$ [17%], 182 ($M\{^{35}Cl\}\text{-}N_2)^{+\cdot}$ [52%], 155 ($M\{^{35}Cl\}$-55)$^+$ [19%], 142 ($M\{^{37}Cl\}\text{-}N_2\text{-}CH_2CO)^{+\cdot}$ [19%], 140 ($M\{^{35}Cl\}\text{-}N_2\text{-}CH_2CO)^{+\cdot}$ [36%].

HRMS (EI) found exact mass = 210.0300 g/mol

calcd. mass ($C_8H_7ClN_4O$) = 210.0308 g/mol (MMU = 0.8)

7.5 Thermolysis of Arylazides

The general procedure was similar to that used by Ohba *et al.*[11a,b]. The azide was dissolved in the appropriate solvent (usually MeOH) at a concentration below 0.5 M and sealed in a pyrex tube. The tube was heated to 170°C for 2 hours in a bomb apparatus. The crude reaction mixture was evaporated under reduced pressure and a ^{1}H NMR was taken. The mixture was then chromatographed on silica to isolate the products.

Thermolysis of 4-Aceto-6-azido-1,2-dihydroquinoxalinone (24) in MeOH.

The procedure was similar to that used by Ohba[11a,b]. The azide (**24**, 100.2 mg, 0.611 mmol, 0.204 M) was dissolved in 3 mL of MeOH in a sealed pyrex tube. The tube was placed in a bomb and heated to 170°C for 2 hours. The bomb was cooled to room temperature and then the tube was removed. The tube was opened and the contents were evaporated under reduced pressure to yield a yellow/brown oil. The oil was chromatographed on silica using 5% MeOH in $CHCl_3$ as the eluent. TLC (silica) showed many products but no recognizable azepine products were found by ^{1}H NMR or mass spectrometry.

Thermolysis of 4-Azidoacetanilide (38) in MeOH.

The azide, **38**, (206.0 mg, 1.170 mmol, 0.39 M) was dissolved in 3 mL MeOH in a sealed tube as described above. The solution was heated to 160°C for 2 hours. The solution was evaporated under reduced pressure to yield a orange-brown oil (mass of

187.5 mg). The oil was flash chromatographed on silica but no recognizable products were obtained.

Thermolysis of 4-Azidoacetophenone (30) in Ethanolamine.

The procedure was similar to that used by Huisgen *et al.*[11c,d]. 4-Azidoacetophenone (600.8 mg, 3.732 mmol, 0.249 M) was dissolved in 15 mL of ethanolamine in a 30 mL round bottom flask fitted with a condenser. The solution was heated to reflux for 90 min. The solution was cooled and poured into 45 mL of water. The solution was acidified with 1M HCl to a pH = 6-7. The aqueous was extracted with 3X30 mL ethyl acetate (EtOAc). The combined organics were evaporated under reduced pressure to yield 448.3 mg of product. The products could not be identified by ^{1}H NMR.

Thermolysis of 30 in ^{n}PrOH.

The azide (415.7 mg, 2.582 mmol, 0.129 M) was refluxed in 20 mL ^{n}PrOH. The reaction was monitored by the disappearance of the azide peak at υ=2100 cm^{-1} relative to the peak at υ=1600 cm^{-1}. The solution was cooled after 50 hours when the azide IR peak had almost disappeared. The solvent was removed by reduced pressure. No recognizable 3H-dihydroazepine products were observed by ^{1}H NMR as described by the literature[9a].

7.6 Photolysis of Arylazides

7.6.1 General Procedure

The general procedure was similar to that used by Schuster *et al.*[9a]. The azide and

nucleophile (typically $HNEt_2$) were dissolved in the appropriate solvent (THF or cyclohexane) in a quartz photolysis tube. The solution was degassed for 15 minutes with dry nitrogen and then irradiated with 300 nm UV light in a Rayonet reactor. The reaction mixture was evaporated at reduced pressure to remove the solvent and a ^1H NMR spectrum was recorded for determination of product yields (the ^1H NMR analysis is outlined in more detail in the first photolysis example).

The product ratios were determined by ^1H NMR which were obtained from at least 128 scans with an estimated error of 2% for the meta- and di-substituted phenylazide photolyses. The estimated error was based on three different acquired fourier transformed FID's that, when separately integrated, yielded the same ratio of products, determined from the integration of the appropriate resonances. The products were isolated by chromatography on silica gel using a Chromatotron apparatus. The products were identified by NMR and mass spectrometry.

7.6.2 Photolysis of para-Substituted Arylazides

Photolysis of 4-Azido-trifluoroacetamido-benzene (33) in 2M $HNEt_2/C_6H_{12}$ to yield 2-diethylamino-5-trifluoroacetamido-3H-dihydroazepine (42).

The azide (14.95 mg, 0.065 mmol, 5 x 10^{-3}M) was dissolved in a 2M $HNEt_2$ in C_6H_{12} solution (13 ml) and photolyzed as described above for 1 hour at 300 nm and 30°C. The solution was evaporated under reduced pressure and the reaction flask was rinsed with three 2 mL volumes of MeOH. The MeOH solution was added to the products and evaporated under reduced pressure to yield 22.2 mg of a black oil. The oil contained three major products by ^1H NMR analysis: 29% unreacted azide, (35), 17% 4-trifluoroacetamido-aniline, (34) and 53% 2-diethylamino-5-trifluoroacetamido-3H-

dihydroazepine, (42) by ^{1}H NMR integration (shown below in Figure 7.1). The appropriate resonances for each of the products is marked in the Figure.

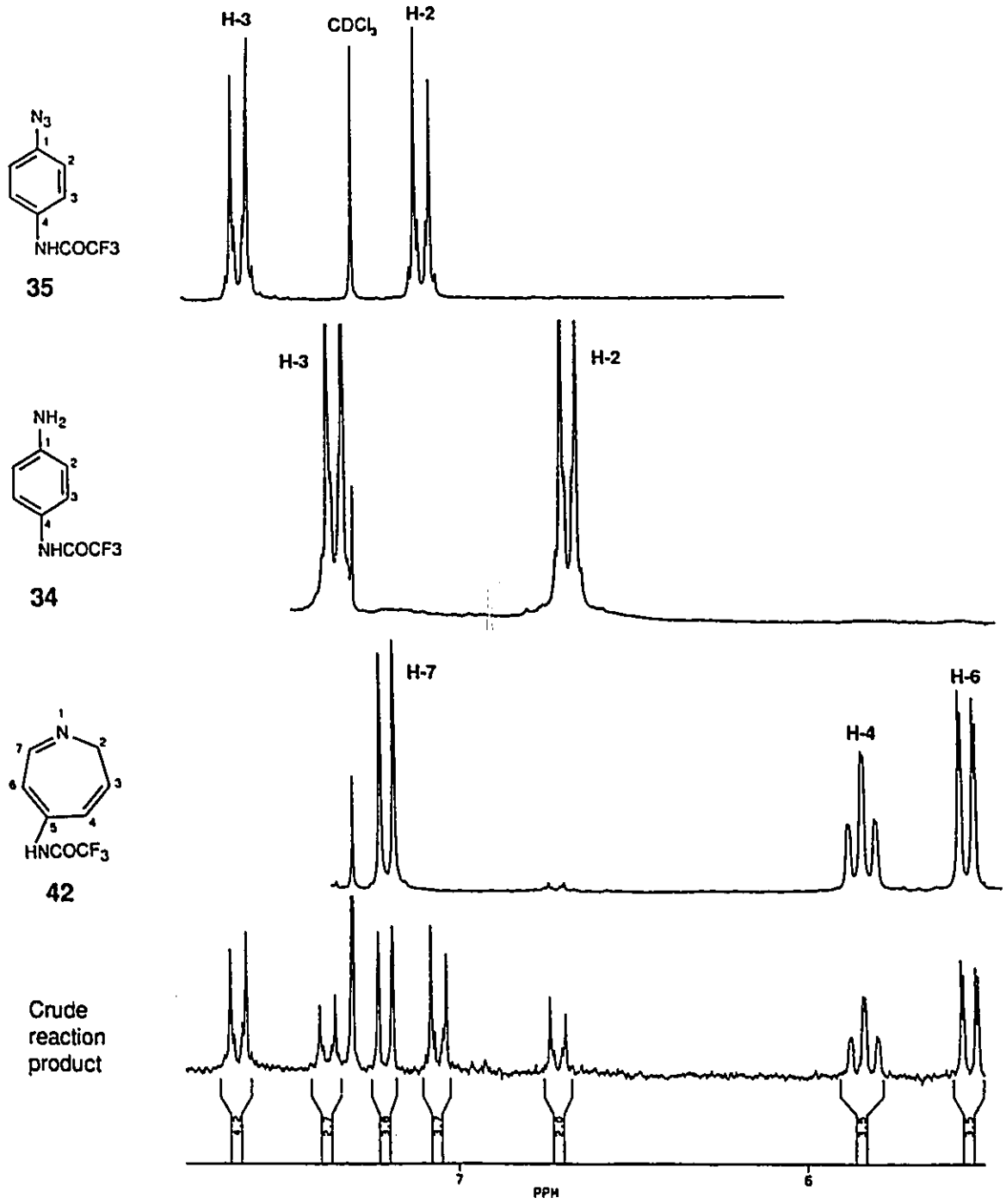

Figure 7.1 ^{1}*H NMR of the crude reaction mixture from the photolysis of* ***35****.*

The mass of the isolated products (22.2 mg) was large because some $HNEt_3$ (36% by mole, 4.0 mg) and MeOH (21%, 1.0 mg) was present in the final mixture along with **35** (13%, 4.3 mg), **34** (8%, 2.3 mg) and **42** (23%, 9.5 mg). The total estimated mass (if **35** was converted only into **34** and **42**) was found to be 21.2 mg illustrating that all the reacted azide was converted into **34** and **42** only.

Ratio of products (by NMR): **35:34:42** = 29:17:53.

Compound **42** showed:

^{1}H NMR ($CDCl_3$) δ 1.14 (H-2''', 6H, br), 2.80 (H-3, 2H, br), 3.36 (H-2'', 4H, br), 5.48 (H-6, 1H, dd, J=8.1, 1.4), 5.79 (H-4, 1H, td, J=7.7, 1.4), 7.14 (H-7, 1H, d, J=8.1), 7.42 (H-5', 1H, br). Owing to conformational exchange of the azepine ring, the H-3 proton resonances were too weak to be reliably distinguished from noise.

Photolysis of 35 in 2M $HNEt_2$/THF: Preparative Scale.

The azide (111.0 mg, 0.483 mmol, 5 x 10^{-3}M) was dissolved in a 2M $HNEt_2/C_6H_{12}$ solution (100 ml) and photolyzed as described above for 75 minutes at 300 nm at 30°C. The product was chromatographed using a Chromatotron (2mm silica, 1% MeOH/5% EtOAc/hexanes for first fraction, then 1% MeOH/15% EtOAc/hexanes for the remaining) to separate the three products **35**, **34** and **42**.

Ratio of products (by ^{1}H NMR): **35:34:42** = 15:20:65.

^{1}H NMR and ^{13}C NMR assignments were confirmed by Spin-Sort, DEPT and ^{1}H-^{13}C HET-CORR experiments.

Compound **42** showed:

^{13}C NMR ($CDCL_3$) δ 14.0 (C-2''', **C**H_3), 29.4 (C-3, **C**H_2), 43.3 (C-2", **C**H_2), 102.2 (C-4, **C**H), 104.7 (C-6, **C**H), 115.7 (C-5''', **C**F_3, q, J_{CF} = 289 Hz), 133.6 (C-5, **C**), 143.3 (C-7, **C**H), 148.1 (C-2, **C**), 155.0 (C-5', **C**=O, q, J_{CF}=37 Hz). Carbon C-3 was indistinguishable from baseline noise because of conformational exchange of the azepine ring.

MS (EI) [RI%] found 275 $(M)^{+\cdot}$ [100%], 260 $(M\text{-}CH_3)^+$ [40%], 246 $(M\text{-}Et)^+$ [32%], 218 $(M\text{-}CF_3)^+$ [15%], 204 $(M\text{-}NEt_2\text{+}H)^{+\cdot}$ [100%].

MS (CI) [RI%] found 276 $(M+H)^+$ [100%].

HRMS (EI) found exact mass = 275.1255 g/mol

calcd. mass ($C_{12}H_{16}F_3N_3O$) = 275.1245 g/mol (MMU = -1.0).

Isolated yields:

Fraction	Product	Yield		
1	**35**	3.7 mg	0.16 mmol	3.3%
2	**34**	1.4 mg	0.007 mmol	1.4%
3	**42**	24.3 mg	0.088 mmol	18.3%

Photolysis of 35 in 2M $HNEt_2/CCl_4$ at 30°C.

The azide (14.5 mg, 0.063 mmol, 5 x 10^{-3}M) was dissolved in a 2M $HNEt_2/CCl_4$ solution (12.5 ml) and photolyzed as described above for 10 minutes at 300 nm and 30°C. Ratio of products (by ^1H NMR): **35**:**34**:**42** = 70:trace:30.

Photolysis of 4-Azido-acetanilide (38) in 2M $HNEt_2/C_6H_{12}$ at 30°C.

12 mL of a 3 x 10^{-3}M solution of 4-azido-acetanilide (**38**, 45.0 mg, 0.256 mmol, in 50 ml) in $HNEt_2/C_6H_{12}$ (2M $HNEt_2$) was photolyzed as described above at 300 nm and

30°C for 30 min. The ^{1}H NMR and TLC showed the 4-amino-acetanilide (**104**) was the major product.

7.6.3 Photolysis of Meta-substituted Arylazides

Photolysis of 3-Azido-trifluoroacetamidobenzene (46g) in 2M $HNEt_2/C_6H_{12}$ at 30°C to yield 2-diethylamino-6-trifluoroacetamido-3H-dihydroazepine (44g) and 2-diethylamino-4-trifluoroacetamido-3H-dihydroazepine (45g).

The procedure was similar to that used by Schuster[9a]. The azide (58.5 mg, 0.254 mmol, $5.1x10^{-3}$M) was dissolved in a 2M solution of $HNEt_2$ (10 ml, 7.07 g, 97 mmol) and C_6H_{12} (40 ml) in a quartz tube fitted with a septum cap. The solution was degassed using dry N_2 for 10 minutes. The solution was then photolyzed for 30 minutes at 300nm and 30°C in a Rayonet apparatus. The solvent was removed by evaporation at reduced pressure and the ^{1}H NMR spectrum was recorded. There were four products present: the starting azide (**46g**, 22%), 3-trifluoroacetamido-aniline (**47g**, <5%), and the 2-closure (**44g**, 46%) and 6-closure (**45g**, 32%) azepine products.

Ratio of products (by ^{1}H NMR): **46g:47g:44g:45g** = 22:trace:46:32.

The 2-closure product, 2-diethylamino-6-trifluoroacetamido-3H-dihydroazepine (**44g**) showed:

^{1}H NMR ($CDCl_3$) δ 1.11 (H-2", 6H, m), 2.70 (H-3, 2H, br), 3.30 (H-2', 4H, m), 5.18 (H-4, 1H, dt, J=8.9, 7.9 Hz), 6.37 (H-5, 1H, dd, J=8.9, 1.5 Hz), 7.21 (H-7, 1H, d, J=1.5 Hz).

The 6-closure product, 2-diethylamino-4-trifluoroacetamido-3H-dihydroazepine (**45g**) showed:

^{1}H NMR ($CDCl_3$) δ 1.11 (H-2", 6H, m), 2.70 (H-3, 2H, br), 3.34 (H-2', 4H, m),

5.66 (H-6, 1H, dd, J=7.8, 6.2 Hz), 6.24 (H-5, 1H, d, J=6.2 Hz), 7.10 (H-7, 1H, d, J=7.8 Hz).

MS (EI) [RI%] found: 275 $(M)^{+\cdot}$ [100%], 260 $(M\text{-}CH_3)^+$ [11%], 246 $(M\text{-}Et)^+$ [42%], 204 $(M\text{-}NEt_2\text{+}H)^{+\cdot}$ [28%], 202 $(M\text{-}HNEt_2)^{+\cdot}$ [35%].

Photolysis of 46g in 2M $HNEt_2$/THF at 35°C.

A $5.4x10^{-3}$M solution of the azide (**46g**) in 2M $HNEt_2$/THF was photolyzed as described above at 35°C for 25 minutes at 300 nm. The solvent was removed by evaporation at reduced pressure and the ^1H NMR spectrum was recorded.

Ratio of products (by ^1H NMR): **46g:47g:44g:45g** = 23:trace:36:40.

Photolysis of 46g in $HNEt_2$/THF at 35°C: Preparative Scale.

A $8.8x10^{-3}$M solution (100 ml) of the azide (**46g**) in 2M $HNEt_2$/THF was photolyzed as described above at 35°C for 60 minutes at 300 nm. The solvent was removed by evaporation at reduced pressure and the ^1H NMR spectrum was recorded. The oil was chromatographed using a Chromatotron (2mm silica plate, 1%MeOH/$CHCl_3$) to yield one fraction (197.7 mg, 80% recovery of all three products).

Ratio of products (by ^1H NMR): **46g:47g:44g:45g** = 63:trace:17:20.

Photolysis of 46g in $HNEt_2$/THF at -70°C.

A $5.5x10^{-3}$M solution of the azide (**46g**, 15.8 mg, 0.0687 mmol) in 2M $HNEt_2$/THF was photolyzed as described above in a dry ice/MeOH bath at -70°C for 25 minutes at 300 nm. The solvent was removed by evaporation at reduced pressure and the ^1H NMR

spectrum was recorded.

Ratio of products (by ^{1}H NMR): **46g:47g:44g:45g** = 52:trace:12:36.

Photolysis of 46g in 0.02M $HNEt_2$/THF at 35°C.

A $4.6x10^{-3}$M solution of the azide (**46g**, 13.9 mg, 0.060 mmol) in 0.0201M $HNEt_2$/THF solution was photolyzed as described above at 35°C for 25 minutes at 300 nm. The solvent was removed by evaporation at reduced pressure and the ^{1}H NMR spectrum was recorded.

Ratio of products (by ^{1}H NMR): **46g:47g:44g:45g** = 44.7:trace:26.3:29.0.

Photolysis of 3-Azido-chlorobenzene (46a) in 2M $HNEt_2/C_6H_{12}$ at 30°C to Yield 6-Chloro-2-diethylamino-3H-dihydroazepine (44a) and 4-Chloro-2-diethylamino-3H-dihydroazepine (45a).

A solution of the azide (**46a**, 223.4 mg, 1.454 mmol, 0.0073 M) was photolyzed as described above for 3.5 hours at 300 nm and 30°C. An oil was isolated. The oil was chromatographed using a Chromatotron (1mm silica plate, 15%EtOAc/hexanes) to yield two fractions. Fraction #1 contained primarily the reduced product, 3-chloro-aniline, **107**, (106.0 mg) and some aliphatic impurities. Fraction #2 contained the azepines, **44a** and **45a**, and trapped solvents (186.5 mg).

Ratio of products (by ^{1}H NMR): **46a:47a:44a:45a** = 49:trace:33:18.

The 2-closure product, 6-Chloro-2-diethylamino-3H-dihydroazepine (**44a**) showed:

R_f (2% MeOH/CH_2Cl_2) = 0.125

^{1}H NMR ($CDCl_3$) δ 1.00 - 1.30 (H-2", 6H, m), 2.64 (H-3, 2H, br), 3.20 - 3.30 (H-2', 4H, m), 5.04 (H-4, 1H, dt, J=8.8, 7.7 Hz), 6.25 (H-5, 1H, m), 7.22 (H-7, 1H, d, J=1.2 Hz).

The 6-closure product, 4-Chloro-2-diethylamino-3H-dihydroazepine (**45a**) showed:

R_f (2% MeOH/CH_2Cl_2) = 0.077

^{1}H NMR ($CDCl_3$) δ 1.00 - 1.30 (H-2", 6H, m), 2.92 (H-3, 2H, br), 3.30 - 3.40 (H-2', 4H, m), 5.50 (H-6, 1H, dd, J=7.9, 6.1 Hz), 6.25 (H-5, 1H, m), 6.99 (H-7, 1H, d, J=7.9 Hz).

MS (EI) [RI%] found: 200 ($M\{^{37}Cl\})^{+\cdot}$ [39%], 199(^{37}M-H)$^+$ [70%], 198($^{35}M)^{+\cdot}$ [100%], 169(^{35}M-Et)$^+$ [37%], 127(^{35}M+H-$NEt_2)^{+\cdot}$ [32%].

MS (CI) [RI%] found: 201 (^{37}M+H)$^+$ [33%], 199(^{35}M+H)$^+$ [100%].

Photolysis of 46a in 2M $HNEt_2/C_6H_{12}$ at 30°C: Preparative Scale.

A 0.007 M solution of the azide (**46a**, 220.1 mg, 1.433 mmol) in 2M $HNEt_2/C_6H_{12}$ (50 mL $HNEt_2$, 35.4 g, 483 mmol; 150 mL C_6H_{12}) was photolyzed as described above for 1 hour at 300 nm and 30°C.

Ratio of products (by ^{1}H NMR): **46a:47a:44a:45a** = 56:trace:22:22.

Photolysis of 46a in 2M $HNEt_2$/THF at 30°C.

A 0.0067 M solution of **46a** (13.4 mg, 0.087 mmol) in 2M $HNEt_2$/THF was photolyzed as described for 25 minutes at 30°C. The solution was evaporated under reduced pressure to yield a yellow oil.

Ratio of products (by ^{1}H NMR): **46a:47a:44a:45a** = 49:trace:33:18.

Photolysis of 46a in $HNEt_2$/THF at -70°C.

A 0.0084 M solution (12.5 ml) of **46a** was photolyzed as described above for 30 minutes at -70°C at 300 nm.

Ratio of products (by ^{1}H NMR): **46a:47a:44a:45a** = 40:12:33:15.

Photolysis of 46a in 0.02M $HNEt_2$/THF at 30°C.

A 0.0076 M solution of **46a** (15.1 mg, 0.098 mmol) in 0.02M $HNEt_2$/THF was photolyzed as described for 60 minutes at 30°C. The solution was evaporated under reduced pressure to yield a yellow oil. An NMR was run to determine the product ratios.

Ratio of products (by ^{1}H NMR): **46a:47a:44a:45a** = 12:trace:59:29.

Photolysis of 3-Azido-bromobenzene (46b) in 2M $HNEt_2/C_6H_{12}$ at 30°C to Yield 6-Bromo-2-diethylamino-3H-dihydroazepine (44b) and 4-Bromo-2-diethylamino-3H-dihydroazepine (45b).

A $7.4x10^{-3}$M solution of the azide (292.9 mg, 1.479 mmol) in 2M $HNEt_2/C_6H_{12}$ (200 ml) was photolyzed for 2 hours at 300 nm and 30°C as described above. The solvent was removed by evaporation at reduced pressure and the ^{1}H NMR spectrum of the residue was recorded. The crude product was chromatographed on a 2 mm Chromatotron plate using 2% MeOH/15% EtOAc/hexanes for the elution solvent. Four fractions were collected. The first fraction contained the starting azide **46b**. The second fraction contained both dihydroazepines, **44b** and **45b**.

Ratio of products (by ^{1}H NMR): **46b:47b:44b:45b** = 49:6:32:13.

The 2-closure product, 6-bromo-2-diethylamino-3H-dihydroazepine (**44b**) showed:

^{1}H NMR ($CDCl_3$) δ 1.11 (H-2", 6H, t, J=7.1 Hz), 3.29 (H-2', 4H, q, J=7.1 Hz), 5.04 (H-4, 1H, dt, J=8.7, 7.4 Hz), 6.40 (H-5, 1H, dd, J=8.7, 1.2 Hz), 7.38 (H-7, 1H, d, J=1.2 Hz).

The 6-closure product, 4-bromo-2-diethylamino-3H-dihydroazepine (**45b**) showed:

^{1}H NMR ($CDCl_3$) δ 1.26 (H-2", 6H, t, J=7.1 Hz), 3.33 (H-2', 4H, q, J=7.1 Hz), 5.52 (H-6, 1H, dd, J=7.9, 6.1 Hz), 6.42 (H-5, 1H, d, J=6.1 Hz), 7.04 (H-7, 1H, d, J=7.9 Hz).

44b and **45b** showed:

MS (EI) [RI%] found: 244(^{81}M {^{81}Br})$^{+\cdot}$ [60%], 242(^{79}M)$^{+\cdot}$ [62%], 229(^{81}M-CH_3)$^+$ [8%], 227(^{79}M-CH_3)$^+$ [10%], 215(^{81}M-Et)$^+$ [35%], 213(^{79}M-Et)$^+$ [37%], 173(^{81}M-NEt_2)$^+$ [42%], 171(^{79}M-NEt_2)$^+$ [42%].

MS (CI) [RI%] found: 245(^{81}M+H)$^+$ [98%], 243(^{79}M+H)$^+$ [100%].

Photolysis of 46b in 2M $HNEt_2/C_6H_{12}$ at 30°C.

A 0.0073 M solution of **46b** (290.0 mg, 1.465 mmol) in 1.92 M $HNEt_2/C_6H_{12}$ (200 ml) was photolyzed as described above for 90 minutes at 300 nm and 30°C.

Ratio of products (by ^{1}H NMR): **46b:47b:44b:45b** = 49:6:32:13.

Photolysis of 46b in 2M $HNEt_2$/THF at 30°C.

A 0.0081 M solution of **46b** (20.9 mg, 0.106 mmol) in 2M $HNEt_2$/THF (13 ml) was photolyzed as described above for 60 minutes at 300 nm and 30°C.

Ratio of products (by ^{1}H NMR): **46b:47b:44b:45b** = 29:15:44:12.

Photolysis of 46b in $HNEt_2$/THF at -70°C.

A 0.0084 M solution of **46b** (20.9 mg, 0.106 mmol) in 1.92 M $HNEt_2$/THF (12.5 ml) was photolyzed as described above for 30 minutes at -70°C at 300 nm.

Ratio of products (by ^{1}H NMR): **46b:47b:44b:45b** = 73:7:20:trace.

Photolysis of 46b in 0.02M $HNEt_2$/THF at 30°C.

A 0.0069 M solution of **46b** (17.7 mg, 0.089 mmol) in 0.02M $HNEt_2$/THF (13 ml) was photolyzed as described above for 60 minutes at 300 nm and 30°C.

Ratio of products (by ^1H NMR): **46b**:**47b**:**44b**:**45b** = 29:trace:52:18.

Photolysis of 3-Azido-Iodobenzene (46h) in 2M $HNEt_2/C_6H_{12}$ at 30°C.

A $8.4x10^{-3}$M solution of the azide (25.8 mg, 0.105 mmol) in 2M $HNEt_2/C_6H_{12}$ was photolyzed for 30 minutes at 300 nm as described above. The solution was evaporated at reduced pressure and the ^1H NMR spectrum of the residue was recorded. No azepine products were identifiable from the ^1H NMR spectrum.

Ratio of products (by ^1H NMR): **46h**:**47h** = 85:15.

Photolysis of 3-Azido-benzonitrile (46c) in 2M $HNEt_2/C_6H_{12}$ at 30°C to Yield 6-Cyano-2-diethylamino-3H-dihydroazepine (44c) and 4-Cyano-2-diethylamino-3H-dihydroazepine (45c).

A $7.4x10^{-3}$M solution (13.4 mg, 0.093 mmol) of the azide in 2M $HNEt_2/C_6H_{12}$ (12.5 ml) was photolyzed for 30 minutes at 300 nm and 30°C as described above. The solvents were removed by evaporation at reduced pressure and the ^1H NMR spectrum of the residue was recorded.

Ratio of products (by ^1H NMR): **46c**:**47c**:**44c**:**45c** = 28:trace:18:14.

The 2-closure product, 6-cyano-2-diethylamino-3H-dihydroazepine (**44c**) showed:

R_f (15%EtOAc/hexanes) = 0.06

^1H NMR ($CDCl_3$) δ 0.97 - 1.24 (H-2", 6H, m), 2.3 (H-3, 2H, br), 3.27 - 3.37 (H-2', 4H, m), 5.10 (H-4, 1H, dt, J=8.6, 7.4 Hz), 6.33 (H-5, 1H, dd, J=8.6, 1.1 Hz),

7.57 (H-7, 1H, d, J=1.1 Hz).

The 6-closure product, 4-cyano-2-diethylamino-3H-dihydroazepine (**45c**) showed:

Rf (15%EtOAc/hexanes) = 0.15

^{1}H NMR ($CDCl_3$) δ 1.07 - 1.27 (H-2", 6H, m), 2.82 (H-3, 2H, br), 3.43 (H-2', 4H, m), 5.70 (H-6, 1H, dd, J=7.6, 6.6 Hz), 6.95 (H-5, 1H, d, J=6.6 Hz), 7.32 (H-7, 1H, d, J=7.6 Hz).

Photolysis of 46c in $HNEt_2/C_6H_{12}$ at 30°C: Preparative Scale.

A 7.3x10^{-3}M solution of the azide (223.4 mg, 1.454 mmol) in 2M $HNEt_2/C_6H_{12}$ (200 ml) was photolyzed for 210 minutes at 300 nm and 30°C as described above. The solvents were removed by evaporation at reduced pressure and the ^{1}H NMR spectrum of the residue was recorded. The crude product was chromatographed using a Chromatotron (1mm silica plate) using 1%MeOH/5%EtOAc/hexanes as the solvent to elute the first fraction. The solvent was switched to 15%EtOAc/hexanes for the remainder of the elutions. Four fractions were obtained. The first two fractions contained the starting azide **46c** and the reduced aniline **47c**. The third fraction contained the 6-azepine product **44c** while the fourth fraction contained the 2-azepine product **45c**.

Ratio of products (by ^{1}H NMR): **46c:47c:44c:45c** = 78:trace:14:8.

Photolysis of 46c in 2M $HNEt_2$/THF at 30°C.

A 7.85x10^{-3}M solution of the azide (14.7 mg, 0.102 mmol) in 2M $HNEt_2$/THF (13 ml) was photolyzed for 25 minutes at 300 nm and 30°C as described above. The solvents were removed by evaporation at reduced pressure and the ^{1}H NMR spectrum of the residue was recorded.

Ratio of products (by ^{1}H NMR): **46c:47c:44c:45c** = 61:trace:20:18.

Photolysis of 46c in 2M $HNEt_2$/THF at -70°C.

A 8.3x10^{-3}M solution of the azide (14.9 mg, 0.103 mmol) in 2M $HNEt_2$/THF (12.5 ml) was photolyzed for 27 minutes at 300 nm at -70°C as described above. The solvents were removed by evaporation at reduced pressure and the ^{1}H NMR spectrum of the residue was recorded.

Ratio of products (by ^{1}H NMR): **46c:47c:44c:45c** = 68:6:19:6.

Photolysis of 46c in 0.02M $HNEt_2$/THF at 30°C.

A 7.96x10^{-3}M solution of the azide (14.9 mg, 0.103 mmol) in 0.02M $HNEt_2$/THF (13 ml) was photolyzed for 60 minutes at 300 nm and 30°C as described above. The solvents were removed by evaporation at reduced pressure and the ^{1}H NMR spectrum of the residue was recorded.

Ratio of products (by ^{1}H NMR): **46c:47c:44c:45c** = 23:trace:29:48.

Photolysis of 3-Azido-acetophenone (46f) in 2M $HNEt_2$/C_6H_{12} at 30°C to Yield 6-Aceto-2-diethylamino-3H-dihydroazepine (44f) and 4-Aceto-2-diethylamino-3H-dihydroazepine (45f).

A 7.7x10^{-3}M solution of the azide (247.2 mg, 1.535 mmol) in 2M $HNEt_2$ (50 ml, 35 g, 480 mmol) and C_6H_{12} (150 ml) was photolyzed for 2 hours at 300 nm and 30°C. TLC (silica, 15% EtOAc/hex) showed the azide (R_f=0.4) had been consumed but showed the presence of the aniline, 3-amino-acetophenone, **47f**, and two other products. The solution was evaporated at reduced pressure to yield a dark oil. A portion was used to record a ^{1}H NMR spectrum. The oil was chromatographed (Chromatotron, 2 mm silica plate) to give

4 fractions. Fraction #1 contained the starting azide, **46f**, and fraction #3 the aniline product, **47f**. Fraction #2 contained the 6-closure azepine product, **44f** while fraction #4 contained the 2-closure azepine product, **45f**.

Ratio of products (by ^{1}H NMR): **46f:47f:44f:45f** = 0:52:2:46.

The aniline, 3-amino-acetophenone, **47f**, showed:

R_f (15%EtOAc/hexanes) = 0.10

^{1}H NMR ($CDCl_3$) δ 2.53 (H-3", 3H, s), 3.70 (H-1', 2H, br), 6.84 (H-6, 1H, ddd, J=7.6, 2.6, 1.6 Hz), 7.20 (H-5, 1H, dd, J=7.6, 7.6 Hz), 7.22 (H-2, 1H, dd, J=2.6, 1.2 Hz), 7.29 (H-4, 1H, ddd, J=7.8, 1.6, 1.2).

The 2-closure product, 6-aceto-2-diethylamino-3H-dihydroazepine (**44f**) showed:

R_f (15%EtOAc/hexanes) = 0.038

^{1}H NMR ($CDCl_3$) δ 1.23 (H-2", 6H, t, J=7.1 Hz), 2.39 (H-6", 3H, s), 3.4 (H-2', 4H, br), 5.21 (H-4, 1H, dt, J=9.0, 7.1 Hz), 6.89 (H-5, 1H, dd, J=9.0, 1.3 Hz), 8.10 (H-7, 1H, d, J=1.3 Hz).

MS (EI) [RI%] found: 206 $(M)^{+\cdot}$ [100%], 191 $(M\text{-}CH_3)^+$ [23%], 177 $(M\text{-}Et)^+$ [29%], 163 $(M\text{-}COCH_3)^+$ [13%].

MS (CI) [RI%] found: 207 $(M\text{-}H)^+$ [100%].

The 6-closure product, 4-aceto-2-diethylamino-3H-dihydroazepine (**45f**) showed:

The ^{1}H and ^{13}C NMR spectra were confirmed by Spin-Sort, DEPT, Selective ^{1}H Decoupling and by ^{1}H-^{13}C HET-CORR experiments. The Selective ^{1}H decoupling experiment involved irradiating a specific proton frequency (^{13}C O2) using a narrow sweep width and acquiring the ^{13}C spectra.

R_f (15%EtOAc/hexanes) = 0.21

^{1}H NMR ($CDCl_3$) δ 1.12 (H-2", 6H, m), 2.32 (H-4", 3H, s), 3.60 (H-2', 4H, br), 5.71 (H-6, 1H, dd, J=7.6, 6.6 Hz), 7.24 (H-5, 1H, dd, J=6.6, 0.7 Hz), 7.36 (H-7, 1H, dd, J=7.6, 0.8 Hz). Owing to conformational exchange of the azepine ring, the H-3 proton resonances were too weak to be reliably distinguished from noise.

^{13}C NMR ($CDCl_3$) δ 12.6 (C-2", **C**H_3), 15.3 (C-2", **C**H_3), 25.5 (C-4", **C**H_3), 29.2 (C-3, **C**H_2), 43.5 (C-2', **C**H_2), 107.6 (C-6, **C**H), 121.3 (C-4, **C**), 137.6 (C-5, **C**H), 147.7 (C-7, **C**H), 196.4 (C-4', **C**=O).

MS (EI) [RI%] found: 206 $(M)^{+\cdot}$ [100%], 191 $(M\text{-}CH_3)^+$ [7%], 177 $(M\text{-}Et)^+$ [57%), 163 $(M\text{-}COCH_3)^+$ [28%].

MS (CI) [RI%] found: 207 $(M+H)^+$ [100%].

Photolysis of 46f in 2M $HNEt_2$/THF at 35°C.

Two separate 0.14 M solutions of **46f** (28.4 mg, 0.176 mmol and 27.1 mg, 0.168 mmol respectively) were photolyzed as described above at 35°C for 20 and 40 minutes respectively.

Ratio of products (by ^{1}H NMR):

Time (min)	**46f : 47f : 44f : 45f**
20	41 : 35.5 : 12.3 : 11.1
40	34 : 39.6 : 14.0 : 12.1

Photolysis of 46f in 2M $HNEt_2$/THF at -70°C.

A 0.11 M solution of **46f** (22.4 mg, 0.139 mmol) was photolyzed as described above in 2M $HNEt_2$/THF (12.5 ml) at -70°C for 27 minutes.

Ratio of products (by ^{1}H NMR): **46f:47f:44f:45f** = 81:7:7:4.5

Photolysis of 46f in 2M $HNEt_2$/THF at -70°C.

Three separate 0.13 M solutions of **46f** (26.7 mg, 0.166 mmol; 26.6 mg, 0.166 mmol; 25.9 mg, 0.161 mmol respectively) were photolyzed as described above in 2M $HNEt_2$/THF (12.5 ml) at -70°C for 60, 90 and 120 minutes respectively.

Ratio of products (by ^1H NMR):

Time (min)	**46f : 47f : 44f : 45f**
60	81 : 8.2 : 7.3 : 3.7
90	79 : 4.0 : 11 : 5.8
120	70 : 13 : 11 : 6.1

Photolysis of 46f in 0.02M $HNEt_2$/THF at 35°C.

A 0.089 M solution of **46f** (18.6 mg, 0.116 mmol) was photolyzed as described above at 35°C for 30 minutes.

Ratio of products (by ^1H NMR): **46f:47f:44f:45f** = 35:37:4:23

Photolysis of 3-Azido-nitrobenzene (46l) in 2M $HNEt_2/C_6H_{12}$ at 30°C.

A $7.4x10^{-3}$M solution of the azide (241.6 mg, 1.473 mmol) in 2.4M $HNEt_2$ in C_6H_{12} was photolyzed for 1 hour at 300 nm and 30°C until no more azide was observed by TLC. The solution was evaporated at reduced pressure and the ^1H NMR spectrum of the residue was recorded. The oil was chromatographed using a Chromatotron on a 2mm silica plate (1% MeOH/5% EtOAc/hexanes for the first three fractions, 15% EtOAc/hexanes for the last fraction) to yield four fractions. The first fraction was unidentifiable by ^1H NMR (R_f (15%EtOAc/hexanes) = 0.46). The second fraction contained some remaining azide, **46l** (R_f (15%EtOAc/hexanes) = 0.43). The third fraction contained

an unknown compound. The fourth fraction contained possible azepines.

Fraction #3 (m-nitrophenyl-diethyl-hydrazine?) showed:

R_f (15%EtOAc/hexanes) = 0.33

^1H NMR ($CDCl_3$) δ 1.08 (114, m), 2.67 (57.8, m), 3.50 (57.6, br), 4.48 (12.8, br), 7.00 - 7.30 (38.7, m), 7.50 (16.2, m), 7.68 (13.1, m).

Fraction #4 showed:

R_f (15%EtOAc/hexanes) = 0.20

^1H NMR ($CDCl_3$) δ 0.7-2.0 (m), 2.3-2.5 (4.18, m), 2.6-2.8 (2.65, m), 3.3-3.8 (21.08, m), 4.0-4.2 (2.0, dt, J=6.6, 4.9 Hz, possibly the 2-closure azepine product H-4), 4.4-4.6 (1.48, m), 5.1-5.2 (0.77, dd, J=10.4, 3.7 Hz), 5.7-5.8 (2.89, dd, J=7.4, 6.9 Hz, possibly the 6-closure azepine product H-6), 7.5-8.0 (6.32, m).

MS (EI) [RI%] found: 209 $(M)^{+\cdot}$ [100%], 194 $(M-CH_3)^+$ [20%], 180 $(M-Et)^+$ [47%], 163 $(M-NO_2)^+$ [61%], 133 $(M-76)^+$ [69%].

MS (EI) [RI%] found: 210 $(M+H)^+$ [100%], 180 $(M-CH_4)^{+\cdot}$ [8%].

Photolysis of 3-Azido-anisole (46d) in 2M $HNEt_2/C_6H_{12}$ at 30°C to Yield 2-Diethylamino-6-methoxy-3H-dihydroazepine (44d) and 2-Diethylamino-4-methoxy-3H-dihydroazepine (45d).

A $7.3x10^{-3}$M solution of the azide (13.6 mg, 0.091 mmol) in 2M $HNEt_2/C_6H_{12}$ (12.5 ml) was photolyzed for 20 minutes at 300 nm and 30°C. The solution was evaporated at reduced pressure and the ^1H NMR spectrum of the residue showed:

Ratio of products (by ^1H NMR): **46d:47d:44d:45d** = 25:trace:16:59.

The 2-closure product, 2-diethylamino-6-methoxy-3H-dihydroazepine (**44d**) showed:

^1H NMR ($CDCl_3$) δ 1.10 - 1.20 (H-2", 6H, m), 2.80 (H-3, 2H, br), 3.20 - 3.40 (H-2', 4H, m), 3.59 (H-6', 3H, s), 5.21 (H-4, 1H, dt, J=9.6, 9.1 Hz),

6.24 (H-5, 1H, dd, J=9.1, 2.0 Hz), 6.91 (H-7, 1H, d, J=2.0 Hz). Owing to conformational exchange of the azepine ring, the H-3 proton resonances were too weak to be reliably distinguished from noise.

The 6-closure product, 2-diethylamino-4-methoxy-3H-dihydroazepine (**45d**) showed: ^{1}H NMR ($CDCl_3$) δ 1.13 (H-2", 6H, t, J=7.1 Hz), 2.80 (H-3, 2H, br), 3.38 (H-2', 4H, q, J=7.1 Hz), 3.56 (H-4', 3H, s), 5.34 (H-5, 1H, d, J=6.1 Hz), 5.59 (H-6, 1H, dd, J=8.0, 6.2 Hz), 6.85 (H-7, 1H, d, J=8.0 Hz).

Photolysis of 46d in 2M $HNEt_2$/THF at 30°C.

A 6.6x10^{-3}M solution of the azide (12.9 mg, 0.087 mmol) in 2M $HNEt_2$/THF (13 ml) was photolyzed for 30 minutes at 300 nm and at 30°C. The solution was evaporated at reduced pressure and the ^{1}H NMR spectrum of the residue was recorded.

Ratio of products (by ^{1}H NMR): **46d:47d:44d:45d** = 30:trace:20:50.

Photolysis of 46d in 2M $HNEt_2$/THF at -70°C.

A 8x10^{-3}M solution of the azide (14.9 mg, 0.100 mmol) in 2M $HNEt_2$/THF was photolyzed at -70°C for 30 minutes at 300 nm. The solution was evaporated at reduced pressure and the ^{1}H NMR spectrum of the residue was recorded.

Ratio of products (by ^{1}H NMR): **46d:47d:44d:45d** = 54:12:trace:33.

Photolysis of 46d in 0.02M $HNEt_2$/THF at 30°C.

A 9x10^{-3}M solution of the azide (17.4 mg, 0.117 mmol) in 0.02M $HNEt_2$/THF (13 ml) was photolyzed for 30 minutes at 300 nm and at 30°C. The solution was evaporated at reduced pressure and the ^{1}H NMR spectrum of the residue was recorded.

Ratio of products (by ^{1}H NMR): **46d:47d:44d:45d** = 21:trace:20:59.

Photolysis of 3-Azido-methylmercaptobenzene (46e) in 2M $HNEt_2/C_6H_{12}$ at 30°C to Yield 2-Diethylamino-6-methylmercapto-3H-dihydroazepine (44e) and 2-Diethylamino-4-methylmercapto-3H-dihydroazepine (45e).

A $7.3x10^{-3}$M solution of the azide (239.5 mg, 1.452 mmol) in 2.4M $HNEt_2/C_6H_{12}$ was photolyzed for 45 minutes at 300 nm and at 30°C. The solution was evaporated at reduced pressure to yield a black oil and the ^{1}H NMR spectrum of the oil was recorded.

Ratio of products (by ^{1}H NMR): **46e:47e:44e:45e** = 48:trace:23:29.

The 2-closure product, 2-diethylamino-6-methylmercapto-3H-dihydroazepine (**44e**) showed:

^{1}H NMR ($CDCl_3$) δ 1.16 (H-2", 6H, m), 2.10 (H-3, 2H, br), 2.23 (H-6', 3H, s), 3.40 (H-2', 4H, m), 5.08 (H-4, 1H, dt, J=8.8, 7.3 Hz), 6.30 (H-5, 1H, dd, J=7.3, 2.5 Hz), 7.46 (H-7, 1H, d, J=2.5 Hz).

The 6-closure product, 2-diethylamino-4-methylmercapto-3H-dihydroazepine (**45e**) showed:

^{1}H NMR ($CDCl_3$) δ 1.16 (H-2", 6H, m), 2.10 (H-3, 2H, br), 2.31 (H-4', 3H, s), 3.40 (H-2', 4H, m), 5.70 (H-6, 1H, dd, J=7.9, 6.1 Hz), 6.02 (H-5, 1H, d, J=6.1 Hz), 6.96 (H-7, 1H, d, J=7.9 Hz).

Photolysis of 46e in 2M $HNEt_2$/THF at 30°C.

A $7.2x10^{-3}$M solution of the azide (15.5 mg, 0.094 mmol) in 2M $HNEt_2$/THF (13 ml) was photolyzed for 60 minutes at 300 nm and at 30°C as described above.

Ratio of products (by ^{1}H NMR): **46e:47e:44e:45e** = 33:trace:30:37.

Photolysis of 46e in 2M $HNEt_2$/THF at -70°C.

A $9.2x10^{-3}$M solution of the azide (18.9 mg, 0.115 mmol) in 2M $HNEt_2$/THF was photolyzed at -70°C for 30 minutes at 300 nm as described above.

Ratio of products (by ^{1}H NMR): **46e:47e:44e:45e** = 73:trace:7:20.

Photolysis of 46e in 0.02M $HNEt_2$/THF at 30°C.

A $7.0x10^{-3}$M solution of the azide (15.0 mg, 0.091 mmol) in 0.02M $HNEt_2$/THF (13 ml) was photolyzed for 25 minutes at 300 nm and at 30°C as described above.

Ratio of products (by ^{1}H NMR): **46e:47e:44e:45e** = 15:trace:43:42.

7.6.4 Photolysis of 3,4-Disubstituted Arylazides

Photolysis of 5-Azido-2-trifluoroacetamido-acetanilide (49) in $HNEt_2$/THF at 30°C.

The azide (**49**, 129.1 mg, 0.4498 mmol, 0.009 M) was photolyzed in 50 mL of a 1.9M $HNEt_2$/THF solution for 1 hour at 300 nm as described above. The solution was evaporated at reduced pressure to yield an oil. The ^{1}H NMR spectrum showed one major product. The oil was chromatographed using a Chromatotron (1mm silica plate, 5% MeOH/$CHCl_3$) to yield three fractions. Fraction #3 was re-chromatographed using a Chromatotron (2mm silica plate, 1.0%MeOH/$CHCl_3$) to remove some more impurities. The first fraction contained the starting azide **49**, the third fraction contained the reduced product, 3-acetamido-4-trifluoroacetamido-aniline (**52**) and the second fraction contained a new product; 4-acetamido-2-diethylamino-5-trifluoroacetamido-aniline, **57**.

Ratio of products (by ^{1}H NMR): **49 : 52 : 58 : 57 : 55 : 56**

= trace : 0 : 0 : 100 : 0 : 0

Fraction #1, **49**, showed:

R_f (10% MeOH/$CHCl_3$) = 0.42

Fraction #2: 4-acetamido-2-diethylamino-5-trifluoroacetamido-aniline (**57**) showed:

R_f (10% MeOH/$CHCl_3$) = 0.32

The ^1H and ^{13}C NMR spectra were confirmed by Spin-Sort, DEPT, ^1H-^{13}C HET-CORR and ^1H-^{13}C long range HET-CORR experiments.

^1H NMR (CD_2Cl_2) δ 0.96 (H-2", 6H, t, J=7.1 Hz), 2.12 (H-4"', 3H, s), 2.90 (H-2', 4H, q, J=7.1 Hz), 6.40 (H-6, 1H, s), 7.24 (H-3, 1H, s), 7.98 (H-4', 1H, br), 9.62 (H-5', 1H, br).

^1H NMR (500MHz, $CDCl_3$) δ 0.96 (H-2", 6H, t, J=7.1 Hz), 2.10 (H-4"', 3H, s), 2.87 (H-2', 4H, q, J=7.1 Hz), 6.35 (H-6, 1H, s), 7.20 (H-3, 1H, s), 8.06 (H-4', 1H, br), 9.57 (H-5', 1H, br).

^{13}C NMR (CD_2Cl_2) δ 12.4 (C-2", **C**H_3), 23.3 (C-4"', **C**H_3), 47.3 (C-2', **C**H_2), 109.7 (C-6, **C**H), 116.2 (C-5"', **C**F_3, q, J_{CF}=288 Hz), 118.8 (C-1, **C**), 120.6 (C-3, **C**H), 127.0 (C-2, **C**), 135.8 (C-5, **C**), 143.3 (C-4, **C**), 155.8 (C-5", **C**=O, q, J_{CF}=37 Hz), 170.3 (C-4", **C**=O).

^{13}C NMR (125MHz, $CDCl_3$) δ 12.4 (C-2", **C**H_3), 23.3 (C-4"', **C**H_3), 47.3 (C-2', **C**H_2), 109.7 (C-6, **C**H), 118.8 (C-1, **C**), 120.6 (C-3, **C**H), 127.0 (C-2, **C**), 135.8 (C-5, **C**), 143.4 (C-4, **C**), 155.7 (C-5", **C**=O, q, J_{CF}=37 Hz), 170.3 (C-4", **C**=O).

MS (EI) [RI%] found: 332 $(M)^{+\cdot}$ [100%], 317 $(M\text{-}CH_3)^+$ [80%], 303 $(M\text{-}Et)^+$ [22%], 287 $(M\text{-}H\text{-}HCOCH_3)^+$ [17%], 261 $(M\text{-}NEt_2\text{+}H)^{+\cdot}$ [25%].

MS (CI) [RI%] found: 333 $(M+H)^+$ [100%], 262 $(M+2H\text{-}NEt_2)^+$ [3%], 206 $(M\text{-}126)^+$ [10%].

HRMS (EI) exact mass = 332.1470 g/mol

calcd. mass ($C_{14}H_{19}F_3N_4O_2$) = 332.1460 g/mol (-1.0 MMU).

Photolysis of 49 in 2M $HNEt_2/C_6H_{12}$ at 30°C.

The azide (**49**, 35.8 mg, 0.125 mmol, 5 mM) was photolyzed in 2M $HNEt_2/C_6H_{12}$ for 30 minutes at 300 nm and 30°C. The solution was evaporated under reduced pressure and the ^1H NMR spectrum of the residue was recorded.

Ratio of products (by ^1H NMR): **49 : 52 : 58 : 57 : 55 : 56**

= 0 : <5 : 0 : >95 : 0 : 0

Photolysis of 49 in $HNEt_2$/THF at -80°C.

The azide (**49**, 17.5 mg, 0.061 mmol, 4.9 mM) was photolyzed in 12.5 mL of a 2M $HNEt_2$/THF solution for 90 minutes at 300 nm as described above at -80°C using a MeOH bath cooled with a cryogen cooling probe. The solution was evaporated at reduced pressure to an oil for which TLC (1% MeOH/15% EtOAc/$CHCl_3$) showed three products: starting azide (**49**, R_f = 0.30), reduced aniline (**52**, R_f = 0.23) and the diamino compound (**57**, R_f = 0.061). The ^1H NMR spectrum of the crude oil showed two major products, **57** and **52**, with only trace amounts of **49**.

Ratio of products (by ^1H NMR): **49 : 52 : 57 : 58 : 55 : 56**

= 0 : 53 : 0 : 47 : 0 : 0

Photolysis of 49 in 0.0036M $HNEt_2$/THF at 30°C: Preparative Scale.

The azide (**49**, 203.5 mg, 0.709 mmol, 3.54 mM) was irradiated in 200 mL of a 3.6 mM $HNEt_2$/THF solution as described in the general procedure for 45 minutes at 300 nm and at 30°C. The solution was evaporated under reduced pressure to yield a reddish/brown oil (249.6 mg, 98% by weight recovery). A ^1H NMR spectrum was recorded of the crude reaction mixture. The oil was chromatographed (4mm silica Chromatotron plate) to yield five fractions. The first fraction was eluted using 1% MeOH/40% EtOAc/59% hexanes and was identified by ^1H NMR as **49** (33.6 mg, 0.117 mmol, 17% recovery). The remaining fractions were eluted by increased addition of EtOAc to the solvent mixture to gradually increase the polarity to 100% EtOAc.

Ratio of products (by ^1H NMR): **49 : 52 : 57 : 58 : 55 : 56**
= 26 : 0 : 0 : 35 : 33 : 5
isolated yields (%) = 17 : 0 : 23 : 0 : 26 : 0

Fraction #1: **49** showed:

R_f (10% MeOH/$CHCl_3$) = 0.42

Fraction #2: an unknown, was a band identified on the Chromatotron but was too not abundant enough to be identified by ^1H NMR or mass spectrometry.

R_f (10% MeOH/$CHCl_3$) = 0.36

Fraction #3: **57** showed:

isolated mass = 53.3 mg, 0.161 mmol, 23% (27% from reacted azide).

R_f (10% MeOH/$CHCl_3$) = 0.32

UV @ 300nm ($c = 6.7 \times 10^{-5}$ M): ε = 11 640 $M^{-1}cm^{-1}$

Fraction #4: the 6-closure azepine product, 4-acetamido-2-diethylamino-5-trifluoroacetamido-3H-dihydroazepine (**56**) showed:

isolated mass = < 5mg.

R_f (10% MeOH/$CHCl_3$) = 0.27

UV @ 300nm (c = 7.7 x 10^{-5} M): ε = 6 738 $M^{-1}cm^{-1}$

^{1}H NMR ($CDCl_3$) δ 1.10 (H-2"', 6H, br), 1.73 (H-4"', 3H, s), 3.09 (H-2", 4H, br), 5.80 (H-6, 1H, d, J=8.5), 6.93 (H-7, 1H, d, J=8.5), 8.65 (H-4', 1H, br) ,9.50 (H-5', 1H, br). Owing to conformational exchange of the azepine ring, the H-3 proton resonances were too weak to be reliably distinguished from noise.

^{13}C NMR ($CDCl_3$) δ 14.0 (C-2"', **C**H_3), 23.1 (C-4"', **C**H_3), 23.1 (C-4"',**C**H_3), 32.7 (C-3, **C**H_2), 43.7 (C-2", **C**H_2), 106.5 (C-6, **C**H), 111.0 (C-4, **C**), 115.8 (C-5"', **C**F_3, q, J_{CF}=286 Hz), 121.6 (C-5, **C**), 137.5 (C-7, **C**H), 146.6 (C-2, **C**), 155.0 (C-5", **C**OCF_3, J_{CF}=37 Hz), 169.5 (C-4", **C**O).

MS (EI) [RI%] found: 332 $(M)^{+\cdot}$ [100%], 317 $(M\text{-}Me)^+$ [74%], 303 $(M\text{-}Et)^+$ [22%], 287 $(M\text{-}HCOCH_3)^{+\cdot}$ [12%], 275 $(M\text{-}NCOCH_3)^+$ [10%], 261 $(M\text{-}HNEt_2)^{+\cdot}$ [38%], 245 $(M\text{-}87)^+$ [18%], 219 $(M\text{-}HNCOCF_3\text{-}H_2)^+$ [20%].

MS (CI) [RI%] found 333 $(M+H)^+$ [100%].

HRMS (EI) exact mass found = 332.1468 g/mol

calcd.($C_{14}H_{19}F_3N_4O_2$) = 332.1460 g/mol (-0.8 MMU).

Fraction #5: 2-closure azepine product, 6-acetamido-2-diethylamino-5-trifluoroacetamido-3H-dihydroazepine (**55**) and trace aniline product **52** (0.006 mmol, 1% by ^{1}H NMR; R_f (10% MeOH/$CHCl_3$) = 0.085).

total isolated mass = 64.4 mg

Compound **55** showed:

yield = 0.186 mmol, 26% (32% from reacted azide) by ^{1}H NMR.

R_f (10% MeOH/$CHCl_3$) = 0.20

UV @ 300nm (c = 6.3 x 10^{-5} M): ε = 6 550 $M^{-1}cm^{-1}$

^{1}H NMR ($CDCl_3$) δ 1.10 (H-2"',6H,br), 1.77 (H-6"', 3H, s), 2.03 (H-3a, 1H, br), 3.31 (H-3b, 1H, br), 3.41 (H-2", 4H, br), 5.47 (H-4, 1H, t, J=7.9 Hz), 7.11 (H-7, 1H, s), 9.20 (H-6', 1H, br), 10.50 (H-5', 1H, br). Both H-3a and H-3b shifts were not observed in the 1D-spectrum and were extracted from the 2-D ^{1}H-^{13}C heteronuclear shift correlated experiment cross sections.

^{13}C NMR: ($CDCl_3$) δ 12.4 (C-2"', **C**H_3), 22.3 (C-6"', **C**H_3), 29.4 (C-3, **C**H_2), 43.4 (C-2", **C**H_2), 105.9 (C-4, **C**H), 114.4 (C-5, **C**), 115.8 (C-5"', **C**F_3, q, J_{CF}=287 Hz), 132.4 (C-6, **C**), 141.0 (C-7, **C**H), 147.8 (C-2, **C**), 155.7 (C-5", **C**O**C**F_3, q, J_{CF}=37 Hz), 172.1 (C-6", **C**O).

MS (EI) [RI%] found: 332 $(M)^{+\cdot}$ [100%], 289 $(M\text{-}COCH_2)^{+\cdot}$ [38%], 261 $(M\text{-}HNEt_2)^{+\cdot}$ [33%], 219 $(M\text{-}HNCOCF_3\text{-}H_2)^+$ [32%], 192 $(M\text{-}140)^+$ [12%].

MS (CI) [RI%] found: 333 $(M+H)^+$ [100%].

HRMS (EI) exact mass found = 332.1468 g/mol

calcd.($C_{14}H_{19}F_3N_4O_2$) = 332.1460 g/mol (-0.8 MMU).

Photolysis of 49 in 0.005M $HNEt_2$/THF at 30°C.

The azide (**49**, 13.0 mg, 0.0453 mmol, 3.8 mM) was irradiated in 12 mL of a 0.005M $HNEt_2$/THF solution as described in the general procedure for 30 minutes at 300 nm and at 30°C. The solution was evaporated under reduced pressure to yield a

reddish/brown oil and a ^{1}H NMR spectrum was recorded. The oil was chromatographed using a Chromatotron (2mm silica plate) to yield five fractions: the first fraction eluted using 1% MeOH/15% EtOAc/84% hexanes was identified by its ^{1}H NMR spectrum as **49**, the next two fractions were eluted using 1% MeOH/40% EtOAc/59% hexanes and the final two fractions were eluted using 100% EtOAc. The ^{1}H NMR spectra were recorded on all the fractions, after removal of solvents by reduced pressure evaporation, for identification.

Ratio of products (by ^{1}H NMR): **49 : 52 : 57 : 58 : 55 : 56**

= 30 : trace : 0 : 2 : 56 : 13

Photolysis of 49 in 0.0036M HN^{i}Pr$_2$/THF at 30°C.

The azide (**49**, 12.2 mg, 0.0425 mmol, 3.5 mM) was irradiated in 12 mL of a solution of 3.6 mM HN^{i}Pr$_2$/THF for 30 minutes at 30°C. The solution was evaporated under reduced pressure to yield an oil (15.6 mg). The ^{1}H NMR spectrum of the oil was recorded and was found to show resonances indicative of some unreacted azide (**49**), some of the reduced aniline product (**52**), 6-acetamido-2-(diisopropyl)-amino-5-trifluoroacetamido-3H-dihydroazepine (**109**) and 4-acetamido-2-(diisopropyl)-amino-5-trifluoroacetamido-3H-dihydroazepine (**110**) but no diamine products (**111** and **112**) were observed.

Ratio of products (by ^{1}H NMR): **49 : 52 : 111 : 112 : 109 : 110**

= 53 : 8 : 0 : 0 : 26 : 11

Photolysis of 49 in 0.005M HNEt$_2$/1,4-dioxane at 80°C.

The azide (**49**, 13.2 mg, 46.0 μmol) was irradiated in a solution of 5 mM HNEt$_2$/1,4-dioxane at 300 nm and at 80°C for 25 minutes. The mixture was evaporated under

reduced pressure to give a reddish/brown oil and a ^{1}H NMR spectrum was recorded. The crude oil was chromatographed (Chromatotron, 1mm silica plate) to yield 5 fractions. The first three fractions were eluted using 1%MeOH/40% EtOAc/59% hexanes and contained the azide **49**, the reduced aniline **52**, and the diamine, **57**. The last two fractions were eluted using 100% EtOAc and contained the azepines **55** and **56**.

Ratio of products (by ^{1}H NMR): **49 : 52 : 57 : 58 : 55 : 56**

= 33 : 5 : trace : 0 : 44 : 19

Photolysis of 49 at Three Different Temperatures and at Constant 5.2 mM $HNEt_2$ Concentration in THF.

The azide **49** (190.7 mg, 0.6645 mmol, 5.11 mM) was dissolved in a 5.2 mM $HNEt_2$/THF solution. The sample was degassed by bubbling with nitrogen for 30 minutes and then divided equally into 10 pyrex test tubes via a double ended needle under a stream of N_2. The solvents were removed by reduced pressure evaporation and a ^{1}H NMR spectrum of each residue was recorded. The data for each reaction is shown in the Table below.

Sample	Temp. /°C	Irradiation Time /min	^{1}H NMR Ratio of Products					
			49	52	58	57	55	56
C5	-70	5	77	0	0	23	0	0
C10		10	57	3	0	40	0	0
C20		20	39	7	0	54	0	0
C40		40	33	11	0	57	0	0
R5	25	5	56	3	0	24	13	4
R10		10	52	3	0	25	15	4
R30		30	23	9	0	41	24	4
H5	55	5	53	0	0	15	26	6
H10		10	51	5	0	15	24	5
H30		30	19	7	0	29	38	7

Photolysis of 49 in 1.8 mM $HNEt_2$/THF.

The azide (49, 6.5 mg, 0.023 mmol, 1.8 mM) was dissolved in 12.5 mL of a 1.8 mM $HNEt_2$/THF solution and then photolyzed for 20 minutes at 300 nm at 30°C. The solvents were removed by reduced pressure evaporation and a ^1H NMR spectrum of the residue was obtained.

Ratio of products (by ^1H NMR): **49 : 52 : 58 : 57 : 55 : 56**

= 0 : 26 : 0 : 15 : 59 : trace

Photolysis of 49 at 35°C and Variable $HNEt_2$ Concentration in THF.

The azide 49 (207.9 mg, 0.724 mmol, 4.5 mM) was dissolved in 80 mL THF. The solution was divided into eight 10.00 mL (± 0.02 ml) portions, using a volumetric pipette, in 30 mL test tubes. A 34.2 mM stock solution of $HNEt_2$/THF was prepared (250 mg, 3.42 mmol, 100 mL solution) and poured into a buret. The stock $HNEt_2$/THF solution was added to each test tube to make eight different concentrations of $HNEt_2$ and the volume of each sample was made equal by addition of more THF to a total volume of 20.0 mL (as shown in the Table below). Each tube was capped with a serum cap and degassed for 15 minutes with dry N_2. The tubes were suspended on a carousel in a distilled water bath at 35°C beside a 300 nm Rayonet bulb. The solutions were rotated and photolyzed at 300 nm for 1 hour, the solvents were removed by evaporation at reduced pressure, the ^1H NMR spectrum of the residues were recorded and the results are tabulated below.

Volume of Stock $HNEt_2$ used /ml	Volume of THF used /ml	Concentration of $HNEt_2$ /mM	Ratio of Products by ^1H NMR					
			49	52	58	57	55	56
10.00	0	17.09	92.5	0	0	3.3	3.5	0.7
8.00	2.00	13.67	90.9	0	0	3.9	4.2	1.0
6.00	4.00	10.25	91.7	0	0	3.7	3.6	1.0
5.00	5.00	8.55	90.1	0	0	4.2	4.2	1.4
4.00	6.00	6.84	89.8	0	0	4.3	4.5	1.5
3.00	7.00	5.13	89.5	0	0	4.2	4.5	1.7
2.00	8.00	3.42	90.6	0	0	4.2	3.4	1.7
1.00	9.00	1.71	93.4	0	0	3.1	1.8	1.6

Photolysis of 49 at 0°C and Variable $HNEt_2$ Concentration in THF.

The azide 49 (207.5 mg, 0.723 mmol, 4.5 mM) was dissolved in 80 mL THF and divided into eight 10.00 mL (± 0.02 ml) portions as described above. The solutions were irradiated at 300 nm at 0°C for 1 hour as described above.

Volume of Stock $HNEt_2$ used /ml	Volume of THF used /ml	Concentration of $HNEt_2$ /mM	Ratio of Products by ^1H NMR					
			49	52	58	57	55	56
10.00	0	16.60	78.1	0	0	12.0	8.9	0.9
8.00	2.00	13.28	79.5	0	0	9.5	9.7	1.3
6.00	4.00	9.96	82.0	0	0	7.5	9.4	1.1
5.00	5.00	8.30	81.4	0	0	7.0	10.6	1.0
4.00	6.00	6.64	77.4	0	0	7.5	13.6	1.5
3.00	7.00	4.98	75.1	0	0	6.4	16.6	1.9
2.00	8.00	3.32	78.2	0	0	4.1	15.9	1.8
1.00	9.00	1.66	84.0	0	0	0.9	12.6	2.4

Photolysis of 49 at 60°C and Variable $HNEt_2$ Concentration in THF.

The azide 49 (206.7 mg, 0.721 mmol, 4.5 mM) was dissolved in 80 mL THF and divided into eight 10.00 mL (± 0.02 ml) portions as described above. The solutions were irradiated at 300 nm at 60°C for 1 hour as described above.

Volume of Stock $HNEt_2$ used /ml	Volume of THF used /ml	Concentration of $HNEt_2$ /mM	Ratio of Products by ^1H NMR					
			49	52	58	57	55	56
10.00	0	16.60	89.5	0	0	2.1	5.2	3.2
8.00	2.00	13.28	76.9	0	0	3.9	13.7	5.4
6.00	4.00	9.96	79.6	0	0	2.9	12.2	5.2
5.00	5.00	8.30	59.6*	0	0	2.7*	32.1*	5.6*
4.00	6.00	6.64	70.9	0	0	3.4	16.4	9.3
3.00	7.00	4.98	84.2	0	0	2.4	7.5	5.9
2.00	8.00	3.32	74.5	0	0	4.1	10.7	10.7
1.00	9.00	1.66	80.9*	0	0	2.1*	5.8*	11.2*

* ^1H NMR integrals were not very reliable.

Photolysis of 49 at -30°C and Variable $HNEt_2$ Concentration in THF.

The azide 49 (258.4 mg, 0.900 mmol, 4.5 mM) was dissolved in 100 mL THF and divided into eight 10.00 mL (± 0.02 ml) portions as described above. The solutions were irradiated at 300 nm at -30°C for 1 hour as described above.

Volume of Stock $HNEt_2$ used /ml	Volume of THF used /ml	Concentration of $HNEt_2$ /mM	Ratio of Products by ^1H NMR					
			49	52	58	57	55	56
10.00	0	16.69	92.9*	0	0	6.3*	0.8*	0
8.00	2.00	13.34	90.3	0	0	7.0	2.7	0
5.00	5.00	8.34	90.3	0	0	6.4	3.3	0
4.00	6.00	6.67	90.0	0	0	7.4	2.6	0
3.00	7.00	5.00	87.1	0	0	7.0	5.9	0
2.00	8.00	3.34	91.1*	0	0	6.4*	2.5*	0
1.00	9.00	1.67	85.4	0	0	6.0	8.1	0.5

* ^1H NMR integrals were not very reliable.

Photolysis of 49 in 3 mM $HNEt_2$/THF at 65°C: Preparative Scale.

The azide (49, 540.6 mg, 1.884 mmol, 2.9 mM) was dissolved in 650 mL of a 3.0 mM $HNEt_2$/THF solution in a quartz reaction flask fitted with a condenser. The solution

was stirred with a magnetic stirrer under a stream of nitrogen while being refluxed by a quartz sleave containing hot oil via a heating probe. The apparatus was mounted inside a 30 cm bore Rayonet unit and photolyzed for 110 minutes. The solution was evaporated under reduced pressure (692.5 mg) and chromatographed (Chromatotron, 541.3 mg used, 4 mm silica plate) using 1% MeOH/15% EtOAc/84% $CHCl_3$ for the first three fractions then 1% MeOH/50% EtOAc/49% $CHCl_3$ for the remaining two fractions. Fraction #1 and contained the starting azide (**49**, 202.9 mg, 0.707 mmol, 38%); fraction #2 contained the 6-closure azirine product (**57**, 7.8 mg, 0.024 mmol, 1.2%); fraction #3 contained a mixture of both **57** and **56** (49.4 mg, 0.149 mmol, 7.9%); fraction #4 contained **56** (123.5 mg, 0.372 mmol, 20%) and fraction #5 contained **55** (93.2 mg, 0.281 mmol, 15%). The overall yield of separated products recovered was 73% after chromatography.

Ratio of products (by ^{1}H NMR):		**49 : 52 : 58 : 57 : 55 : 56**	
		=	32 : 3 : 0 : 5 : 33 : 28
Isolated yields	(mg)	=	202.9 : 0 : 0 : 7.8 : 93.2 : 123.5
	(mmol)	=	0.707 : 0 : 0 : 0.024 : 0.281 : 0.372
	(%)	=	38 : 0 : 0 : 1.2 : 15 : 20

Photolysis of 49 in 2M $HNEt_2$/Cyclohexane at 30°C and -30°C.

The azide (**49**, 35.8 mg, 0.125 mmol, 5 mM) was dissolved in 25 mL of a 2M $HNEt_2$ (5 ml, 3.5 g, 48 mmol, 1.93 M, 387 equivalents)/cyclohexane solution. The solution was divided into two quartz photolysis tubes and each tube was irradiated for 30 minutes at 300 nm as described above, one at 30°C and the other at -30°C. The products were analyzed by ^{1}H NMR.

Ratio of products (by ^{1}H NMR): **49 : 52 : 58 : 57 : 55 : 56**

(at 30°C) = 0 : 0 : 0 : 100 : 0 : 0
(at -30°C) = 0 : 50 : 0 : 50 : 0 : 0

Photolysis of 49 in KOMe/MeOH/1,4-dioxane at 30°C.

The procedure used was similar to that of Hayes *et al.*[9v]. The azide (**49**, 38.3 mg, 0.133 mmol) was dissolved in 15 mL 1,4-dioxan. A solution of 3M KOMe/MeOH (15 ml) was added and the mixture was degassed with nitrogen for 15 minutes. The solution was irradiated at 300 nm for 60 minutes and then neutralized with concentrated HCl/MeOH (1:1 v:v). The mixture was filtered through celite to remove the precipitated KCl. The precipitate was washed with dry MeOH until they appeared white in colour. The combined organics were evaporated under reduced pressure to yield a red oil (46.2 mg) which was used to record a ^{1}H NMR spectrum. The ^{1}H NMR spectrum was too complex for interpretation.

Photolysis of 4-Azido-1,2-di(trifluoroacetamido)-benzene (48) in $HNEt_2\backslash C_6H_{12}$ at 30°C.

The azide (**48**, 22.8 mg, 0.0669 mmol, 0.0053 M) was photolyzed in a 2M $HNEt_2\backslash C_6H_{12}$ solution (12.5 ml) at 300 nm as described above. After 45 minutes, when no more azide was observed by TLC (silica, 10%MeOH/$CHCl_3$, R_f=0.5), the solution was evaporated at reduced pressure to yield an oil. The ^{1}H NMR spectrum of the oil was recorded and showed two products: one being the aniline; 3,4-di(trifluoroacetamido)-aniline (**54**, 46%) and the other a new product; 2-diethylamino-4,5-di(trifluoroacetamido)-aniline (**64**, 54%).

2-Diethylamino-4,5-di(trifluoroacetamido)-aniline, **64**, showed:

^{1}H NMR ($CDCl_3$) δ 1.15 (H-2''', 6H, t, J=7.2), 2.65 (H-2'', 4H, q, J=7.2), 6.78 (H-3, 1H, s), 7.00 (H-6, 1H, s).

MS (EI) [RI%] found: 386 $(M)^{+\cdot}$ [93%], 371 $(M\text{-}CH_3)^+$ [100%], 357 $(M\text{-}Et)^+$ [43%].

Photolysis of 48 in 0.005M $HNEt_2$\THF at 30°C.

The azide (**48**, 16.9 mg, 0.0496 mmol, 0.0041 M) was photolyzed in a 0.005M $HNEt_2$\THF solution (12 ml) at 300 nm and at 30°C as described above for 30 minutes. The ^{1}H NMR spectrum of the crude product showed only the diamino product **64** (80%), the reduced aniline **54** (20%) and some minor unidentifiable peaks in the aromatic region (<10%).

Photolysis of 5-Azido-2-chloro-acetanilide (91) in 1.9 M $HNEt_2$/THF at 30°C.

The azide (**91**, 142.1 mg, 0.675 mmol, 3.4 mM) and $HNEt_2$ (117.5 mg, 1.61 mmol, 8.0 mM, 2.4 equivalents) was dissolved in 200 mL THF, degassed for 15 minutes by bubbling with nitrogen and then irradiated at 300 nm at 30°C for 30 minutes. The solution was evaporated under reduced pressure to a yellow oil (166.0 mg) and the ^{1}H NMR spectrum was recorded. The oil contained five products by TLC (1% MeOH/50% EtOAc/hexanes) and from the ^{1}H NMR spectrum these were assigned: the azide (**91**, R_f = 0.57); the reduced aniline product (**90**, R_f = 0.21); the 2-closure azepine product, 6-acetamido-5-chloro-2-diethylamino-3H-dihydroazepine (**92**, R_f = 0.03); the 6-closure azepine product, 4-acetamido-5-chloro-2-diethylamino-3H-dihydroazepine (**84**, R_f = 0.03); and an unknown product, possibly the 6-closure diamine product, 4-acetamido-5-chloro-2-

diethylamino-aniline, **93**. the oil was chromatographed (Chromatotron, 2mm silica plate) using 1% MeOH/50% EtOAc/49% hexanes for the first four fractions, then 1% MeOH/50% EtOAc/49% $CHCl_3$ for the fifth fraction and finally 10% MeOH/90% EtOAc for the last fraction. Fraction #1 contained the stating azide **91** (65.9 mg), fraction #2 contained a mixture of **91** and the 6-azepine product **84** (54.0 mg), fraction #3 contained only **84** (30.8 mg), fraction #4 contained traces of the 2-azepine product **92** (3.0 mg), fraction #5 contained **92** (39.6 mg) and the final fraction, #6, contained tar that could not be identified by ^{1}H NMR.

Ratio of products (by ^{1}H NMR):			**91** : **90** : **92** : **84** : unknown
		=	50.7 : 0 : 27.8 : 18.3 : 3.1
Isolated products	(mg)	=	65.9 : 0 : 39.6 : 30.8 : 0
	(mmol)	=	0.31 : 0 : 0.16 : 0.12 : 0
Yield	(%)	=	46 : 0 : 23 : 18 : 0

Fraction #3: 4-acetamido-5-chloro-2-diethylamino-3H-dihydroazepine, **84**, showed:

^{1}H NMR ($CDCl_3$) δ 1.10 (H-2‴, 6H, br), 1.35 (H-4‴, 3H, s), 2.09 (H-2″, 4H, br), 5.83 (H-6, 1H, d, J=8.1), 6.75 (H-4′, 1H, br), 7.19 (H-7, 1H, d, J=8.1). Owing to conformational exchange of the azepine ring, the H-3 proton resonances were too weak to be reliably distinguished from noise.

^{13}C NMR ($CDCl_3$) δ 12.2 (C-2‴,**C**H_3), 15.9 (C-2‴,**C**H_3), 24.4 (C-4‴, **C**H_3), 30.3 (C-3, **C**H_2), 43.1 (C-2″, **C**H_2), 108.0 (C-6, **C**H), 114.1 (C-4, **C**), 117.2 (C-2, **C**), 139.0 (C-7, **C**H), 145.9 (C-5, **C**), 168.9 (C-4″, **C**=O).

MS (EI) [RI%] found: 257 (M{^{37}Cl})$^{+\cdot}$ [34%], 255 (M{^{35}Cl})$^{+\cdot}$ [100%], 226 (M{^{35}Cl}-Et)$^+$ [18%], 220 (M-Cl)$^+$ [36%], 212 (M{^{35}Cl}-$COCH_3$)$^+$ [22%], 184 (M{^{35}Cl}-$NCOCH_2$-CH_3)$^+$ [17%], 72 (M-$C_6H_3ClNHCOCH_3$)$^+$ [39%].

MS (CI) [RI%] found 258 ($M\{^{37}Cl\}+H)^+$ [33%], 256 ($M\{^{35}Cl\}+H)^+$ [100%], 220 $(M-Cl)^+$ [7%], 185 ($M\{^{35}Cl\}-NEt_2+2H)^{+\cdot}$ [17%].

Fraction #5: 6-acetamido-5-chloro-2-diethylamino-3H-dihydroazepine, **92**, showed:

^1H NMR ($CDCl_3$) δ 1.88 (H-2‴, 6H, br), 2.04 (H-6‴, 3H, s), 3.33 (H-2″, 4H, br), 5.22 (H-4, 1H, t, J=7.9), 7.19 (H-7, 1H, s). Owing to conformational exchange of the azepine ring, the H-3 proton resonances were too weak to be reliably distinguished from noise.

MS (EI) [RI%] found: 257 ($M\{^{37}Cl\})^{+\cdot}$ [34%], 255 ($M\{^{35}Cl\})^{+\cdot}$ [100%], 240 ($M\{^{35}Cl\}-CH_3)^+$ [23%], 214 ($M\{^{37}Cl\}-COCH_3)^+$ [24%], 212 ($M\{^{35}Cl\}-COCH_3)^+$ [71%], 184 ($M\{^{35}Cl\}-NCOCH_2-CH_3)^+$ [42%], 72 $(M-C_6H_3ClNHCOCH_3)^+$ [88%].

MS (CI) [RI%] found: 258 ($M\{^{37}Cl\}+H)^+$ [33%], 256 ($M\{^{35}Cl\}+H)^+$ [100%], 220 $(M-Cl)^+$ [18%].

Fraction #6: an unknown (possibly 4-acetamido-5-chloro-2-diethylamino-aniline, **93**) showed:

^1H NMR ($CDCl_3$) δ 7.48 (H-3, 1H, s), 6.23 (H-6, 1H, s).

Photolysis of 91 in 1.9 M $HNEt_2$/THF at 30°C.

The azide (**91**, 9.7 mg, 0.046 mmol, 3.7 mM) and $HNEt_2$ (2.5 ml, 1.77 g, 24.1 mmol, 1.9 M, 524 equivalents) was dissolved in 10 mL THF, degassed for 15 minutes with N_2 and irradiated at 300 nm at 30°C for 20 minutes. The solution was evaporated under reduced pressure to give a yellow oil (11.8 mg) and a ^1H NMR spectrum was recorded. The oil contained five products according to TLC (10% MeOH/$CHCl_3$): the azide (**91**, R_f = 0.82); the reduced aniline product (**90**, R_f = 0.06); the 2-closure azepine product (**92**, R_f = 0.66); the 6-closure azepine product (**84**, R_f = 0.67); and an unknown product (R_f =

0.27), possibly the hydrazine product, N,N-diethyl-N'-(3'acteamido-4'-chloro-phenyl)-hydrazine, or the 2-closure diamine product, 2-acetamido-3-chloro-6-diethylamino-aniline.

Ratio of products (by ^{1}H NMR): **91** : **90** : **92** : **84** : unknown

= 19.2 : 9.3 : 35.8 : 17.9 : 17.8

Photolysis of 91 in 1.9 M $HNEt_2$/THF at -70°C.

The azide (**91**, 11.5 mg, 0.0546 mmol, 4.4 mM) and $HNEt_2$ (2.5 ml, 1.77 g, 24.1 mmol, 1.9 M, 524 equivalents) was dissolved in 10 mL THF, degassed for 15 minutes with N_2 and irradiated at 300 nm at -70°C for 20 minutes. The solution was evaporated under reduced pressure to give a yellow oil (12.6 mg) and the ^{1}H NMR spectrum was recorded.

Ratio of products (by ^{1}H NMR): **91** : **90** : **92** : **84** : unknown

= 76.5 : 4.5 : 14.1 : 3.7 : 0.7

Photolysis of 91 in 7.5 mM $HNEt_2$/THF at 30°C.

The azide (**91**, 9.7 mg, 0.0461 mmol, 3.7 mM) and $HNEt_2$ (6.9 mg, 0.094 mmol, 7.5 mM, 2.05 equivalents) was dissolved in 12.5 mL THF, degassed for 15 minutes with N_2 and irradiated at 300 nm at 30°C for 10 minutes as described above to yield a yellow oil (11.2 mg).

Ratio of products (by ^{1}H NMR): **91** : **90** : **92** : **84** : unknown

= 46.6 : 0 : 20.7 : 25.9 : 6.7

7.7 Stability Studies on Selected Photolysis Products.

The azepines **55** and **56** along with the 6-diamine product **57** from the photolysis reaction of **49** were individually irradiated to determine if secondary photolysis was prevalent. The above products were stable at room temperature in the dark for at least a month. Similar thermal stability was observed for all the meta-substituted ring expanded products.

Thermal stability of 42 after 11 months at -5°C.

The crude reaction product from the photolysis of **42** (at 30°C in 2M $HNEt_2/C_6H_{12}$) was stored in the freezer wrapped in foil for 11 months, periodically left at room temperature for a few days. After the 11 month period a ^1H NMR spectrum was obtained on the sample and the integration of the resonances were compared to the original spectra. The relative ratios were essentially unchanged (< 6% error).

Ratio of Products:	**35 : 34 : 42**
Original Spectra:	29 : 17 : 53
11 months later:	27 : 14 : 59

Re-photolysis of 55, 56 and 57 in $HNEt_2$/THF.

The photolysis products **55** (7.7 mg, 0.0232 mmol), **56** (9.2 mg, 0.0277 mmol), **57** (6.3 mg, 0.0190) and the starting azide **49** (5.5 mg, 0.0192 mmol) were separately dissolved in 12 mL 5.1 mM $HNEt_2$/THF solutions. The solutions were degassed with nitrogen for 10 minutes and then irradiated in a rayonet using a carousel for 30 minutes. A separate solution of **56** (9.2 mg, 0.0277 mmol) in 12 mL of 5.1 mM $HNEt_2$/THF was irradiated for 120 minutes as well. The solutions were evaporated under reduced pressure

and their ^{1}H NMR spectra were recorded. The 2-azepine product **55** showed no significant change. The 6-azepine product **56** after 30 minutes of irradiation showed the presence of the azepine (49%) and another aromatic resonance at 5.89 ppm (51%) and after 120 minutes no aromatic resonances were observed. The 6-diamine product **57** after 30 minutes of irradiation showed numerous other products in the aromatic region in low yield as well as **57**.

7.8 Attempted Experiments Directed Towards the Synthesis of Amino-imino-azepines from 3H-Dihydroazepines.

Trifluoroacetamide Deprotection of 5-Nitro-2-trifluoroacetamido-acetanilide (51) with K_2CO_3/MeOH.

The trifluoroacetamide (**51**, 55.9 mg, 0.192 mmol, 12.8 mM) was dissolved in 15 mL MeOH and the solution was saturated with K_2CO_3 (500 mg). The solution was refluxed for 5 hours cooled to room temperature. Half the solution was removed, evaporated under reduced pressure and the products were rinsed from the salts with chloroform. The chloroform solutions were combined, evaporated under reduced pressure and the ^{1}H NMR spectrum showed the reduced product; 2-acetamido-4-nitro-aniline (**50**) and some other unidentifiable resonances in the aromatic region. The remaining solution was left at room temperature for 2 days after which it was worked-up in a similar fashion and its ^{1}H NMR spectrum recorded. The spectrum showed only the reduced aniline product **50**.

Attempted Deprotection of 6-Acetamido-2-diethylamino-5-trifluoroacetamido-3H-dihydroazepine (55) with K_2CO_3/MeOH.

The azepine (**55**, 11.8 mg, 0.0355 mmol, 12 mM) was treated with 3 mL of a saturated solution of K_2CO_3 (116 mg) in MeOH as described above at room temperature for 5.5 hours. The solution was worked-up as described earlier and analyzed by ^{1}H NMR to contain a small amount of the starting material, **55**, and no other identifiable products.

Attempted Deprotection of 55 with Methanolic Ammonia.

The azepine (**55**, 6.8 mg, 0.021 mmol, 4.2 mM) was dissolved in 5 mL of freshly distilled dry MeOH and NH_3 gas was bubbled through the solution at room temperature. The solution was left for 6 hours and then evaporated at 15°C under reduced pressure to give an oil. The oil was found to contain only **55** as evidenced by the ^{1}H NMR spectrum. The solution was evaporated, treated again with anhydrous MeOH and NH_3 for a further 14 hours at which time no products were visible according to TLC, mass spectra and ^{1}H NMR.

Attempted Oxidation of 4-acetamido-2-diethylamino-5-trifluoroacetamido-3H-dihydroazepine (56) with Iron (III) Chloride.

The azepine (**56**, 0.4 mg, 0.0012 mmol) was dissolved in 1 mL of dry MeOH and $FeCl_3$ (7 mg) was added in a 1.3 mL quartz cuvette. The reaction was monitored by the UV absorption of **56**. After 3 days no change was observed.

Oxidation of 4-Acetamido-5-chloro-2-diethylamino-3H-dihydroazepine (84) with DDQ.

The azepine (**84**, 6.7 mg, 0.0263 mmol, 0.0263 M) was dissolved in 1 mL of deuterated benzene in a 5 mm NMR tube fitted with a septum. A ^{1}H NMR spectrum was recorded and then 2,3-dichloro-5,6-dicyano-1,4-benzoquinone (DDQ, 8.0 mg, 0.0352 mmol, 0.035 M, 1.3 equivalents) was added and the reaction was followed by ^{1}H NMR. The solution immediately turned black and a precipitate formed. An impurity at 6.13 ppm in the ^{1}H NMR spectrum was used as a standard for integration. After 10 minutes 67% of the azepine **93** resonance had disappeared and after 35 minutes no more **84** was observed. After 2.5 hours the solution was transferred to a 30 mL round bottom flask. The tube was rinsed with *n*-butylamine (10 ml, 7.4 g, 0.10 mol, 3850 equivalents) and added to the flask with stirring. The black solution turned reddish brown. TLC (1% MeOH/50% EtOAc/hexanes) showed the starting azepine (**84**, R_f = 0.37) and two other products (R_f = 0.86 and 0.06). After 90 minutes no change was observed and the flask was fitted with a condenser, heated and refluxed for 120 minutes. TLC showed no change and the solution was cooled to room temperature, then evaporated under reduced pressure and the ^{1}H NMR spectrum of the residue was recorded. The spectrum showed only the starting azepine **84** and *n*-butylamine.

Attempted Substitution Reaction of 84 with *n*-Butylamine Using Silver Salts as a Catalyst.

The azepine (**84**, 7.7 mg, 0.030 mmol, 1.5 mM) was dissolved in 20 mL *n*-butylamine (14.8 g, 20 mol, 6.7 x 10^5 equivalents) and refluxed for 16 hours. The solution was cooled, evaporated under reduced pressure to yield an oil and its ^{1}H NMR was recorded. The spectrum showed the presence of **84** and *n*-butylamine and some

aromatic resonances at 4.53 (singlet) and 7.32 (multiplet). The solution was evaporated under reduced pressure and then 10 mL of a solution of CH_2Cl_2 and silver tetrafluoroborate ($AgBF_4$, 5.8 mg, 0.03 mmol, 1 equivalent) was added. After 1 minute 2ml of *n*-butylamine was added and the solution was left at room temperature for 2 hours. The solution was evaporated under reduced pressure and the ^1H NMR spectrum of the residue showed no new signals.

APPENDIX 1

Steady-State Kinetics for the 6-Closure Ring Expansion of 3-Acetamido-4-trifluoroacetamido-phenylnitrene, ^{1}59.

The steady-state reaction for the 6-closure of ^{1}**59**, to yield 4-acetamido-2-diethylamino-5-trifluoroacetamido-3H-dihydroazepine (6-azepine product **56**) and 4-acetamido-2-diethylamino-5-trifluoroacetamido-aniline (6-diamine product **57**), was calculated for the ratio of products **57/56** to simplify the calculation. The ratio **57/56** was expressed in terms of rate constants and the concentration of diethylamine. Under steady-state reaction conditions the rate of formation of the 6-azirine **61** and 6-didehydroazepine **63** intermediates remains constant. From this assumption the following expression for **57/56** was calculated:

Under steady-state conditions, the rate of change in 6-didehydroazepine (**63**) production was zero:

$$\frac{d[\mathbf{63}]}{dt} = 0 = k_{6d}[\mathbf{61}] - (k_6^o + k_{-6d} + k_{nuc6d}[HNuc])[\mathbf{63}] \qquad \text{(A1)}$$

Therefore the concentration of **63** was:

$$[\mathbf{63}] = \frac{k_{6d}[\mathbf{61}]}{(k_6^o + k_{-6d} + k_{nuc6d}[HNuc])} \qquad \text{(A2)}$$

The rate of 6-azepine (**56**) production was dependent on the concentration of **63** and diethylamine therefore:

$$\Phi_{56} = k_{nuc6d}[HNuc][\mathbf{63}] \qquad \text{(A3)}$$

where Φ_{56} is the rate of production of **56**.

Therefore Φ_{56} can be expressed in terms of [**61**] by substituting equation **A2** into **A3**:

$$\Phi_{56} = \frac{k_{nuc6d}[HNuc]k_{6d}[\mathbf{61}]}{k_6^o + k_{-6d} + k_{nuc6d}[HNuc]} \qquad \text{(A4)}$$

The rate of **57** production, Φ_{57}, can be expressed in terms of concentration of **61** and diethylamine:

$$\Phi_{57} = k_{nuc6a}[HNuc][\mathbf{61}] \qquad \text{(A5)}$$

The ratio of **57** over **56** (Φ_{57}/Φ_{56}) was obtained by dividing equation **A5** by **A4**:

$$\frac{\Phi_{57}}{\Phi_{56}} = \frac{(k_6^o + k_{-6d})k_{nuc6a}[HNuc][\mathbf{61}] + k_{nuc6d}k_{nuc6a}[\mathbf{61}][HNuc]^2}{k_{6d}k_{nuc6d}[\mathbf{61}][HNuc]} \qquad \text{(A6)}$$

Equation **A6** simplifies to:

$$\frac{\Phi_{57}}{\Phi_{56}} = \frac{(k_6^o + k_{-6d})k_{nuc6a}}{k_{6d}k_{nuc6d}} + \frac{k_{nuc6a}}{k_{6d}}[HNuc] \qquad \text{(A7)}$$

Therefore a plot of Φ_{57}/Φ_{56} versus the diethylamine concentration yielded:

$$Slope = \frac{k_{nuc6a}}{k_{6d}} \qquad \text{(A8)}$$

and

$$Intercept = \frac{(k_6^o + k_{-6d})k_{nuc6a}}{k_{6d}k_{nuc6d}} \qquad \text{(A9)}$$

The ratio of equations **A8/A9** yielded a simplified expression for the relative rate of 6-didehydroazepine rearrangement (k_{-6d} and k_6^o) to its trapping with diethylamine (k_{nuc6d}):

$$\frac{Intercept}{Slope} = \frac{k_6^o + k_{-6d}}{k_{nuc6d}} \qquad (A10)$$

Similarly, for the 2-closure products, a plot of Φ_{58}/Φ_{55} yielded:

$$Slope = \frac{k_{nuc2a}}{k_{2d}} \qquad (A11)$$

and:

$$Intercept = \frac{(k_2^o + k_{-2d})\,k_{nuc2a}}{k_{2d}k_{nuc2d}} \qquad (A12)$$

The ratio of equations **A11/A12** yielded a simplified expression for the relative rate of 6-didehydroazepine rearrangement (k_{-2d} and k_2^o) to its trapping with diethylamine (k_{nuc2d}):

$$\frac{Intercept}{Slope} = \frac{k_2^o + k_{-2d}}{k_{nuc2d}} \qquad (A13)$$

References

1a Swanson, D.P., Chilton, H.M. and Thrall, J.H., *Pharmaceuticals in Medical Imaging.*, Macmillan Publishing Co., New York, N.Y., U.S.A., **1990**.

1b Young, S.W., *Magnetic Resonance Imaging: Basic Principles.*, Raven Press, New York, N.Y., U.S.A., **1988**.

1c Kean, D. and Smith, M., *Magnetic Resonance Imaging: Principles and Applications.*, William Heinemann Medical Books, London, U.K., **1986**.

2a Sanders, J.K.M. and Hunter, B.K., *Modern NMR Spectroscopy*, Oxford Univ. Press, New York, NY, U.S.A., **1987**.

2b Pavia, D.L., Lampmann, G.M. and Kris, G.S.Jr., *Introduction to Spectroscopy*, Saunders College, Philadelphia, PA, U.S.A., **1979**, pp. 81-165.

3a Lauffer, R.B., *The Strem Chemiker*, 1988, *XII(1)*,1-9.

3b Lauffer, R.B., *Chem.Rev.*1987,*87(5)*,901-927.

3c Lauffer, R.B., *Mag. Res. Quart.*, **1990**, *6*, 65-84.

3d Hahn, E.L., *Phil. Trans. R. Soc. Lond., A*, **1990**, *333*, 403-411.

3e Lauffer, R.B., *Invest. Rad.*, **1990**, *25*, S32-S33.

3f Fiel, R.J., Musser, D.A., Mark, E.H., Mazurchuk, R. and Alletto, J.J., *Mag. Res. Imag.*, **1990**, *8*, 255-259.

3g Geraldes, C.F.G.C., Sherry, A.D. and Kiefer, G.E., *J. Mag. Res.*, **1992**, *97*, 290-304.

4a Eaton, D.R., McClellan, W.R. and Weiher, J.F. *Inorg. Chem.*, **1968**, *7(10)*, 2040-2046.

4b Eaton, D.R., Josey, A.D. and Benson, R.F., *J. Am. Chem. Soc.*, **1967**, *89*, 4040-4050.

4c Jesson, J.P., Trofimenko, S. and Eaton, D.R., *J. Am. Chem. Soc.*, **1967**, *89*, 3148-3158.

4d Eaton, D.R. and McClellan, W.R., *Inorg. Chem.*, **1967**, *6*, 2134-2138.

4e Eaton, D.R. and Phillips, W.D., *J.Chem.Phys.*, **1965**, *43(2)*, 392-398.

4f Eaton, D.R., Josey, A.D., Phillips, W.D. and Benson, R.E., *J.Chem.Phys.*, **1962**, *37(2)*, 347-360.

4g Eaton, D.R., Phillips, W.D. and Caldwell, D.J., *J. Am. Chem. Soc.*, **1963**, *85*, 397-406.

4h Eaton, D.R., Josey, A.D., Benson, R.E., Phillips, W.D. and Cairns, T.L., *J. Am. Chem. Soc.*, **1962**, *84*, 4100-4106.

5a Li, Y.Z. and Schuster, G.B., *J. Org. Chem.*, **1988**, *53*, 1273-1277.

5b Dewar, M.J.S. and Thiel, W., *J. Am. Chem. Soc.*, **1977**, *99*, 4899-4907.

5c Dewar, M.J.S., Zoebisch, E.G., Healy, E.F. and Stewart, J.J.P., *J. Am. Chem. Soc.*, **1985**, *107*, 3902-3909.

5d Dewar, M.J.S. and Thiel, W., *J. Am. Chem. Soc.*, **1977**, *99*, 4907-4917.

5e Boyd, D.B. and Lipkowitz, K.B., *J. Chem. Ed.*, **1982**, *59*, 269-274.

5f Drzaic, P. and Brauman, J.I., *J. Am. Chem. Soc.*, **1984**, *106*, 3443-3446.

5g Ertl, P., *Monatsh. Chem.*, **1991**, *122*, 1015-1018.

5h Quirante, J.J., Enr˜quez, F. and Hernando, J.M., *J. Molec. Struct. (Theochem.)*, **1992**, *254*, 493-504.

5i Broughton, H.B., Green, S.M. and Rzepa, H.S., *J. Chem. Soc., Chem. Commun.*, **1992**, 37-39.

5j Fabian, W.M.F., *Z. Naturforsch.*, **1990**, *45a*, 1328-1334.

5k Zakzhevskii, V.G. and Danovich, D.K., *J. Struct. Chem.*, **1989**, *30*, 474-477.

5l Dewar, M.J.S. and Storch, D.M., *J. Am. Chem. Soc.*, **1985**, *107*, 3898-3902.

5m Bingham, R.C., Lo, D.H. and Dewar, M.J.S., *J. Am. Chem. Soc.*, **1975**, *97*, 1285-1301.

5n Smolinsky, G., Wasserrman, E. and Yager, W.A., *J. Am. Chem. Soc.*, **1962**, *84*, 3220.

6a PCMODEL available from Dr. K. Gilbert, Serena Software, P.O. Box 3076, Bloomington, IN, 47402-3076, U.S.A.

6b AMPAC available from the Quantum Chemistry Program Exchange, Bloomington, IN, 47405, U.S.A.

7a McWeeny, R., *Spins In Chemistry*, Polytechnic Press, Brooklyn, NY, U.S.A., **1970**.

7b McConnell, H.M., *J. Chem. Phys.*, **1958**, *28*, 1188-1192.

8a Iddon, B., Meth-Cohn, O., Scriven, E.F.V., Suschitzky, H., Gallager, P.T., *Angew. Chem. Int. Ed. Engl.*, **1979**, *18*, 900-917.

8b Maier, G., *Angew. Chem. Int. Ed. Engl.*, **1967**, *6*, 402-413.

8c Hassenrück, K. and Martin, H.D., *Synthesis*, **1988**, 569-586.

9a Li, Y.-Z., Kirby, J.P., George, M.W., Poliakoff, M. and Schuster, G.B., *J. Am. Chem. Soc.*, **1988**, *110(24)*, 8092-8098.

9b Meijer, E.W., Nijhuis, S. and van Vroonhoven, F.C.B.M., *J. Am. Chem. Soc.*, **1988**, *110*, 7209-7210.

9c Kobayashi, T., Ohtani, H., Suzuki, K. and Yamaoka, T., *J. Phys. Chem.*, **1985**, *89*, 776-779.

9d Poe, R., Grayzar, J., Young, M.J.T., Leyva, E., Schnapp, K.A. and Platz, M.S., *J. Am. Chem. Soc.* **1991**, *113*, 3209-3211.

9e Soundararajan, N. and Platz, M.S., *J. Org. Chem.* **1989**, *55*, 2034-2044.

9f Young, M.J.T. and Platz, M.S., *J. Org. Chem.* **1991**, *56*, 6403-6406.

9g Purvis, R., Smalley, R.K., Suschitzky, H. and Alkhader, M.A., *J.Chem.Soc. I*, **1984**, 249-254.

9h Purvis, R., Smalley, R.K., Strachan, W.A. and Suschitzky, H., *J.Chem.Soc. I*, **1978**, 191-195.

9i Mustill, R.A. and Rees, A.H., *J.Org.Chem.*, **1983**, *48*, 5041-5043.

9j Gritson, N.P. and Pritchina, E.S., *Journal of Information Recording Materials*, **1989**, *17*(5-6), 391-404.

9k Chapman, O.L. and Le Roux, J.-P., *J. Am. Chem. Soc.*, **1978**, *100(1)*, 282-285.

9l Leyva, E., Munoz, D. and Platz, M.S., *J. Org. Chem.* **1989**, *54*, 5938-5945.

9m Kanakarajan, K., Goodrich, R., Young, M.J.T., Soundararajan, S. and Platz, M.S., *J. Am. Chem. Soc.* **1988**, *110*, 6536-6541.

9n Shields, C.J., Chrisope, D.R., Schuster, G.B., Dixon, A.J., Poliakoff, M. and Turner, J.J., *J. Am. Chem. Soc.*, **1987**, *109*, 4723-4726.

9o Leyva, E., Platz, M.S., Persy, G. and Wirz, J., *J. Am. Chem. Soc.*, **1986**, *108*, 3783-3790.

9p Shields, C.J., Falvey, D.E., Schuster, G.B., Buchardt, O. and Nielson, P.E., *J.Org.Chem.*, **1988**, *53*, 3501-3507.

9q DeGraff, B.A., Gillespie, D.W. and Sundberg, R.J., *J. Am. Chem. Soc.*, **1974**, *96(24)*, 7491-7496.

9r Carroll, S.E., Nay, B., Scriven, E.F.V., Suschitzky, H. and Thomas, D.R., *Tetrahedron Lett.*, **1977**, *36*, 3175.

9s Larmara, K. and Smalley, R.K., *Tetrahedron*, **1991**, *47*, 2277-2290.

9t Scriven, E.F.V., Suschitzky, H. and Thomas, D.R., *J. Chem. Soc., Perkin*, **1979**, 53-59.

9u Iddon, B., Pickering, M.W., Suschitzky, H. and Taylor, D.S., *J. Chem. Soc., Perkin*, **1975**, 1686-1690.

9v Hayes, R., Schofield, J.M., Smalley, R.K., Scopes, D.I.C., *Tetrahedron* **1990**, *46*(6), 2089-2096.

9w Schrock, A.K. and Schuster, G.B., *J. Am. Chem. Soc.* **1984**, *106*, 5234-5240.

9x Dunkin, I.R. and Thomson, P.C.P., *J. Chem. Soc., Chem. Commun.* **1980**, 499-501.

9y Patel, D.I., Scriven, E.F.V., Smalley, R.K. and Suschitzky, H., *J. Chem. Soc., Perkin Trans. I* **1985**, 1911-1915.

9z Schrock, A.K. and Schuster, G.B., *J. Am. Chem. Soc.*, **1984**, *106*, 5228-5234.

9a' Khan, Z.U., Patel, E.F.V., Smalley, D.I., Scriven, R.K. and Suschitzky, H., *J. Chem. Soc., Perkin Trans. I* **1983**, 2495-2500.

9b' Sundberg, R.J., Suter, S.R. and Brenner, M., *J. Am. Chem. Soc.*, **1972**, *94(2)*, 513-520.

9c' Liang, T.-Y. and Schuster, G.B., *J. Am. Chem. Soc.*, **1987**, *109*, 7803-7810.

9d' Nielson, P.E. and Buchardt, O., *Photochem. and Photobiol.*, **1982**, *35*, 317-323.

9e' Purvis, R., Smalley, R.K., Suschitzky, H. and Alkhader, M.A. *J. Chem. Soc., Perkin Trans. I* **1984**, 249-254.

9f' Leyva, E., Chang, D.H.S., Platz, M.S., Watt, D.S., Crocker, P.J., Kawada, K., *Photochem. and Photobio.*, **1991**, *54*(3), 329-333.

9g' Younger, C.G. and Bell, R.A., *J. Chem. Soc., Chem. Commun.*, **1992**, 1359-1361.

9h' Doering, W. von E. and Odum, R.A., *Tetrahedron*, **1966**, *22*, 81.

10a Cadogan, J.I.G. and Todd, M.J., *J.Chem.Soc.(C)*, **1969**, 2808-2823.

10b Cadogan, J.I.G., *Quart.Rev.*, **1968**, *22*, 222-251.

10c Cadogan, J.I.G., Grace, D.S.B., Lim, P.K.K. and Tait, B.S., *J.Chem.Soc.I*, **1975**, 2376-2385.

10d Atherton, F.R. and Lambert, R.W., *J.Chem.Soc I*, **1973**, 1079-1084.

10e de Boer, T., Cadogan, J.I.G., McWilliam, H.M. and Rowley, A.G., *J.Chem.Soc. II*, **1974**, 554-558.

10f Cadogan, J.I.G. and Tweddle, N.J., *J.Chem.Soc. I*, **1978**, 1278-1284.

10g Odum, R.A. and Brenner, M., *J. Am. Chem. Soc.*, **1966**, *88*, 2074-2075.

11a Ohba, Y., Kubo, S., Nakai, M., Nagal, A. and Yoshimoto, M., *Chem.Soc.Jap.*, **1986**, 59, 2317-2320.

11b Ohba, Y., Kubo, S., Nishiwaki, T. and Aratani, N., *Heterocycles*, **1984**, *22(3)*, 457-460.

11c Appl, M. and Huisgen, R., *Chem. Ber.*, **1959**, *92*, 2961-2967.

11d Huisgen, R., Vossius, D. and Appl, M., *Chem. Ber.*, **1958**, *91*, 1-21.

12a Hafner, K., König, C., *Angew. Chem.*, **1963**, *75*, 89.

12b Vogel, E., Altenbach, H., Drossard, J., Schmickler, H. and Stegelmeier, H., *Angew. Chem. Int. Ed.*, **1980**, *19*, 1016-1018.

12c Lwowski, W., Maricich, T.J., Mattingly, T.W.jr., *J. Am. Chem. Soc.*, **1963**, *85*, 1200-1202.

12d Hafner, K., *Angew. Chem. Int. Ed.*, **1964**, *3*, 165-173.

12e Hafner, K., Zinser, D., Moritz, K-L., *Tetrahedron Lett.* **1964**, *26*, 1733-1737.

12f Marsh, F.D., and Simmons, H.E., *J. Am. Chem. Soc.* **1965**, *87*, 3529-3530.

12g Paquette, L.A., Kuhla, D.E., Barrett, J.H. and Haluska, R.J., *J. Org. Chem.*, **1969**, *34*, 2866-2878.

12h Paquette, L.A., Kuhla, D.E. and Barrett, J.H., *J. Org. Chem.*, **1969**, *34*, 2879-2884.

12i Paquette, L.A. and Kuhla, D.E., *J. Org. Chem.*, **1969**, *34*, 2885-2896.

13a Paquette, L.A., *J. Am. Chem. Soc.* , **1963**, *85*, 3288-3292.

13b Paquette, L.A. and Farley, W.C., *J. Am. Chem. Soc.* , **1967**, *89*, 3595-3600.

13c Paquette, L.A., *J. Am. Chem. Soc.* , **1964**, *86*, 4092-4095.

13d Paquette, L.A., *J. Am. Chem. Soc.* , **1964**, *86*, 4096-4099.

13e Paquette, L.A., *J. Am. Chem. Soc.* , **1963**, *85*, 4053-4054.

14a Splitter, J.S. and Calvin, M., *Tetrahedron Lett.* , **1968**, *12*, 1445-1448.

14b Meyer, E. and Griffin, G.W., *Angew. Chem. Int. Ed. Engl.*, **1967**, *6*, 634.

14c Tsui, F.P., Chang, Y.H., Vogel, T.M. and Zon, G., *J. Org. Chem.*, **1976**, *41*, 3381-3388.

15a Padwa, A., Smolanoff, J. and Tremper, A., *J. Org. Chem.*, **1979**, *41*, 543-549.

15b Anderson, D.J. and Hassner, A., *Synthesis*, **1975**, 483-495.

15c Prinzbach, H., Bingmann, H., Fritz, H., Markert, J., Knothe, L., Eberbach, W., Brokatzky-Geiger, J., Sekutowski, J.C. and Krüger, C., *Chem. Ber.*, **1986**, *119*, 616-644.

15d Gockel, U., Hartmannsgruber, U., Steigel, A. and Sauer, J., *Tetrahedron Lett.*, **1980**, *21*, 595-598.

15e Dittmar, W., Sauer, J. and Steigel, A., *Tetrahedron Lett.*, **1969**, 5171-5174.

15f Hassner, A. and Anderson, D.J., *J. Org. Chem.*, **1974**, *39*, 3070-3076.

15g Sano, T., Horiguchi, Y. and Tsusa, Y., *Heterocycles*, **1979**, *12*, 1427-1432.

15h Sano, T., Horiguchi, Y. and Tsusa, Y., *Heterocycles*, **1986**, *24*, 273.

15i Sano, T., Horiguchi, Y., Tanaka, K. and Tsusa, Y., *Chem. Pharm. Bull.*, **1985**, *33*, 5197-5201.

15j Sano, T., Horiguchi, Y. and Tsusa, Y., *Heterocycles*, **1978**, *9*, 731-738.

15k Takahata,H., Tomiguch, A. and Yamazaki, T., *Heterocycles*, **1981**, *16*, 1569-1572.

15l Martin, H.-D., Mais, F.-J., Mayer, B., Hecht, H.-J., Hekman, M. and Steigel, A., *Monatsh. Chem.*, **1983**, *114*, 1145-1147.

16a Misiti, D., Moore, H.W. and Folkers, K. *Tetrahedron Lett.* , **1965**, *16*, 1071-1074.

16b Rickards, R.W. and Smith, R.M., *Tetrahedron Lett.* , **1966**, 2361-2365.

17a Anderson, M. and Johnson, A.W., *J. Chem. Soc.*, **1965**. 2411-2422.

17b Childs, R.F. and Johnson, A.W., *J. Chem. Soc.*, **1966**, 1950-1955.

18a Katritzky, A.R., Aurrecoechea, J.M., Quian, K., Kozoil, A.E. and Palenik, G.J., *Heterocycles*, **1987**, *25*, 387-391.

18b Lablache-Combier, A. and Surpateanu, G., *Tetrahedron Lett.*, **1976**, 3081.

19a Smith, P.A.S., Platz, M.S. and Wentrup, C. in: *Azides and Nitrenes, Reactivity and Utility*, Scriven, E.F.V. (Ed.), Academic Press, New York, N.Y., U.S.A., **1984**, pp 95-204, pp 359-394 and pp 395-433 respectively.

19b Platz, M.S., Leyva, E. and Haider, K., *Organic Photochemistry, Vol. 11*, Padwa, A. (Ed.), Marcel Dekker, Inc, New York, N.Y., U.S.A., **1991**, pp 367-429.

20 Wayner, D.D.M., *CRC Handbook of Organic Photochemistry, Vol. II*, Scaiano, J.C. (Ed.), CRC Press, Inc., Boca Raton, Florida, U.S.A., **1991**, 395-399.

21a Greene, T.W., *Protective Groups in Organic Synthesis*, J. Wiley, New York, N.Y., U.S.A., **1981**.

21b Newman, H., *J. Org. Chem.*, **1965**, *30*, 1287.

21c Schwartz, M.A., Rose, B.F. and Vishnuvajjala, B., *J. Am. Chem. Soc.*, **1973**, *95*, 612.

21d Imazawa, M. and Eckstein, F., *J. Org. Chem.*, **1979**, *44*, 2039.

22a Bellamy, F.D. and Ou, K., *Tetrahedron Lett.* **1984**, *25*, 839-842.

22b Mendenhall, G.D. and Smith, P.A.S., *Organic Synthesis, Collective Vol. 5*, Baumgarten, H.E. (Ed), John Wiley and Sons, Inc., New York, NY, U.S.A., **1973**, 829-833.

23a Godovikova, T.I., Rakitin, O.A. and Khmel'nitskii, *Russ. Chem. Rev.*, **1983**, *52*, 440-445.

23b *Organic Synthesis, Collective Vol. 4*, Mallory, F.B. (Ed.), John Wiley and Sons, Inc., New York, NY, U.S.A., **1963**, 74-78.

24 Turro, N.J., *Modern Molecular Photochemistry*, The Benjamin/Cummings Publishing Co. Inc., Menlo Park, California, **1978**.

25a Satake, K., Saitoh, H., Kimura, M. and Morosawa, S., *J. Chem. Soc., Chem. Commun.*, **1988**, *16*, 1121-1123.

25b Anderson, D.J., Hassner, A. and Tang, D.Y., *J. Org. Chem.*, **1974**, *39*, 3076-3080.

25c Streef, J.W. and Van der Plas, H.C., *Heterocycles*, **1987**, *26*, 685-688.

26 Rose, M.E. and Johnstone, R.A.W., *Mass Spectrometry for Chemists and Biochemists*, Cambridge University Press, Cambridge, U.K., **1987**.

27a Nitta, M., Shibata, K. and Miyano, H., *Heterocycles*, **1989**, *29*, 253-256.

27b Takeuchi, H., Maeda, M., Mitani, M. and Koyama, K., *J. Chem. Soc., Perkin I*, **1987**, 57-60.

28 Imajo, S., Nakanishi, K., Roberts, M., Lippard, S.J. *J. Am. Chem. Soc.* **1983**, *105*, 2071-2073.

29a Perkin, W.H. Jr. and Riley, G.C., *J. Chem. Soc.*, **1923**, 2399-2408.

29b Plochl, J., *Chem. Ber.*, **1886**, *19*, 6.

30 Terpko, M.O. and Heck, R.F., *J. Org. Chem.* **1980**, *45*, 4992-4993.

31 Komiyama, M. and Bender, M.L., *J. Am. Chem. Soc.*, **1977**, *99(24)*, 8021-8024.

32 Weast, R.C. (Ed.), *Handbook of Chemistry and Physics, 57th Ed.*, CRC Press, Inc., Cleveland, Ohio, U.S.A., **1976**, C83.

33 Leffler, J.E. and Temple, R.D., *J. Am. Chem. Soc.*, **1967**, *89*, 5235-5246.

34 Spauschus, H.O. and Scott, J.M., *J. Am. Chem. Soc.*, **1951**, *73*, 208.

35 Forster, M.O. and Schaeppi, J.H., *J. Chem. Soc.*, **1912**, *101*, 1359-1366.

36 Rupe, H. and von Majewski, K., *Ber.*, **1900**, *33*, 3401.

37 Ugi, I., Perlinger, H. and Behringer, L., *Chem. Ber.*, **1958**, *91*, 2330.

38 Lieber, E., Chao, T.S. and Rao, C.N.R., *J. Org. Chem.*, **1957**, *22*, 654.